

A MULTI-DISCIPLINED FIELD-BASED STUDY OF  
SEDIMENTARY BASIN EVOLUTION ALONG  
SEISMICALLY ACTIVE TRANSPRESSIONAL FAULT  
SYSTEMS IN THE MONGOLIAN ALTAI

Thesis submitted for the degree of Doctor of Philosophy at the  
University of Leicester

By

James Peter Howard BSc (Liverpool)

Department of Geology

The University of Leicester

April 2004

UMI Number: U188577

All rights reserved

INFORMATION TO ALL USERS

The quality of this reproduction is dependent upon the quality of the copy submitted.

In the unlikely event that the author did not send a complete manuscript and there are missing pages, these will be noted. Also, if material had to be removed, a note will indicate the deletion.



UMI U188577

Published by ProQuest LLC 2013. Copyright in the Dissertation held by the Author.  
Microform Edition © ProQuest LLC.

All rights reserved. This work is protected against  
unauthorized copying under Title 17, United States Code.



ProQuest LLC  
789 East Eisenhower Parkway  
P.O. Box 1346  
Ann Arbor, MI 48106-1346



# A Multi-disciplined field-based study of sedimentary basin evolution along seismically active transpressional fault systems in the Mongolian Altai

James Peter Howard

## **Abstract**

This PhD project documents processes controlling the generation, evolution and preservation of intracontinental transpressional basins, one of the least understood major basin types. Field data were collected in three actively deforming transpressional basins along the eastern margin of the Mongolian Altai. The Mongolian Altai is an active intracontinental mountain range comprising discrete ranges, uplifted by outward-directed thrust and oblique-slip faults linked to regionally extensive, dextral strike-slip faults. Between ranges numerous transpressional basins exist in various stages of their evolution. Thus the Mongolian Altai is an excellent natural laboratory for studying the origin and development of intraplate transpressional basins.

Analysis of Landsat TM imagery allows the identification of five interlinked sediment accumulation sites which control modern sediment transport, deposition and storage within the Altai region. At present, small sediment volumes exit the Mongolian Altai and the most significant sediment sinks are range flanking transpressional basins such as the Dzereg, Dariv and Shargyn basins. In these basins, strata are uplifted, deformed and exposed by active faulting and folding in internal zones and along basin margins. Mesozoic strata are confined to an elongate trough coincident with Cenozoic basins, suggesting Cenozoic basins are reactivated older depocentres. The upward fining and asymmetric thickness distribution of Mesozoic strata, and the presence of interpreted Mesozoic normal faults, suggest that the basins formed during Mesozoic extension or transtension.

Transpressional reactivation of the Altai began in the Oligocene, presumably in response to the distant Indo-Eurasian collision. Cenozoic strata coarsen upward and are dominated by alluvial sediment shed from adjacent ranges. Compartmentalised uplift and erosion of basin sediments and synchronous downslope sedimentation characterise the transpressional phase of basin evolution. Transpressional basins have variable bounding fault geometries and a low preservation potential. Consequently recognising ancient examples requires a detailed investigation of their stratigraphy, bounding faults and regional tectonic setting.

## **Acknowledgements**

I would like to thank many people for their help and support during my time at Leicester. Firstly many thanks to Dickson Cunningham and Sarah Davies for their support both in the field and in Leicester particularly while writing up this thesis. Thanks also to my family for their long term support, both emotional and financial throughout both my undergraduate and postgraduate degrees. Emma Cosham has constantly been there during my writing up putting up with my grumpy moods and long hours working with constant goodwill. The future looks good for us; any couple who can make it through simultaneously writing up a PhD and rearing a puppy can survive anything. Thanks to Marc Reichow for constant friendship during my time in Leicester, I have particularly good memories of field trips in Spain and Arran before everything got stressful. Thanks to Nat Thomas and Gary Shawley for many nights out in Leicestershire. Matt Hooper gave good advice on supervisors and when presenting talks at conferences and, along with Dave Gladwell could always be relied upon to be somewhere near a pub. All the other PhD students have helped in one way or another and made my time in Leicester far more enjoyable.

Particular thanks are also due to all the people who helped during fieldwork in Mongolia, particularly Tsogoo, Tsogoo, Oralmaa, my field team, and to Badarch who arranged it all.

# Table of Contents

## Chapter 1

<b>Introduction</b>	<b>1</b>
1.2 Wider context for this project	5
1.3 Chapter synopsis	5

## Chapter 2

<b>A TM Landsat study into modern sediment transport and deposition within the greater Altai region</b>	<b>9</b>
2.1 Introduction	9
2.2 Method	11
2.3 Geomorphology of the Altai and western Gobi Altai region	11
2.4 Glaciation in the Altai	12
2.5 Structural geology of the Altai	13
2.6 Drainage systems in the Altai	14
2.6.1 INTRODUCTION	14
2.6.2 INTRAMONTANE BASINS	15
2.6.2.1 <i>Externally drained basins</i>	15
2.6.2.1.1 Description	15
2.6.2.1.2 Interpretation	16
2.6.2.2 <i>Internally drained basins</i>	16
2.6.2.2.1 Description	16
2.6.2.2.2 Interpretation	17
2.6.3 DEPOSITION WITHIN MOUNTAIN RIVER VALLEYS	18
2.6.3.1 <i>Description</i>	18

2.6.3.2 <i>Interpretation</i>	20
2.6.4 RANGE-FLANKING TRANSPRESSIONAL BASINS	21
2.6.4.1 <i>Description</i>	21
2.6.4.2 <i>Interpretation</i>	22
2.6.5 SHALLOW PERIPHERAL BASINS	23
2.6.5.1 <i>Description</i>	23
2.6.5.2 <i>Interpretation</i>	24
2.6.6 EXTERNAL DEPOCENTRES	25
2.6.6.1 <i>The Junggar Basin</i>	25
2.6.6.1.1 Description	25
2.6.6.1.2 Interpretation	25
2.6.6.2 <i>The Valley of Lakes</i>	26
2.6.6.2.1 Description	26
2.6.6.2.2 Interpretation	26
2.7 The influence of tectonic uplift on drainage patterns	27
2.8 Discussion	28

## Chapter 3

<b>The Stratigraphic and structural evolution of the Dzereg Basin, western Mongolia: clastic sedimentation, transpressional faulting and basin destruction in an intraplate, intracontinental setting</b>	<b>34</b>
3.1 Abstract	34
3.2 Introduction	35
3.3 Geology of the Altai region	37
3.4 Previous work on flanking basins in the Mongolian Altai	38

3.5 Geology of the Dzereg Basin	39
3.6 Basin stratigraphy	41
3.6.1 JURASSIC	42
3.6.2 LOWER CRETACEOUS (YELLOW SANDSTONE UNIT)	42
3.6.2.1 <i>Description</i>	42
3.6.2.2 <i>Interpretation</i>	43
3.6.3 LOWER CRETACEOUS (THE LOWER RED BED UNIT/ WESTERN RED BED UNIT)	45
3.6.3.1 <i>Description</i>	45
3.6.3.2 <i>Interpretation</i>	46
3.6.4 OLIGOCENE (THE OASIS UNIT)	49
3.6.4.1 <i>Description</i>	49
3.6.4.2 <i>Interpretation</i>	50
3.6.5 MIOCENE (TAN CONGLOMERATE UNIT/ LOWER YELLOW CONGLOMERATE UNIT)	51
3.6.5.1 <i>Description</i>	51
3.6.5.2 <i>Interpretation</i>	52
3.6.6 PLIOCENE AND LOWER PLEISTOCENE (UPPER RED BED UNIT/ UPPER YELLOW CONGLOMERATE UNIT/ GREY CONGLOMERATE UNIT)	55
3.6.6.1 <i>Description</i>	55
3.6.6.2 <i>Interpretation</i>	56
3.6.7 QUATERNARY (ALLUVIAL FAN DEPOSITS)	58
3.7 Structural geology of the study area	59
3.8 Discussion	60
3.9 Conclusions	66

## Chapter 4

<b>Stratigraphy of the Dariv and Shargyn basins</b>	<b>69</b>
4.1 Introduction	69
4.2 Mesozoic Stratigraphy	70
4.2.1 PREVIOUS WORK	70
4.2.2 JARGALANT FORMATION – MIDDLE JURASSIC	70
4.2.2.1 <i>Description</i>	71
4.2.2.2 <i>Interpretation</i>	75
4.2.3 DARIV (a) FORMATION – UPPER JURASSIC	80
4.2.3.1 <i>Description</i>	80
4.2.3.2 <i>Interpretation</i>	81
4.2.4 IHKES NUUR FORMATION – UPPER JURASSIC – LOWER CRETACEOUS	83
4.2.4.1 <i>Description</i>	83
4.2.4.2 <i>Interpretation</i>	87
4.2.5 GURVEN EREEN FORMATION – LOWER CRETACEOUS	91
4.2.5.1 <i>Description</i>	91
4.2.5.2 <i>Interpretation</i>	98
4.2.6 DZEREG (DZERI) FORMATION – LOWER CRETACEOUS	105
4.2.6.1 <i>Description</i>	106
4.2.6.2 <i>Interpretation</i>	112
4.3 Cenozoic Sediments	118
4.3.1 INTRODUCTION	118
4.3.2 PREVIOUS WORK	118

4.3.3 RED HILL FORMATION – OLIGOCENE (BEGER SUITE)	119
4.3.3.1 <i>Description</i>	119
4.3.3.2 <i>Interpretation</i>	124
4.3.4 EAGLE VALLEY FORMATION – MIOCENE	129
4.3.3.1 <i>Description</i>	130
4.3.3.2 <i>Interpretation</i>	131
4.3.5 THE GOSHU FORMATION – PLIOCENE TO LOWER PLEISTOCENE	134
4.3.5.1 <i>Description</i>	134
4.3.5.2 <i>Interpretation</i>	135
4.3.6 UNDIFFERENTIATED CENOZOIC SEDIMENTS	136
4.3.6.1 <i>Description</i>	136
4.3.6.2 <i>Interpretation</i>	137
4.3.7 QUATERNARY DEPOSITS	138

## **Chapter 5**

<b>The structural evolution of the Dariv and Shargyn basins</b>	<b>140</b>
5.1 Introduction	140
5.2 Cenozoic basin structure	141
5.2.1 EXTERNAL (BASIN BOUNDING) STRUCTURES	142
5.2.2 INTERNAL BASIN STRUCTURES	143
5.2.2.1 <i>The North and South Forebergs</i>	144
5.2.2.2 <i>The Southern Saddle Domain</i>	146
5.2.2.3 <i>The Central Ridge Section</i>	147
5.2.3 INTERPRETATION OF THE CENOZOIC BASIN STRUCTURE	149
5.2.3.1 <i>Stage 1 – Initiation</i>	150
5.2.3.2 <i>Stage 2 – Structural linkage</i>	152

5.2.3.3 Stage 3 – Recent – future	156
5.3 Mesozoic basin evolution	158
5.3.1 REGIONAL MESOZOIC TECTONICS	157
5.3.2 DISTRIBUTION OF MESOZOIC SEDIMENT	160
5.3.3 MESOZOIC STRUCTURES	161
5.3.4 SUMMERY	166
5.4 Synthesis of Cenozoic basin evolution incorporating sedimentary and structural data	167
5.5 The future	170
5.6 The Shargyn Basin	171
5.6.1 PREVIOUS WORK	171
5.6.2 DESCRIPTION	171
5.6.3 INTERPRETATION	173
5.6.3.1 <i>The Mesozoic Shargyn Basin</i>	173
5.6.3.2 <i>The Cenozoic Shargyn Basin</i>	173

## Chapter 6

<b>Conclusions and wider implications</b>	<b>176</b>
6.1 Introduction	176
6.2 Review of transpressional basin types	176
6.3 Mongolian Altai transpressional basins	180
6.4 Identification of transpressional basins in the rock record	182
6.5 Future work	185
6.6 Summary of major conclusions	187



# Index of Figures

## Chapter 1

After page

**Figure 1.1a** - Digital elevation model showing the distribution of central Asian mountain ranges. **1.1b** - Digital elevation model showing the Altai and Gobi Altai. 1

**Figure 1.2** - Oblique shuttle view looking north and showing Altai, western Gobi Altai and the large range flanking depocentres, the Valley of Lakes and the Junggar Basins. The three transpressional basins investigated in this study are shown. 3

## Chapter 2

**Figure 2.1** - Landsat TM montage of the Altai region showing national borders along with major towns, mountains and rivers mentioned in the text. Inset map is a digital elevation model showing the major topographic features of Asia. 9

**Figure 2.2** – Landsat TM montage of the greater Altai area, showing areas of uplift versus sedimentary basins (pale tones). 11

**Figure 2.3** - View down a U-shaped valley on the western flanks of Tsambagarav Uul (Fig. 2.1). 12

**Figure 2.4** - Interpreted TM Landsat montage showing major Cenozoic faults and known kinematics. Interpretation based on image analysis, ground truthing and historical seismicity. Loose-leaf copy in appendix 3. 13

**Figure 2.5** - Interpreted TM Landsat montage showing catchment areas, drainage divides and major rivers in the greater Altai area.

Inset map shows the upstream catchment areas for major river systems. Loose-leaf copy in appendix 3. 14

**Figure 2.6** - Interpreted TM Landsat montage showing major drainage divides and the distribution of major sedimentary basins. Five major types of sedimentary basin are distinguished. Loose-leaf copy in appendix 3. 14

**Figure 2.7** - Map showing distribution of intramontane basins and corresponding drainage systems. 15

**Figure 2.8a** – Major rockfall in the high Altai close to Tal Nuur. The apparent failure of the whole face suggests possible co-seismic triggering. **2.8b** - Debris flows in the northern Dariv Basin (Fig. 2.1). 15

**Figure 2.9** – Alluvial/fluvial fans and deltas of various forms are recognised within the Altai. **2.9a** – Tolbo Nuur lake in the central Altai, here large alluvial fans prograded into the lake from the actively uplifting flanking range. **2.9b** - The Khovd Delta in northern Har Us Nuur lake represents a major depocentre for sediment eroded from the Altai. **2.9c** – Delta forming on the southern banks of Har Us Nuur lake which stores sediment transported axially within the Dzereg Basin. **2.9d** – Small fluvial delta deposited in the Valley of Lakes by the only river to transport sediment from the flanking transpressional basins to the external depocentres. The small size of the delta reflects the limited volume of sediment that passes through Har Us Nuur lake. **2.9e** - Two major terminal fans that dry out due to downwards infiltration of water and surface evaporation in the southern peripheral basins. 16

**Figure 2.10** - Detailed image showing major structures, drainages and drainage divides within Sutai Uul. 17

<b>Figure 2.11</b> - Map showing the distribution of sedimentation within Altai mountain valleys and their drainage systems.	18
<b>Figure 2.12</b> – Photograph showing a tributary to the Khovd river incising through low relief, actively uplifting terrain.	18
<b>Figure 2.13</b> - Detailed image of Tsambagarav Uul, distinguishing discrete areas of active faulting and range uplift separated by areas of inactive degraded terrain and sediment accumulation.	19
<b>Figure 2.14</b> - View across region of degraded terrain in the central Altai showing sinuous ridges of exposed bedrock that are overlapped by low-angle fan deposits, and meandering stream that flows in broad valley.	19
<b>Figure 2.15</b> - Map showing distribution of range flanking transpressional basins and corresponding drainage systems.	21
<b>Figure 2.16</b> - Map showing distribution of shallow peripheral basins and corresponding drainage systems.	23
<b>Figure 2.17</b> - Detailed image showing the shallow Baruun Huuray peripheral basin south of the Altai. The image shows reactivated vs. unreactivated terrain.	23
<b>Figure 2.18</b> - Map showing distribution of external depocentres and corresponding drainage systems.	25
<b>Figure 2.19</b> - Detailed images showing the Dariv range (a) and the Jargalant range (b), the two most easterly ranges in the Altai.	32

## Chapter 3

**Figure 3.1** - Digital topographic map of western Mongolia and Altai region. Areas of Cenozoic sediment accumulation, including the Dzereg Basin are shown. Inset map shows regional fault patterns and areas of Cenozoic deformation in central Asia. 35

**Figure 3.2** - Topographic map of part of western Mongolia showing the Altai Mountains and the depression to the east, called the Valley of Lakes. 35

**Figure 3.3** - Space shuttle photograph of the southeastern Altai region (Photo #ST574-713-003) including Cenozoic flanking basins to the east and the Valley of Lakes. Major regional faults are shown. 37

**Figure 3.4** - MSS Landsat image and interpretation showing complex relationships between structure and sedimentation within the Dzereg Basin. Range bounding faults and thrust faults within the basin that deform Mesozoic-Cenozoic sediments are visible. 38

**Figure 3.5** - Geological map of the Dzereg Basin region showing basement rocks and previously mapped sedimentary units (after Zaitsev, 1978). 40

**Figure 3.6a** - View southwest from the northeast basin margin. In the foreground, deformed Mesozoic-Cenozoic basin sediments are eroded into small hills and cut by gullies. **3.6b** - View south along the northeast basin margin of tilted and folded Cretaceous and Oligocene-Miocene basin sediments. Prominent northeast-vergent anticlines are visible. 40

**Figure 3.7** - Detailed geological map of the NE side of the Dzereg basin. The geology is dominated by northeast vergent folds and thrust faults which deform Mesozoic-Cenozoic basin fill. 41

**Figure 3.8** - Detailed geological map of the SW Dzereg basin. The geology is dominated by a northeast vergent anticline which exposes Mesozoic-Cenozoic basin fill. 41

**Figure 3.9a** - Generalised stratigraphic sections for northeast and southwest study areas within the Dzereg Basin. Stratigraphy is subdivided into separate units which correlate with formation names taken from Devjatkin, (1981). Ages of each formation are interpreted from fossil evidence (Devjatkin, 1981). Directions of palaeocurrent flow as well as positions of detailed logs are shown. **3.9b** - Ternary plot showing bulk composition for the main units. 42

**Figure 3.10** - Detailed graphic logs 1 and 2 for the NE Dzereg. 42

**Figure 3.11a1 & a2** - View and interpretation of the major anticline on the northeast basin margin showing the angular unconformity between the lower Cretaceous Yellow Sandstone Unit and the Lower Red Bed Unit. **3.11b** - Large sheets of symmetrical wave ripples in facies AF. **3.11c** - The angular unconformity between the lower Cretaceous Lower Red Bed Unit and the Oligocene Oasis Unit (N47° 08' 306", E93° 03' 579"). **3.11d** - View of the Tan Conglomerate Unit showing a channel body (facies BF) **3.11e** - Cross-stratified sandstone and conglomerate (Facies BF) in the lower Tan Conglomerate Unit. 43

**Figure 3.12** - Detailed graphic logs 1-4 for the SW Dzereg Basin. 46

**Figure 3.13a** - Erosive contacts between facies BF and EF within the Tan Conglomerate Unit. Hammer for scale (length 30 cm). **3.13b** - Calcrete horizons within facies BF in the Tan Conglomerate Unit. Facies BF sandstone overlies an erosive contact. **3.13c** - Asymmetric anticline on the southwest basin margin. **3.13d1 & 2** - View and interpretation of the variation of folding along strike. 51

**Figure 3.14** - Detailed graphic logs 3-6 for the NE Dzereg basin. 52

**Figure 3.15** - Cross-sections to show the interpreted evolution of the Dzereg basin from the Jurassic to the present day. 60

## Chapter 4

**Figure 4.1** – Oblique shuttle view of the Altai region showing the Dzereg, Dariv and Shargyn basins. 69

**Figure 4.2** – Interpreted Kosmos satellite image showing the 8 study areas within the Dariv and Shargyn Basins. Major structures that uplift mountain ranges and bound active ridges within the basin are also shown. 69

**Figure 4.3** – Correlation panel showing generalised stratigraphic sections from the Dzereg, Dariv and Shargyn Basins, Section VIII, the Dariv Section is taken from Sjostrom, 2001. Inset map shows the location of sections. Formation names correspond to those of Devjatkin, 1981. Correlation is based on palaeontological data (listed in appendix 1), field mapping of formations and major changes in lithology. The direction of measured palaeocurrent is shown on sections and on 6 inset maps. Loose-leaf copy in appendix 3. 69

**Figure 4.4** – Aerial photograph and interpretation for areas 5 & 6 showing the location of the Shargyn Section (X), the Radio Mast Section (XI) and the relationship between the Jargalant Formation (Jj) and the Palaeozoic basement rocks (X). 71

**Figure 4.5** – Aerial photograph and interpretation for area 7 (Fig. 4.2). The location of the Dariv Section (VIII) and Sandstorm Section (IX) are shown, along with structures that uplift the ridges and deform the Mesozoic and Cenozoic basin fill. 71

**Figure 4.6a & b** - Photographs showing good exposures of the sandstone and pebble conglomerates of the central Jargalant Formation. **4.6c** - 14 cm diameter wood fragments found within the upper Jargalant Formation in area 5. **4.6d** - The gradational upper contact between the grey/yellow Jargalant Formation and the overlying red Dariv (a) Formation. **4.6e** - Photograph showing the Middle Jurassic Jargalant Formation (grey/green) thrust over Cretaceous red/blue beds. **4.6f** - The Jargalant Formation at the Dariv Section. 72

**Figure 4.7a** - View north across the Dariv (a) Formation red beds and the Jargalant Formation. The shallow saline lake in the centre of the Dariv Basin is visible in the distance. **4.7b** - View south across the Dariv (a) Formation showing one of two major caliche horizons visible on aerial photographs. 81

**Figure 4.8a** – Photograph showing conglomerates of the Ikkes Nuur Formation in the Green Valley Section. **4.8b** – Photograph showing dessication cracks in faces EF within the Ikkes Nuur Formation, Green Valley Section. 84

**Figure 4.9** – Aerial photograph and interpretation for the North Foreberg showing the different sections studied, the structures that uplift the ridge and locations mentioned in the text. 85

**Figure 4.10a** - Photograph showing the Ihkes Nuur Formation in the North Canyon Section of the North Foreberg. **4.10b** – Close up photograph showing the Ihkes Nuur Formation in the North Canyon Section. 85

**Figure 4.11a** – Log 17 from the Ihkes Nuur Formation in the North Canyon Section. Key to sedimentary logs is on following page. **4.11b** – Key to sedimentary logs. 85

**Figure 4.12** – Aerial photograph and interpretation of the Central Ridge in the Dariv Basin. Structures that uplift the ridge and the location of the Central Ridge Sections (north) and (south) are shown. 85

**Figure 4.13** – Log S1 from the upper Ihkes Nuur Formation in the Shargyn Section. 86

**Figure 4.14a** – View south down the Central Ridge Section (South) showing general exposure of the grey Gurven Ereen Formation sediments and the overlying Dzereg Formation. **4.14b** – soft sediment deformation in facies I, in the Gurven Ereen Formation, Central Ridge Section (South). **4.14c** – View north showing the exposures in the North Foreberg Section. **4.14d** – Climbing ripples in the Gurven Ereen Formation, East Ridge Section. 91

**Figure 4.15** – Log VI from the Central Ridge Section (south) showing the Gurven Ereen, Dzereg and Dariv (b) Formations. 91

**Figure 4.16** – Log 10 from the East Ridge Section of the North Foreberg. 94



<b>Figure 4.17</b> – Log S2 from the Gurven Ereen Formation in the Shargyn Section (Fig. 4.2).	97
<b>Figure 4.18a</b> – Soft sediment deformation in the Gurven Ereen Formation in the Shargyn Section. <b>4.18b</b> – View of well-laminated lacustrine sediments from the upper part of the Gurven Ereen Formation in the Shargyn Section. <b>4.18c</b> – Soft sediment deformation due to loading in the Gurven Ereen Formation in the Shargyn Section.	97
<b>Figure 4.19</b> – Log S3 from the upper Gurven Ereen Formation in the Shargyn Section.	97
<b>Figure 4.20a</b> – Facies LA and LB in the Central Ridge Section (south). <b>4.20b</b> – Facies LB low angle cross-stratification in delta front sediments. <b>4.20c</b> – View showing the facies association L. <b>4.20d</b> – Lacustrine sediments in the Central Ridge Section (north). <b>4.20e</b> – Exposure in the Central Ridge Section (north) showing structure within the ridge and lacustrine sediments.	107
<b>Figure 4.21a</b> – View south down the East Ridge Section, towards the Red Hill. <b>4.21b</b> – View north across the Base 1 Section showing the Dzereg Formation. <b>4.21c</b> – Very fine lamination from the Dzereg Formation in the Shargyn Section. <b>4.21d</b> – Climbing ripple lamination in a facies I sandstone bed in the Dzereg Formation in the Shargyn Section. <b>4.21e</b> – Bivalves from the Dzereg Formation in the Shargyn Section.	109
<b>Figure 4.22</b> – Log Base 1 from the Base 1 Section showing the Dariv (b) Formation.	109

<b>Figure 4.23</b> – Log S4 from the Dzereg Formation in the Shargyn Section.	111
<b>Figure 4.24</b> - Map and section through a theoretical delta to explain the distribution of facies within facies association L in the Dzereg Formation.	113
<b>Figure 4.25a</b> - View to the west of the Base 1 section showing the channelised conglomerate bodies (facies D) within yellow/brown siltstone beds (facies EF). <b>4.25b &amp; c</b> – Photographs and interpretation of a facies D channel body with a multi-stage fill. Internal erosion surfaces are picked out in red. Dariv (b) Formation, Base 1 Section.	120
<b>Figure 4.26</b> – Log 4 from the Base 1 section showing the Dariv (c) Formation.	120
<b>Figure 4.27a</b> – Large siltstone rip-up clast in the base of a conglomerate bed in the Base 1 Section. <b>4.27b</b> – View of an exceptionally thick multi-story channel (Facies D) within the Base 1 Section. <b>4.27c</b> – Close up of the multi-story channel shown in fig. 4.27a. <b>4.27d</b> – Gleyed roots preserved within a red siltstone bed in the Base 1 Section of the Dariv (b) Formation.	120
<b>Figure 4.28</b> – Log 8 from the East Ridge Section of the North Foreberg showing The Dariv (c) Formation.	121
<b>Figure 4.29</b> – Log 9 from the Dariv (b) Formation in the East Ridge Section.	121

<p><b>Figure 4.30a</b> - Laterally extensive pebble conglomerate channels in the East Ridge Section, North Foreberg area. <b>4.30b</b> – Basal contact of the Dariv (b) Formation with the Cretaceous red beds of the Dzereg Formation. <b>4.30c</b> – Channelised sandstone and conglomerate in the upper Dariv (b) Formation within the Eagle Valley. <b>4.30d</b> – Channelised conglomerate body just north of Dariv town. <b>4.30e</b> – Close up of channelised conglomerate bed in the Dariv (b) Formation. <b>4.30f</b> - Close-up of an erosive basal contact in the Dariv (b) Formation showing remnants of a planar laminated sandstone below.</p>	121
<p><b>Figure 4.31</b> - Log 11 and log 15 from the Dariv (b) Formation in the Eagle Valley Section.</p>	122
<p><b>Figure 4.32</b> – Log E1 from the Eagle Valley Section of the North Foreberg showing the Dariv (c) Formation.</p>	130
<p><b>Figure 4.33a</b> – View south across the Eagle Valley showing exposure of the Dariv (c) Formation. <b>4.33b</b> - Multi-coloured strata in the Dariv (c) Formation. <b>4.33c</b> - Multi-coloured strata in the Dariv (c) Formation, Eagle Valley Section. <b>4.33d</b> - Coarse sediment (facies AC) has loaded and deformed the underlying calcitic siltstone within the Dariv (c) Formation.</p>	130
<p><b>Figure 4.34</b> – Photograph showing typical section of the Goshu Formation (Pliocene to Lower Pleistocene).</p>	134
<p><b>Figure 4.35</b> – Log 13 from the Goshu Formation in the Eagle Valley Section.</p>	134
<p><b>Figure 4.36</b> – Log 14 from the Goshu Formation in the Eagle Valley Section.</p>	134

**Figure 4.37a** – Badland exposure of the undifferentiated Cenozoic strata. **4.37b** – Horizontal stratification in the undifferentiated Cenozoic deposits. **4.37c** – Carbonate cemented channel conglomerate in the upper part of the undifferentiated Cenozoic strata. 136

**Figure 4.38** – Map showing drainage patterns within the Dariv Basin, indicating catchment areas and areas of deposition. 138

**Figure 4.39a** – View south across the basin centre from the top of the East Ridge in the North Foreberg. **4.39b** - View northeast across the Eagle Valley in the North Foreberg area. 139

## Chapter 5

**Figure 5.1** - Digital elevation model showing western Mongolia and adjacent parts of China and Russia. Sedimentary basins are shown in pale tones. Major Cenozoic thrust and strike-slip faults are also shown. 140

**Figure 5.2** - Kosmos image covering the Dariv Basin. Showing the major structural domains within the basin along with basin bounding structures. The summit of Dariv Nuruu preserves part of a Paleogene peneplane recognised throughout the region (Devjatkin *et al.*, 1975). 141

**Figure 5.3** - Aerial photo of degraded thrust scarp along the western margin of the Dariv Basin. 141

**Figure 5.4** - Aerial photograph of the North Foreberg overlain by geological map showing the distribution of major stratigraphic units and structures referred to in the text. 144

<p><b>Figure 5.5a &amp; b</b> - View north across the North Canyon Section (Fig. 5.4) showing exposed basin stratigraphy in the North Foreberg. <b>5.5c</b> - View south down the East Ridge showing asymmetric east verging folds in the Cretaceous Dzereg (Dzerik) Formation. <b>5.5d</b> - View northwest up the East Ridge showing the major syncline to the west of the frontal thrust.</p>	145
<p><b>Figure 5.6a</b> - Photograph looking north showing the southern extent of the North Foreberg in the Base 1 locality. <b>5.6b</b> - Photograph showing the frontal, east directed, thrust that uplifts the Southern Foreberg.</p>	145
<p><b>Figure 5.7</b> - Aerial photograph of the South Foreberg overlain by geological map showing the distribution of stratigraphic units and geological structures.</p>	146
<p><b>Figure 5.8</b> - Cross-section through sediments exposed in the northern Shargyn Basin, adjacent to Tsetseg Dariv Uul.</p>	147
<p><b>Figure 5.9</b> - Aerial photograph mosaic and interpretation of the Central Ridge domain of the Dariv Basin.</p>	148
<p><b>Fig. 5.10a</b> - Aerial photograph showing part of the southern Central Ridge. Individual beds can be traced and crest lines act as proxies for bedding. <b>5.10b</b> - View south over the southern Central Ridge. The ridge contains folds with steep or sub-vertical axes. <b>5.10c</b> - View southeast across the southern Dariv Basin. Low relief uplifts extend southwest and southeast from the Central Ridge.</p>	148
<p><b>Figure 5.11</b> - Three stage evolutionary model for the Cenozoic Dariv Basin. EVA – Eagle Valley Anticline.</p>	150

<b>Figure 5.12</b> - Conjugate fault model for the Dariv Basin. This model predicts some of the features observed, however the real basin is complicated by the influence of the sinistral Shargyn Fault in the southeast.	152
<b>Figure 5.13</b> - Figure shows three stage, progressive evolution of the North Foreberg taking into account north-east directed shortening and clockwise rotation adjacent to the Tonhil dextral strike-slip fault.	152
<b>Figure 5.14</b> - A four stage interpretation for the evolution of the North Foreberg based on the actual geometry of structures seen in the field and the implications of the models shown in Figs. 5.12 & 5.13.	153
<b>Figure 5.15</b> - A block diagram showing the interpreted 3D structure of the present day Dariv Basin.	156
<b>Figure 5.16</b> - Model showing contractional foreland setting for the Mesozoic Dariv Basin from Sjostrom <i>et al.</i> (2001).	159
<b>Figure 5.17</b> - Geological map of the southern Altai showing previously mapped sedimentary units and basement rocks.	160
<b>Figure 5.18</b> - Cross-sections showing a compressional model for the evolution of the Dariv Basin.	163
<b>Figure 5.19</b> - Cross-sections showing an extensional model for Dariv Basin evolution.	165
<b>Figure 5.20</b> - Interpreted Landsat TM montage of the Shargyn Basin showing major thrust and strike-slip faults bounding the adjacent ranges.	171

**Figure 5.21a** - View across the Shargyn Basin showing the broad marsh area in the basin centre, and in the background, alluvial fans derived from adjacent ranges. **5.21b** - Active aeolian dune fields within the northwest Shargyn Basin. 172

**Figure 5.22a** - Simple model for block rotation in a conjugate strike-slip fault system. **5.22b** - Actual fault geometry of the Shargyn Basin. 174

## Chapter 6

**Figure 6.1a** – Model for transpressional basin development at a restraining bend. . Modified from Nilsen & Sylvester (1995). **6.1b** - Map showing the main structural features of the Pedroso-As Pontes-Moinonovo fault zone and the location of the As Pontes Basin. Modified from Sáez & Cabrera (2002) **6.1c** - Sketch map of the As Pontes Basin, Spain which corresponds well with model “a” above. Modified from Sáez & Cabrera (2002). 177

**Figure 6.2** – sketch cross-sections showing the orientation of basin bounding faults in ramp and full ramp basins and their extensional counterparts (Cobbold *et al.*, 2003). 178

**Figure 6.3** - Cross-sections through the transpressional basins with a full ramp geometry discussed in the text. **6.3a** - The >100 km wide Fergana Basin in the Kyrghyz Tien Shan (Cobbold *et al.*, 1994). **6.3b** - The Tadzhik depression containing the 30km wide Vaksh sub-basin (Thomas *et al.*, 1996). **6.3c**- The 20 km wide El Bolson Basin adjacent to the large Niriuhau foreland (modified from Diraison *et al.*, 1998). **6.3d** - The Dzereg Basin (Howard *et al.*, 2003; chapter 3). 178

**Figure 6.4a** - Sketch model showing a basin developing between basement blocks (grey) uplifted at the thrust termination zones of two parallel strike-slip faults. This basin is not subsiding but sediment is stored in the depression between the uplifted ranges. The basin is bound by active faults on one side only. **6.4b** - Cross-section interpretation for the early Cenozoic evolution of the Dariv Basin which is an actively deforming transpressional piggyback basin.

179



## Index of tables

**Table 3.1 and 4.2** – Facies chart for major stratigraphic units identified in the Dzereg, Dariv and Shargyn basins. Loose-leaf copy in appendix 3. 41/71

**Table 6.1** – Table comparing the first order characteristics of different continental basin types. 183

## Appendices

on page

**Appendix 1** – Table showing fauna and flora reported from Western Mongolia Mesozoic and Cenozoic strata. 192

**Appendix 2** – Tables useful for the field recognition of palaeosols. 193

**Appendix 3** (inside back cover) – Loose-leaf copies of figures 2.4, 2.5, 2.6, 4.3, and table 3.1/4.2. 194

# Chapter 1

## Introduction

Transpressional basins that develop in intracontinental, intraplate settings are one of the least understood of all major basin types. Although transpressional basins are found on many continents, previous work has mainly focussed on larger basins that develop at plate margins, leaving intraplate examples under-represented in the literature. The sedimentary fill of modern and ancient intraplate transpressional basins preserves a record of both local and regional orogenic activity in intraplate transpressional mountain ranges. Transpressional basins also host important resources such as water, hydrocarbons and placer mineral deposits. By studying the linked processes of tectonic uplift, erosion, sediment transport and deposition within active transpressional mountain ranges, the evolution of transpressional basins and their overall preservation potential can be better understood and new insights for identifying and interpreting ancient transpressional basins in the rock record can be gained. An improved understanding of transpressional basin evolution may also facilitate the efficient recognition and recovery of resources.

Although intracontinental transpressional basins occur on all continents, the largest number of actively forming examples occur adjacent to the Tien Shan, Altai and Gobi Altai ranges in central Asia (Fig. 1.1a) which are being uplifted in response to the Indo-Eurasian collision to the southwest. A dozen particularly good examples of transpressional basins occur along the eastern flanks of the Altai. The Altai is an actively uplifting transpressional mountain range in western Mongolia, China and Russia (Fig. 1.1a). The Mongolian Altai comprise a number of discrete, spaced ranges bound by thrust faults at restraining bends, fault step-

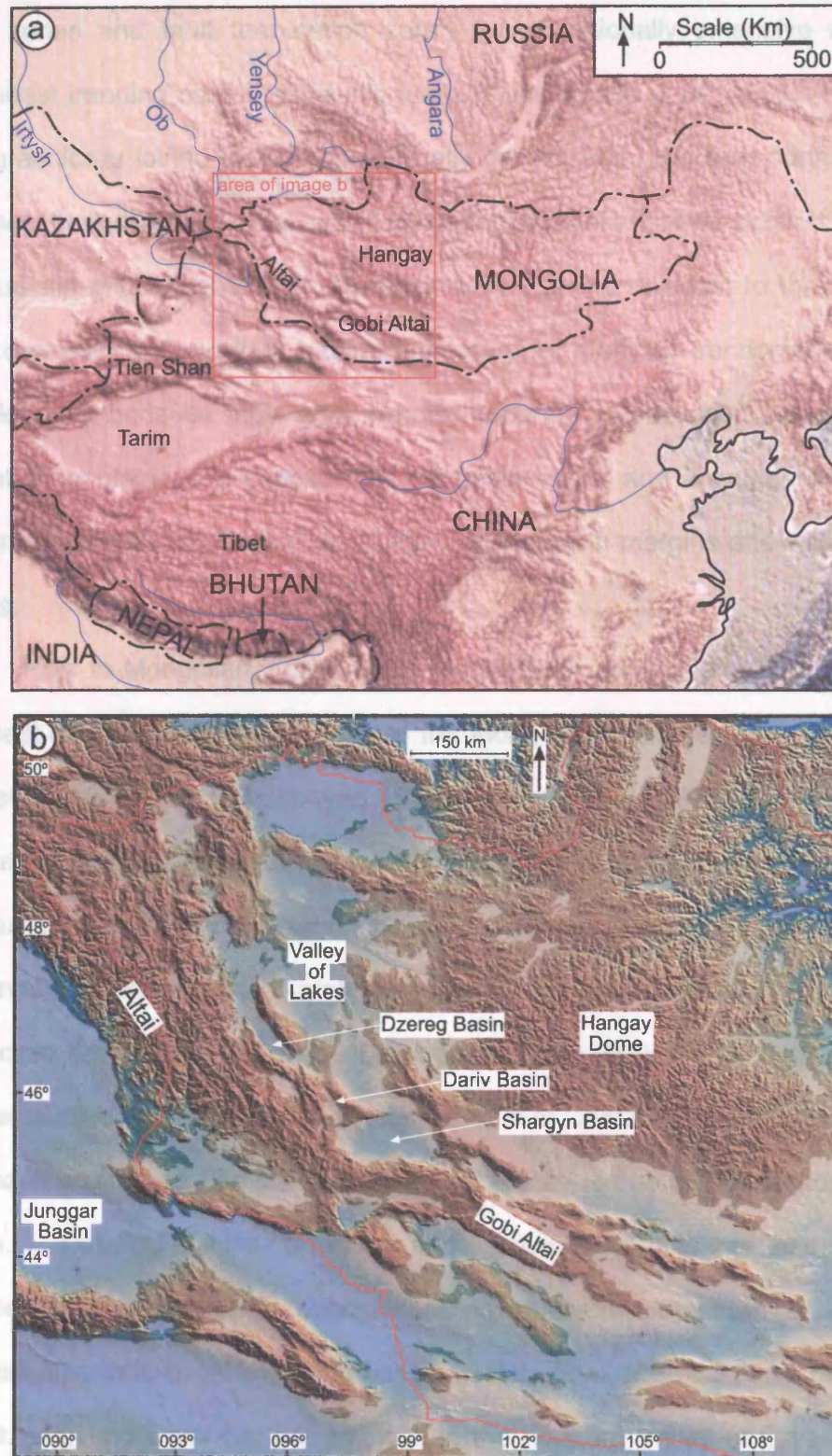


**Figure 1.1a** - Digital elevation model showing the distribution of central Asian mountain ranges. **1.1b** - Digital elevation model showing the Altai and Gobi Altai. The location of the Dzereg, Dariv and Shargyn Basins are shown.

over zones and fault termination zones along regionally extensive northwest-southeast trending dextral strike-slip faults (Cunningham *et al.*, 1996). The Altai is topographically joined to, but kinematically distinct from, the east-northeast-west-northwest trending Gobi Altai, which is uplifted and deformed by sinistral strike-slip, oblique-slip and thrust faults. Transpressional basins adjacent to the Mongolian Altai represent an excellent natural laboratory for studying transpressional basin development because they exist in both moderate to advanced stages of basin evolution, contain good exposure of the basin strata, and are undergoing active deformation by thrust faulting and folding at the basin margins and within internal zones.

Prior to Mongolian independence in 1991, Russian geologists documented the best-exposed sections in each of the Mongolian transpressional basins (e.g. Devjatkin, 1970, 1981; Khosbayer, 1973; Devjatkin *et al.*, 1975; Rasnitsyn, 1985). These studies established a regional stratigraphic framework constrained by numerous biostratigraphic data. However, a lack of detailed sedimentological observations hindered interpretation of depositional environments. Since 1991 the Mesozoic sedimentary fill of the Dzereg and Dariv Basins (Fig. 1.1b) has been further studied (e.g. Graham, 1997; Sjostrom *et al.*, 2001). These studies focus on Mesozoic strata and, like previous work, are limited to one or two sections in each basin. Detailed facies analysis and sedimentary logging has permitted interpretation of Mesozoic depositional environments. Sjostrom *et al.* (2001) discuss Mesozoic basin evolution based on data from three sections, one each in the Dzereg and Dariv basins, and one in the northern Valley of Lakes (Fig.1.1). They conclude that a foreland basin existed east of a palaeo-Altai mountain range during the Mesozoic. Cenozoic strata in the Dzereg, Dariv and Shargyn Basins remained unstudied by western geologists prior to this study. The structural

architecture of the Altai range has been extensively documented both in the field (e.g. Baljunnayam, 1993; Cunningham *et al.*, 1996a & b, 2002, 2003) and via analysis of satellite imagery (e.g. Schlupp, 1996), however, deformation within the transpressional basins has not previously been studied in detail.

This PhD project seeks to expand existing knowledge of transpressional basin evolution through detailed field investigations of three Mongolian transpressional basins. Two field seasons (summers of 2001 and 2002) were carried out in the adjacent Dzereg, Dariv and Shargyn basins, close to the intersection of the Altai and Gobi Altai ranges (Fig. 1.1b & 1.2). Each basin exists between actively uplifting ranges and is bound by basin-directed thrust faults.

On a local scale, this project aims to document the dynamic link between the uplift of basin-bounding ranges and the progressive accumulation of sediment eroded from these ranges in the adjacent basins. The field area provides the opportunity to document the middle stages of transpressional basin inversion which is manifested by uplift and deformation of older basin strata along the basin margins and within internal zones. Documenting the interplay between processes of faulting and folding, uplift, and erosion of the existing basin fill and evolving sediment distribution networks also enhances understanding of the facies architecture preserved in ancient transpressional basins. By documenting vertical and lateral changes in sedimentary facies, sediment composition, variations in observed palaeoflow indicators, palaeontological data, and the distribution and orientation of observed faults and folds, insights into the timing and location of initial range uplift in the Altai and the progressive evolution of the Mongolian Altai range can also be gained. This study demonstrates that the basins have a Mesozoic and Cenozoic history. It is therefore important to examine the possible influence an inherited fault network may have had on Cenozoic transpressional



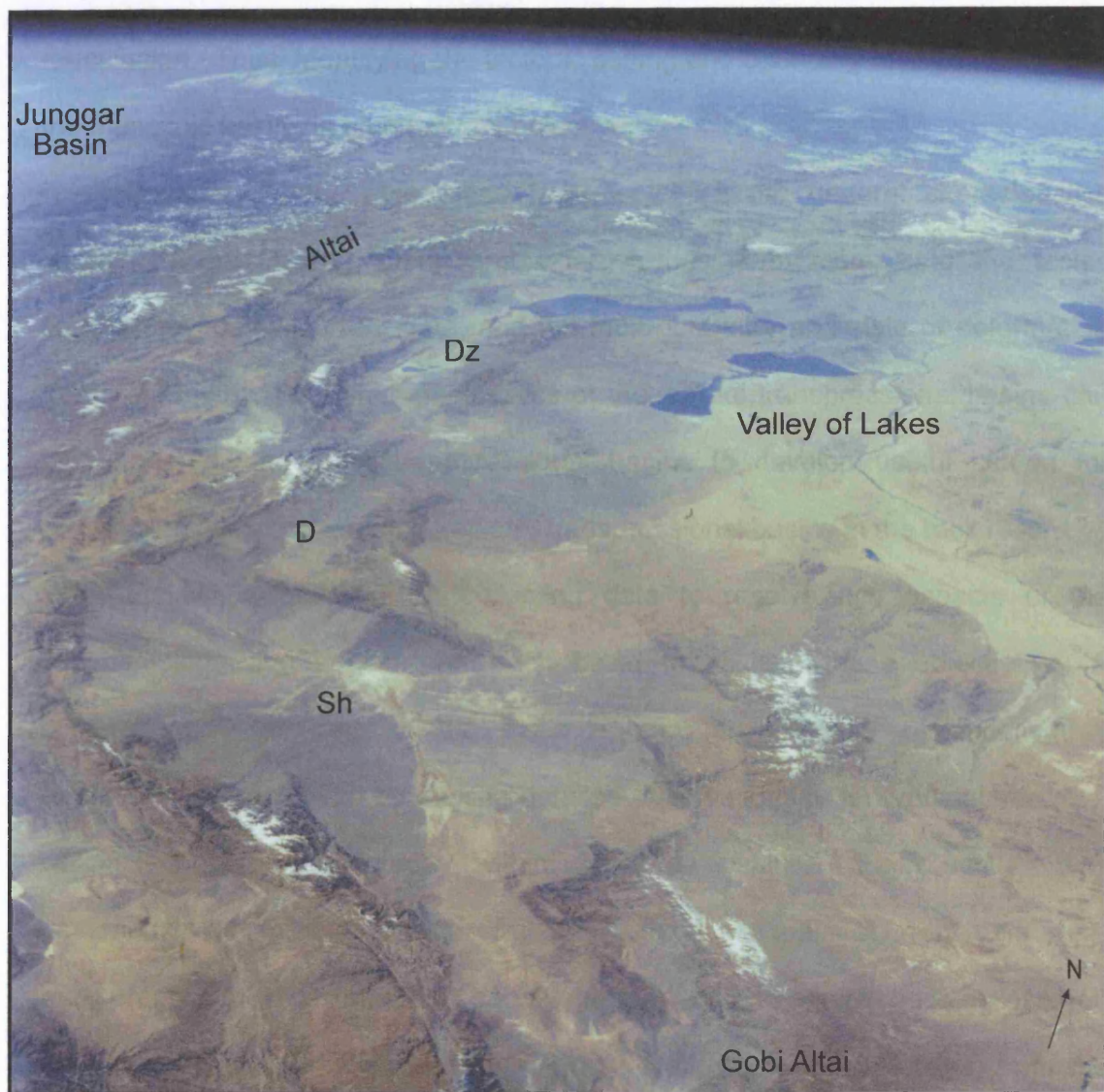


**Figure 1.2** - Oblique shuttle view looking north and showing Altai, western Gobi Altai and the large range flanking depocentres, the Valley of Lakes and the Junggar Basins. The three transpressional basins investigated in this study are shown. Sh - Shargyn Basin, D - Dariv Basin and DZ - Dzereg Basin. Each of these basins lies between discrete fault bounded ranges. Scale varies within photograph, the base width is approximately 300 km. Image courtesy of Earth Sciences and Image Analysis Laboratory, NASA Johnson Space Centre (<http://eol.jsc.nasa.gov>).

Basins. Lateral changes in facies and formation thickness were documented within and between the three basins by correlating between sections. Faults and folds that bound the basins and internally deform basin strata were identified on satellite imagery and ground truthed. Many faults are unexposed, but uplifted and eroded ridges and alluvial surfaces indicate their presence at depth. Observed and inferred faults and folds were combined with stratigraphic data to produce cross-sections through deformed basin sediments. Important areas undergoing intense

reactivation. Thus, identifying the tectonic setting and bounding fault geometries of the Mesozoic basins is an important objective.

Broader generic objectives are to establish the general characteristics shared by the Dzereg, Dariv and Shargyn basins by comparing the facies architecture, palaeocurrent data, and the fault geometry and style of deformation from each. Any general characteristics of these Altai transpressional basins can be compared with other transpressional basins to develop useful criteria for recognising intracontinental, intraplate, transpressional basins in the rock record.

Fieldwork focussed on collecting data to resolve key aspects of the sedimentology and structure of each basin to achieve these objectives. A comprehensive analysis of the three-dimensional geometry of sedimentary formations was achieved by making detailed observations in ten vertical sections, which record the stratigraphy within the three basins. Each section was documented on millimetre-scale stratigraphic logs and palaeocurrent data were measured from cross-stratified sandstone and conglomerate beds, preserved ripples, imbricated pebbles and tool marks. Data (and interpretations) from the detailed sections are supported by observations made at many other exposures within each basin. These data form the basis of a detailed facies analysis and environmental interpretation for the Mesozoic to recent evolution of the three Altai basins. Lateral changes in facies and formation thickness were documented within and between the three basins by correlating between sections. Faults and folds that bound the basins and internally deform basin strata were identified on satellite imagery and ground truthed. Many faults are unexposed, but uplifted and tilted ridges and alluvial surfaces indicate their presence at depth. Observed and inferred faults and folds were combined with stratigraphic data to produce cross-sections through deformed basin sediments. Important areas undergoing intense

intrabasinal deformation were mapped using Mongolian base maps and aerial photographs and, where appropriate, these have been reproduced in the thesis. Satellite imagery and aerial photography were utilised, both in the lab and in the field, to identify areas of exposure, trace structures and document modern drainage networks and the distribution of basin types in the Altai region.

## 1.2 The wider context for this project

This project represents part of an ongoing, multi-disciplined investigation into the geology and active tectonics of Mongolia by the Orogenic Processes Group at the University of Leicester. In particular, this project complements previous work on the structural architecture of the Altai and Gobi Altai (e.g. Cunningham *et al.*, 1996a & b, 2002, 2003). These earlier investigations have provided a structural framework for the Altai ranges making this investigation of the adjacent sedimentary basins a logical progression toward understanding the evolution of the Altai region.

## 1.3 Chapter synopsis

What follows is a brief distillation of the main objectives, methods and broad conclusions of each subsequent chapter.

Chapter 2 is an investigation into modern sediment transport and deposition within the greater Altai region based on analysis of TM Landsat imagery. The results of this analysis provide a regional context for detailed investigations of individual transpressional basins documented in subsequent chapters. A five-fold subdivision of linked drainage systems, each comprising a catchment area, river system and area of sediment deposition is identified within the Altai and Gobi Altai. Active faulting and range uplift have a major influence on these drainage systems.



The analysis reveals that, at present, little sediment is transported out of the Altai to the Valley of Lakes, which is the major external depocentre to the northeast of the study area (Fig. 1.1b). Instead, structurally compartmentalised transpressional basins along the eastern margin of the Altai and the northern margin of the Gobi Altai are the most volumetrically important depocentres for modern sediment eroded from the Mongolian Altai and westernmost Gobi Altai.

Chapter 3 describes the stratigraphic and structural evolution of the Dzereg Basin. The elongate Dzereg Basin is bound on each side by active ranges with flower structure internal geometries. Structural and stratigraphic field data were collected from deforming belts, uplifted by basinward-directed thrust faults. Mesozoic sediment is present within the basin but is not observed within adjacent ranges. This suggests that the Cenozoic basins are reactivated Mesozoic depocentres. The geometry of thrust faults and fault propagation anticlines within the basin, suggest the presence of inverted Mesozoic normal faults that initially formed during Jurassic-Cretaceous extensional (possibly transtensional) rifting. Cenozoic transpressional reactivation began in the Oligocene, and the Cenozoic sediment record is dominated by coarsening upward alluvial fans derived from adjacent ranges. Deformation, uplift and erosion of existing basin fill occurs coincidently with deposition of modern sediment closer to the basin centre. This dynamic interplay between deformation, erosion and sedimentation characterises transpressional basin evolution, and produces a complex facies architecture.

Chapter 4 concerns the Mesozoic-Cenozoic stratigraphy of the Dariv and Shargyn basins. The Dariv Basin contains extensive exposures of its sedimentary fill. Seven detailed vertical sections and numerous other exposures were documented, and palaeocurrent data recorded. A single vertical section in the north-eastern Shargyn Basin was also investigated. These sections are

correlated, and when combined with other stratigraphic data, provide the basis for a detailed palaeoenvironmental reconstruction of the Dariv Basin from the Jurassic to the present day. The Mesozoic sediment forms an asymmetric wedge, thickening toward the west, which fines upward. Jurassic sediment was deposited in alluvial and fluvial fans that flanked an axial river system, Cretaceous sediment was deposited in a long-lived lake which developed on a broad floodplain. The Cenozoic fill is significantly thinner and initially dominated by a fining upward floodplain succession overlain by a coarsening succession recording the progradation of alluvial fans, derived from the flanking ranges, into the basin. The Cenozoic sediment records the progressive evolution of catchment areas and river systems within the evolving basin bounding ranges.

In Chapter 5 the structural evolution of the Dariv and Shargyn basins is discussed. The Dariv and Shargyn basins are bound by active thrust and strike-slip faults. Movement on these faults has resulted in widespread contractional deformation of the sedimentary fill, both within the basin and along its margins. The surface expression of deformation varies from large uplifted thrust ridges, containing widespread exposure of the deeper basin fill, to low domes or ridges that offset alluvial fan surfaces. It is shown that Cenozoic structures within the Dariv Basin form a rhomboid of active deformation related to ongoing uplift of the adjacent Sutai Uul restraining bend. An inverted Mesozoic normal fault is interpreted in the centre of the basin which, combined with the marked asymmetry of the Mesozoic basin fill, suggests that the Dariv Basin represents the southward extension of the extensional (possibly transtensional) Mesozoic rift basin documented further north in the Dzereg Basin.

The Shargyn Basin lies between regional conjugate strike-slip faults and its basin centre is the lowest point in western Mongolia. The Shargyn Basin fill is

comparable to the Dariv and Dzereg basins and it is suggested that the Shargyn Basin has undergone subsidence linked to block rotation during the Cenozoic. This is unlike the Dariv and Dzereg basins where sediment was trapped between the uplifting ranges in the absence of significant Cenozoic subsidence.

In Chapter 6 the broader implications of this PhD project for understanding transpressional basins in general are discussed. A review of intraplate transpressional basins in the literature reveals four broad types of transpressional basins. This subdivision is based on the geometry of bounding faults, and includes basins formed by flexural subsidence at restraining bends, ramp basins bound on each side by basinward-directed thrust faults, transpressional piggyback basins, and transrotational basins. Furthermore, a continuum exists from strike-slip basins forming in strike-slip dominated deforming belts to thrust dominated foreland basin settings with minor strike-slip motion. The Mongolian basins investigated in this study represent three of these major basin types. Flexural basins forming adjacent to restraining bends were not documented during this project. The development of three adjacent basins with different bounding fault geometries in the same regional tectonic setting underscores the potential problems facing those wishing to identify transpressional basins in the rock record. A comparison with other basin types reveals that to identify an ancient transpressional basin in the rock record, a multi-disciplined investigation of the basin stratigraphy, internal structure and fault kinematics must be combined with knowledge of the regional tectonic setting.

## Chapter 2

# A TM Landsat study into modern sediment transport and deposition within the greater Altai region

## 2.1 Introduction

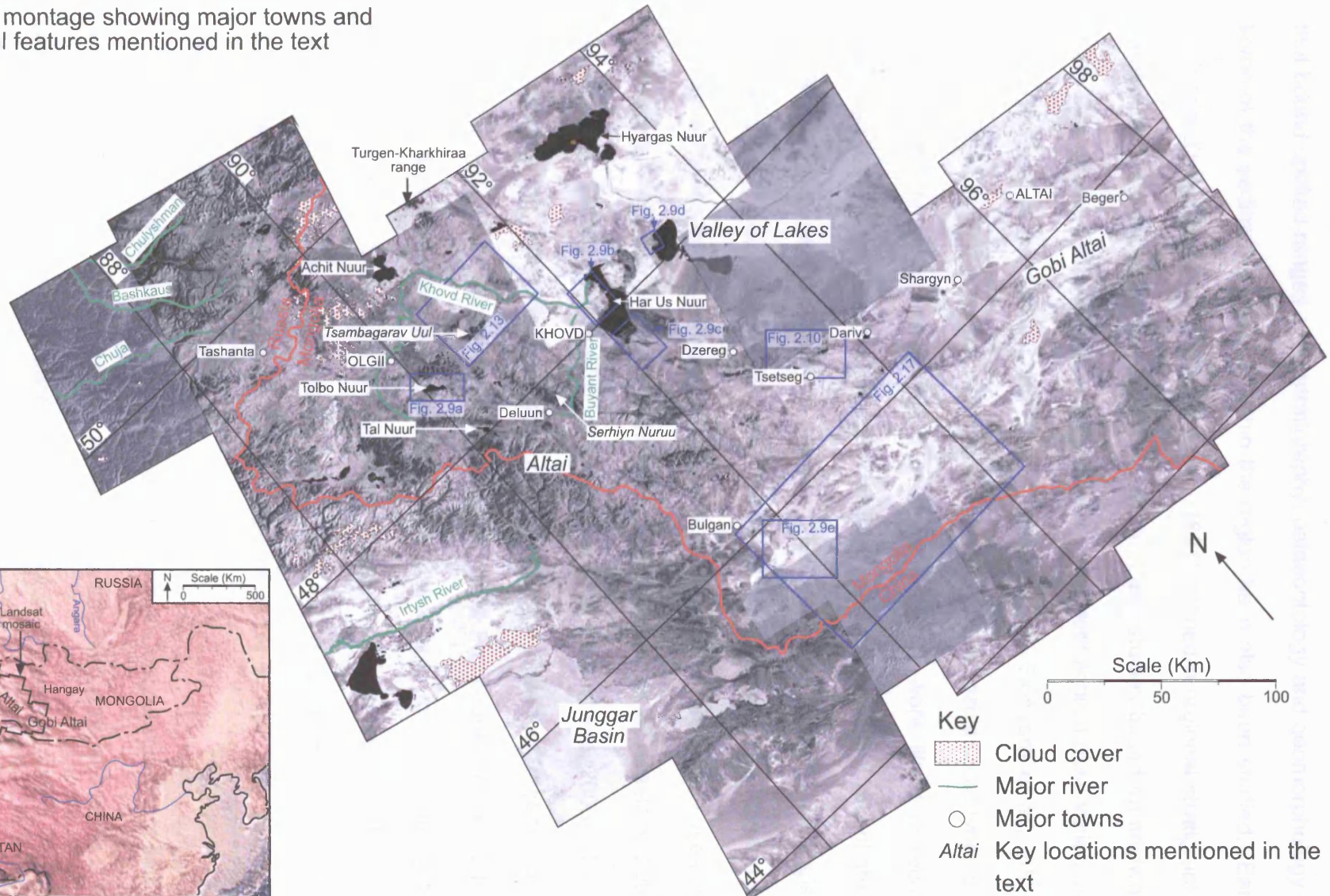
The Altai and Gobi Altai are tectonically active Cenozoic mountain ranges. The Altai lies in China, western Mongolia, and extends north-westwards into Russia (Fig. 2.1). The Gobi Altai trends east-west through southern Mongolia (Fig. 2.1). The ranges are structurally linked and have been actively uplifted since the Oligocene, probably as a response to the far-field effects of the Indo-Eurasia collision 2500 km to the southwest (Tapponnier & Molnar, 1979; Cunningham *et al.*, 2003).

Investigations into the geology and geomorphology of the Altai and Gobi Altai prior to 1991 were mainly restricted to Russian and Mongolian workers (e.g. Shuvalov, 1969; Devjatkin *et al.*, 1975; Khosbayer, 1973; Devjatkin, 1981; Togtoh & Baatarhuyag, 1991). However, since Mongolia opened its borders, western scientists have worked throughout the region. Many workers have focussed on the structural architecture of the Altai and Gobi Altai, using either satellite imagery or field observations, or both (e.g. Tapponnier & Molnar, 1979; Cunningham *et al.*, 1996a & b, 2002, 2003; Bayasgalan 1999a, b). These studies have documented the complex interlinked network of dextral strike-slip, oblique-slip and thrust faults

---

**Figure 2.1** (following page) - Landsat TM montage of the Altai region showing national borders along with major towns, mountains and rivers mentioned in the text. The locations of figs. 2.9, 2.10, 2.13 and 2.17 are shown. Inset map is a digital elevation model showing the major topographic features of Asia. The study area is highlighted by the black box, which encompasses the Altai and western Gobi Altai.

A map of the Gobi Desert region in Central Asia. The map shows the Gobi Altai, Hangay, and Tien Shan mountain ranges, and the Tarim and Junggar basins. The map includes labels for Russia, Kazakhstan, Mongolia, China, India, Nepal, and Bhutan. A scale bar indicates 0 to 500 km, and a north arrow is present.



that bound uplifted ranges. The stratigraphy, palaeontology and geomorphology of some of the sedimentary basins within the region have also been studied. Early work (e.g. Devjatkin *et al.*, 1970; Devjatkin, 1981) defined a regional stratigraphic framework constrained by abundant fossil finds. Later studies based on fieldwork in the Dzereg and Dariv Basins include detailed sedimentological observation and facies analysis of Mesozoic strata (e.g. Graham, 1997; Sjostrom *et al.*, 2001). Sjostrom *et al.* (2001) introduces discussion of potential Mesozoic basin types and conclude that Mesozoic sediments in western Mongolia were likely to record deposition in a flexural foreland basin. This PhD represents the first recent study of Cenozoic sediment in the Altai region. Geomorphologists and glaciologists working in the area have particularly focussed on understanding Quaternary climatic variations based primarily on fieldwork in the northern Valley of Lakes and northeastern Altai ranges (e.g. Lehmkhul, 1998; Lehmkhul & Haselein, 2000; Grunert *et al.*, 2000; Komatsu *et al.*, 2001; Fedeneva & Dergacheva, 2003). These geomorphological investigations have documented the timing of recent glacial cycles as discussed below. Chlachula (2001) and Prokopenko *et al.* (2001) present studies based on fieldwork in the lake Baikal area to the northeast but include regional interpretations of Quaternary climate that cover western Mongolia. No previous study has incorporated image analysis to document the regional distribution of drainage networks and catchment areas in the Altai, and their relationship to active faulting and block uplift.

This chapter aims to provide an understanding of Cenozoic sediment source areas and their links to active depocentres both within, and adjacent to the Altai, and to document links between active faulting, erosion and sedimentation. A major question is how modern sedimentation is distributed throughout the region from intramontane to completely external depocentres. The results of the analysis

provide a regional context for detailed investigations of individual Cenozoic basins presented in subsequent chapters. This study is largely based on interpretation of TM Landsat imagery and some ground truthing undertaken during geological fieldwork in Mongolia during the summers of 2001 and 2002.

## 2.2 Method

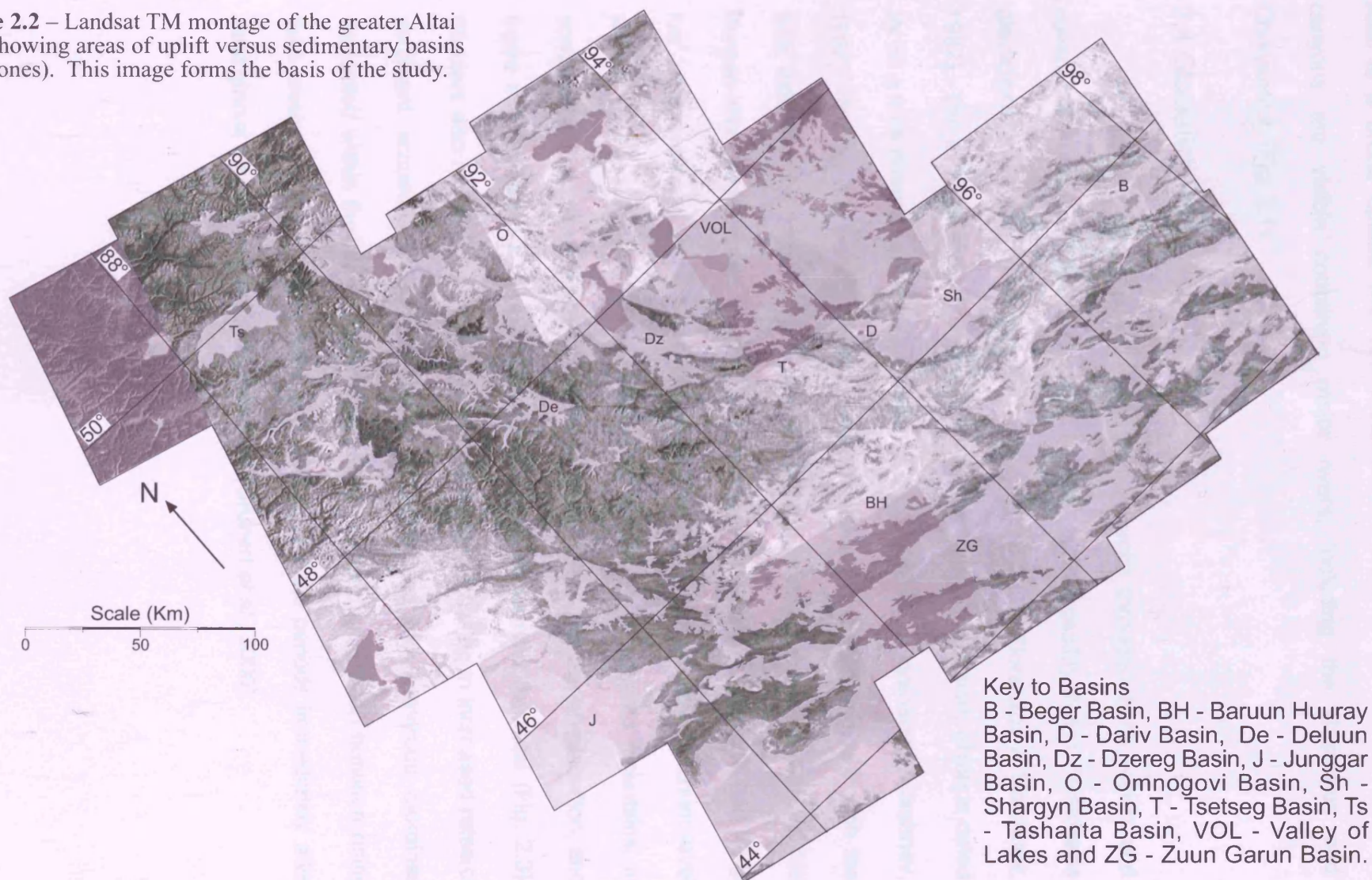
A montage of twenty-three Landsat TM images, covering approximately 150,000 km<sup>2</sup> of the Altai and Gobi Altai ranges, was created using Research Systems ENVI V.3.6 software (Fig. 2.2). Band 5 is shown because it provides the brightest response for most geological materials. Various features were identified and mapped, including types of basins, drainage networks, catchment divides, areas of active sediment deposition, faults, lakes and marsh areas. The results are presented as a series of maps and key geomorphological features, and their tectonic implications, are discussed.

## 2.3 Geomorphology of the Altai and western Gobi Altai region

Figure 2.2 distinguishes areas of uplift from sedimentary basins in the Altai region. The topographically linked Altai and Gobi Altai mountain belts stretch through the centre of the image, bound on each side by broad depressions. The Altai trends northwest-southeast and highest elevations are found in the west, where a continuous high range with many glacier-clad peaks forms the border between Mongolia and China. The eastern (Mongolian) Altai comprises discrete uplifted blocks separated by areas of lower topography containing major river systems, e.g. the Buyant river (Fig. 2.1). The Gobi Altai is a major geomorphic feature that extends eastwards for 600 km, although individual ranges have lower relief than those in the Altai (Fig. 2.1). In the northwest of the image, the Russian



**Figure 2.2** – Landsat TM montage of the greater Altai area, showing areas of uplift versus sedimentary basins (pale tones). This image forms the basis of the study.





Altai is a broad upland with few intramontane depressions. However, deep canyons are visible containing major rivers, including the Bashkaus and Chulyshman (Fig. 2.1).

## 2.4 Glaciation in the Altai

Permanent ice cover exists on high summits throughout the region and covers a total area of 328 km<sup>2</sup> (Lehmkuhl, 1998). Two (possibly three) Pleistocene glaciations are documented in the Altai (Devjatkin, 1981; Florensov & Korzhnev, 1982). The last glacial maximum (LGM) was the Sartan Glaciation, which is dated as  $32 \pm 6$  ka (thermoluminescence) and  $25.3 \pm 0.6$  ka (<sup>14</sup>C; Florensov & Korzhnev, 1982). During this period the Altai was extensively glaciated and, although the total extent of ice in the region has not been quantified, extensive work in the Turgen-Kharkhiraa mountains (Fig. 2.1) indicates that this range alone had 1300 km<sup>2</sup> permanent ice at the LGM (Lehmkuhl, 1998). The modern equilibrium level altitude (ELA) is approx 3405 – 3480 m in the Turgen-Kharkhiraa mountains, in comparison to a calculated 2900 – 3000 m at the LGM. The Sartan glaciation, and those that preceded it, eroded U-shaped valleys throughout the Altai (Fig. 2.3). Glaciers also mobilised a large amount of sediment, resulting in increased rates of sediment accumulation in the Valley of Lakes and the numerous moraines deposited within the range (Lehmkuhl, 1998). A good correlation between rising lake levels, especially those east of the Altai, and the periods immediately after past glacial maxima has been documented (Grunert *et al.*, 2000).

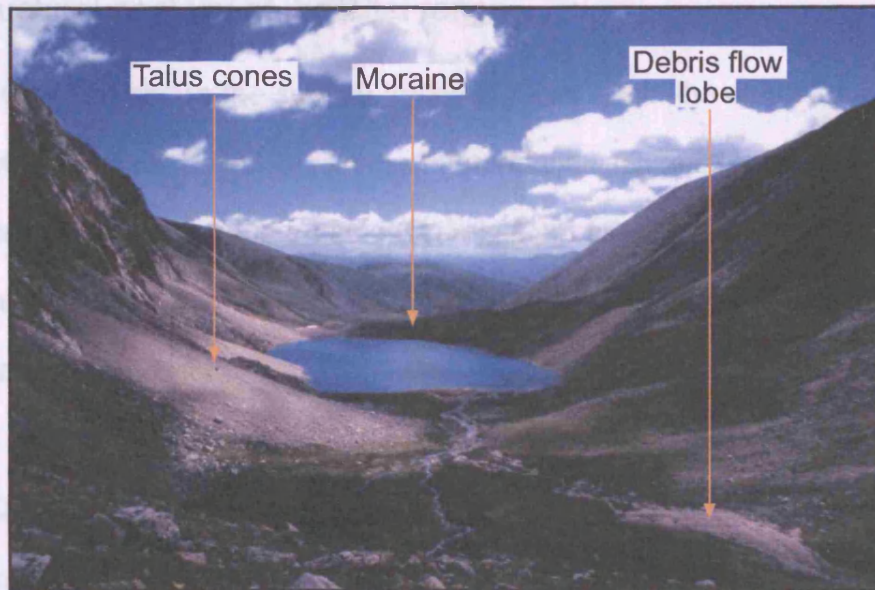


**Figure 2.3** - View down a U-shaped valley on the western flanks of Tsambagarav Uul (Fig. 2.1). Photographer is standing at the toe of the modern glacier. Note the remobilisation of moraine sediment as debris flows. Moraines represent a major sediment source.

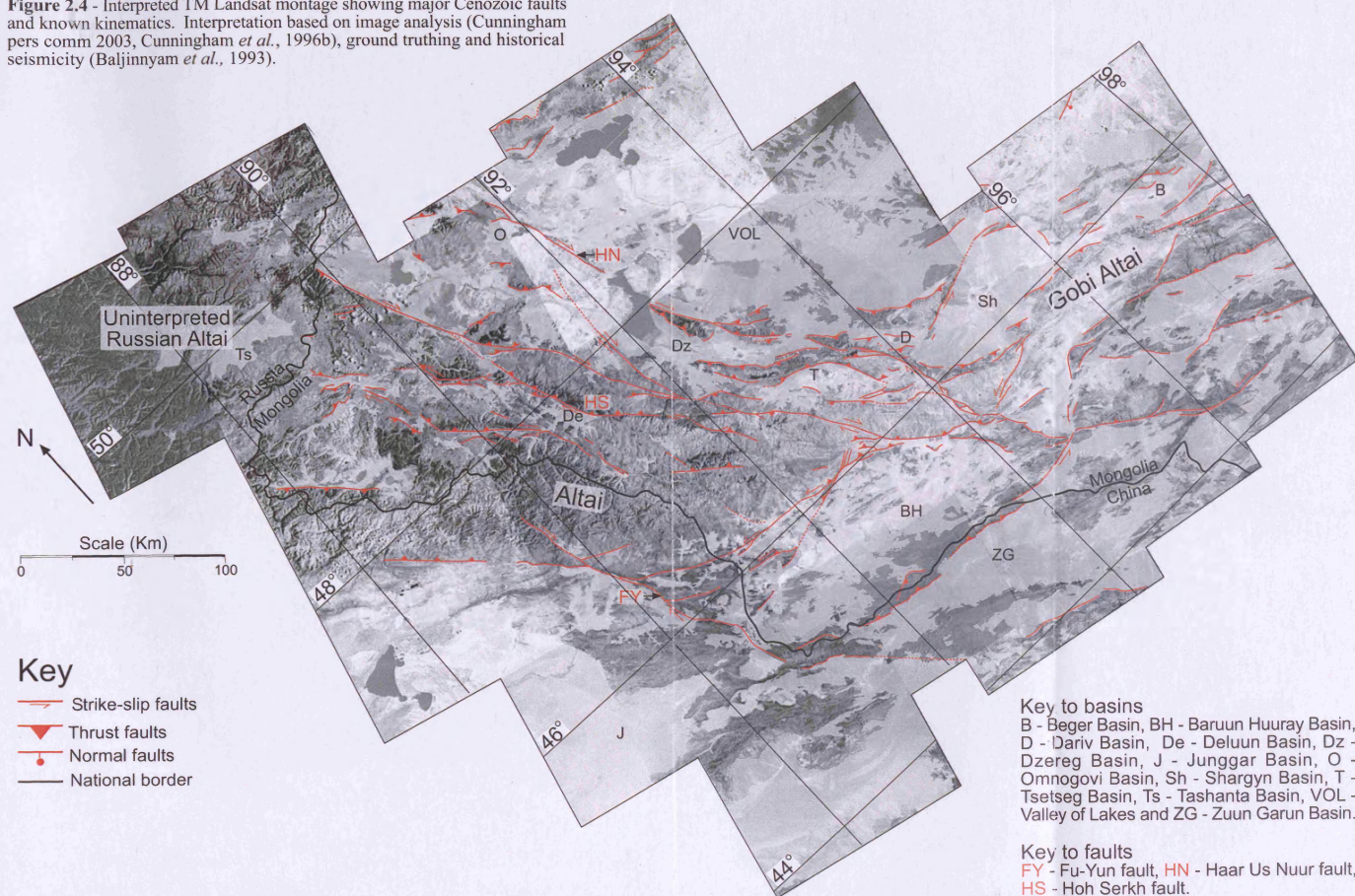
geomorphological spectra (Balinyam *et al.*, 1993; Cunningham *et al.*, 1996a, 2005). Figure 2.4 also shows that, whereas the Altai and Gobi Altai may be topographically linked, they are tectonically separate. Cenozoic construction of the Mongolian Altai and Gobi Altai has occurred by thrusting and oblique-slip faulting at strike-slip termination zones, fault step-over zones and other transpressional fault settings (Cunningham *et al.*, 2005). In the east-west trending Gobi Altai, several major east-west-trending strike-slip faults are found (Balinyam *et al.*, 1993). In the Altai, the major strike-slip faults within the range trend northwest-southeast and are dextral (Balinyam *et al.*, 1993). Regional fault trends in the Altai follow a first order basement anisotropy resulting from the accretion of Palaeozoic terranes to the Tuva-Mongol block along northwest-southeast oriented sutures (Sengör *et al.*, 1993). These faults have uplifted discrete, spaced ranges with thrust faults at their margins. Most active ranges are asymmetric and are separated by sedimentary basins.

## 2.5 Structural geology of the Altai range

Figure 2.4 shows the surface traces of faults within the study area and their sense of movement based on image interpretation (Cunningham, pers. comm., 2004), and extensive ground truthing (Cunningham *et al.*, 1996a & b, 2002, 2003). Only faults with known Cenozoic movements are shown. Most are in the Mongolian Altai and not the Chinese Altai where Cenozoic displacements are not obvious on the imagery (Fig. 2.4). The Chinese Altai contains west-directed thrust faults (Qu & Zhang, 1994) and it is possible that the mountainous topography of the Chinese Altai is a relict of Palaeozoic-Mesozoic mountain building with only limited Cenozoic reactivation. Many faults in the Mongolian Altai are active based on records of historical seismicity, documentation of Quaternary scarps, and other geomorphological criteria (Baljinnyam *et al.*, 1993; Cunningham *et al.*, 1996a, 2003). Figure 2.4 also shows that, whereas the Altai and Gobi Altai may be topographically linked, they are kinematically separate. Cenozoic construction of the Mongolian Altai and Gobi Altai has occurred by thrusting and oblique-slip faulting at strike-slip termination zones, fault step-over zones and other transpressional fault settings (Cunningham *et al.*, 2003). In the east-west trending Gobi Altai, several major east-west sinistral strike-slip faults are found (Baljinnyam *et al.*, 1993). In the Altai, the major strike-slip faults within the range trend northwest-southeast and are dextral (Baljinnyam *et al.*, 1993). Regional fault trends in the Altai follow a first order basement anisotropy resulting from the accretion of Palaeozoic terranes to the Tuva-Mongol block along northwest-southeast oriented sutures (Şengör *et al.*, 1993). These faults have uplifted discrete, spaced ranges with thrust faults at their margins. Most active ranges are asymmetric and are separated by sedimentary basins.



**Figure 2.4** - Interpreted TM Landsat montage showing major Cenozoic faults and known kinematics. Interpretation based on image analysis (Cunningham pers comm 2003, Cunningham *et al.*, 1996b), ground truthing and historical seismicity (Baljinnyam *et al.*, 1993).



The tectonic geomorphology of the Russian Altai is poorly resolved on the imagery presented here and faults are difficult to identify. However, Cenozoic thrust, strike-slip and localised extensional faulting is documented within different areas of the Russian Altai (Dehandschutter *et al.*, 2002; Thomas *et al.*, 2002).

## 2.6 Drainage systems in the Altai

### 2.6.1 Introduction

Many factors may affect the evolution of mountain range geomorphology and these factors may vary across a region. Controls may include active uplift, the distribution and style of faulting, bedrock geology, local climatic variations and vegetative cover (Ahnert, 1998, Summerfield, 1991). Within the Altai, five types of drainage system are distinguished. Each type consists of a catchment area, drainage network and area of sediment storage. Each drainage system links with another as sediment travels downslope and, therefore, systems are not isolated. Instead, each system represents a dynamic response to both internal and external factors on a local and regional scale. The distribution of major catchment divides and rivers within the Altai is shown on figure 2.5. The distribution of different basin types is shown in figure 2.6. The five types of drainage system identified are named after their associated depocentres. They are (1) intramontane basins, (2) depocentres within mountain river valleys, (3) shallow peripheral basins, (4) range flanking transpressional basins and (5) fully external depocentres. In the following section; the characteristic features of the five types of drainage system are individually described and interpreted. This is followed by discussion of drainage system interactions and regional tectonic implications.

**Figure 2.5** - Interpreted TM Landsat montage showing catchment areas, drainage divides and major rivers in the greater Altai area. The location of Figs. 2.10, 2.13 and 2.17 are also shown. Inset map shows the upstream catchment areas for major river systems.

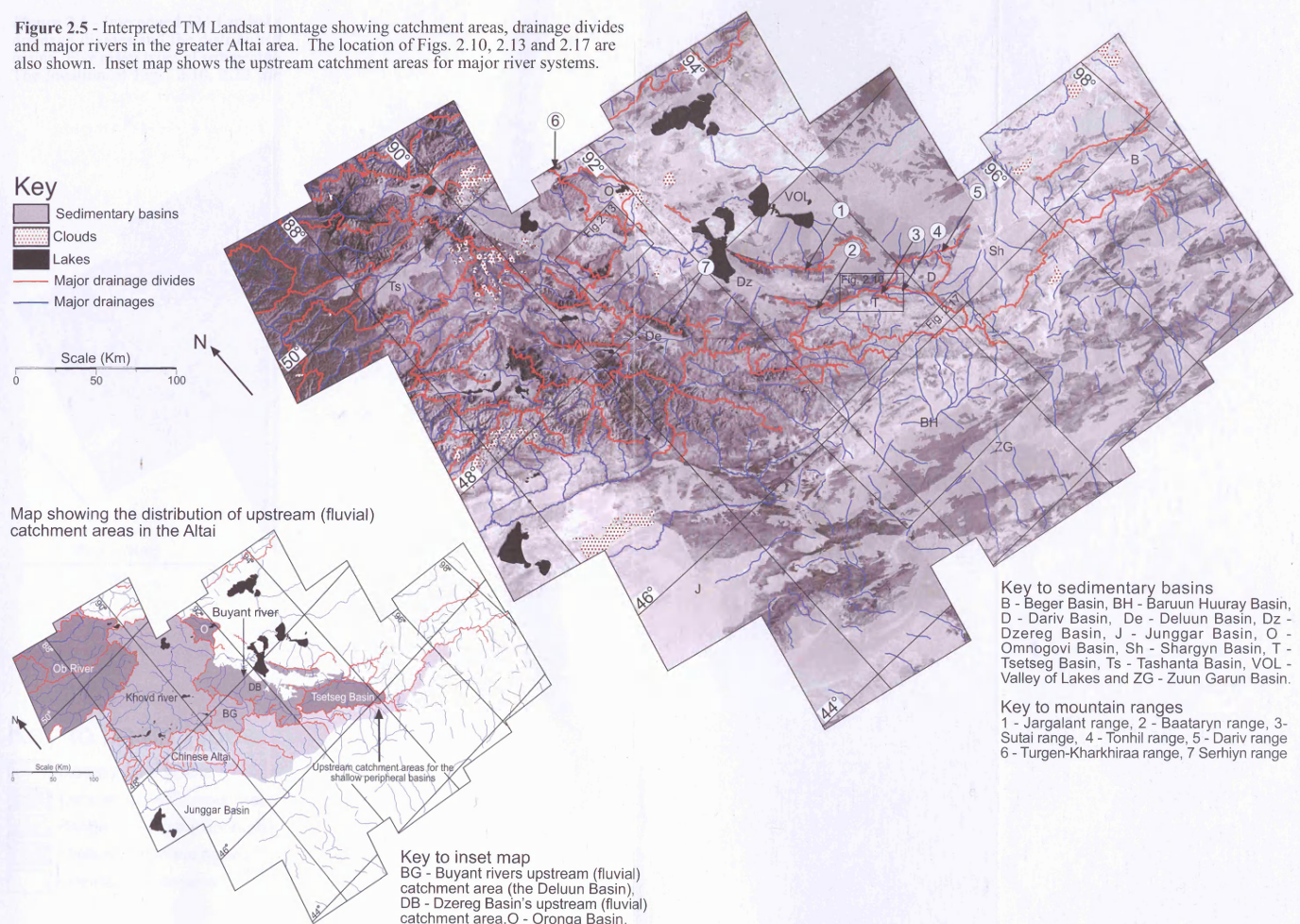
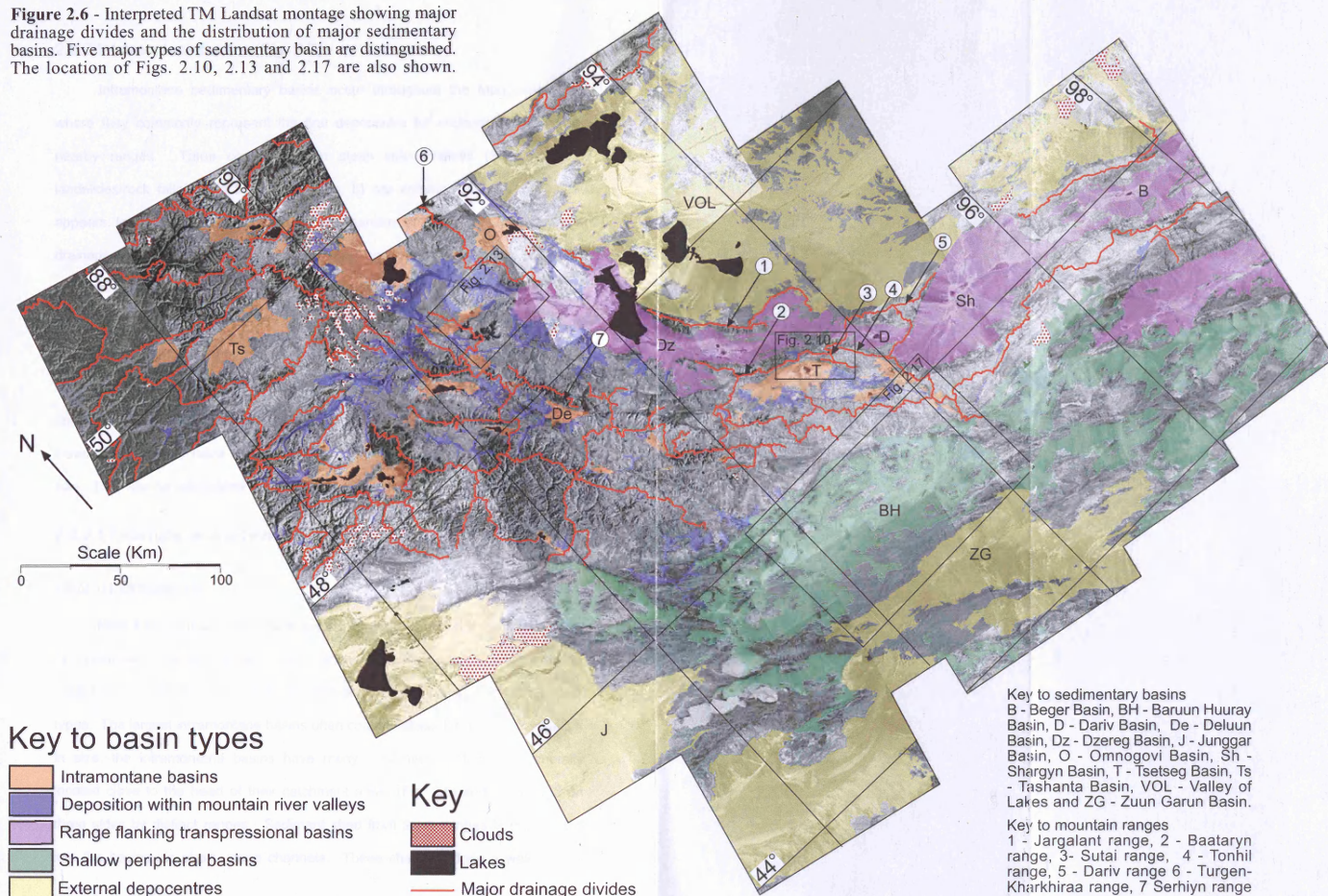




**Figure 2.6** - Interpreted TM Landsat montage showing major drainage divides and the distribution of major sedimentary basins. Five major types of sedimentary basin are distinguished. The location of Figs. 2.10, 2.13 and 2.17 are also shown.



## 2.6.2 Intramontane basins (Fig. 2.7)

Intramontane sedimentary basins occur throughout the Mongolian Altai, where they commonly represent the first depocentre for sediment eroded from nearby ranges. Talus cones form in steep sided valleys (Fig. 2.3) and landslides/rock falls/debris flows (Fig. 2.8a, b) are common. Mass movement appears to be an important transport mechanism bringing sediment into the drainage network and some landslides may have been seismically triggered. Moraine deposits throughout the glaciated high Altai also provide an important sediment source. Precipitation is highest on peaks greater than 3000 m which receive more than 300 mm/yr of rain and, rarely, up to 400 mm/yr in the northwest Altai (Arakawa, 1969; Lehmkuhl, 1998). In contrast, the basins receive less rainfall, <150 mm/yr (Arakawa, 1969; Lehmkuhl, 1998). Of all basin types, intramontane basins have the greatest variability in surface area and catchment size. They can be subdivided into externally and internally drained types.

### 2.6.2.1 Externally drained intramontane basins

#### 2.6.2.1.1 DESCRIPTION

Most intramontane basins are externally drained and are concentrated in the northwest of the Altai range. Basins range in size from approximately 4 km<sup>2</sup> to 1050 km<sup>2</sup> (average 125 km<sup>2</sup>), which is relatively small compared to the other basin types. The largest intramontane basins often contain lakes. Despite their variation in size, the intramontane basins have many similarities. They are generally located close to the head of their catchment areas (Fig. 2.6) and are bound on three sides by distinct ranges. Sediment shed from these ranges is transported into the basins via short, steep channels. These channels drain a well-defined



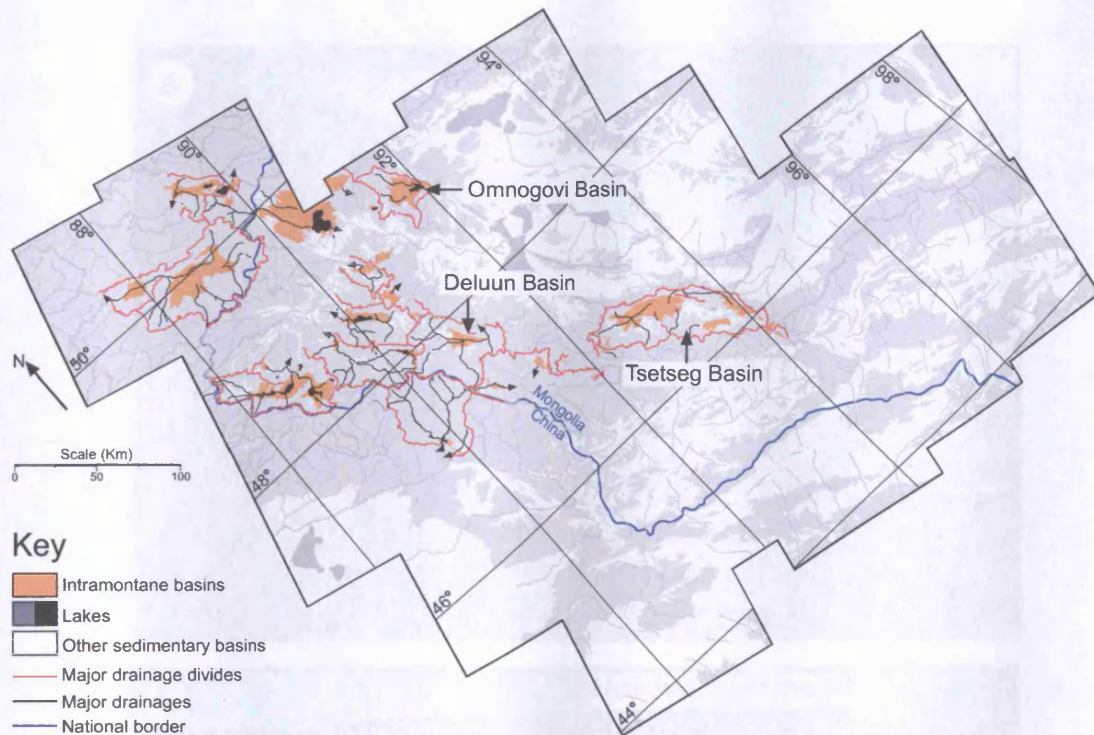


**Figure 2.7** - Map showing distribution of intramontane basins and corresponding drainage systems.

# **SPECIAL NOTE**

**ITEM SCANNED AS SUPPLIED  
PAGINATION IS AS SEEN**

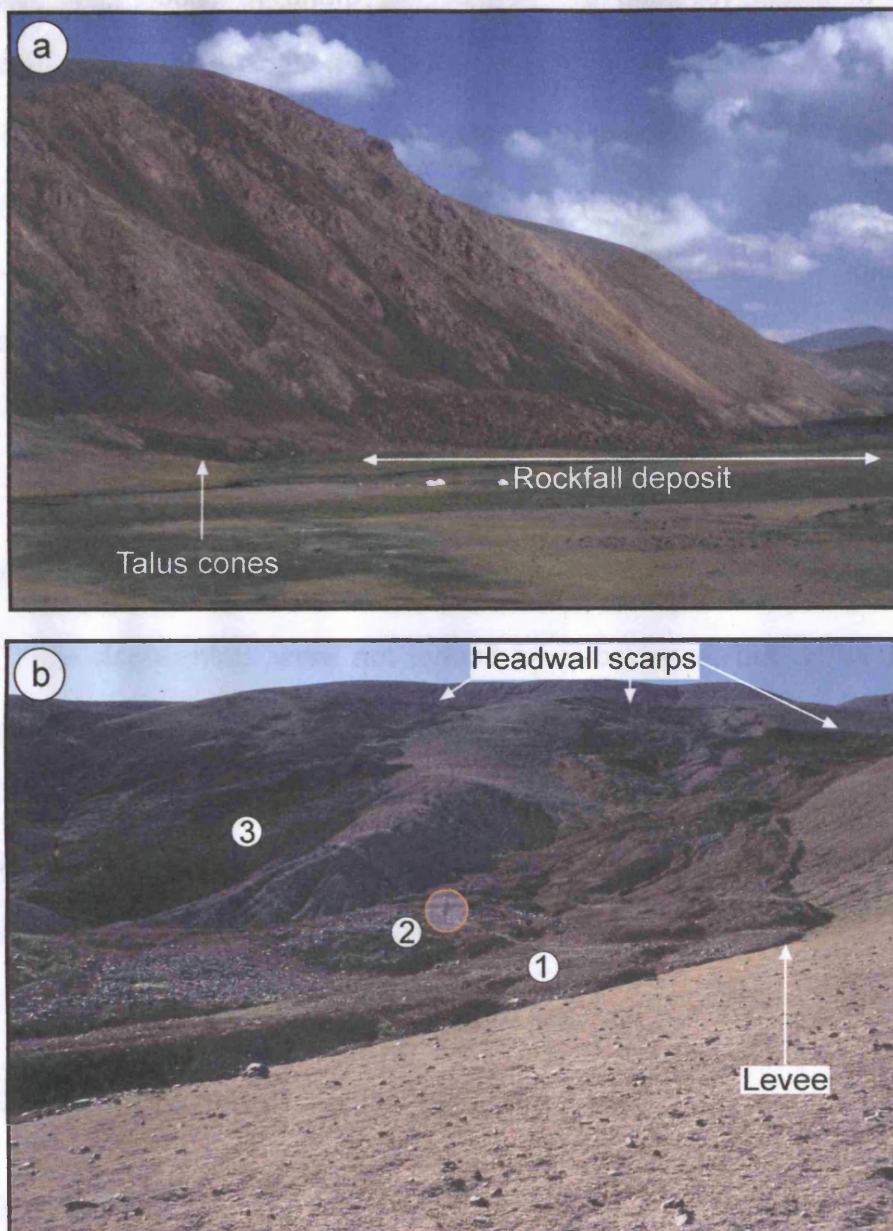


**Figure 2.8a** – Major rockfall in the high Altai close to Tal Nuur (Fig. 2.1). The white Gers (tents) are 5 m across. The apparent failure of the whole face suggests possible co-seismic triggering. **2.8b** - Debris flow deposits in the northern Dariv Basin (Fig. 2.1), 1-3 indicate successive individual flows. The person standing in the centre of the image (orange circle) provides scale.



catchment area bound by sharp ranges that are generally glaciated or show evidence for past glaciations (Fig. 2.6). The channels rarely store sediment, except where they have backfilled adjacent to an over-filled basin. Instead their sediment is commonly deposited as alluvial fans at the basin margins (Fig. 2.9a). The rivers and streams draining these depocentres generally flow northwest or southeast (Fig. 2.5), following the regional structural trend. Only one intramontane basin is observed on the Chinese side of the range (Fig. 2.7). This depocentre has formed along the Fu-Yun strike-slip fault as a small pull-apart basin (Fig. 2.4).

#### 2.6.2.2.2 INTERPRETATION

These depocentres were not formed by subsidence, but rather are relict areas between uplifted ranges that became passive sedimentary sinks for material eroded off the adjacent ranges. These basins may also have been topographically uplifted during sedimentation, but at a slower rate than the surrounding ranges. Elongate intramontane basins are oriented northwest-southeast, parallel to major range bounding structures (Fig. 2.6).

#### 2.6.2.2 Internally drained intramontane basins

##### 2.6.2.2.1 DESCRIPTION

Two internally drained intramontane basins bound by major ranges are identified, the Tsetseg and Omnogovi basins (Fig. 2.6). The Tsetseg Basin has a catchment area of approximately 400 km<sup>2</sup> and is bound by the Sutai and Baataryn ranges to the north and northeast (Fig. 2.6), and by unnamed ranges to the south and southwest. The low relief Tonhil range forms the eastern basin margin. The Omnogovi Basin has a catchment of approximately 490 km<sup>2</sup> and is bound by the Turgan-Kharkhiraa range on its north-western margin. A low, unnamed, ridge

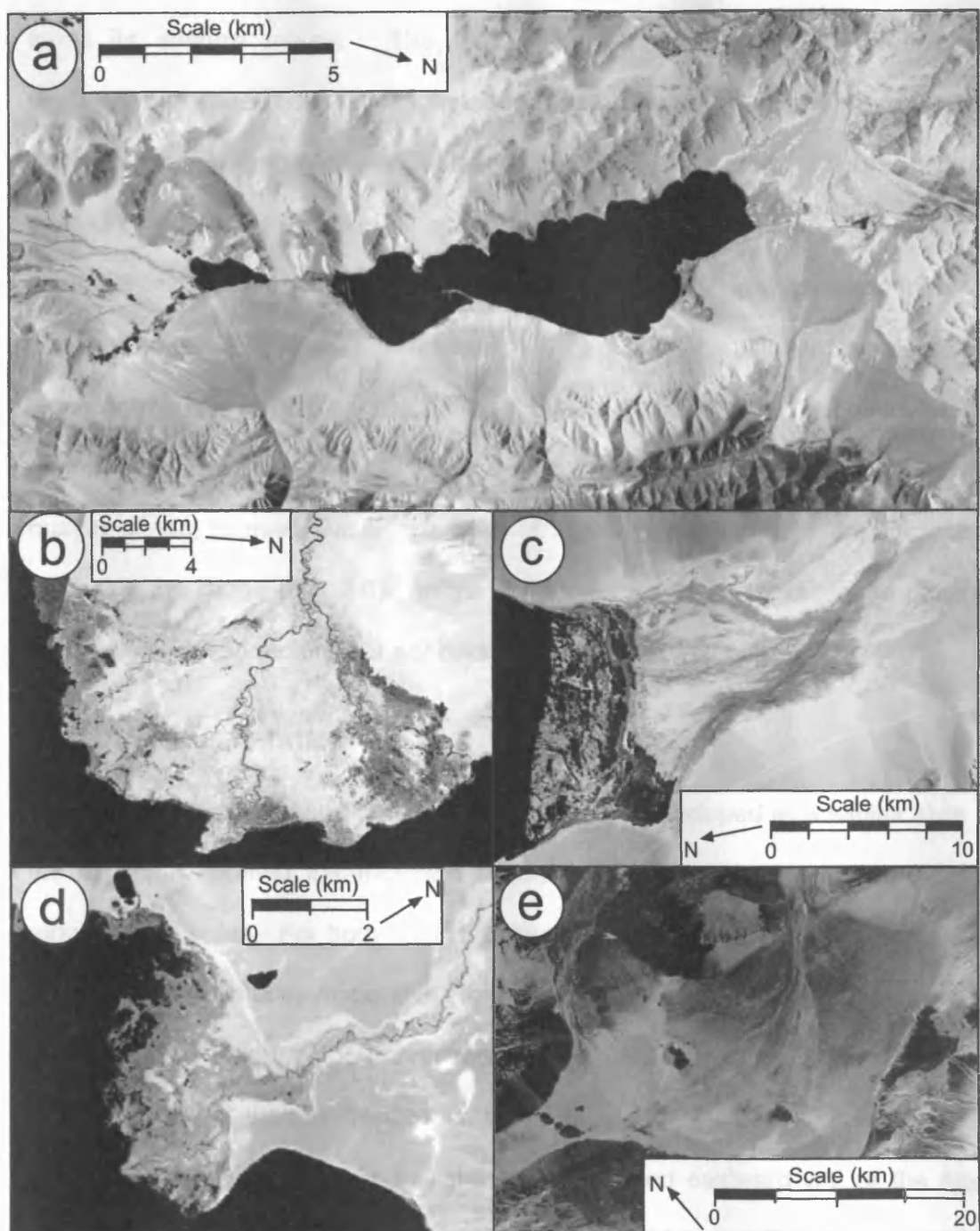


**Figure 2.9** – Alluvial/fluviol fans and deltas of various forms are recognised within the Altai (examples located on Fig. 2.1). **2.9a** – Tolbo Nuur lake in the central Altai, here large alluvial fans prograded into the lake from the actively uplifting flanking range. **2.9b** – The Khovd Delta in northern Har Us Nuur lake represents a major depocentre for sediment eroded from the Altai. **2.9c** – Delta forming on the southern banks of Har Us Nuur lake which stores sediment transported axially within the Dzereg Basin. **2.9d** – Small fluvial delta deposited in the Valley of Lakes by the only river to transport sediment from the flanking transpressional basins to the external depocentres. The small size of the delta reflects the limited volume of sediment that passes through Har Us Nuur lake. **2.9e** – Two major terminal fans that dry out due to downwards infiltration of water and surface evaporation in the southern peripheral basins.

forms its eastern margin. The larger Tsetseg Basin contains three active depocentres, while the smaller Omnogovi Basin contains one, with a lake at its centre. The topography of the Tsetseg Basin floor is subdued, although bedrock exposures onlapped by basin fill occur within the basin. Sediment is supplied to these basins via predominantly short (<10 km), semi-straight streams from the adjacent ranges (Fig. 2.5). Both basins are dominated by alluvial fans deposited along active range fronts (e.g. Tsetseg Basin, Fig. 2.10); no exposure of the underlying basin fill is present. River valleys adjacent to the less active western margin of the Tsetseg Basin are sites of active deposition and are filling and onlapping the range (Fig. 2.6). In the Omnogovi Basin similar drainage patterns are seen, however sediment is not backfilling the main channels.

#### 2.6.2.2.2 INTERPRETATION

The Omnogovi and Tsetseg basins probably developed in a similar style to the externally drained intramontane basins but have been isolated by uplifted ranges on all sides. For both basins, uplift of ranges along their eastern margins appears to be ultimately responsible for their isolation. This interpretation is based on the relative height of bounding ranges. In both cases, the eastern range is significantly lower than the ranges on the other side of the basin. Consequently, prior to their uplift, it is likely that the basins drained eastward out of the Altai. However, these antecedent drainages were presumably not sufficiently powerful to cut through the uplifting ranges. The Tsetseg Basin contains the greater volume of sediment, based on surface area and more sediment is backfilling the adjacent channel systems. This suggests that the Tsetseg Basin is perhaps at a more advanced stage than the Omnogovi Basin. The Deluun Basin (Fig. 2.5), source of the Buyant river, is an example of a basin that is becoming progressively isolated

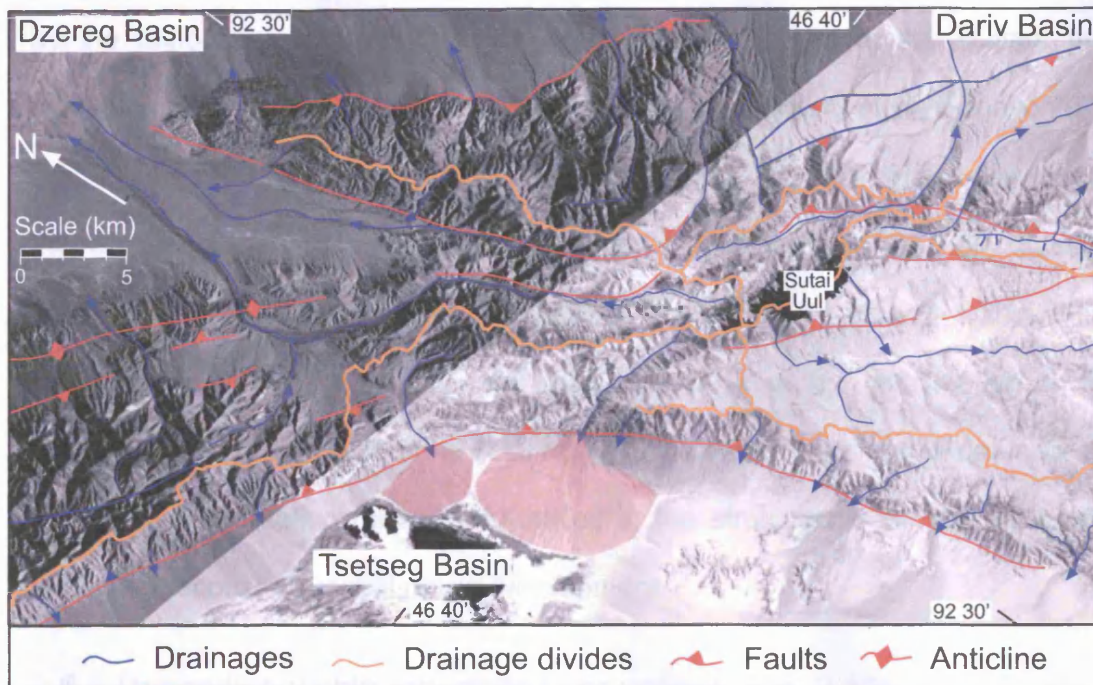


**Figure 2.10** - Detailed image showing major structures, drainages and drainage divides within Sutaï Uul. Note that many drainages are deflected northwest or southeast by active structures. Also, note the asymmetry of drainages adjacent to major faults. Red shading indicates major fans derived from the Sutaï massif.

by the tectonic uplift of bounding ranges. In this example, the Buyant river continues to exit the basin through Serhiyn Nuruu via a deeply incised canyon (Fig. 2.5), but further uplift along the Hoh Serkh fault (Fig. 2.4) may eventually exceed the rate of incision and the basin may then become isolated and internally drained.

No data exist regarding the age of the oldest sediments within these intramontane basins, but such data would provide important information on the timing of the tectonic uplift of the Altai range. Systematic variation in dates for the onset of sedimentation might be identified in the stratigraphy of different basins and could record sequential range development.

### 2.6.3 Deposition within mountain river valleys (Fig. 2.11)

#### 2.6.3.1 DESCRIPTION

Large river systems within the Altai, particularly those draining intramontane basins, commonly flow through valleys with gradients that allow some sediment deposition and storage. Sediment deposited within these valleys varies from coarse cobble lags, that are temporarily stored at low flow stage within a braided system (Fig. 2.12), to finer grained overbank deposits. The type of deposit depends primarily upon proximity to the river source and river gradient. The fluvial network may be the primary locus of deposition in those catchment areas lacking an intramontane basin or, as documented above, where sediment is backfilling the feeder channels into intramontane basins. In most cases, however, the fluvial system contains sediment reworked and deposited downstream from intramontane basins (Fig. 2.6).

Three river systems are particularly important in transporting sediment east or west away from the centre of the Altai. It is these channel systems that contain the most significant fluvial deposits, based on surface area. The Khovd and



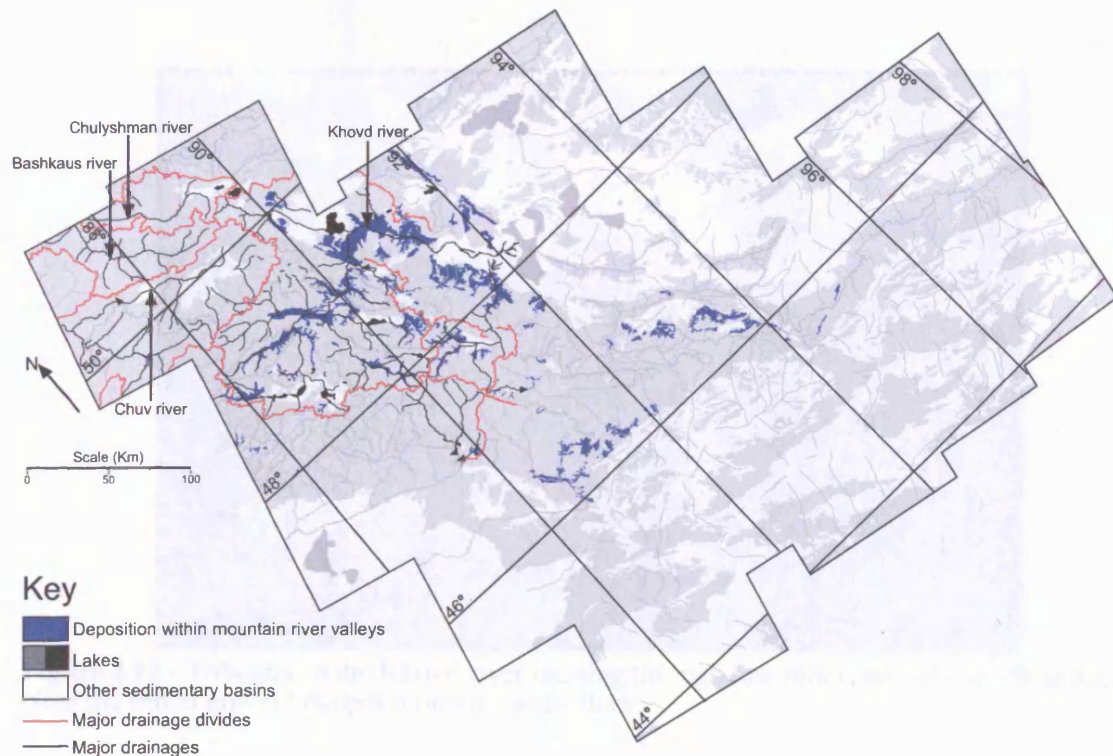


**Figure 2.11** - Map showing the distribution of sedimentation within Altai mountain valleys and their drainage systems.



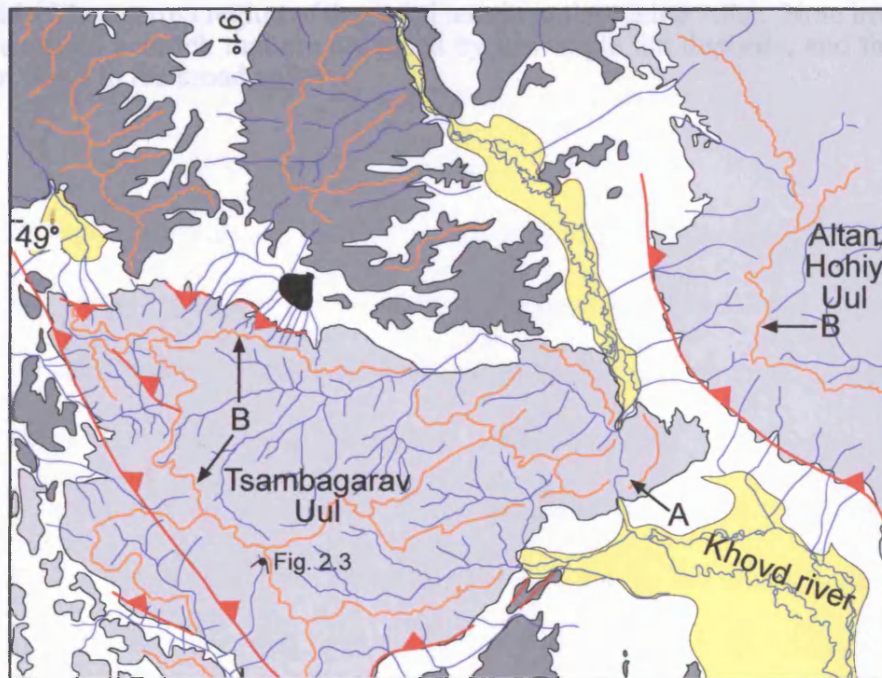
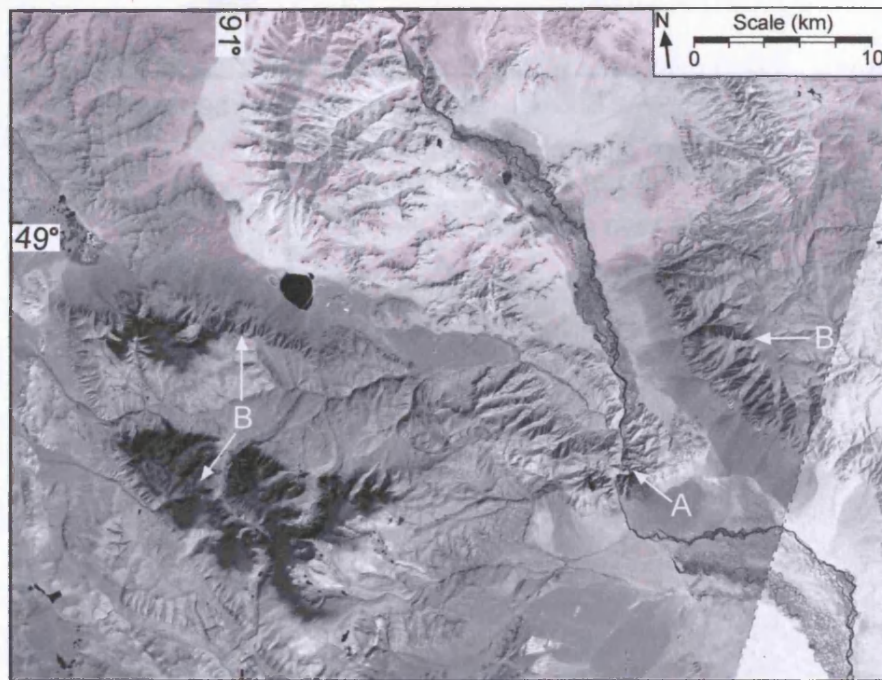
**Figure 2.12** - Tributary to the Khovd river incising through low relief, actively uplifting terrain. Note the broad gravel braidplain on the valley floor.







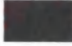
Buyant river systems in Mongolia, and the Chulyshman/Bashkaus/Chuja rivers in Russia (Fig. 2.1), drain multiple catchment areas amounting to approximately 50% of the range area (Fig. 2.5). The Khovd river drains 12 small catchments, many containing intramontane basins, totalling an area of more than 14,100 km<sup>2</sup> or approximately one third the surface area of the Mongolian Altai (Fig. 2.5).

Tributaries flowing northeast or southwest along the regional structural grain join the Khovd river, which flows east-northeast towards Achit Nuur (Fig. 2.1). From there the river turns southeast and flows through the easternmost end of Tsambagarav Uul (Fig. 2.13) before draining southeast into Har Us Nuur lake. The river deposits sediment where it flows through terrain that is not being actively uplifted, and is a single canyon channel where it incises through actively uplifting terrain. Areas of relict topography, as seen in figures 2.13 and 2.14, are common within the Altai between tectonically active ranges.

The Chulyshman, Bashkaus and Chuja rivers are located in the northwest of the image. The Tashanta Basin (Fig. 2.5) receives sediment from adjacent ridges and drains into the Chuja river which flows northwest. On this image only limited sections of the three rivers are present and there appears little evidence for deposition within channels. This is because the channels are predominantly confined to steep sided gorges although, where the channel margins broaden, sediment is deposited adjacent to the river.

Southwest of Har Us Nuur, the smaller Buyant river system (Fig. 2.5) drains the Deluun Basin which has a catchment area of approximately 1550 km<sup>2</sup>. The Buyant river is initially deflected southeast by Serhiyn Nuruu, an active fault bounded range, before incising through the range to flow northeast, via the city of Khovd, into Har Us Nuur lake. This drainage system is of a smaller order than the Khovd system, but is included in this summary of major drainages because a



Key		
	Actively uplifting terrane	 Drainages
	Floodplain	 Drainage divides
	Inactive, mature terrane	 Faults
	Lakes	

**Figure 2.13** - Detailed image of Tsambagarav Uul, note the discrete areas of active faulting and range uplift separated by areas of inactive degraded terrain and sediment accumulation. A – the large braided Khovd river has incised a canyon through the uplifting Tsambagarav Uul. B – Note also the drainage asymmetry exhibited by immature drainages in the uplifting ranges. Short, steep drainages characterise the active range fronts with longer drainages on the inactive sides. This figure is located on Fig. 2.1. The location of Fig. 2.3 is shown.



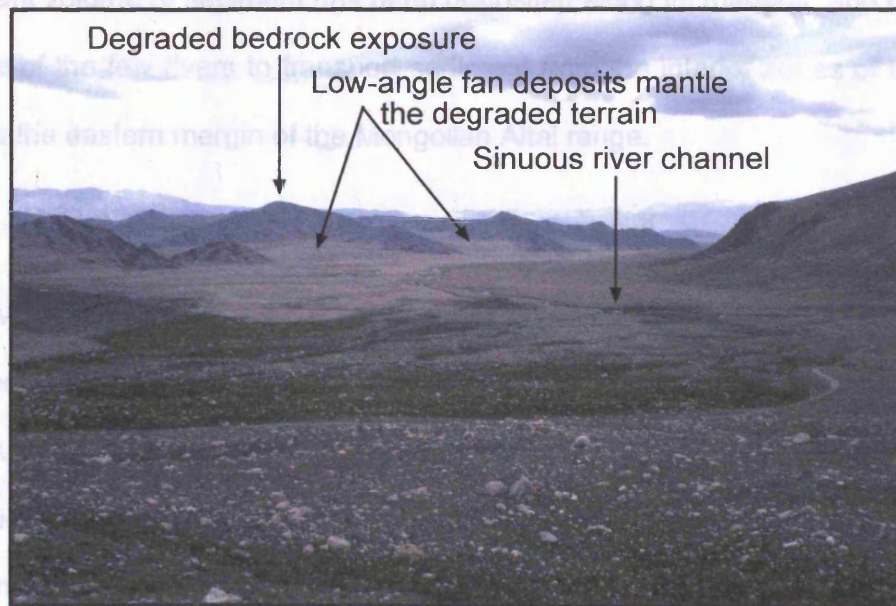


**Figure 2.14** - View across region of degraded terrain in the central Altai. Note irregular sinuous ridges of exposed bedrock that are onlapped by low-angle fan deposits, and the meandering stream that flows in the broad valley.

An important question is whether the Khovd river formed during initial uplift of the Altai, or whether the Khovd system cut back into the range by progressive drainage basin capture. The river must have existed prior to uplift of easternmost Tsambagarav Uul or it would have been unable to incise through the range (Fig. 2.13). It appears from the course of the river that it originally drained the Achil Nur lake in the north. The volume of sediment in the intramontane basins (estimated from surface area), and the fact that they have not all been cannibalised yet, suggests that the rest of the drainage system may have developed by successive capture of drainage basins. The Khovd river now drains a large area and flows along a low gradient through the range over a length of 130 km. This low gradient results in broad plain development and the associated deposition of wide floodplain deposits (Fig. 2.13).

significant volume of sediment has been deposited along its margins, and because it is one of the few rivers to transport sediment from the interior zones of the Altai towards the eastern margin of the Mongolian Altai range.

#### 2.6.3.2 INTERPRETATION

Mountain valleys that contain sediment from rivers that drain the Altai represent an important short-term sediment sink.

Major drainages, such as the Khovd river, that transport sediment across the regional structural trend are the dominant mechanism for sediment transport out of the range and into the flanking basins. The Khovd drainage is a major river system and has the ability to incise through uplifting ranges, e.g. eastern Tsambagarav Uul (Fig. 2.13). This erosive power relates to its large catchment area and consequently larger water volumes.

An important question is whether the Khovd river formed during initial uplift of the Altai, or whether the Khovd system cut back into the range by progressive drainage basin capture. The river must have existed prior to uplift of easternmost Tsambagarav Uul or it would have been unable to incise through the range (Fig. 2.13). It appears from the course of the river that it originally drained the Achit Nuur lake in the north. The volume of sediment in the intramontane basins (estimated from surface area), and the fact that they have not all been cannibalised yet, suggests that the rest of the drainage system may have developed by successive capture of drainage basins. The Khovd river now drains a large area and flows along a low gradient through the range over a length of 330 km. This low gradient results in braidplain development and the associated deposition of wide floodplain deposits (Fig. 2.13).

The other channel systems documented in Russia are of similar importance as the Khovd river, but only the source regions can be seen on the Landsat mosaic analysed in this study. The rivers drain a large area and merge to the northwest to form the Ob river (Fig. 2.5) which flows 2800 km northwards to the Arctic Ocean.

## 2.6.4 Range-flanking transpressional basins (Fig. 2.15)

### 2.6.4.1 DESCRIPTION

Along the northeast margin of the Altai and adjacent to the Gobi Altai are a series of distinct flanking basins. These basins form a succession of depocentres from the Dzereg Basin to the Beger Basin (and beyond) on the northern flanks of the Gobi Altai (Fig. 2.15). They are bound by juvenile mountain ranges, which are uplifted by thrust faults relating to ongoing regional transpression (Howard *et al.*, 2003). The basins themselves vary in size from the large Dzereg (approximately 3260 km<sup>2</sup>) and Shargyn basins (approximately 2970 km<sup>2</sup>) to the smaller Dariv Basin (approximately 360 km<sup>2</sup>), but all contain well-exposed sections of Mesozoic-Cenozoic basin fill (Sjostrom *et al.*, 2001; Howard *et al.*, 2003). These basins contain widespread evidence for ongoing contractional deformation with faulting and folding leading to uplift and erosion of recent basin fill (Howard *et al.*, 2003). The climate experienced by the flanking basins is semi-arid with rainfall decreasing toward the southeast. The Dzereg Basin receives 100-150 mm/yr of rainfall with the more southerly basins receiving as little as 50 mm/yr (Arakawa, 1969; Lehmkuhl, 1998). The basins are usually dominated by alluvial fan sedimentation and have marshlands in their centres. The Dzereg Basin also contains a major lake, Har Us Nuur, in its northern part.

These basins contain fluvial, lacustrine and aeolian sediment and alluvial fans derived from adjacent ranges. They receive sediment from two types of

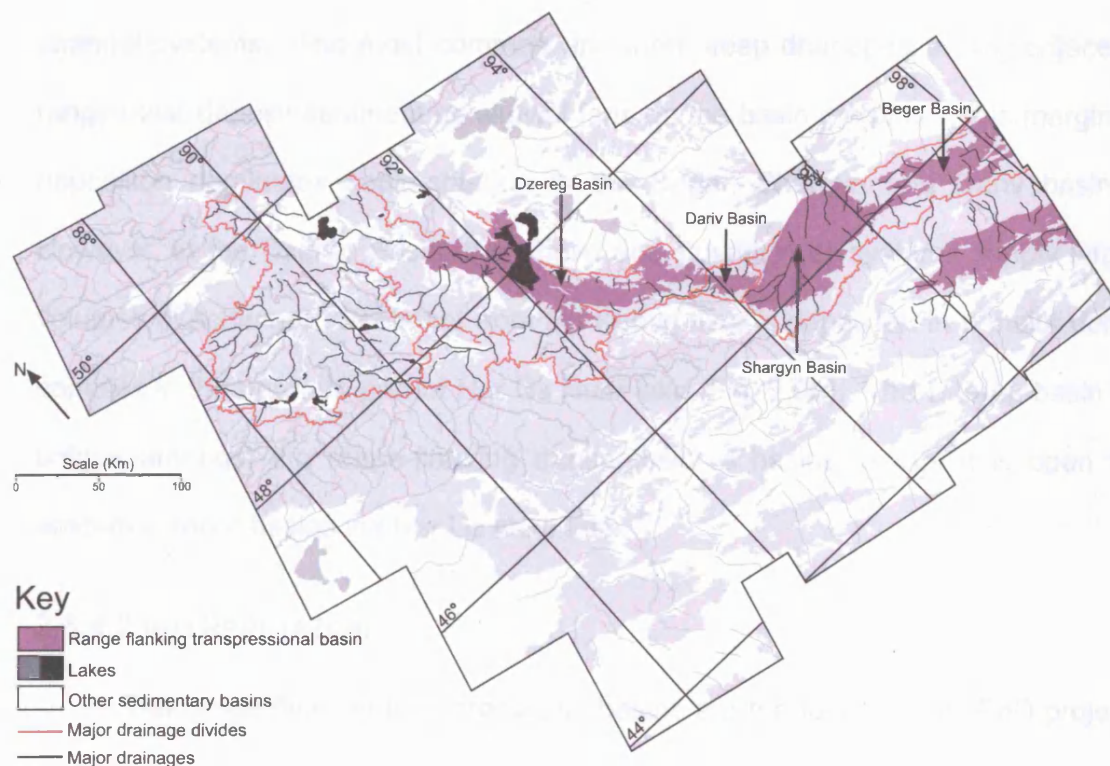


**Figure 2.15** - Map showing distribution of range-flanking transpressional basins and corresponding drainage systems.



channel systems. The most common are short steep drainages exiting adjacent ranges that deposit sediment as alluvial fans on the basin margins. This marginal deposition dominates sedimentation in the Beger, Shargyn and Dariv basins. However, in the Dzereg Basin, the Khovd and Buyant river systems supply large volumes of sediment. Sediment from the Khovd river is deposited in a major delta complex in the northern part of Har Us Nuur lake (Fig. 2.9b). The Dzereg basin is unique amongst the range-flanking transpressional basins in that it is open to eastern exterior basins via Har Us Nuur lake.

#### 2.6.4.2 INTERPRETATION

The range flanking transpressional basins are the focus of this PhD project and subsequent chapters concern the evolution of three of them, the Dzereg, Dariv and Shargyn basins. These three basins have tectonically active thrust and oblique-slip faults on one or more of their margins, and are undergoing internal deformation. The range flanking transpressional basins form a continuous sediment sink limiting sediment transport eastward into the Valley of Lakes. The large volume of Jurassic-Cretaceous sediment within the range flanking transpressional basins suggests they were also important depocentres during the Mesozoic. The Mesozoic sedimentary succession suggests that these basins were a repository for sediment produced during Mesozoic orogenic events and this is further investigated in chapters 3, 4 and 5. The majority of the sediment transported from the northern Mongolian Altai is deposited in the Khovd river delta at the northwest end of Har Us Nuur Lake in the northern Dzereg Basin (Fig. 2.9b & c). Only limited quantities of sediment will pass through the lake and be transported east into the Valley of Lakes (2.9d).

## 2.6.5 Shallow peripheral basins (Fig. 2.16)

### 2.6.5.1 DESCRIPTION

A broad belt of sedimentary basins that lack well defined bounding ranges lie to the south of the Altai. Fluvial and alluvial fan sediments drape a relict topography and basement is exposed through the sedimentary fill as inliers and inselbergs, suggesting that the basin fill is shallow in most places (Fig. 2.17). These basins are in a more arid zone than basins within the Altai and aeolian transport may be an important mechanism carrying sediment both within and between individual basins. Locally aeolian deposits are reported within some shallow peripheral basins investigated during fieldwork in the Gobi Altai (Cunningham, pers. comm., 2004). The shallow peripheral basins receive sediment from the westernmost Gobi Altai and the southernmost Altai (Figs. 2.5 & 2.6). Short straight drainages with small catchment areas in the Gobi Altai supply sediment to the south (Fig. 2.5). Catchment area size increases to the west, where long drainages (<140 km) with a well-developed dendritic pattern and deep canyon incision exist. Individual catchment areas in the west are well defined and cover areas on the order of 1800 km<sup>2</sup>. Rainfall of between 200-300 mm/yr occurs within the Altai, but decreases eastward into the Gobi Altai, where some basins receive less than 50 mm/yr on average (Arakawa, 1969). Once streams reach the range margins they enter a broad expanse of relict topography, with only limited uplift along active faults (Fig. 2.4). This results in a marked change in fluvial style, characterised by less confined channel systems and alluvial and fluvial fan deposition (Fig. 2.17). Figure 2.17 shows an enlargement of the broad area south of the Altai in which extensive basement exposure is visible. Drainage patterns appear random and are difficult to trace across the image. Two streams with

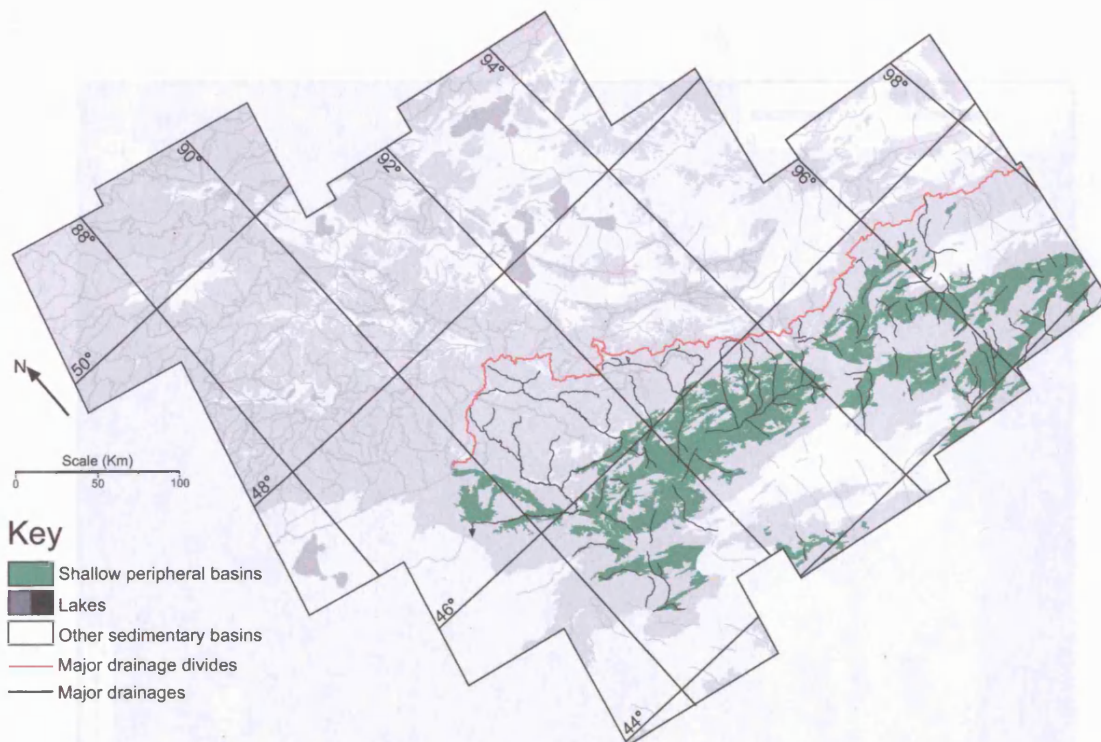


**Figure 2.16** - Map showing distribution of shallow peripheral basins and corresponding drainage systems.

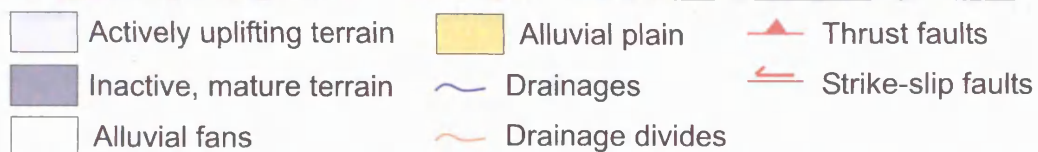
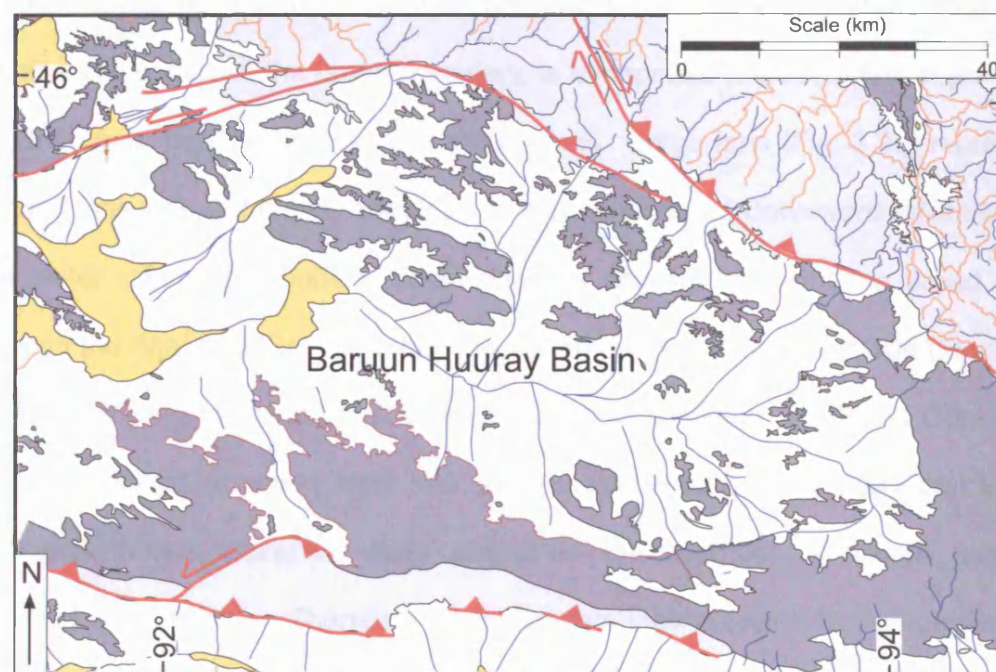
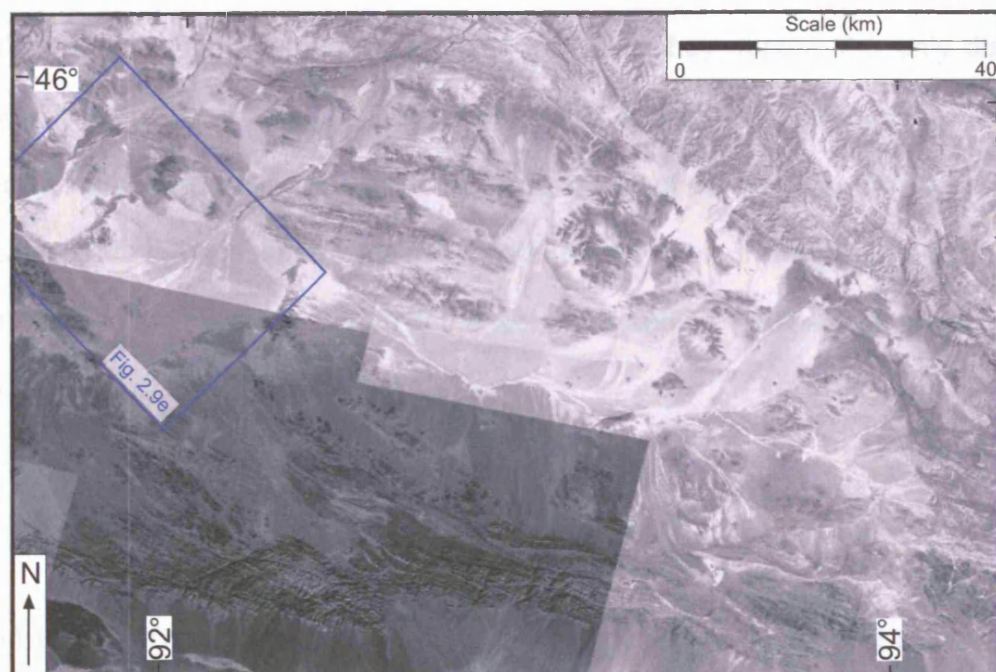


**Figure 2.17** - Detailed image of the shallow Baruun Hurray peripheral basin south of the Altai. The image shows reactivated and unreactivated terrain. Sediment eroded from the reactivated terrain is deposited in low areas of mature remnant landscape. This results in patches of sediment accumulation but no laterally continuous basin fill. These shallow peripheral basins may represent the earliest stages and basal accumulations of future Cenozoic transpressional basins.



larger catchment areas occur in the northwest of figure 2.17. Where they cross faults bounding the southern margins of the Altai, they deposit the only distinct fluvial fans in the area (Fig. 2.9e). The total catchment area available to the shallow peripheral basins is small compared to that of the flanking transpressional basins. This is because the main drainage divide within the Altai and Gobi Altai lies closer to the southern margin of the Gobi Altai and the south-western margin of the Altai (Fig. 2.5).

#### 2.6.5.2 INTERPRETATION

The shallow peripheral basins are not subsiding, rather sediment is infilling relict topography adjacent to the Altai. The deposition of fluvial and alluvial fans and the change from straight channels confined within valleys to meandering river systems that occurs at the range boundary, is a response to a reduction in gradient and, therefore, transport capacity of the streams. Large fans (Fig. 2.9e) represent terminal fans where the river dries due to evaporation and downward infiltration of river water. Similar peripheral basin deposits occur throughout the broad area between the Altai and Tien Shan beyond the area of the image montage (Fig. 2.1). These basins receive and store sediment from the southern Altai and Gobi Altai preventing fluvial transport west into the Junggar Basin. It is likely that these peripheral basins represent early stages in the evolution of range flanking transpressional basins. Therefore the sediments they contain may be analogous to the basal sedimentary accumulations of the more mature flanking transpressional basins described in later chapters.

## 2.6.6 External depocentres (Fig. 2.18)

These large basins (Fig. 2.6) flank the Altai and lie outside the actively deforming zone.

### 2.6.6.1 The Junggar Basin

#### 2.6.6.1.1 DESCRIPTION

Southwest of the Altai lies the Junggar Basin, which has a broad belt of exposed basement rock on its eastern margin, with local shallow sediment cover (Fig. 2.6). Catchment areas within the Chinese Altai average 2000 Km<sup>2</sup> and contain dendritic drainage systems with deep, steep sided canyons that drain well-defined catchment areas. At the margins of the range, small rivers flow out into the Junggar Basin via bedrock channels until they meet one of two major rivers (the Irtysh or Orongka rivers, Fig. 2.18). These rivers initially drain westward, however the Irtysh river turns northwest into Russia eventually reaching the Arctic Ocean (Fig. 2.1).

#### 2.6.6.1.2 INTERPRETATION

The Junggar Basin is a regional depocentre that has been extensively studied because of its known hydrocarbon occurrences (Hendrix *et al.*, 1992; Carroll *et al.*, 1995; Allen & Vincent, 1997; Vincent & Allen, 2001). The relative underfilling of the eastern Junggar Basin, adjacent to the Altai, is due to a combination of smaller catchment areas in the Chinese Altai, storage of sediment in the shallow basins south of the range, the presence of long-lived mature river systems which transport sediment northwest into the northern Junggar Basin and Russia (Fig. 2.1) and probable deflation by prevailing northwest winds. The lack of

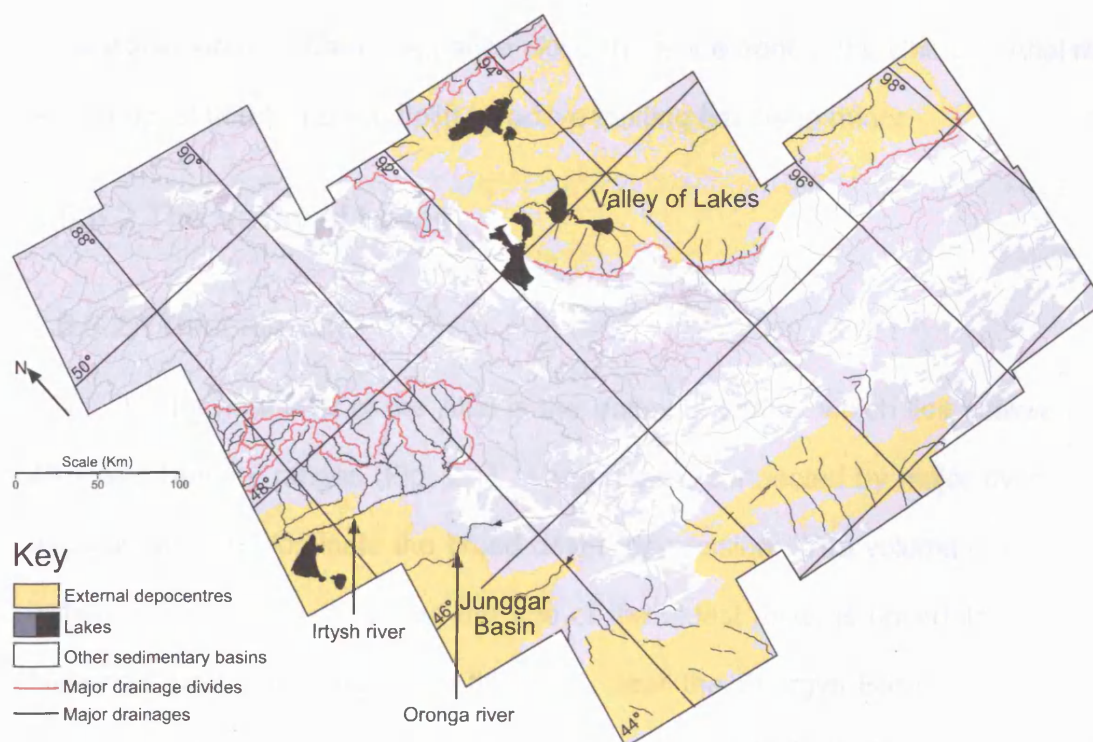


**Figure 2.18** - Map showing distribution of external depocentres and corresponding drainage systems.

a Cenozoic foreland basin sequence along the entire front of the Chinese Altai may also suggest that Cenozoic uplift by active faulting has been minor.

## 2.6.6.2 The Valley of Lakes

### 2.6.6.2.1 DESCRIPTION

To the northeast of the Altai is the Valley of Lakes, which lies between the Altai and Hangay ranges (Fig. 2.1). Large lakes, connected by major rivers, and large dune fields dominate the broad desert depression. The volume of sediment within the Valley of Lakes, and the age of the oldest units, is uncertain, although Mesozoic strata are reported in the south near the Shargyn Basin (Tomurtogoo, 1999). Russian geophysical data suggest that at least 500 to 700 m of Neogene-Quaternary sediment is present, although, in the absence of a large isostatic gravity anomaly, it is unlikely that the total sediment thickness exceeds 1-2 km (Baljinnyam *et al.*, 1993). Sediment is supplied to the Valley of Lakes from the Altai via short steep rivers on the western flanking ranges, which drain only a small fraction of the total Altai surface area, and also via the outlet from the Har Us Nuur Lake in the northern Dzereg Basin. The dune fields contain predominantly elongate, sinuous crested dunes with occasional barchan forms. Dune styles were observed both on the satellite imagery and during an aeroplane flyover.

### 2.6.6.2.2 INTERPRETATION

The Valley of Lakes initially appears to be the major depocentre storing sediment derived from the Mongolian Altai. However, this study demonstrates that only a small proportion of sediment eroded from the Altai actually reaches the Valley of Lakes. Only drainage systems in the most easterly Altai ranges feed directly into the Valley of Lakes and little coarse material can pass through Har Us



Nuur lake. In fact, the Valley of Lakes probably receives very little non-aeolian sediment from the Altai at the present time. Widespread, apparently active, dune forms identified on the imagery suggest that aeolian transport may be an important mechanism for transporting sediment within the Valley of Lakes. However, Grunert *et al.* (2000) report three stages of longitudinal dune development related to past glacial maxima, in the Uvs Nuur Basin just north of Hyargas Nuur (Fig. 2.1). The dunes are now stabilised by vegetation and have thick palaeosol development. However, without close investigation these dunes might be considered active, because the prevailing wind direction has not changed since their deposition. The only active dunes reported in the Uvs Nuur Basin are small barchan dunes that rework older dune deposits destabilised by overgrazing. Consequently, while the widespread dune-fields in the southern and central Valley of Lakes appear active, it is possible that some may be stabilised and inactive.

## 2.7 The influence of tectonic uplift on drainage patterns

Tectonic influence on drainage patterns exists on all scales within the Altai from the effects of mountain range growth on regional drainage networks, such as that described during discussion of the Khovd river system, to the small-scale influence of an individual fault. Drainage asymmetry within an individual range is the most common sign of a structural influence in the Altai. Short, straight drainages forming parallel drainage networks, which drain away from a linear, often northwest-southeast trending, catchment divide, are seen in many ranges in the Mongolian Altai (Figs. 2.10 & 2.13). Short steep channels form on active range fronts and longer channels on the inactive side. Therefore, the asymmetric drainage divides are often useful in establishing the probable direction of

underlying thrust faults that uplift the range and the overall asymmetry of block tilting (Cunningham *et al.*, 2003).

## 2.8 Discussion

While the five types of modern depositional system in the Altai region are characterised by different drainage patterns and basin types, the structural geology of the range is the principal control on sedimentation. The distribution of evolving ranges along thrust and strike-slip faults is the fundamental control, at every scale, on the geomorphology of the Altai range. A first-order division of the Altai into two structural domains, one dominated by westward vergent thrusting along the western Altai, principally in China, and one by transpressional uplift in Mongolia, has previously been established (Cunningham *et al.*, 2003). This difference exerts the primary control on drainage development and geomorphology. The western Altai forms a single continuous range from north to south with well-defined catchment areas containing dendritic drainages that flow directly into the Junggar Basin. In the Mongolian Altai, late Cenozoic growth of discrete individual ranges separated by areas of tectonic inactivity and sediment deposition created a completely different geomorphological style. Tectonic uplift patterns favour a predominantly northwest-southeast transport direction. Rivers originating from Mongolian Altai ranges flow between uplifted blocks and develop more complex drainage patterns than those seen in the Chinese Altai. As the Mongolian Altai developed, some drainages were able to keep up with, and incise through, block uplifts (e.g. the Khovd river). In other examples, uplift along faults caused deflection of major rivers (e.g. the Buyant river) or damming of rivers creating internally drained intramontane basins.

Other factors that may influence the development of depositional systems include climate. Glaciations have eroded U-shaped valleys and deposited sediment as moraine. Moraine deposits represent a readily transportable sediment source in the upper reaches of many catchment areas. The variation in precipitation around the region, and the corresponding variation in vegetation, match well with observed changes in catchment area and channel morphology. In the Chinese Altai, precipitation is greater and vegetation is correspondingly thicker, with the widespread development of forests. Greater precipitation allows extensive erosion in the Alpine domain, multiple dendritic tributary development and deep valley incision with steep slopes stabilised by vegetation. In the Mongolian Altai, precipitation decreases from north to south and from west to east with decrease in altitude. In the northern Altai drainage networks with large catchment areas have developed perennial rivers, due to a combination of glacial melt and high precipitation rates. These river systems have a greater opportunity to incise and maintain forward flow during tectonic uplift. In the southern Altai, where there is less precipitation and more evaporation, depositional systems are different. Precipitation within the range leads to the development of medium-sized catchment areas that feed large river systems, supplying sediment to the range margins. However, once these rivers enter the broad tectonically inactive area south of the Altai they rapidly lose their water by infiltration and evaporation, creating terminal fans that are periodically remobilised by ephemeral streams. In the eastern Altai, low precipitation in minor catchment areas produces ephemeral sheetflood sedimentation on alluvial fans (Howard *et al.*, 2003). Broad areas in the south and east have little vegetative cover and wind streaking or dune development is recognised on the imagery, suggesting deflation is an important sediment transport process.

Bedrock geology is another possible control on drainage development. The influence of bedrock lithology on drainage systems is hard to quantify because the Altai has a heterogeneous basement. One possible factor is that rocks were accreted parallel to the northwest-southeast regional trend, so any weak horizons are likely to be oriented this way. This may have influenced the trend of drainages to develop parallel to the structural trend.

At first sight, the Altai lies between two major sedimentary depocentres that appear to receive sediment eroded from the range. This study has shown that this is not necessarily true, especially in the case of the Valley of Lakes. Instead, a hierarchy of sedimentary depocentres exists within the Altai. The only drainages to actively transport sediment from within the range to the eastern basin margins are the Khovd and Buyant river systems. Other drainages drain away from the northwest-southeast trending ridge lines and into adjoining troughs. The absence of a river system that flows from the flanking transpressional basins eastward to the Valley of Lakes is important and means that the Valley of Lakes receives Altai sediment only from the most adjacent ranges on its western and south-western side. This means that the flanking transpressional basins, rather than the external basins, are the important modern depocentres, in terms of sediment volume, for sediment eroded from the Altai. Dust storms were observed in the range flanking transpressional basins during fieldwork and may transport some fine sediment from the flanking basins into the Valley of Lakes. However, previous work has shown that significant aeolian sediment transport into the Valley of Lakes occurred mainly during glacial periods (Lehmkhul, 1998; Grunert *et al.*, 2000). On the south-western range margin sediment storage in the shallow peripheral basins and the northward transport of sediment from the Chinese Altai into Russia by the Irtysh river, limit the volume of Altai sediment reaching the Junggar Basin. Major dust

storms are commonly observed from space over the Junggar basin (Wilkinson, pers. comm., 2003). Therefore, sediment volumes within the eastern Junggar may be further limited by aeolian deflation.

Transport of sediment as dust is also potentially an important mechanism for removing sediment from the Altai region as a whole. The predominant transport direction is south-eastward, towards the Chinese loess plateau (Sun, 2002). The Altai and Gobi Altai may be an important source area for these loess deposits. Natsagdorj *et al.* (2003) report data on the spatial distribution of dust storms in Mongolia and the frequency of their occurrence. The Valley of Lakes and the depressions south of the Altai are areas with the greatest proportion of dusty days nationally (61-127 and 91-120 respectively). Abundance of dust is ascribed to the limited vegetative cover, strong winds, low rainfall and overgrazing of pastureland. In contrast, within the high Altai there are less than 10 dusty days per year (Natsagdorj *et al.*, 2003).

Making a quantitative measurement of the total amount of sediment eroded from the Altai is difficult. The volume of sediment stored in basins both within and adjacent to the range is unknown as is the amount of sediment removed from the Altai region by aeolian deflation. The initial topography of the range is also unconstrained, but the presence of a remnant peneplain on ranges within the Altai suggests that the total sediment volume of the regions basins, combined with the aeolian outflow, should balance with the volume of material required to fill all of the Altai valleys up to the relict peneplain surface. However, at first order the volume of sediment within Altai basins appears too small. Thus the peneplain may not have been fully developed across the region or a large amount of sediment may have been removed by the wind.

One outstanding question is how did the Altai develop? Were ranges randomly uplifted or was there a systematic growth outwards from a central zone? This question cannot yet be categorically answered. The major ranges >3000 m high are distributed throughout the region and form the sites of ongoing transpressional uplift. Glaciers exist on most major ranges at present, and evidence for previous glaciers extending to lower elevations (U-shaped valleys and moraines) are seen in all but the most easterly flanking ranges. The degree of fluvial incision and drainage maturity both decrease toward the east, suggesting that the Altai may be growing eastward. This is further supported by the isolation of the two internally drained basins by ranges growing on their eastern side and by the absence of glacially eroded valleys in Jargalant Nuruu and Dariv Nuruu (Fig. 2.19). This study suggests that further information on the growth of individual ranges may be contained within the sedimentary record of intramontane basins, about which very little is currently known.

The preservation potential of the different types of sediment depocentre varies. Deposition within mountain river valleys is temporary, probably stable only until the next major flood event. Intramontane basins are small and shallow but their preservation potential is good because regional, rather than discrete block uplift would be required to remove all the sedimentary fill from the intramontane areas. The range flanking transpressional basins contain greater volumes of sediment than the intramontane basins, and are deeper. This presents some advantage in terms of preservation potential. However, the basins are bound by active thrust faults that deform and uplift the basin fill as the basins develop and close. The range flanking transpressional basins will be preserved only if movement on their bounding faults ceases. The shallow peripheral basins contain only a thin sediment veneer over basement rock. There is, however, only limited

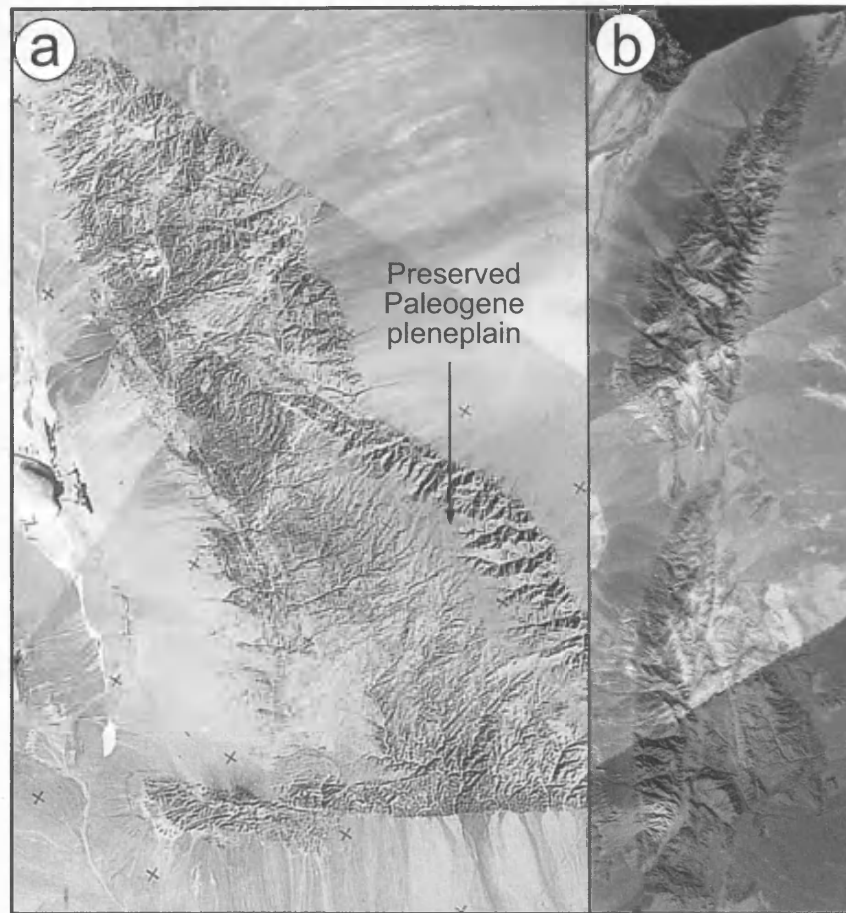


**Figure 2.19** - Detailed images showing the Dariv range (a) and the Jargalant range (b), the two most easterly ranges in the Altai (located on Fig. 6). The absence of U-shaped valleys suggests that these ranges lay below the equilibrium level altitude during the last glacial maximum. Note the preserved Paleogene peneplain surface on the summit of the Dariv range.

faulting and tectonic uplift adjacent to the ranges at present, so their preservation potential is good. The external depocentres are large and tectonically inactive. Away from their margins they have the greatest preservation potential.

The Altai is relatively understudied compared to similar sized ranges elsewhere (e.g. the Alps), but contains a great deal of interest to the geologist or geomorphologist studying the links between fault movement, range growth and multi-stage sediment storage and dispersal within a dynamic and evolving orogen.



## Chapter 3

# The stratigraphic and structural evolution of the Dzereg Basin, western Mongolia: clastic sedimentation, transpressional faulting and basin destruction in an intraplate, intracontinental setting

This chapter was published in *Basin Research* in June 2003. Only the facies letters have been altered in order to correspond with those used in Chapter 4.

### 3.1 Abstract

The Dzereg Basin is an actively evolving intracontinental basin in the Altai region of western Mongolia. The basin is sandwiched between two transpressional ranges which occur at the termination zones of two regional-scale dextral strike-slip fault systems. The basin contains distinct upper Mesozoic and Cenozoic stratigraphic sequences that are separated by an angular unconformity, which represents a regionally correlative peneplanation surface. Mesozoic strata are characterized by northwest and south-southeast-derived thick clast-supported conglomerates (Jurassic) overlain by fine-grained lacustrine and alluvial deposits containing few fluvial channels (Cretaceous). Cenozoic deposits consist of dominantly alluvial fan and fluvial sediments shed from adjacent mountain ranges during the Oligocene to Holocene. The basin is still receiving sediment today, but is actively deforming and closing. Outwardly propagating thrust faults bound the ranges, whereas within the basin, active folding and thrusting occurs within two marginal deforming belts. Consequently, active fan deposition has shifted towards

the basin centre with time, and previously deposited sediment has been uplifted, eroded and redeposited, leading to a complex facies architecture. The geometry of folds and faults within the basin and the distribution of Mesozoic sediments suggest that the basin formed as a series of extensional half-grabens in the Jurassic-Cretaceous which have been transpressionaly reactivated by normal fault inversion in the Tertiary. Other clastic basins in the region may therefore also be inherited Mesozoic depocentres. The Dzereg Basin is a world class laboratory for studying competing processes of uplift, deformation, erosion, sedimentation and depocentre migration in an actively forming intracontinental transpressional basin.

### 3.2 Introduction

Central Asia contains numerous Cenozoic basins that have developed in foreland, transpressional, transtensional and rift related settings. These basins are a record of ongoing tectonic activity related to widespread deformation associated with the Indo-Eurasia collision (Fig. 3.1). Most workers interested in the distant effects of the Indo-Eurasian collision have focussed on the structural architecture of the major mountain ranges of central Asia and the evidence for or against crustal extrusion towards the east (e.g., Tapponnier and Molnar, 1979; Yin and Harrison, 1996, and references therein). In contrast, fewer studies have investigated the detailed stratigraphy and structure of Cenozoic basins adjacent to the major central Asian ranges to discover what information they hold about local orogenic activity, and overall processes of basin evolution and basin destruction in an intracontinental, intraplate setting.

In this paper, we present a detailed description of the stratigraphy and structural evolution of the Dzereg Basin which is an individual transpressional basin on the eastern flanks of the Altai in western Mongolia (Fig. 3.2). Our

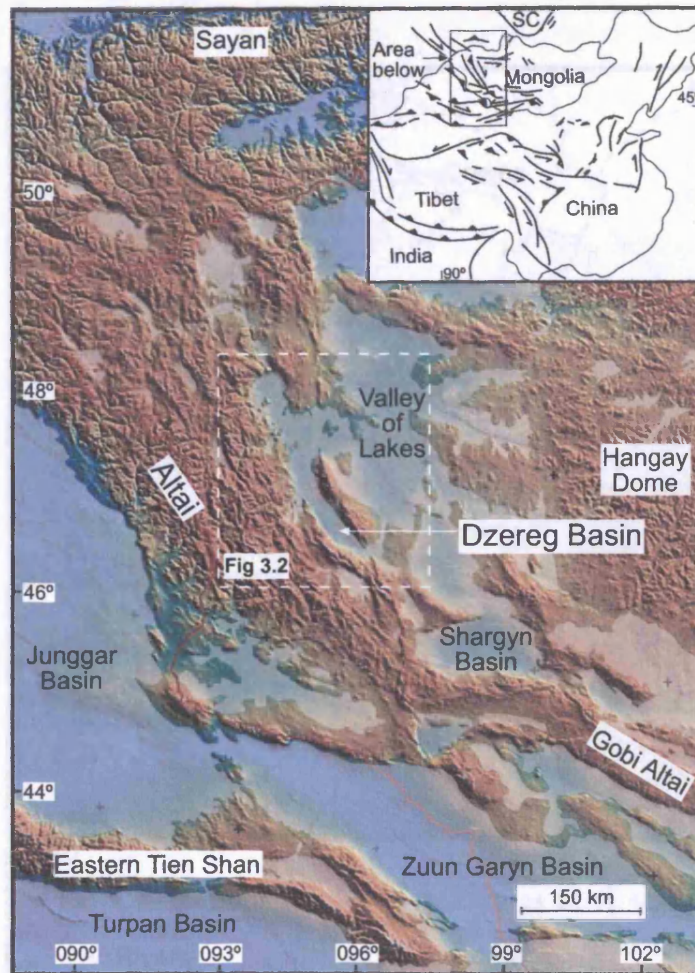


**Figure 3.1** - Digital topographic map of western Mongolia and Altai region. Areas of Cenozoic sediment accumulation indicated by pale tones. Note particularly the small basins on the eastern margin of the Altai, such as the Dzereg Basin, which is the focus of this study. Inset map shows regional fault patterns and areas of Cenozoic deformation in central Asia. Area of Fig. 3.2 is shown. SC - Siberian Craton.

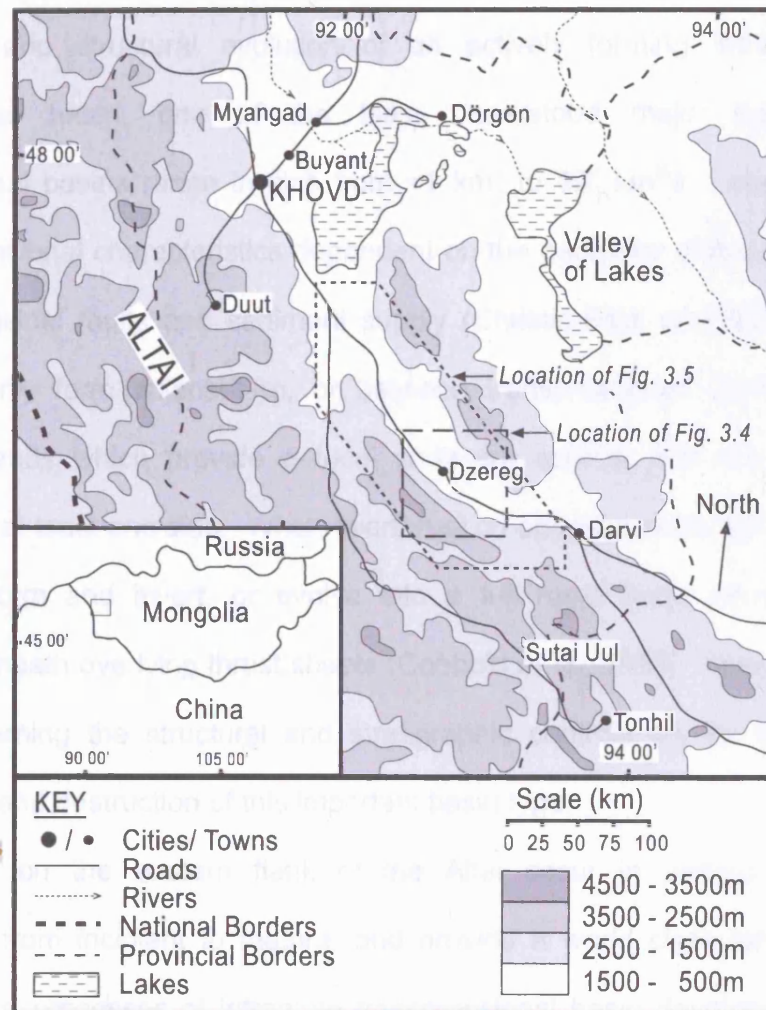


**Figure 3.2** - Topographic map of part of western Mongolia showing the Altai Mountains and the depression to the east, called the Valley of Lakes. The town of Dzereg and the Dzereg Basin are located on the eastern flank of the Altai.



objective is to present detailed stratigraphic and structural data that constrain the stratigraphic and structural evolution of an actively forming intracontinental transpressional basin, one of the least understood major basin types. Transpressional basins range in size from  $<1 \text{ km}^2$  to  $10^3 \text{ km}^2$ 's and can have diverse dimensional characteristics dependent on the geometry of basin bounding faults, intrabasinal faults and sediment supply (Christie-Blick and Biddle, 1985). They commonly form adjacent to, or between transpressional uplifts such as restraining bends which provide a local sediment source, and are commonly overthrust on at least one side. When overthrust on opposite sides, the basin may internally deform and invert, or evolve into a full ramp basin which may be concealed beneath overlying thrust sheets (Cobbold *et al.*, 1993). Many questions remain concerning the structural and stratigraphic controls on the localisation, development and destruction of this important basin type.

Basins on the eastern flank of the Altai occur in various stages of development from incipient to mature, and provide a world class laboratory for studying active processes of intraplate transpressional basin development. The study of transpressional basins in western Mongolia also has important regional implications. Basin sediments on the flanks of the Altai are a record of renewed Mesozoic-Cenozoic tectonism in the region and help constrain the timing and spatial progression of faulting and topographic uplift. In addition, the climate of western Mongolia is semi-arid and the clastic basins host an important water resource. Future groundwater extraction is dependent on correct identification of underground aquifers, their sedimentary facies context, and overall basin architecture.

### 3.3 Geology of the Altai region

The basement geology in the Altai region is complex and reflects an extended period of Palaeozoic crustal growth and widespread magmatism (Şengör *et al.*, 1993). Various basement terranes have been identified which are interpreted to represent arc complexes, subduction accretion belts and continental fragments (Badarch *et al.*, 2002, in press). These terranes accreted between older Precambrian blocks in Siberia, China and central Mongolia. In the Altai region, the terranes are elongate northwest and contain a dominant basement grain defined by regional foliation trends and faults systems. This fundamental structural anisotropy has strongly influenced all subsequent Phanerozoic deformation.

Cenozoic reactivation of the Mongolian Altai began at the end of the Oligocene, presumably as an intracontinental response to far field stresses derived from the Himalayan collision over 2500 km to the south (Tapponnier & Molnar, 1979; Devjatkin, 1981; Zoback, 1992). The range contains a large number of northwest-southeast trending faults that bound tectonically active mountain ranges. Movement on these faults is dominated by right-lateral strike-slip and oblique-slip with uplift occurring predominantly due to transpression at restraining bends and terminal splays. Some faults can be traced for hundreds of kilometres and are clearly visible on satellite imagery (Fig. 3.3). Many individual ranges contain faults that show opposing senses of vergence suggesting flower structure cross-sectional geometries (Cunningham *et al.*, 1996a). Fault plane solutions for historic earthquakes confirm the dextral transpressional nature of active deformation in the region and indicate maximum horizontal stress is oriented northeast-southwest (Khil'ko *et al.*, 1985; Baljinnyam *et al.*, 1993). GPS data indicate that the Altai is moving northwest at approximately 1 cm/yr relative to Siberia (J. Deverchere, pers. comm., 2001). Evidence for prehistoric earthquakes exists in the large fault scarps



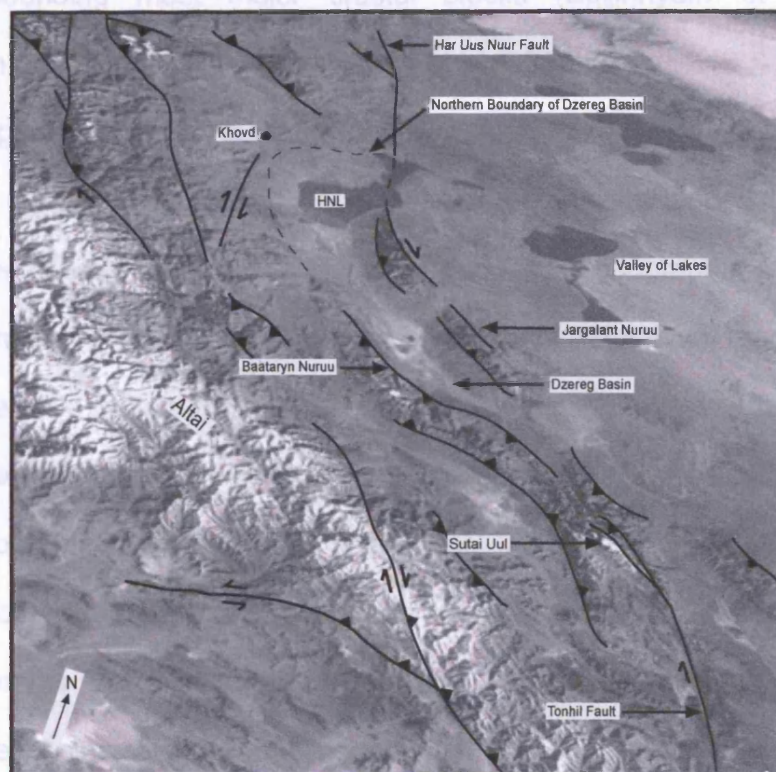


**Figure 3.3** - Space shuttle photograph of the southeastern Altai region (Photo #ST574-713-003) including Cenozoic flanking basins to the east and the Valley of Lakes. Major regional faults are shown. The Dzereg Basin is located between active thrust bounded ranges, which are restraining bends along the Tonhil and Har Uus Nuur dextral strike-slip fault systems, thus the Dzereg Basin occupies an intracontinental transpressional setting. The Dzereg Basin is divided into a northern and a southern depocentre. This study is principally focussed on the evolution of the southern Dzereg Basin. The width at the base of the photo is approximately 250 km and top to bottom is approximately 700 km. HNL - Har Uus Nuur lake.

Clastic basins are widespread along the eastern flank of the Altai. Previous work on clastic sedimentary deposits in the Altai region includes Devetkin (1981) who studied exposures in the Valley of Lakes and other flanking basins to produce a general stratigraphy for the entire Altai region. This work also includes a biostratigraphy for Mesozoic and Cenozoic basin deposits in the region. The Dzereg Basin contains an upper Mesozoic-Cenozoic sedimentary succession that is exceptionally well exposed due to active folding and faulting along the basin margins. Detailed information on the sedimentology and stratigraphy of Jurassic and Lower Cretaceous rocks in the Dzereg Basin and elsewhere in western



presently bounding most major crustal blocks (Baljinnyam *et al.*, 1993, Cunningham *et al.*, 1996a & b, Cunningham *et al.*, 2002).

The geomorphology of the Mongolian Altai reflects its youthful nature. Relief rarely exceeds 2500 m and summits are commonly flat-topped, preserving a late Cretaceous-early Palaeocene planation surface. Topographic asymmetry is apparent in many ranges and is due to the presence of a dominant range-bounding fault on one side which typically defines a sub-linear mountain front. Rivers generally drain eastwards, however their courses are strongly influenced by active faulting, topographic uplift and block tilting (Figs. 3.3 & 3.4). Short steep streams incise the active sides of ranges, whereas larger drainage basins with shallower gradient streams characterise inactive sides. Active sedimentation occurs in intramontane basins, along some mountain river valleys, and in larger flanking basins on the east side of the Altai such as the Dzereg Basin (Figs. 3.1 and 3.2). Some basins are internally closed leading to rapid accumulation of sediment. Most basins however, have river outlets that remove some sediment from the basin.

### 3.4 Previous work on flanking basins of the Mongolian Altai

Clastic basins are widespread along the eastern flank of the Altai. Previous work on clastic sedimentary deposits in the Altai region includes Devjatkin (1981) who studied exposures in the Valley of Lakes and other flanking basins to produce a general stratigraphy for the entire Altai region. This work also includes a biostratigraphy for Mesozoic and Cenozoic basin deposits in the region. The Dzereg Basin contains an upper Mesozoic-Cenozoic sedimentary succession that is exceptionally well exposed due to active folding and faulting along the basin margins. Detailed information on the sedimentology and stratigraphy of Jurassic and Lower Cretaceous rocks in the Dzereg Basin and elsewhere in western

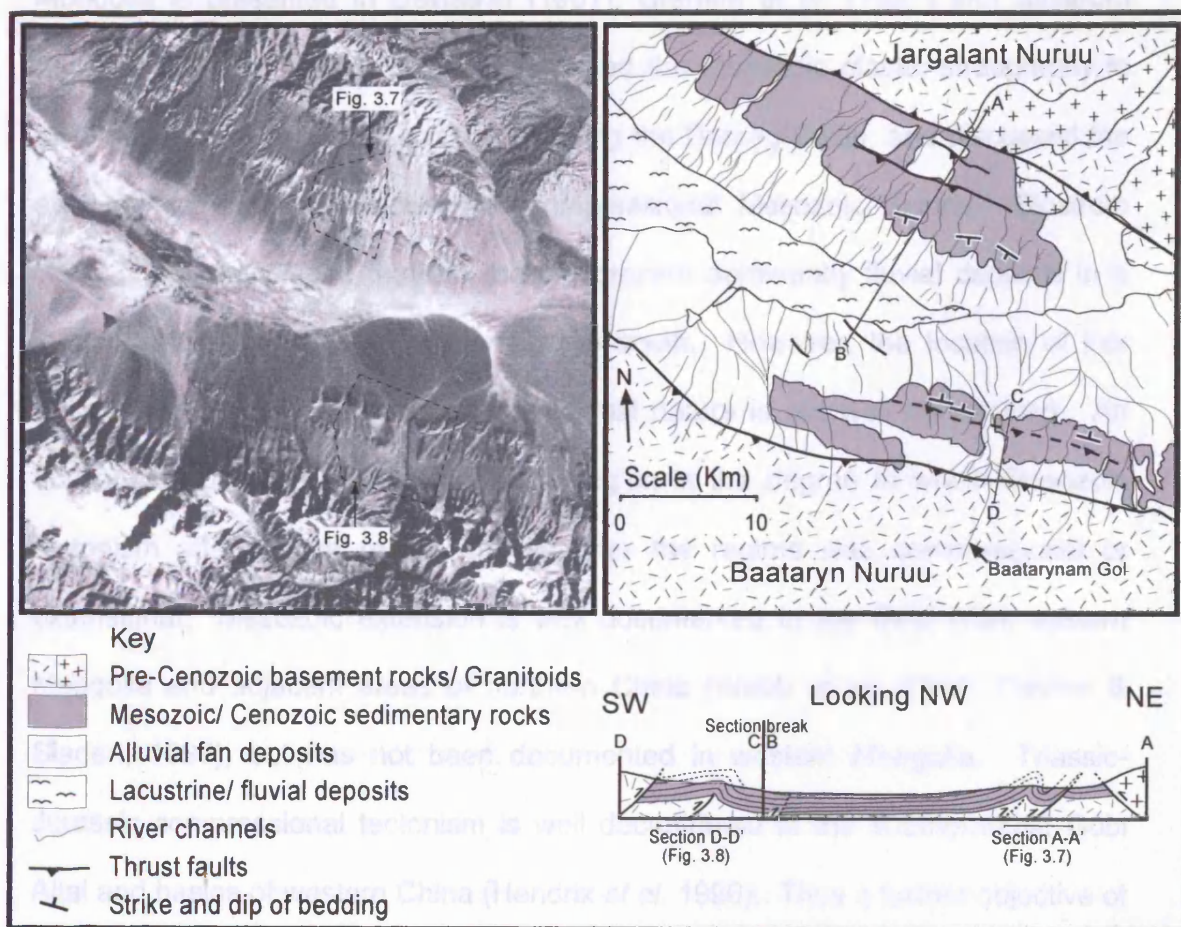


**Figure 3.4 - MSS Landsat image and interpretation showing complex relationships between structure and sedimentation within the Dzereg Basin. Range bounding faults and thrust faults within the basin that deform Mesozoic-Cenozoic sediments are visible. Modern streams cross ridges of deformed sedimentary rocks to deposit sediment in the basin centre. Basin cross-section is summarized from detailed maps and sections shown in Figs. 3.7 and 3.8. Locations of Figs. 3.7 and 3.8 are shown. Area of map is shown in Fig. 3.2.**

### 3.5 Geology of the Dzereg Basin

The Dzereg Basin is situated on the eastern flank of the Altai mountain two fault-bounded ridges, the Baataryn Nuruu range to the west and the lower Jargalant Nuruu range to the east. Immediately south of the Dzhirgatal Range of Sulai Uul (4090 m), the highest peak in the region (Figs. 3.2 and 3.3). The regionally important Har Us Nuur strike-slip fault terminates within the Jargalant Nuruu range forming a clear scarp on its northeast side (Fig. 3.3). The Jargalant Nuruu range is



Mongolia is presented in Devjatkin (1981), Graham *et al.* (1997) and Sjöström (2001). Sjöström (1997, 2001) documented the Mesozoic clastic stratigraphy in several western Mongolian basins, including the Dzereg Basin, and discussed the evidence for both extensional and compressional Mesozoic Basins. Sjöström (1997, 2001) concluded that the rocks represent dominantly fluvial deposits in a foreland basin north of an orogen to the south. However, the location of this orogen and its compressional or extensional nature is not well constrained. An outstanding problem in the entire Altai region is the degree to which Mesozoic tectonism affected the region and whether the regime was compressional or extensional. Mesozoic extension is well documented in the Gobi Altai, eastern Mongolia and adjacent areas of northern China (Webb *et al.*, 1999; Traynor & Sladen, 1995), but has not been documented in western Mongolia. Triassic-Jurassic compressional tectonism is well documented in the southernmost Gobi Altai and basins of western China (Hendrix *et al.* 1996). Thus a further objective of this study was to evaluate evidence for Mesozoic deformation in the Dzereg Basin region and to determine whether pre-existing Mesozoic basin architecture has influenced Cenozoic sedimentation patterns, and whether reactivation of older faults is responsible for deformation of the basin fill.

### 3.5 Geology of the Dzereg Basin

The Dzereg Basin is situated on the eastern flank of the Altai between two fault-bounded ridges, the Baataryn Nuruu range to the west and the lower Jargalant Nuruu range to the east. Immediately south of the Dzereg Basin is Sutai Uul (4090 m), the highest peak in the region (Figs. 3.2 and 3.3). The regionally important Har Us Nuur strike-slip fault terminates within the Jargalant Nuruu range forming a clear scarp on its northeast side (Fig. 3.3). The Jargalant Nuruu range is

considered a single restraining bend for this fault system with shortening focussed along the range's southwest side within and adjacent to the Dzereg Basin (Cunningham *et al.*, 1996a). Likewise, the Baataryn Nuruu and Sutai Uul ranges form a terminal bend for the regionally important Tonhil strike-slip fault (Fig. 3.3). Thus, the Dzereg Basin has formed between active transpressional ranges which accommodate shortening at the termination zones of two major strike-slip faults.

Both the Jargalant Nuruu and the Baataryn Nuruu ranges contain folded Vendian and Palaeozoic volcanic and sedimentary units intruded by Palaeozoic granites (Fig. 3.5). Similar rocks are believed to underlie the Dzereg Basin (Devjatkin *et al.*, 1975). The Jargalant Nuruu and Baataryn Nuruu ranges have non-parallel trends, therefore the width of the Dzereg Basin varies from 20 km in the south to more than 40 km at its northern end (Fig. 3.3). The basin is divided into two parts, a smaller southern sector where fieldwork for this study was carried out, and a larger northern sector that opens into Har Us Nuur lake (Fig. 3.3). The southern sector of the basin contains small lakes and large areas of swampy ground. Small drainages feed these lakes, but the basin lacks an axial river system. Sediment is delivered to the basin mainly via large alluvial fans, which in places define a bajada. Evidence for active deformation along the basin margins includes asymmetric ridges, dipping Mesozoic and Cenozoic strata and visible fault scarps (Fig. 3.4). This deformation influences the location of erosion, sediment transport and sediment accumulation. For example, on the southwest side of the basin, an uplifted ridge obstructs or deflects drainages entering the basin (Fig. 3.4) so that antecedent drainages have converged to feed a single stream (Baatarynam Gol, Fig. 3.4). This single stream now deposits sediment onto the largest fan complex in the southern Dzereg Basin (Figs. 3.4 and 3.6a). Active transpressional deformation along the entire length of the Dzereg Basin is closing the basin while

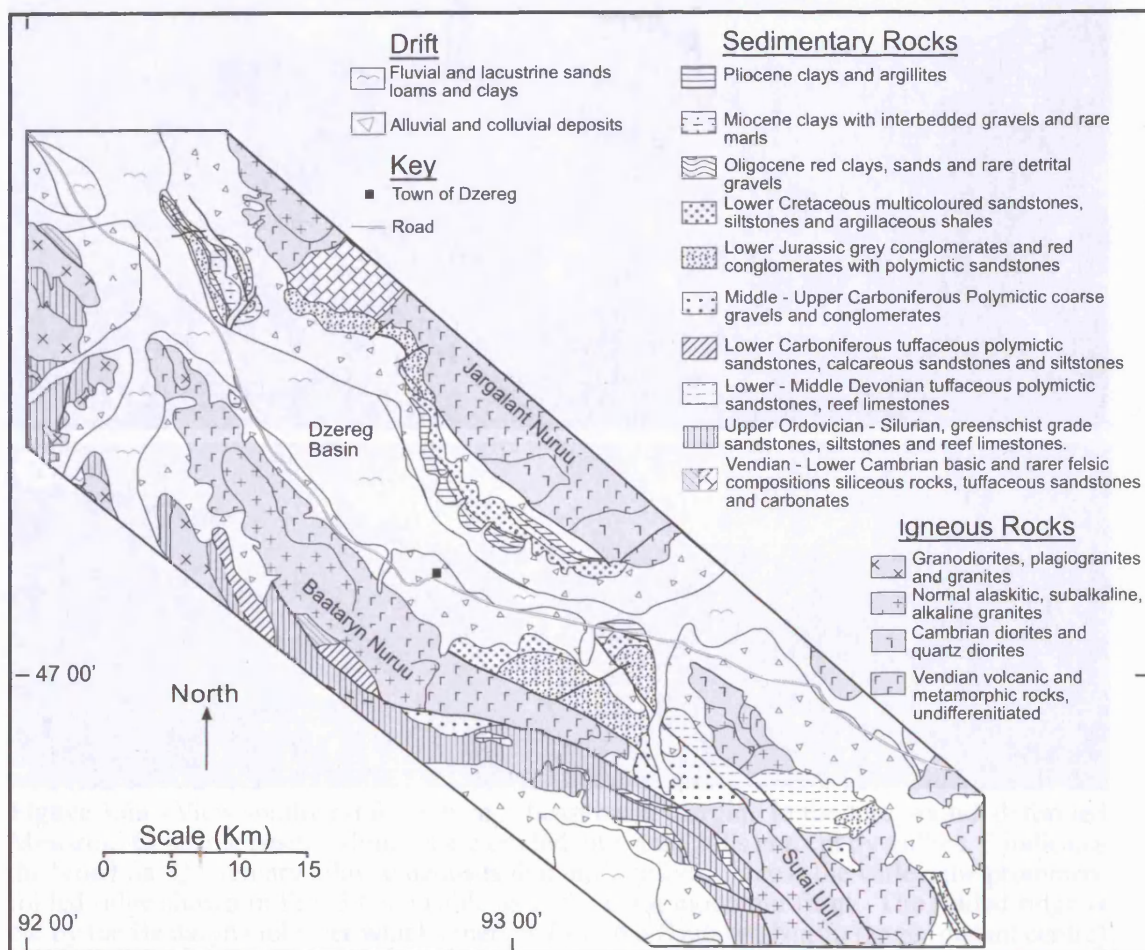


**Figure 3.5** - Geological map of the Dzereg Basin region showing basement rocks and previously mapped sedimentary units (after Zaitsev, 1978). Area of map is shown in Fig. 3.2.



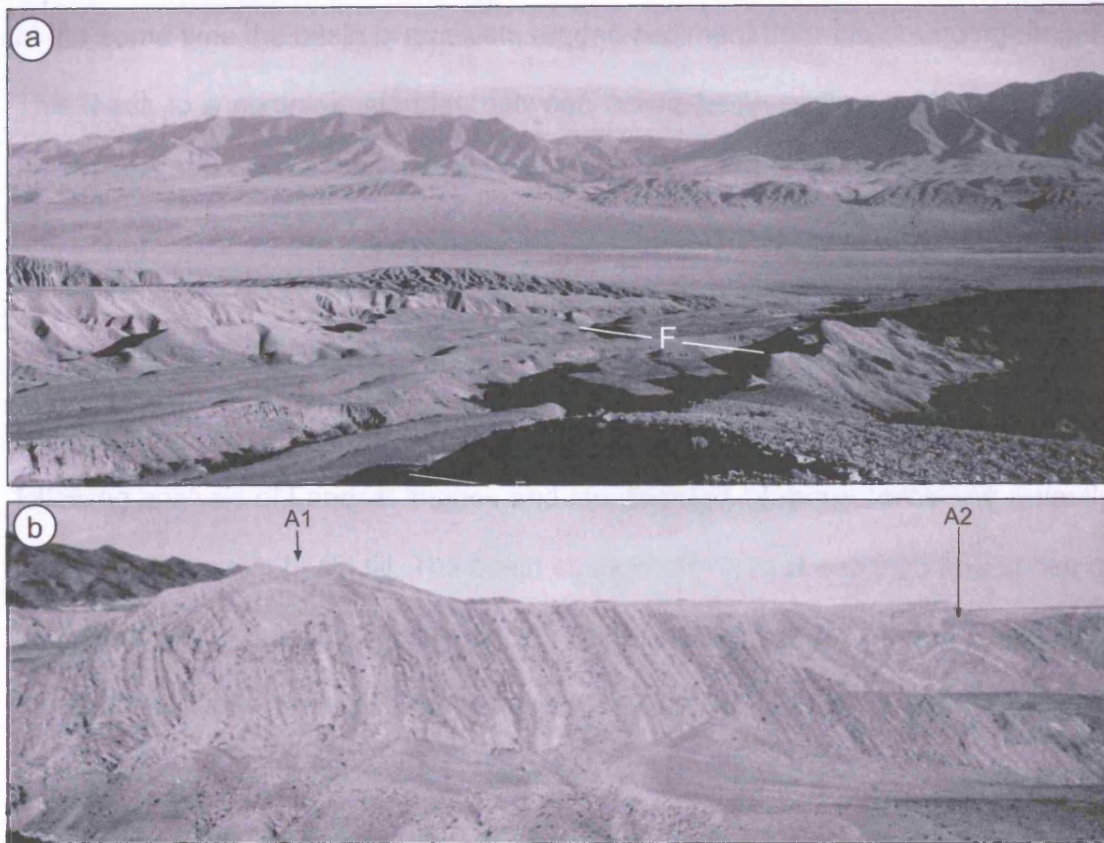


**Figure 3.6a** - View southwest from the northeast basin margin. In the foreground, deformed Mesozoic-Cenozoic basin sediments are eroded into small hills and cut by gullies. F indicates the broad flat Quaternary alluvial deposits that infill gullies. Across the valley, the prominent folded ridge shown in Fig. 3.6 is visible as is the main mountain front. The folded ridge is cut by the Baataryn Gol river which emerges from the Baataryn Nuruu range (distant centre) and is actively depositing a large alluvial fan in the basin centre (c.f. Fig. 3.3 for aerial perspective). **3.6b** - View south along the northeast basin margin of tilted and folded Cretaceous and Oligocene-Miocene basin sediments. Prominent northeast-vergent anticlines are visible (A1 and A2).

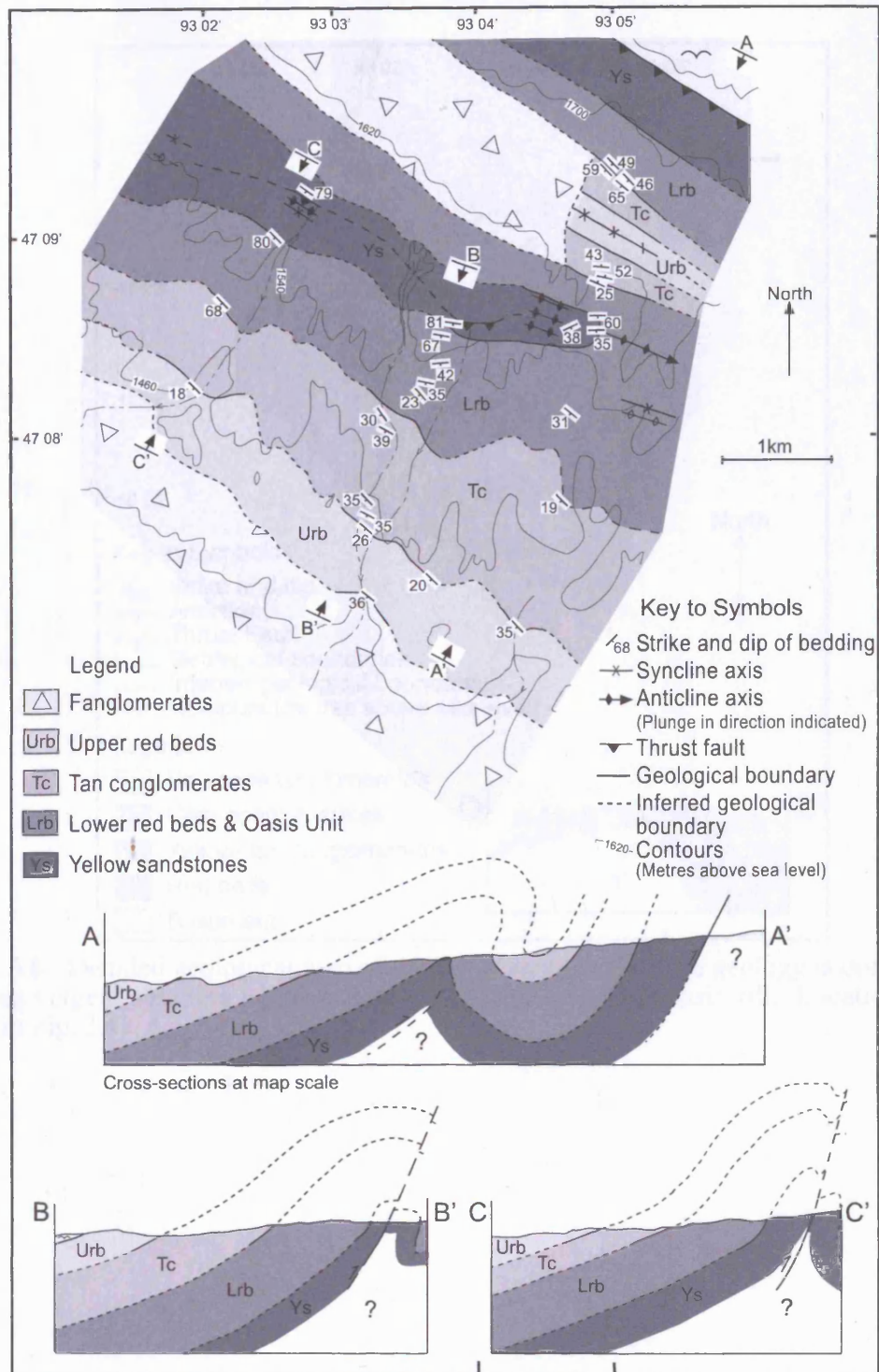
at the same time the basin is receiving eroded sediment from the bounding ranges. This leads to a complex interplay between active basin sedimentation and basin destruction.

### 3.6 Basin stratigraphy

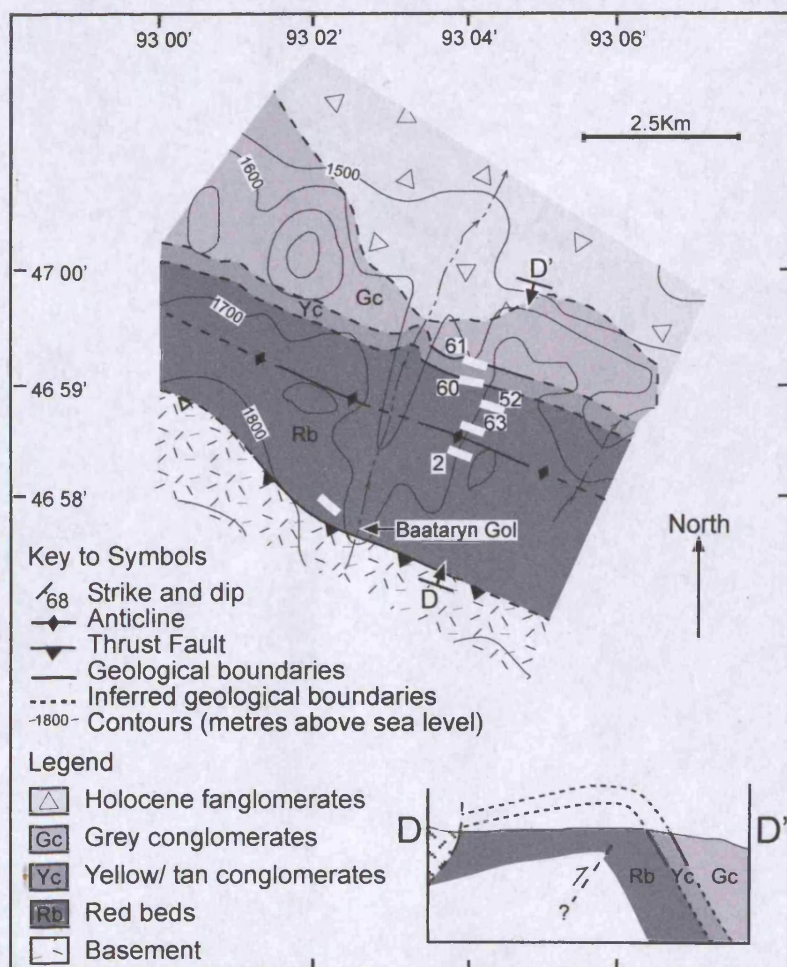
Field data were collected during August 2000 from two locations within the southern Dzereg Basin (Fig. 3.4, 3.7 and 3.8). These locations were chosen following analysis of Landsat images and identification of areas containing recently deformed Cenozoic basin fill. The basin stratigraphy is best exposed in a series of uplifted ridges and incised gullies on the northeast side of the Dzereg Basin. On the southwest basin margin, exposure is more limited (Figs. 3.6a and 3.6b). The chronostratigraphy published by Devjatkin *et al.* (1975), Devjatkin (1981) and Rasnitsyn (1985) is used to correlate units across the basin. The specific fossil data that constrain the age of each major stratigraphic unit are listed in Appendix 1. The stratigraphy is described upwards from the oldest sediments.

Table 3.1 summarises the facies identified within the field area. Facies codes are the authors own and do not correspond with existing facies systems (e.g. Miall, 1996) because no present system documents the range of facies identified. Table 3.1 contains four broad groups of facies: 1) alluvial fan sheetflood facies (facies AC and AF), 2) fluvial/overbank facies (facies BC-F), 3) mass flow deposits (Facies G and H), 4) lacustrine facies and related deltas (facies I to M). The letters C and F following a facies code indicate coarse and fine end members of particular facies.





**Figure 3.7** - Detailed geological map of the NE side of the Dzereg basin. The geology is dominated by northeast vergent folds and thrust faults which deform Mesozoic-Cenozoic basin fill. Location of map is shown in Fig. 3.3. A prominent asymmetric fold (Fig. 3.9a) shown in section A-A' continues to the northwest where it is cut by a northeast-directed thrust fault. This thrust fault is interpreted to be blind at the line of section A-A'. The unconformable contact between the Lower Red Bed Unit and the Oasis Unit (Fig. 3.9) is traced for only 150m, and these two units were mapped together.



**Figure 3.8** - Detailed geological map of the SW Dzereg basin. The geology is dominated by a northeast vergent anticline which exposes Mesozoic-Cenozoic basin fill. Location of map is shown in Fig. 3.4.



Table 3.1 – Facies chart for major stratigraphic units identified in the Dzereg, Dariv and Shargyn basins.

Facies	Description	Process	Interpretation
AC	Erosive base. Laterally extensive pebble sheets, massive or upward fining, clast supported and <60 cm thick. Occasional lamination or cross-stratification.	Fining upward indicates waning flow during deposition and lateral extent suggests a broad unconfined flow. Usually associated with Facies AF.	Coarse sheetflood deposit. Massive beds may be hyperconcentrated gravity flow deposits
AF	Sharp, often erosive base. Occasional basal pebble/granule lag overlain by a fining upward sandstone succession. Some/all of a characteristic vertical sequence of sedimentary structures: Laminæ, planar or trough-cross stratification, laminæ, massive sandstone. Upper surface may be rippled. Associated with facies EF/EC.	Basal lamination representing upper phase flow overlain by fining upwards sandstone and structures characteristic of waning flow.	Sheetflood deposit.
BC	Massive clast-supported cobble/pebble conglomerate with some interbedded sandstone. Laterally extensive <3 m thick. Rare normal grading. Interbedded with facies AF.	Lateral migration of a cobble dominated channel system. Reworking of sedimentary structures and little preservation of overbank material (Facies AF and EF).	Deposits of a coarse bedload braided river system on a fluvial or alluvial fan.
BF	Massive laterally extensive pebble conglomerate and sandstone sheets with many internal erosion surfaces. Abundant imbrication and cross-stratification and occasional normal grading.	Variable clast size and complex internal structure results from the migration of channel macroforms within a braided gravel-bed river system.	Deposits of a braided river system.
C	15-30 cm thick pebble conglomerate with minor erosive bases and rare cross-stratification. Grade laterally into coarse sandstone. No internal erosion surfaces.	Coarse sediment deposited over the floodplain during a flood event. Slightly channelised base indicated more confined flow than facies AF and AC.	Crevasse splay deposit.
D	Well-defined channels containing clast supported pebbles (rarely cobbles) that fine up between internal erosion surfaces. Interbedded with sandstone sheets. Cross-stratification, lamination and deformation of underlying strata are common. Occasional silt (facies EF) drapes.	Bedload gravel and sand transport in a fluvial system with variable discharge. Gravel and sandstone bodies record the migration of bedforms. Intermittent siltstone (facies EF) horizons indicate flow was ephemeral.	Deposits of an ephemeral, sinuous mixed-load river. Massive beds may represent hyperconcentrated flood gravels.
EF	Intermittently laminated siltstones and rare mudstones. Containing organic material. Large colour variations.	Slow setting of silt from suspension after inundation of the floodplain. Primary lamination is commonly reworked by bioturbation and rooting. Colour variation records hydromorphic processes in action on the floodplain.	Overbank deposits.
EC	Massive silt-rich sandstone or sand-rich siltstone sheets often containing matrix-supported granules.	Deposition either by (1) transport of clay within fluvial systems as sand-grade aggregates (Nanson <i>et al.</i> , 1988; Talbot <i>et al.</i> , 1994), where post depositional breakdown of the aggregates produces a matrix supported sand rich siltstone (2) muddy debris flow (3) reworking of interbedded sandstone and siltstone by bioturbation. These options cannot be distinguished without microscopic analysis of the sediment.	Overbank deposits or debrites.
F	Lenticular sand sheets containing extensive cross-stratification that are laterally extensive over 100's m. > 1 m high foresets are mantled with pebbles and granules with occasional pebble sheets.	Migration of sand-bed channel. Cross-stratification represents both the migration of 3D bedforms and preservation of bank attached foresets resulting in a broad range of measured palaeocurrent.	Deposits of a high sinuosity sand bed river system.
G	Coarsening upward clast supported granule/pebble or pebble/cobble conglomerate.	Deposit of a wet or hyperconcentrated debris flow from which the matrix drained after deposition.	Hyperconcentrated gravity flow deposits.
H	Pebbles and granules supported in a fine sand or siltstone matrix. Massive or coarsening upward.	Cohesive debris flow in which large grains are carried by a dense matrix.	Cohesive debris flow deposit.
I	Sandstone dominated sheets that fine upward from an occasionally pebbly base and contain structures indicating waning flow. Dish and pillar structures or laminations form the upper part of beds. Massive beds are rare and contain evidence of burrowing. Commonly interbedded with lacustrine fines (Facies J & K).	Fining upward with a structure indicative of waning flow suggests the influx of coarse sediment into a lake as an individual flood event. This facies represents sheetflood facies AF entering a lake.	Deposits of a sheetflood entering a lake.
J	Very well laminated siltstone and claystone often showing fine variations between lamina. Individual laminations have a large lateral extent in good exposure. Can be associated with gypsum horizons.	Slow settling of silt or clay particles from suspension in the water column. Background sedimentation with the variation in lamination picking out periodic changes in climate or water column composition. Lack of bioturbation put down to anoxic bottom waters or elevated salinity. Gypsum horizons are precipitated from concentrated water, water concentration varies.	Lacustrine deposits recording conditions hostile to burrowing benthic organisms.
K	Massive siltstone and claystone, occasionally micritic. Sometimes associated with gypsum horizons.	Reworked lacustrine sediments often associated with gypsum. Lamination removed by either sub-aqueous burrowing – suggesting conditions supported benthic life or sub aerial exposure, often difficult to establish which. Gypsum deposited during concentration of water by evaporation.	Lacustrine deposits reworked by burrowing organisms or hydromorphic processes.
Facies association L	LA Coarsening upwards interbedded sandstone and laminated, massive or bioturbated siltstone. Sand beds have sharp planar bases.	Distal influence of prograding fluvial system into lacustrine environment. Preservation of lamination implies anoxic conditions. Bioturbated or massive siltstones suggest oxic conditions.	Prodelta deposits.
	LB Massive or coarsening upward sandstone with low-angle planar lamination or cross-stratification. Commonly affected by small-scale soft sediment deformation e.g. dish and pillar structures and minor slumping.	Deposition of sandstone over the delta surface. Slumping and dish and pillar structures form due to loading of saturated prodelta sediments.	Delta front deposits.
	LC Large (>1 m) trough cross-stratified sandstone beds with erosive bases, often with lag surfaces and occasional siltstone drapes.	The migration of mouth bars close to the mouth of the fluvial system. Silt drapes suggest periodic pauses in fluvial input, possibly seasonal.	Mouth bar deposits.
	LD Ripple cross-stratified sandstone with a coarse lag surface, commonly bioturbated.	Reworking of abandoned delta surface by wind derived currents into ripples etc. Lag surface results from continual reworking of sediment and winnowing of coarse fraction. Bioturbation affects the surface if it is exposed for extended periods.	Reworked delta top deposits.
	LE Erosive based conglomerate sheets and interbedded fine sediment (Facies EF). Commonly hard and resistant to erosion due to intensive caliche formation.	Sub aerial deposits on the delta top. Laterally extensive channels reflect channel migration and the extensive carbonate concretion indicate long-term exposure and non-deposition.	Delta top deposits.
M	Micritic limestone containing ostracods and gastropods.	Deposition of calcium carbonate in a temporary lake environment.	Temporary lake deposits.

### 3.6.1 Jurassic

The oldest sediments within the Dzereg Basin are coarse, well indurated conglomerates best exposed at the southern end of the basin and outside the area described in this paper (Fig. 3.5). Sjostrom (1997) reported a 1180 m thick, upwards fining Lower-Middle Jurassic succession comprising 640 m of red, clast-supported, subrounded conglomerate with an increasing sandstone component upward. This is overlain by sandstones and siltstones with occasional coal horizons. Palaeocurrent data indicate source areas were both to the northwest and southeast (Sjostrom 1997).

### 3.6.2 Lower Cretaceous (Yellow Sandstone Unit)

#### 3.6.2.1 DESCRIPTION

The 180 m thick Yellow Sandstone Unit lies at the base of the studied section (Fig. 3.9) and is only exposed on the northeast side of the Dzereg Basin (Fig. 3.7). At one location, an indurated well-sorted, texturally mature granite clast conglomerate occurs stratigraphically beneath the Yellow Sandstone Unit (northeast of Fig. 3.7). However elsewhere, the base of the unit is bounded by a thrust fault (Fig. 3.6b) that places it in contact with Holocene fan conglomerates (Fig. 3.7).

Limited exposures in the lower 100 m of the Yellow Sandstone Unit reveal interbedded siltstones with thin (<30 cm) and locally thicker (5 m and 8 m) sandstone beds. Overall, sandstone bed thickness increases upwards. The upper 75 m of the Unit was studied in detail (Log NE1-Fig. 3.10).

---

**Figure 3.10** (following page) - Detailed graphic logs 1 and 2 for the NE Dzereg. Locations: Log NE1: N47° 08' 564'', E93° 03' 758''; Log NE2: N47° 08' 521'', E93° 03' 684''. Letters in facies column refer to Table 3.1.

Fig. 3.9a

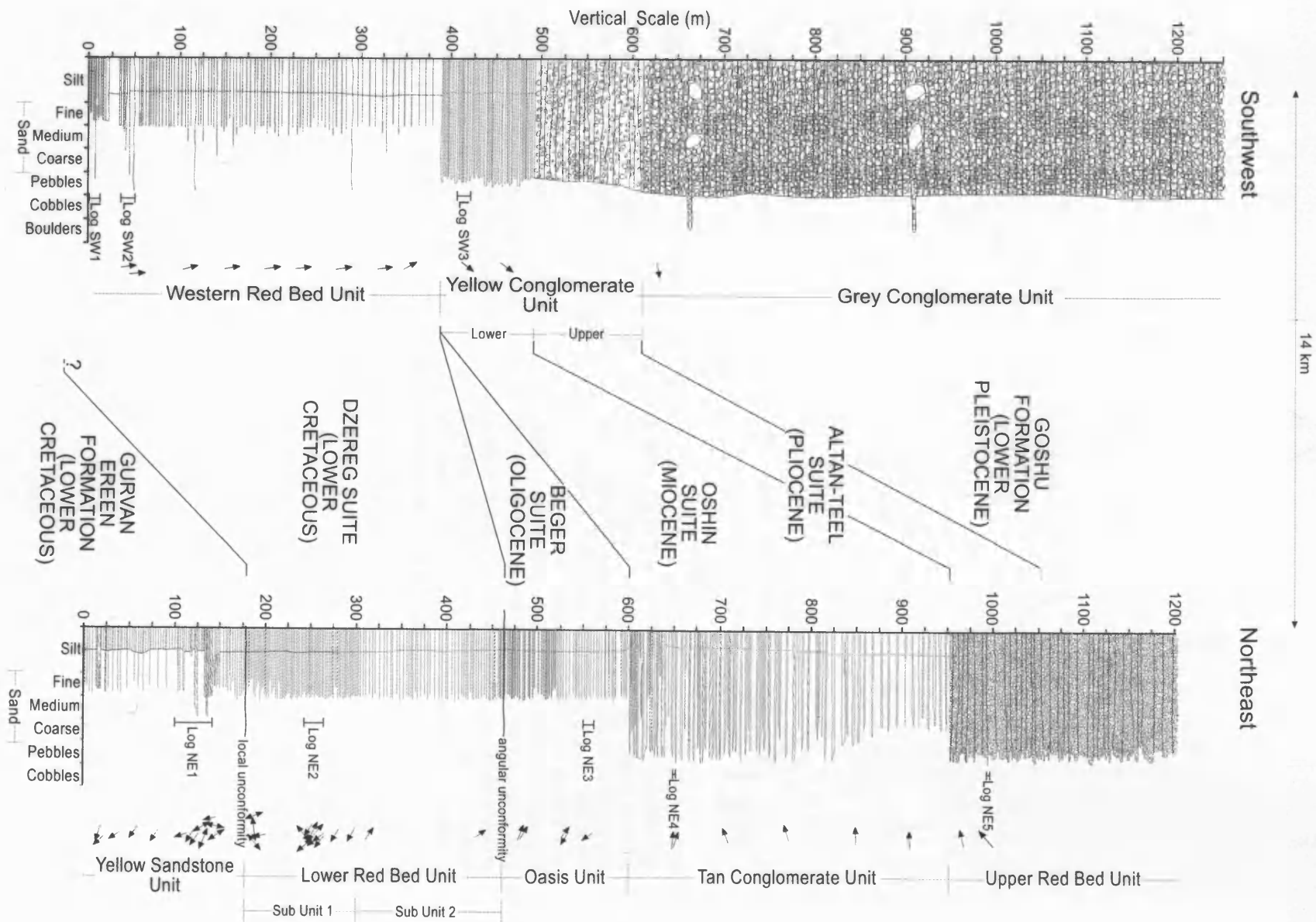
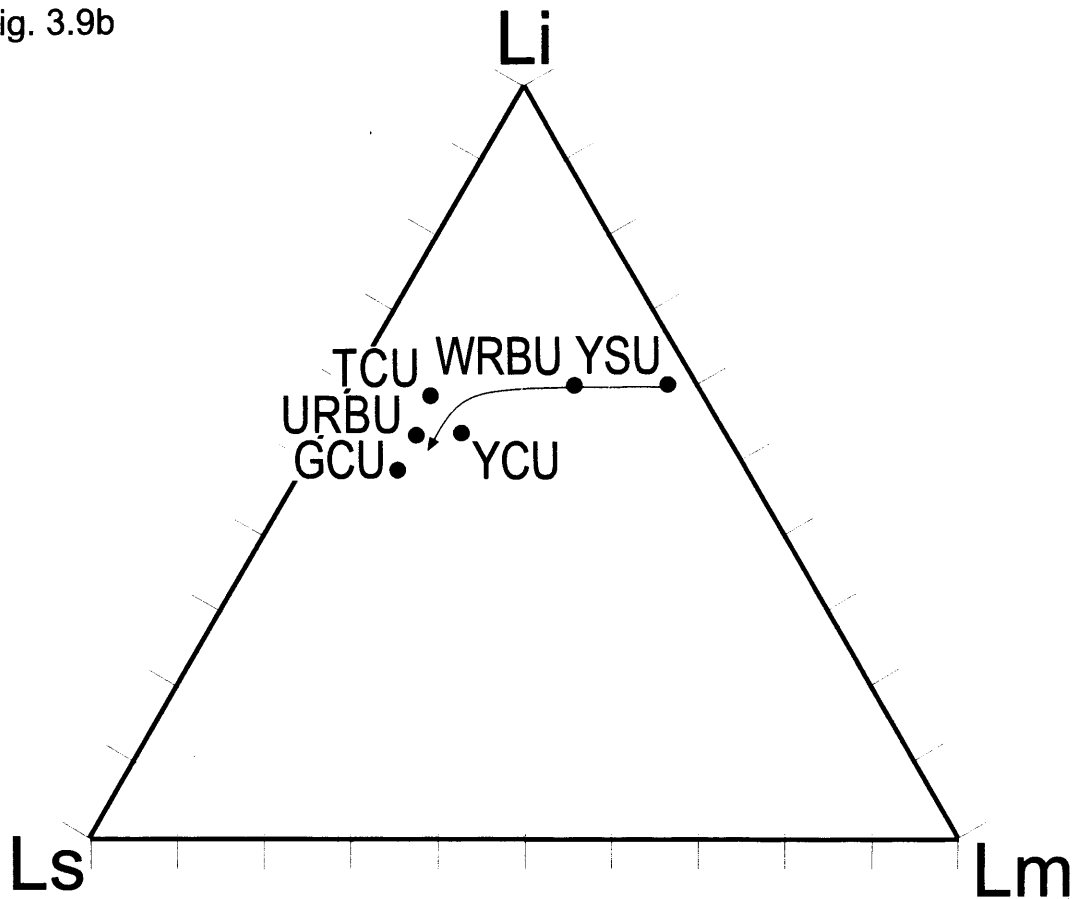
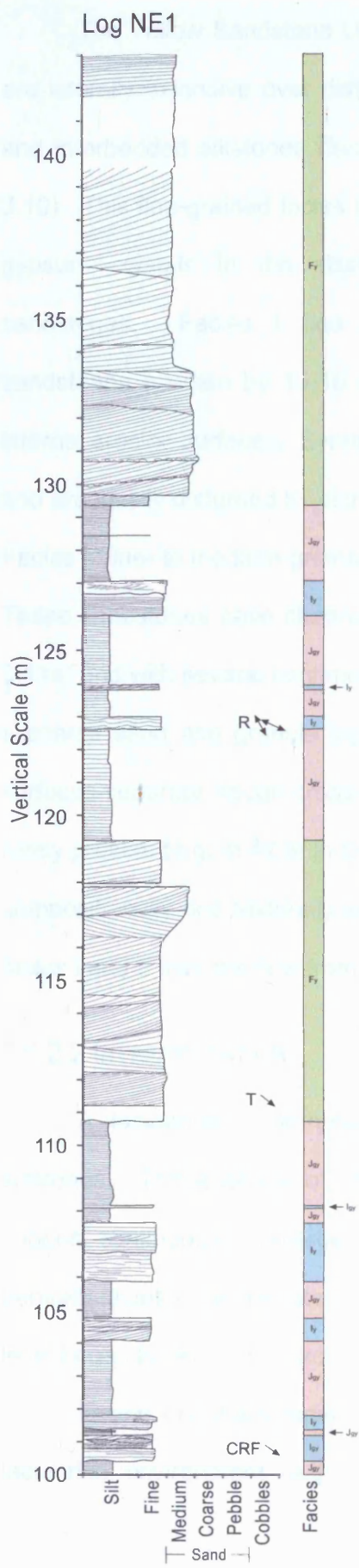


Fig. 3.9b



**Figure 3.9a** - Generalised stratigraphic sections for northeast and southwest study areas within the Dzereg Basin. Sections are from areas 14 km apart. See figures 3.7 and 3.8 for relevant geological maps. Stratigraphy is subdivided into separate units which correlate with formation names taken from Devjatkin, (1981). Ages of each formation are interpreted from fossil evidence (Devjatkin, 1981). Directions of palaeocurrent flow as well as positions of detailed logs are shown. **3.9b** - Ternary plot showing bulk composition for the main units. Li = igneous clasts, Ls = sedimentary clasts and Lm = metamorphic clasts. Individual points represent summary compositions based on thin section analysis and outcrop clast composition estimates. Note that the percentage of sedimentary clasts increases upwards in the succession as basin fill sediments are reworked during basin closure. Abbreviations are YSU = Yellow Sandstone Unit, WRBU = Western Red Bed Unit, TCU = Tan Conglomerate Unit, URBu = Upper Red Bed Unit, YCU = Yellow Conglomerate Unit and GCU = Grey Conglomerate Unit.





### Key for sedimentary logs

- Laminated sediments
- Cross-stratification
- Irregular laminations
- Laminated clay in silt
- Asymmetric ripples
- Pebble lag surfaces
- Clast supported conglomerate
- Matrix supported conglomerate
- Climbing ripples
- Convolute bedding
- Bioturbation
- Loading structures
- Water escape structures

### Paleocurrent measurements:

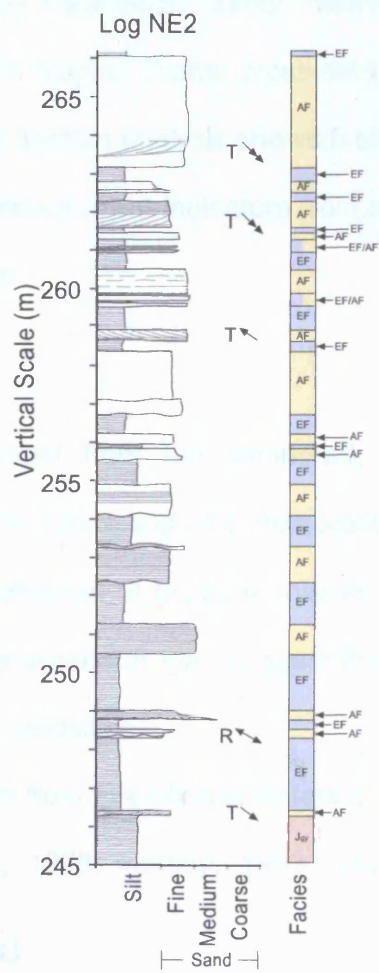
- Im - Imbrication
- T - Trough axis
- R - Ripple crest
- CRF - Climbing ripple foreset

### Facies colour

- AF
- AC
- BF
- BC
- D
- EF
- EC
- F
- H
- I
- J

### Sediment colour

- no letter - red
- gy - grey
- g - green
- y - yellow
- o - orange
- b - brown
- w - white





The Yellow Sandstone Unit comprises three facies (J, I & F; Table 3.1) that are laterally extensive over distances of 300-500 m. Laminated grey mudstones and interbedded siltstones (facies J) dominate the lower 29 m of log NE1 (Fig. 3.10). This fine-grained facies is interbedded with sandstone facies I and F. Rare gypsum crystals in the siltstones are generally present beneath facies I sandstones. Facies I fine sandstones comprise erosive-based, laminated sandstones overlain by 10-15 cm-thick trough cross-stratified sets separated by internal erosion surfaces. Symmetrical ripples are restricted to sandstone bed tops and are locally disturbed by dish and pillar structures and/ or traces of bioturbation. Facies F fine- to medium-grained sandstones dominate the upper 13 m of log NE1. These sandstones have channel-shaped, erosive bases tens of metres wide (Fig. 3.11a) and with several centimetres of local relief. The basal surface is overlain by a coarse sand and granule lag with siltstone intraclasts. Minor internal erosion surfaces separate trough cross-sets, 1-4 m in height. Planar cross-sets are more rarely present (e.g. at 42 m in log NE1). Thin section analysis shows facies F to be compositionally and texturally immature. Palaeocurrent indicators from sandstone facies I and F indicate flow from the northwest.

#### 3.6.2.2 INTERPRETATION

A lacustrine environment is interpreted from the laminated, facies J, siltstones. The absence of rootlet horizons, reddening and desiccation cracks suggest continuous submergence. The localisation of gypsum crystals (facies J) beneath facies I may be later diagenetic phenomena or may suggest that the lake level began to fall prior to facies I sandstone deposition.

Facies I is characteristic of deposition from sheetfloods entering a shallow lacustrine environment (e.g. Hardie *et al.*, 1978; Hartley, 1993; Miall, 1996).

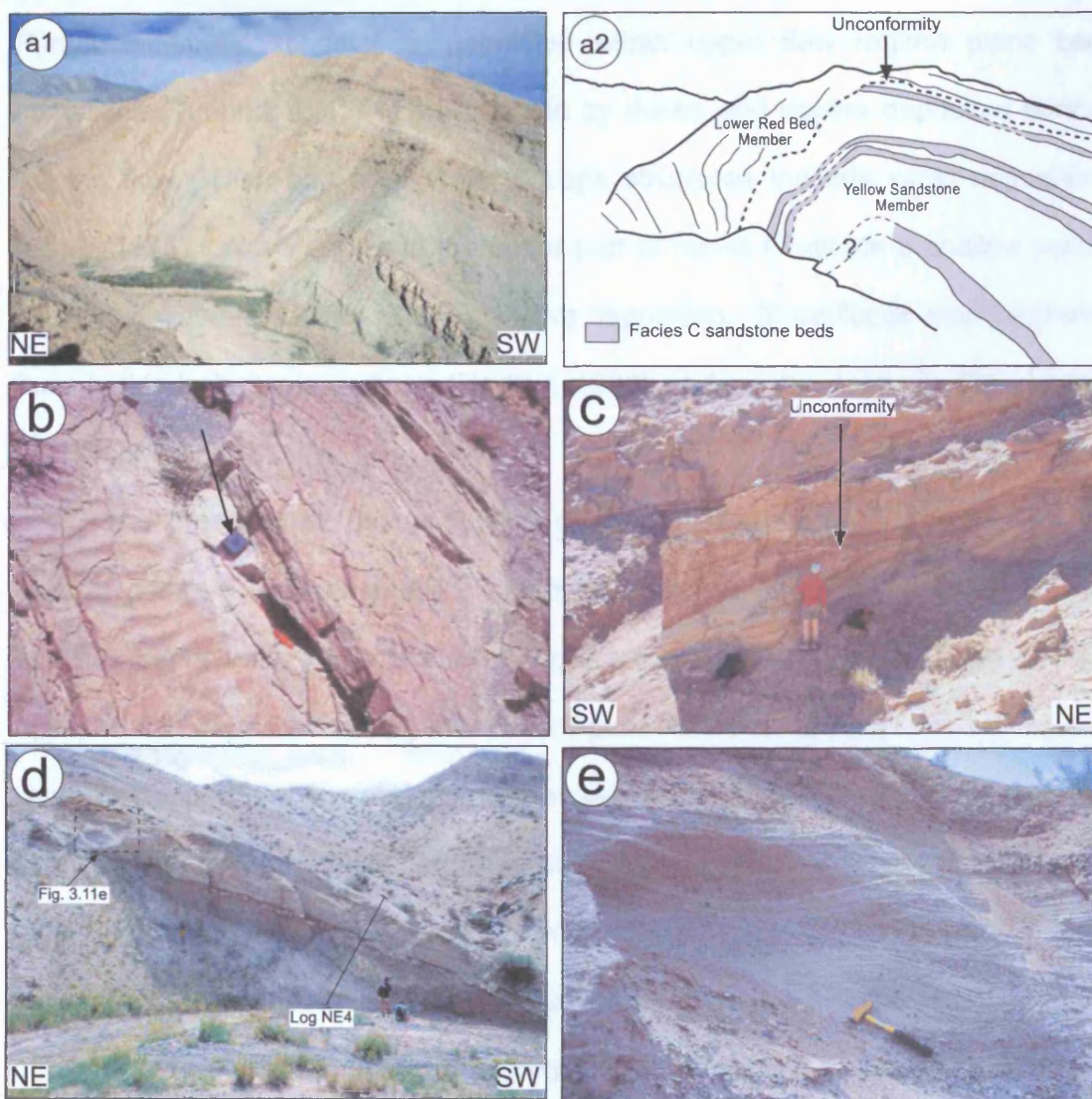


**Figure 3.11a1 & a2** - View and interpretation of the major anticline on the northeast basin margin showing the angular unconformity between the lower Cretaceous Yellow Sandstone Unit and the Lower Red Bed Unit. **3.11b** - Large sheets of symmetrical wave ripples in facies AF. Note the variation in ripple crest orientation over a few centimetres vertical section. (arrow points to compass = 8 cm long). **3.11c** - The angular unconformity between the lower Cretaceous Lower Red Bed Unit and the Oligocene Oasis Unit ( $N47^{\circ} 08' 306''$ ,  $E93^{\circ} 03' 579''$ ). The erosion associated with this unconformity can be traced in outcrop over 150 m and may relate to a regional planation event. **3.11d** - View of the Tan Conglomerate Unit showing a channel body (facies BF), the location of Log NE 4 and the location of Fig 3.11e. **3.11e** - Cross-stratified sandstone and conglomerate (Facies BF) in the lower Tan Conglomerate Unit.

Parallel-laminated sandstones, deposited within upper flow regime plane bed conditions (Tunbridge, 1981) are overlain by dunes and ripples deposited during waning flow. Dish and pillar water escape structures indicate rapid deposition (Lowe, 1975). Wave ripples in the upper part of facies I indicate a shallow water cover and wave-reworking following active deposition. Sheetfloods may originate from braided channels in flood (Hartley, 1993) or from the toes of alluvial fans (Hardie *et al.*, 1978).

The presence of poorly defined channels, basal mudstone clasts and a uniform palaeocurrent orientation suggest an alluvial origin for facies F cross-stratified sandstones. The lack of fine-grained overbank deposits suggests that facies F was deposited during intermittent peak flow events when channel banks were overtopped and fine material was eroded and transported downstream. The depositional environment is interpreted as a sinuous, shallow, sand-bed river (e.g. Miall, 1996; Williams, 1971; Parkash *et al.*, 1983; Kelly & Olsen, 1993). The western Eyre Basin (Australia) provides a modern analogue with bedload transport of sand grade material (here mud aggregates) occurring over wide areas as small channels increase in width to several kilometres during flood events (Williams, 1971; Gibling *et al.*, 1998). The presence of channels indicates a reduction in lake area, allowing the alluvial system to migrate over the exposed lakebed. The northwest-derived palaeocurrents represent an axial drainage.

The Yellow Sandstone Unit is equivalent to the lower Cretaceous Gurvan Ereen Formation (Togtoh & Baatarhuyag, 1991). The age is based on the presence of phyllopods, ostracods, molluscs, insects, fish (Devjatkin *et al.*, 1975; Rasnitsyn, 1985) and a small Ornithischian dinosaur (Khosbayar, 1973).

### 3.6.3 Lower Cretaceous (the Lower Red Bed Unit/ Western Red Bed Unit)

#### 3.6.3.1 DESCRIPTION

The unconformity at the base of the Lower Red Bed Unit is exposed only in a major fold on the northeast side of the basin. At this location, the uppermost thick sandstone bed in the Yellow Sandstone Unit (facies F) is truncated by an erosive-based channel (Fig. 3.11a). The 420 m thick Lower Red Bed Unit can be divided into two Sub-units (Figs. 3.7 and 3.9). The youngest Sub-unit correlates with a 380 m thick Western Red Bed Unit on the southwest basin margin (Fig. 3.9). These Sub-units contain four facies (AC, AF, EF & J; Table 3.1).

Sub-unit 1 is 130 m thick (Fig. 3.10, Log NE2). It is dominated by intermittently laminated red siltstone (facies EF), interbedded with facies AF sandstones with rare intervals of laminated grey siltstone (facies J). Facies AF comprises fine-to medium-grained, soft, nodular, red/ green sandstone with extensive sheets of symmetrical wave ripples (Fig. 3.11b). Ripple crest orientation varies dramatically over a few centimetres of vertical section. Facies AF sandstones have sharp basal contacts with facies J and EF and fine upwards. The thickest facies AF sandstone beds are erosive. Paleocurrent data indicate consistent southeast flow within Sub-unit 1.

Sub-unit 2 represents the top 160 m of the Lower Red Bed Unit on the northeast basin margin (Fig. 3.9). Thick (5 m) laminated red/brown siltstone intervals with desiccation horizons (facies EF) and subordinate grey/green siltstones (facies J) dominate Sub-unit 2. Well-sorted, soft, sandstones (facies AF) commonly contain cross-stratification, mud lenses up to 2 m wide and faint

bioturbation in their upper part. Facies AF beds are rarely erosive-based, but locally overlie an upward coarsening sandy mudstone interval (facies EF).

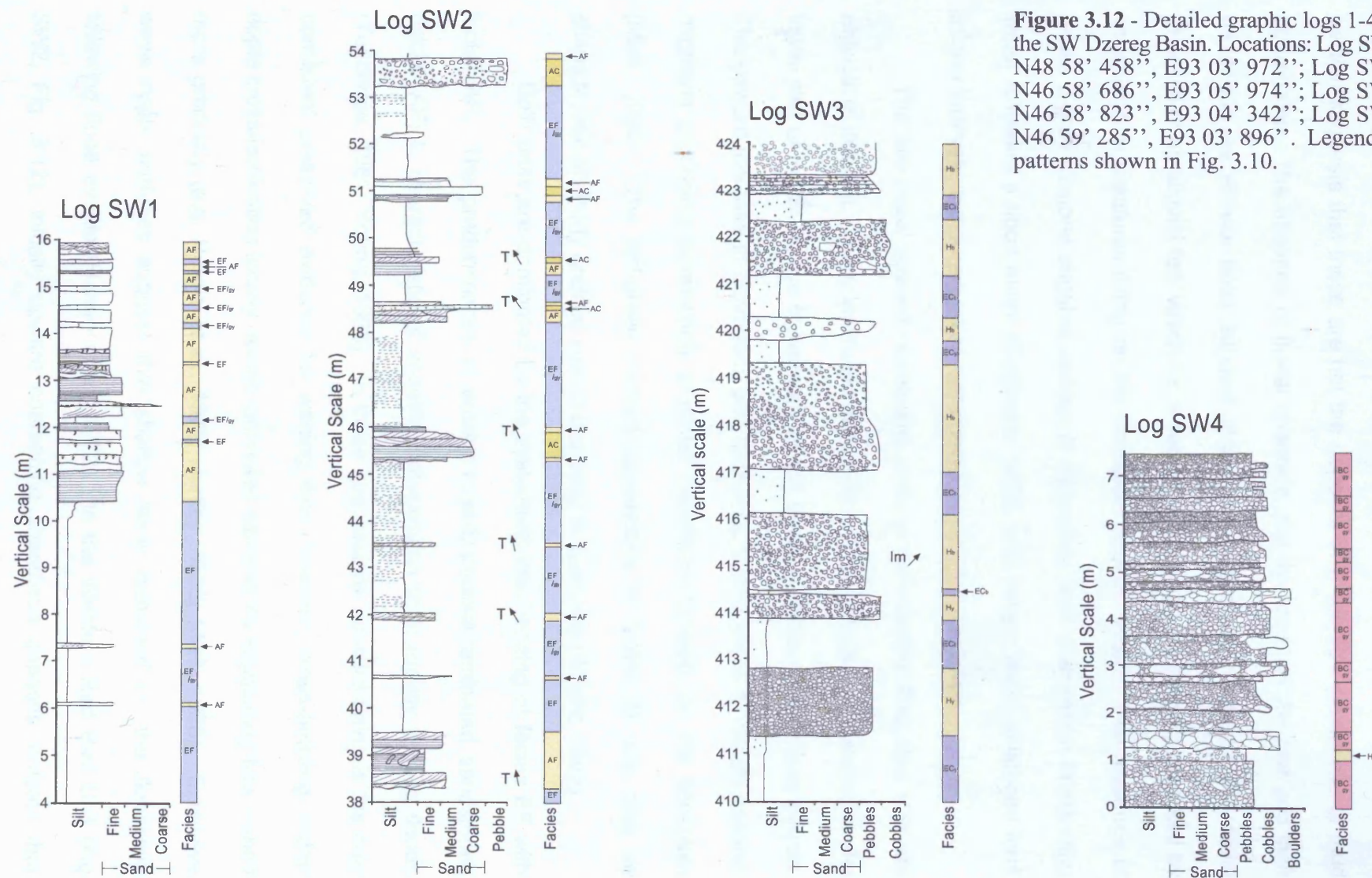
The 380 m thick Western Red Bed Unit represents the equivalent stratigraphy on the southwest basin margin. Red/green siltstones (facies EF) interbedded at 2-4 m intervals with facies AF dominate the succession, which is similar to Sub-unit 2 of the Lower Red Bed Unit (northeast basin margin). The base of the unit contains two 12-14 m thick upward coarsening units (Log SW1, Fig. 3.12) and facies AC, an upward fining massive or trough cross-stratified pebble and granule conglomerate (Log SW2, Fig 3.12). Facies AC horizons are usually associated with facies AF. The Western Red Bed Unit is slightly coarser than its equivalent on the northeast basin margin,

Facies I sandstones contain a high percentage of volcanic lithic fragments, plagioclase, undulose quartz, mafic minerals and some clay minerals. Facies AC conglomerates consist of subangular grains dominated by volcanic lithic clasts (Fig. 3.9b). Palaeocurrent measurements in facies AF on both flanks of the basin show a consistent current orientation from the southeast.

### 3.6.3.2 INTERPRETATION

The red siltstone beds (facies EF) that dominate these units formed by the settling of silt from suspension following periodic inundation of a floodplain or a distal alluvial fan (e.g. Wright, 1992; Collinson, 1996). The absence of a consistent lamination may result from one of three processes: 1) Continental red beds are prone to biological reworking which can effectively mix original lamination. 2) Mud transported as aggregates (e.g. Rust & Nanson, 1989; Nanson *et al.*, 1986) would deposit sediment with a clotted texture and limited lamination (Talbot *et al.*, 1994). 3) The sediments may have been deposited by a mass flow process, which would





not produce laminae. The presence of intermittent lamination throughout the section suggests that these are not the deposits of mass flow processes or mud aggregates. The absence of fluvial channels, the thickness of the unit and their deposition as alluvial fines suggest that these sediments represent the distal deposits of an alluvial fan, which have subsequently been biologically reworked by vegetation or creatures living on the floodplain (Burch, 1992). The presence of facies J grey siltstone suggest periods of deposition from suspension in standing water following a flood event (Collinson, 1996) and, where these siltstones form thicker intervals, temporary lakes were developed on the floodplain.

The two basal upward coarsening units in the Western Red Bed Unit are atypical of this unit. Thinly laminated and ripple cross-laminated sandstones, in the lower part of log SW1, are interpreted as the distal deposits of rare flood events. The upward increase in sandstone bed thickness is interpreted to record channel migration producing increasingly proximal sheetflood deposits on the floodplain (Miall, 1996). The red-green mottled appearance of facies EF can also be characteristic of poorly drained soils in proximity to channels (Wright, 1992).

Both units are dominated by the systematic interbedding of facies EF with facies AF. The predominance of erosive-based, parallel laminated sandstones (facies AF) is characteristic of sheetflood deposition from rapidly waning floods (Tunbridge, 1981; Young, 1993). In these successions, upward fining is the only consistent preserved evidence for waning flow, however, cross-bedding and/or ripple cross-lamination locally overlie laminated sandstones suggesting flow waned more gradually (e.g. Hardie *et al.*, 1978; Hartley, 1993; Miall, 1996). Extensive wave ripple surfaces suggest that shallow lakes remained on the floodplain following flood events (Hardie *et al.*, 1978). In the Western Red Bed Unit (log SW2, Fig. 3.12), initially upward coarsening sheetflood deposits indicate that



inundation of the floodplain did not represent the peak flow period of the event. This is unusual, but Stear (1985) describes a flood event in the south-western Karoo region of South Africa where multiple floodwater pulses occurred within a single flood event in a sandy ephemeral stream. These floodwater pulses are attributed to the convergence of numerous smaller tributaries into a main channel, producing several flood peaks. The rare occurrence of pebble conglomerate beds (facies AC) may represent an especially energetic flooding event or a more proximal source.

The predominance of facies EF in Sub-unit 2 suggests deposition in a more distal environment that was reached by fewer sheetfloods, than in Sub-unit 1. Desiccation cracks and bioturbation provide more evidence for deposition on a subaerial floodplain environment. A major change in palaeoflow from northwest in Sub-unit 1 to southeast in Sub-unit 2 suggests that a new source area was uplifted at this time. The Western Red Bed Unit is significantly coarser than Sub-unit 2 of the Lower Red Bed Unit and is therefore interpreted to record a more proximal position in the fan system.

The Lower Red Bed Unit and Western Red Bed Unit are considered equivalent to the Dzereg (Zerik) Formation (Togtoh & Baatarhuyag, 1991) and its lithological characteristics are strikingly similar to the description of that formation given near Darvi (Fig. 3.2) by Sjöström (1997). The Dzereg Formation is reported as lower Cretaceous (Albian-Aptian) in age on the basis of fresh water molluscs, phyllopods and ostracods (Devjatkin *et al.*, 1975; Devjatkin, 1981; Rasnitsyn, 1985).

### 3.6.4 Oligocene (The Oasis Unit)

#### 3.6.4.1 DESCRIPTION

The 140 m thick Oasis Unit overlies an angular unconformity with the Lower Red Bed Unit on the northeast basin margin (Figs. 3.9 and 3.11c) and comprises four facies (AF, AC, D & EF; Table 3.1). Thick (3-4 m) erosive-based channelised sandstones (facies D) dominate the lower part of the unit and are usually preceded by 1-2 m of interbedded siltstone (facies EF) and sandstone (facies AF). Facies D has a basal pebble and mudstone rip-up clast lag and local internal granule/pebble bands up to 10 cm thick overlain by massive sandstones. Up section, sandstones contain tabular cross-stratification up to 1 m in height separated by rare laminated and current ripple cross-laminated sandstones containing 1-2 cm diagenetic calcium carbonate nodules. Locally, mudstone lenses <40 cm thick occur within facies D.

Facies EF siltstones dominate the upper section of the Oasis Unit and are interbedded with sandstones (facies AF) and rare channelised sandstones (facies D). Facies AF forms thin (<20 cm) beds with climbing ripples whereas facies D sandstones contain dish and pillar structures and load structures that intrude into silt layers. Facies EF beds contain calcium carbonate concretions on distinct horizons that become increasingly common upwards, especially where facies D is less common. Log NE3 (Fig. 3.12) characterises a sandstone-rich section that contains the only true coarse bed in the Oasis Unit; an angular clast-supported pebble conglomerate (facies AC). Palaeoflow indicators in the lower part of the Oasis Unit suggest a southeast source and those in the upper part suggest a northwest source.

#### 3.6.4.2 INTERPRETATION

The basal angular unconformity and time gap at the base of the Oasis Unit (Fig. 3.11c) records a regional late Mesozoic-early Cenozoic period of tectonic quiescence and peneplanation. The older Mesozoic sediments dip 20° more steeply towards the basin than the overlying Cenozoic sediments. The Oligocene Oasis Unit marks the onset of renewed tectonism in the Altai region.

Shallow sandstone-dominated channels with gravel lags (facies D) in the lower part of the Oasis Unit are interpreted as deposits of shallow streams that are characteristic of the medial to distal portions of alluvial fans (Miall, 1996). The lack of channel incision into older channels and the aggradational character suggests that significant accommodation was available. Large tabular cross sets within the channels represent the migration of bars. Soft-sediment deformation indicates that some of the channels migrated rapidly onto saturated interchannel deposits. Facies D channels within the lower part of the Oasis Unit represent a more proximal alluvial environment than the Lower Red Bed Unit, but facies EF siltstones become more important upwards, indicating an increasingly distal environment. Extensive carbonate concretions are interpreted as calcretes developed in overbank deposits. An increasing abundance of calcrete surfaces, suggesting lower rates of sedimentation, correlates with a decrease in channel density suggesting an increased distance from major channels allowed prolonged pedogenesis (e.g. Wright, 1992). The upper part of the Oasis Unit does not contain channelised sandstones and is dominated by sheetflood deposits (Facies AF & AC). Paleocurrent data indicate that the channels originated in the southeast whereas the subsequent sheetfloods originated in the northwest.

The channelised beds may indicate northwards progradation of the southerly sourced fan system that deposited the Red Bed Unit and Western Red

Bed Unit. Alternatively, initial uplift of Sutai Uul (Fig. 3.3) in the south (represented by the basal unconformity?) may have created a new, more proximal source area. The change to sheetflood-dominated sedimentation in the upper Oasis Unit is interpreted as a decrease in sediment supply from the southern alluvial fan.

The Oasis Unit corresponds lithologically to the Beger Suite (Devjatkin, 1981) which is Oligocene in age based on varied fauna found in the Dzereg Basin. The dominant species in the unit are the micro-mammals (including *Cylindrodontitae*, *Cricetidae*, *Rhizomyidae* and *Ctenodactylidae*; Devjatkin, 1981).

### 3.6.5 Miocene (Tan Conglomerate Unit/ Lower Yellow Conglomerate Unit)

#### 3.6.5.1 DESCRIPTION

The upward fining, 350 m thick Tan Conglomerate Unit conformably overlies the Oasis Unit on the northeast basin margin (Fig. 3.9). Facies BF erosive, matrix-supported, cross-bedded channelised conglomerates dominate the base of the unit (Figs. 3.11d and 3.11e). Clasts are <3 cm in size and include granite, quartzite, phyllite and volcanic lithologies (Fig. 3.9b). Channel fills are 10-20 m wide with preserved channel depths of 30-100 cm and are in erosive contact with fine-grained, green, cross-stratified, channelised sandstones. Facies EF laminated siltstones, with common calcium carbonate nodule horizons, first occur 20 m above the base of the unit and are deeply incised by basal erosion surfaces associated with facies BF (Figs. 3.13a and 3.13b). The middle section through the unit, has minor soft-sediment deformation affecting facies EF (log NE4, Fig. 3.14). Isolated wide, shallow channels (facies D) within silt units (facies EF) dominate the upper section. Facies D sandstone channels are 10-20 m wide and 2-3 m deep with >1

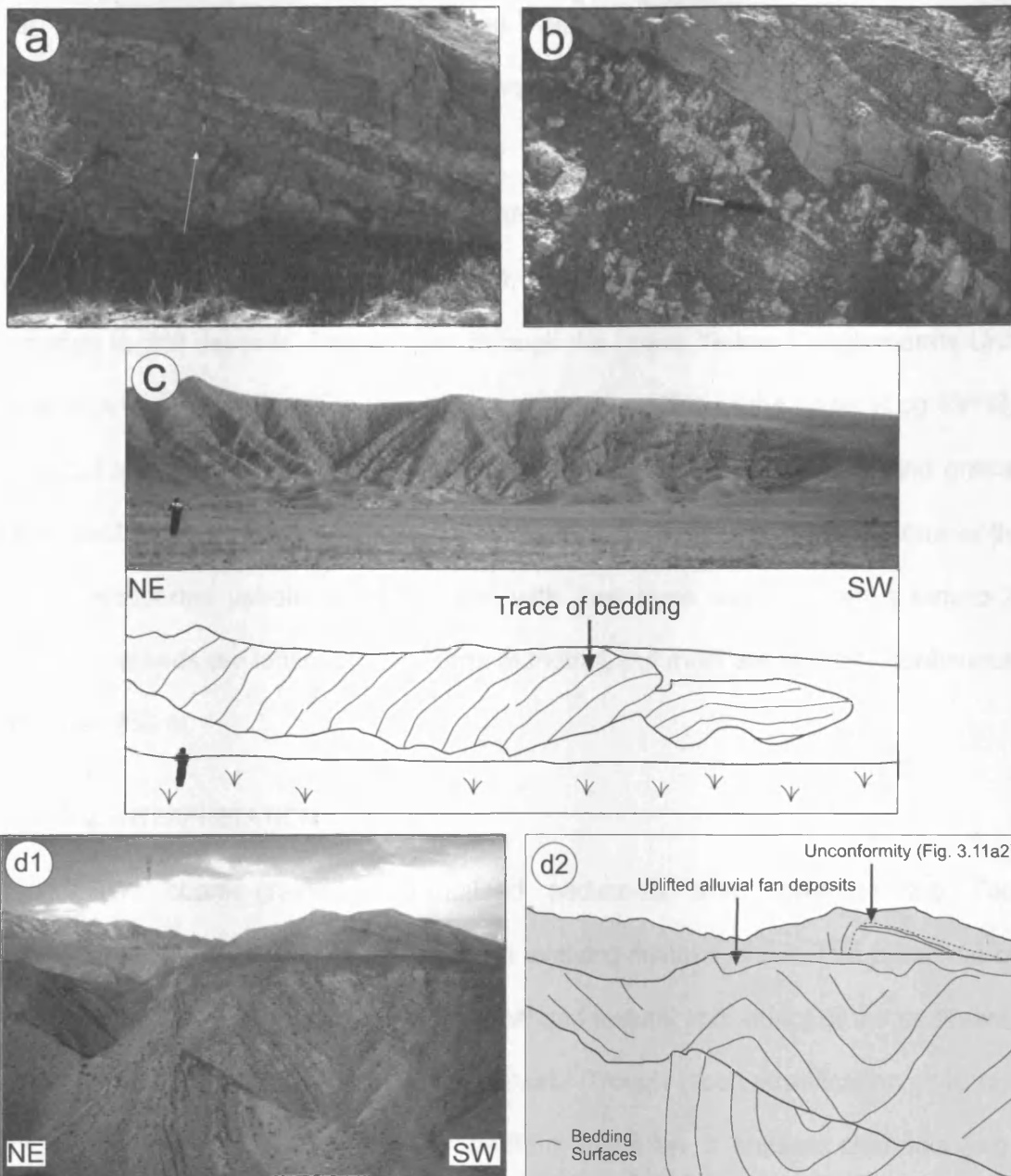


**Figure 3.13a** - Erosive contacts between facies BF and EF within the Tan Conglomerate Unit. Hammer for scale (length 30 cm). **3.13b** - Calcrete horizons within facies EF in the Tan Conglomerate Unit. Facies BF sandstone overlies an erosive contact. **3.13c** - Asymmetric anticline on the southwest basin margin interpreted as a fault propagation fold above a blind thrust. **3.13d1 & 2** - View and interpretation of the variation of folding along strike. Three anticline-syncline pairs replace the single large anticline-syncline pair (Fig. 3.10a) in the distance.



m high 25-30° foresets orientated perpendicular to channel margins. Palaeocurrents within the Tan Conglomerate Unit are consistently from the east.

The lower Yellow Conglomerate Unit on the southwest basin margin is equivalent in age to the Tan Conglomerate Unit of the northeast basin margin (Fig. 3.9). The basal contact is not exposed, but it can be located by a sharp colour change in drift deposits. The section through the Lower Yellow Conglomerate Unit was examined in only one location on the southwest side of the basin (Log SW13, Fig. 3.13c). Facies EC, silty clays contain isolated matrix-supported sand grains and pebbles that increase in abundance upwards. Facies H is a predominantly matrix-supported pebble conglomerate, with clast sizes ranging from 5 mm to 2 cm. Some beds are lenticular over tens of metres, but most are laterally continuous for over 250 m.

#### 3.6.5.2 INTERPRETATION

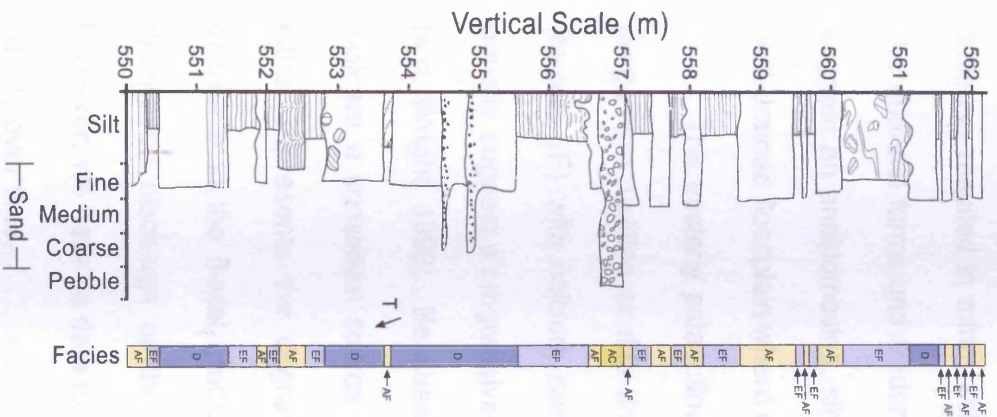
The coarse-grained channelised sediments that dominate the Tan Conglomerate Unit were deposited in an evolving fluvial system. The presence of phyllite clasts and the overall mineralogical and textural immaturity of the sediment, suggest that transport distances were short. Trough cross-stratification (<40 cm high sets) in BF are interpreted as bedform migration in shallow channels (e.g. Miall, 1996), with conglomeratic bodies deposited during peak flow conditions. The lower part of the Tan Conglomerate Unit is interpreted as braided river deposits with minimal preservation of overbank deposits.

Channels with bank-attached foresets orientated perpendicular to

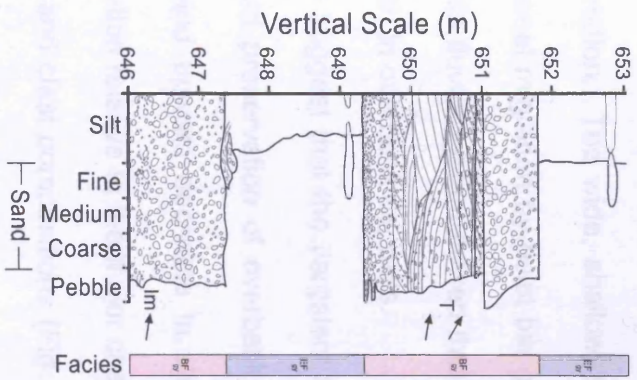
---

**Figure 3.14** (following page) - Detailed graphic logs 3-6 for the NE Dzereg basin. Locations: Log NE3: N47° 08' 190'', E93° 03' 499''; Log NE4: N47° 07' 944'', E93° 03' 286''; Log NE5: N47° 07' 521'', E93° 03' 151''; Log NE6: N47° 07' 237'', E93° 03' 142''. Legend for patterns shown in Fig. 3.10.

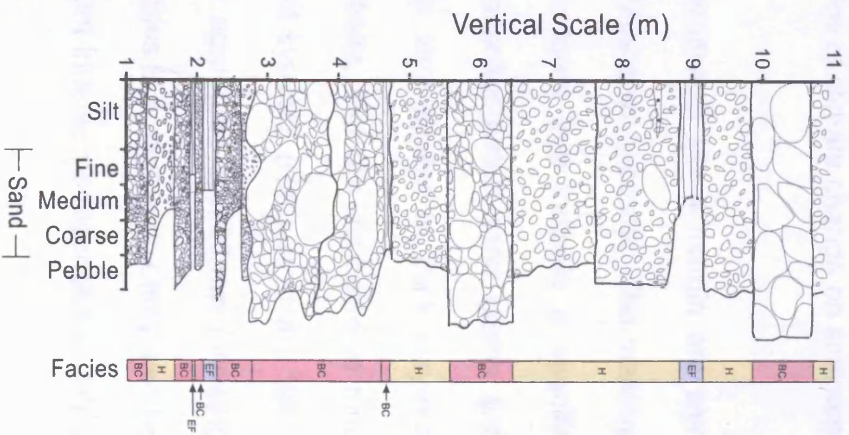
# Log NE3



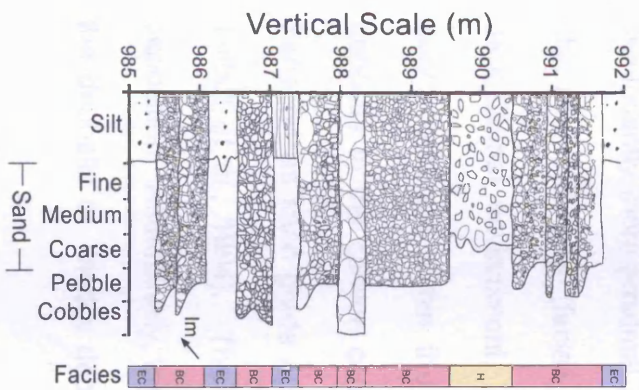
# Log NE4



# Log NE6



# Log NE5



palaeoflow (facies D) are interpreted to record pointbar migration. Channel bank collapse resulted in minor soft-sediment deformation. The wide, shallow, sheet-like channel forms and evidence for lateral channel migration by point bar growth suggest an anastomosing, sinuous stream. This fluvial system flowed through a well-drained floodplain where calcretes developed in overbank deposits.

The easterly palaeoflow data (Fig. 3.9a) suggest that the Jargalant Nuruu range was uplifted at this time. The increased preservation of overbank fines (facies EF) with calcium carbonate nodules and upward decrease in channel density suggest a progressively more distal location relative to the major channels (e.g. Wright, 1992). Because palaeoflow data and clast compositions (Fig. 3.9b) indicate a consistent source area within the Jargalant range, this upward trend either represents the degradation of the Jargalant range associated with a decrease in the fluvial gradient, or a change in the transport mechanism, e.g. decreased discharge or the avulsion of major channels away from the area. However, we have no data to quantify the influence of climate change on sediment supply over time.

The time-equivalent sediments on the southwest basin margin are also significantly more proximal than the underlying Mesozoic deposits. The massive clay-rich siltstones (facies EC) contain few features that indicate a specific depositional environment. The presence of matrix-supported sand grains and quartz granules within the clay-rich siltstone is very similar to thick clay-rich deposits in the canyon country, southwest Australia, that are attributed to mud transport as sand grade aggregates within fluvial systems (Nanson *et al.*, 1988; Talbot *et al.*, 1994). The texture results from aggregate breakdown following deposition. Alternatively, the matrix-supported grains in a mud matrix may also be the deposits of muddy debris flows or result from intense pedogenesis of thinly

laminated interchannel silts and sands. Further microscopic analysis of the nature of the grains would be required to distinguish between these three possibilities. Dependant on the mode of deposition microscopic analysis should allow the identification of remnant mud aggregates or any primary lamination or, their absence in the case of a debris flow deposit.

The matrix-supported conglomerates (facies H) are interpreted as debrites (e.g. Collinson, 1996; Nemec & Postma, 1993) based on the lateral extent of most conglomerate beds, limited imbrication and interbedding with fine sediment (facies EC). These debris flows were probably generated by rare but intense rainstorms that flushed out material stored in the catchment area (e.g. Collinson, 1996). The material flushed from the Dzereg Basin's catchment is mature with a significant proportion of well-rounded quartz grains. Facies H and EC were deposited on an alluvial fan from a south-western source, possibly the incipient Baataryn Range. An exact fan location cannot be determined for the mud aggregates and fine debris flows.

The Tan Conglomerate Unit and Yellow Sandstone Unit are referred to as the Oshin Suite by Devjatkin, (1981) and Sjostrom, (1997). The Oshin suite is thought to be Miocene, on the basis of mammal remains reported from the Dzereg Basin by Devjatkin (1981).

### 3.6.6 Pliocene and Lower Pleistocene (Upper Red Bed Unit/ Upper Yellow Conglomerate Unit/ Grey Conglomerate Unit)

#### 3.6.6.1 DESCRIPTION

The Upper Red Bed Unit has a conformable basal contact and comprises at least 400 m of poorly exposed conglomerate beds. The unit crops out on the south-western limb of a major anticline but is present as only a thin drape within an adjacent syncline (Fig. 3.7, section A-A'). Facies H, BC and EC (Table 3.1, Log NE5, Fig. 3.14) can be traced laterally over hundreds of metres. Massive, red-stained, clast-supported pebble/cobble conglomerates (facies BC) are preserved as 30 cm thick beds. Facies BC is locally massive, but generally fines upwards over 20-50 cm from a cobble lag into massive pebble beds between 40-100 cm thick. Facies H is a rare matrix supported pebbly sandstone which exhibits significant lateral variability. The conglomerate facies (H and BC) contain angular to subrounded clasts of variable composition including, quartz, volcanic rocks, diorite, phyllite, schist and small amounts of limestone (Fig. 3.9b). Localised lenses of poorly-laminated siltstone (facies EC) that are <50 cm thick and contain pebbles and coarse-grained sand interrupt the sequence. Rare imbrication, measured in facies BC, suggest a northeast source.

On the southwest side of the basin, the lower part of the Upper Red Bed Unit is equivalent to the Upper Yellow Conglomerate Unit (Fig 3.9). Massive-bedded conglomerates (facies H) with lenses of facies EC dominate the unit (Fig. 3.9). There are very few beds of clast-supported conglomerate (facies BC) within the Yellow Conglomerate Unit and all are associated with its gradational upper contact with the Grey Conglomerate Unit. The lateral extent of individual beds of

facies H is hard to establish due to limited exposure. Palaeocurrent data are rare, but some imbricated pebbles suggest flow from the southwest.

The Grey Conglomerate Unit is time equivalent to the upper part of the Upper Red Bed Unit (Fig. 3.9). Its gradational basal contact is placed where conglomerate facies BC begin to dominate the section. Facies BC has a highly variable clast composition, with clasts ranging from 2–40 cm in size. Bed thickness ranges from 15–20 cm for the pebble layers to >60 cm for boulder layers. In individual pebble beds predominantly clast-supported bases fine upwards into matrix-supported tops. Rare matrix-supported conglomerates (facies H) are also occasionally present.

#### 3.6.6.2 INTERPRETATION

The conglomerate-dominated Upper Red Bed Unit is coarser than any of the preceding units. Clast angularity and composition (including phyllite and schist, Fig. 3.9b) suggest short transport distances and the interpreted southwest palaeoflow indicates a sediment source within the proximal Jargalant Nuruu range northeast of the basin. Massive beds, and vertical grading (facies BC) combined with a low proportion of fine material (facies EC) are characteristic of a braided-stream dominated fluvial or alluvial fan setting (Nemec & Postma, 1993). Facies BC coarse cobble conglomerates (e.g. 2.5 and 3 m in log NE5) probably represent channel lag surfaces interpreted as the preserved traction load of a peak flood event. The massive pebble conglomerate layers are interpreted to be deposits of channel bars. Matrix-supported conglomerates (facies H) are present only once within log NE5 (4.5 m), and are interpreted as deposits from minor debris flows produced during fan surface reworking by rainwash processes, bank collapse or



unstable local slopes or stream flow processes. The fine deposits (facies EC) are a minor component and are characteristic deposits of muddy debris flows.

The overlying Grey Conglomerate Unit is dominated by facies BC interpreted to record channel lag surfaces and channel bar deposits within a braided system. A few beds (e.g. 1-1.3 m on log SW4-Fig. 3.12) are matrix-supported (facies H), and interpreted to be debrites (Collinson, 1996; Nemec & Postma, 1993). The similarity of these facies and their clast compositions with those of the modern alluvial fan sediments suggest a braided stream environment on a proximal alluvial fan derived from the adjacent Baataryn Nuruu range.

The lower section of the Upper Red Bed Unit represents the Pliocene Altan-Teel Suite in the Dzereg Basin. The Pliocene age is based on mammal remains and a few fresh water molluscs (Devjatkin, 1981). The Upper Yellow Conglomerate Unit is considered to be of Miocene age by Togtoh & Baatarhuyag (1991), although there is no supporting faunal evidence. We suggest that the upper conglomeratic part of the Yellow Conglomerate Unit is also the Pliocene Altan-Teel suite based on the significant facies change and the unit's similarities with sections described elsewhere in the flanking basins (Devjatkin, 1981). The upper part of the Upper Red Bed Unit and the whole of the Grey Conglomerate Unit are both regarded as Lower Pleistocene on the basis of mammal remains and belong to the Goshu Formation (Togtoh & Baatarhuyag, 1991 and Devjatkin, 1981). No evidence of a contact between the Altan-Teel suite and the Goshu Formation was observed within the Upper Red Bed Unit (Fig. 3.9).

### 3.6.7 Quaternary (Alluvial Fan Deposits)

Quaternary alluvial fans unconformably overlie the steeply dipping northeast and southwest sections. Each of the alluvial fan deposits has similar characteristics. Adjacent beds are highly variable in terms of grain size, degree of matrix support, thickness and lateral continuity, and all contain a proportion of sandstone and siltstone. Palaeocurrent indicators are rare, but limited imbrication suggests palaeoflow directly away from the respective mountain fronts. Crosscutting relationships between these fans and local structures are useful in constraining the timing of recent structural events. Clast compositions demonstrate reworking of older basin sediments into the Quaternary fan deposits.

On the northeast basin margin, the oldest fan forms a cap over all the high ground and has a basal angular unconformity with the Mesozoic and Cenozoic rocks indicating that the fan was deposited during or after the deformation and uplift of the Cenozoic sediments. A second fan infills the area between the folded and uplifted Cenozoic sediments within the basin and the mountain front (Fig. 3.4) but has now been displaced by the most recent northeast-verging thrust fault. The third and youngest sediments are represented by about 8 m of conglomerate in all present day gullies (Fig. 3.4 and 3.6a). The modern fan system incises and bypasses the older sedimentary units and deposits alluvial fans within the present day basin centre to the southwest (Fig. 3.4). Quaternary fan sedimentation on the southwest side of the basin occurred in two stages. The first alluvial fan infilled the area behind a major thrust ridge (Fig. 3.4 and 3.8) extending back to the mountain front in the southwest (Fig. 3.4). This has subsequently been incised by the modern fan system, which has cut a long, straight valley through the uplifted ridge to feed the modern fan near the basin centre (Fig. 3.4).

### 3.7 Structural geology of the study area

Active deformation within the Dzereg Basin is characterised by shortening on both sides of the basin in zones adjacent to the mountain front. On the northeast side of the Dzereg Basin, upthrusting along the southwest side of the Jargalant Nuruu range uplifted and deformed the Cenozoic sediments. Several faults are sharply defined and appear to be active. The major structure in the area is a prominent northeast vergent anticline-syncline pair (Figs. 3.7 and 3.11a). Along strike, this fold pair is modified and shortening is accommodated in different ways. For example, towards the northwest the major anticline is replaced by three smaller folds (Fig. 3.13d) and then faulted. The fault is expressed on the surface by a line of springs in three deep gullies and by a fault scarp cutting alluvial fan deposits. This fault is interpreted to be a northeast-directed thrust which places Cretaceous sediments over younger Miocene sediments. The fault is blind in the southeast where fault propagation folds (a prominent anticline-syncline pair) accommodate shortening. Another northeast-directed thrust occurs between the Jargalant range front and the fault described above. It cuts the surface of the alluvial fan and is marked by a line of springs. The clear geomorphological expression of this fault suggests it may be the most recently active intrabasinal fault. Upslope, the major range-bounding fault is a southwest-directed thrust previously documented by Cunningham *et al.* (1996a). Together these thrusts define a small triangle zone that (Cunningham *et al.*, 1996a) reported further southeast.

Small-scale tectonic structures are fairly rare. Sedimentary units are tilted, but otherwise not deformed away from the major thrusts and only a few minor folds were observed outside the fold and thrust zones.

On the southwest side of the Dzereg Basin, major faults and folds deform the basin fill and are clearly visible on Landsat images (Fig. 3.4). A km-scale asymmetric anticline verges towards the basin centre in the area of Fig. 3.8 (Fig. 3.13c). The fold is well exposed and is also expressed geomorphologically by tilted beds which define the surface topography of a small ridge (Fig. 3.4). Because of its asymmetric basinward vergence, this fold is interpreted as being passively driven by a blind thrust below. This fold is believed to be actively forming because modern incision by local streams is developed within the fold hinge, but not on the fold limbs. Other active deformation within the southern Dzereg Basin occurs along the southwest basin margin and within the basin interior further to the northwest where isolated ridges, bounded by sharp fault lines, can be seen on satellite imagery.

### 3.8 Discussion

The stratigraphic and structural data indicate that the present day Dzereg Basin is the product of two distinct evolutionary phases (Fig. 3.15). During the late Cenozoic, basin evolution was dominated by transpressional deformation associated with regionally extensive strike-slip faults and linked thrusts. However, our new structural and sedimentological data suggest that the basin initially formed during the Mesozoic in a different tectonic regime. The Mesozoic sediments are dominated by fine-grained terrestrial and lacustrine sediments with few preserved fluvial channels. Conversely, the Cenozoic deposits consist predominantly of coarse channelised sandstone and conglomeratic sheets interpreted to be of fluvial or alluvial fan origin.

The sediments comprising the lower Cretaceous Yellow Sandstone Unit were supplied to the Dzereg Basin via a low sinuosity, shallow, ephemeral, sand-

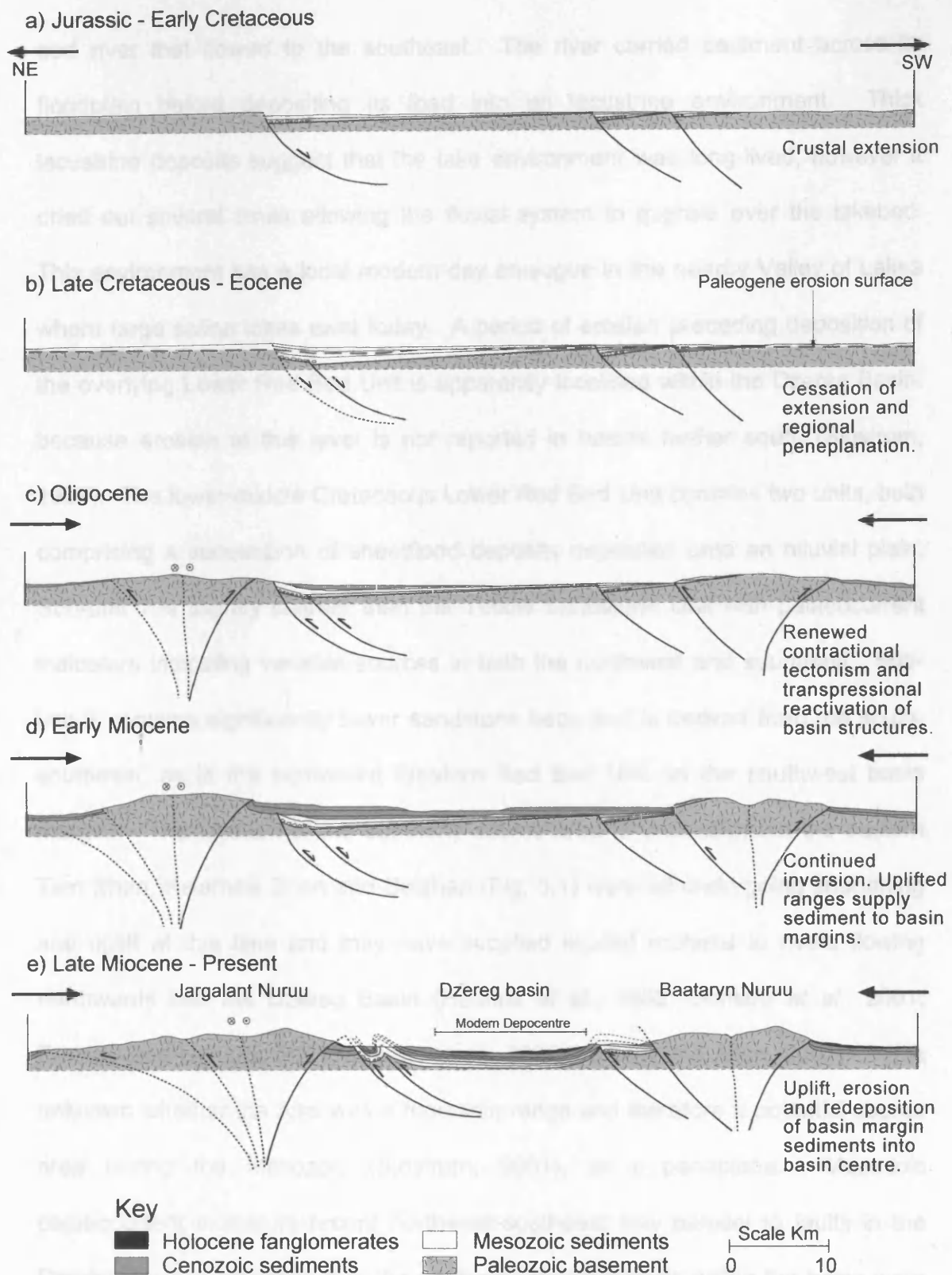


**Figure 3.15** - Cross-sections to show the interpreted evolution of the Dzereg basin from the Jurassic to the present day. a) Regional extension controlled the initial Jurassic – early Cretaceous basin formation. b) Tectonic quiescence and regional peneplanation occurred in the Paleogene. c) The onset of transpression and uplift of the Jargalant Nuruu and Baataryn Nuruu ranges and basin closure began in the Oligocene. d & e) Transpression continues to the present day with deformation stepping well into the basin from both margins leading to uplift, erosion and redeposition of Mesozoic and Cenozoic sediment downslope as the basin closes.

bed river that flowed to the southeast. The river carried sediment across its floodplain before depositing its load into an lacustrine environment. Thick lacustrine deposits suggest that the lake environment was long-lived, however it dried out several times allowing the fluvial system to migrate over the lakebed. This environment has a local modern-day analogue in the nearby Valley of Lakes where large saline lakes exist today. A period of erosion preceding deposition of the overlying Lower Red Bed Unit is apparently localised within the Dzereg Basin, because erosion at this level is not reported in basins further south (Sjostrom, 1997). The lower-middle Cretaceous Lower Red Bed Unit contains two units, both comprising a succession of sheetflood deposits deposited onto an alluvial plain. Sub-unit 1 is slightly coarser than the Yellow Sandstone Unit with palaeocurrent indicators indicating variable sources in both the northwest and southeast. Sub-unit 2 contains significantly fewer sandstone beds and is derived from the south-southeast, as is the equivalent Western Red Bed Unit on the southwest basin margin. The location of the southerly source area is uncertain, but the eastern Tien Shan, Kelameili Shan and Beishan (Fig. 3.1) were all undergoing shortening and uplift at this time and may have supplied eroded material to rivers flowing northwards into the Dzereg Basin (Hendrix *et al.*, 1992; Dumitru *et al.*, 2001; Dumitru and Hendrix, 2001; Greene *et al.*, 2001; Vincent and Allen, 2001). It is unknown whether the Altai was a mountain range and therefore a potential source area during the Mesozoic (Sjostrom, 2001), or a peneplane. Mesozoic palaeocurrent indicators record northwest-southeast flow parallel to faults in the Dzereg Basin, suggesting that the northwest trending faults within the basin were active in the Mesozoic and influenced the course of river systems and flow reversals (Fig. 3.15a).



The Cenozoic sediments are dominated by fluvial and alluvial fan deposits and with the exception of the Oligocene Oasis Unit, are coarse-grained, more proximal deposits than the underlying Mesozoic sediments. The Oasis Unit overlies an angular unconformity with the Lower Red Bed Unit indicating that a period of tilting and erosion occurred prior to Oligocene deposition (Fig. 3.15b). This unconformity is interpreted to be part of a regionally developed peneplanation surface recognised throughout the Altai region (Devjatkin *et al.*, 1975). The thick sandstone beds and associated siltstone facies that dominate the Oasis Unit are interpreted to be deposits of a shallow sand-dominated, ephemeral stream on the margins of an alluvial fan. Palaeocurrents in the Oasis Unit are comparable with Mesozoic source areas in the northwest and southeast, however the nature of the sediments and their interpreted environment of deposition do not support a distant Altai source region. Instead, we suggest that the Sutai range, which lies directly southeast of the Dzereg Basin, provided a local sediment source for the lower section of the Oasis Unit (Fig. 3.3). The Sutai range contains the highest mountains in the region and supplies sediment to the southernmost Dzereg Basin today. It is located at the transpressional termination zone of the regionally important Tonhil fault (Fig. 3.3) and connects with the Baataryn Nuruu range to the northwest (Fig. 3.3). The Sutai range is higher, broader and has accommodated greater shortening than the Baataryn Nuruu range and is therefore believed to have been the site of initial Cenozoic uplift southeast of the Dzereg Basin. In contrast, in the upper part of the Oasis Unit palaeocurrent data indicate renewed source areas in the Altai region to the northwest of the Dzereg Basin.

Palaeocurrent indicators in the fluvial sediments of the Tan Conglomerate Unit and the debrite dominated lower Yellow Sandstone Unit record easterly and south-westerly source areas, respectively. These units record the initial uplift of

the modern basin flanking ranges (Jargalant Nuruu and Baataryn Nuruu) during Miocene transpressional deformation along the Tonhil fault and at the termination zone of the Har Us Nuur fault (Fig. 3.15d). The sediment on both basin margins becomes increasingly conglomeratic through the Pliocene and lower Pleistocene.

Modern sedimentation is occurring in the central third of the basin where large individual fans and coalesced smaller fans are fed by ephemeral rivers (Fig. 3.15e). These rivers have incised through the deformed belts at the basin margins, are transporting eroded crystalline basement material from the flanking ranges, and are eroding Mesozoic-Cenozoic basin sediment from the folded and faulted ridges within the basin. Thus former basin-marginal sediments are being scavenged and redeposited in the basin centre as the basin closes.

*Did the Dzereg Basin initially form in a contractional foredeep environment?*

It is possible that the Dzereg Basin initiated as a depocentre associated with Mesozoic shortening and uplift of the Altai. However, to our knowledge, Mesozoic contractional faults have not been identified anywhere within the interior of the Mongolian Altai (Cunningham *et al.*, 1996a; Cunningham, 2002) nor were they documented in this study in the Dzereg Basin despite attempts to find them. The nearest documented Jurassic contractional tectonism is in the Tien Shan, Turfan Basin and northeast Junggar Basin area 250 km's to the southwest (Hendrix and Davis, 2001, and references therein). Therefore, it is uncertain whether the Altai was an elevated range that provided eroded material to the east in the Mesozoic. Mesozoic sediments today are not documented from the interior of the Mongolian Altai and are confined to a relatively narrow belt (approx. 30-40 km's wide) along the eastern margin of the range which includes the Dzereg Basin. Existing stratigraphic data for this belt do not support a foredeep wedge geometry typical of

contractional settings. However, little is known about the age and thickness of the sedimentary succession beneath the Valley of Lakes. Another possibility is that the Dzereg and other neighbouring basins initially formed as depocentres marginal to discrete thick-skinned basement cored uplifts similar to the Laramide basins of western North America (Sjostrom *et al.*, 2001). This interpretation also requires the existence of Mesozoic thrust faults in the Mongolian Altai.

*Was Mesozoic crustal extension responsible for initiation of the Dzereg Basin?*

An extensional origin for the Dzereg Basin appears to be better supported by local structural data. The northeast-vergent faults and folds on the northeast margin of the Dzereg Basin (Fig. 3.7) are opposite in both dip direction and vergence from the faults expected to develop in an evolving restraining bend setting (i.e., the faults root into the basin centre, not the adjacent mountain range). The faults are unlikely to be linked thrusts rooting into the southwest basin margin because the amount of displacement on each of the thrusts within the basin, as constrained by relative relief and uplifted fan surfaces, is interpreted to be of the order of hundreds of metres and not kilometres (Fig. 3.4 and 3.5). Therefore, there is no reason why multiple thrusts would form to accommodate northeast-directed compressional stress instead of continued thrust displacement on a single fault at the basin margin. In other words, it is unlikely that separate thrusts initiated and propagated forward into the basin without more significant thrust displacements and crustal thickening to the southwest. The geometry of faults and distribution of uplifted topography does not suggest that a critical taper was ever achieved within an evolving Cenozoic thrust wedge. We therefore suggest that the steep northeast-vergent thrusts and overlying folds within the basin may be reactivated older normal faults that formed during the Mesozoic (Fig. 3.15a). This could explain

why deformation is widely distributed, rather than localised only along the basin margins. Thus, we cautiously suggest that ongoing Cenozoic closure of the Dzereg Basin is by outward thrusting of the main range-bounding faults and inversion of older Mesozoic normal faults within the basin interior (Fig. 3.15e).

The suggestion that the major thrust faults within the basin are reactivated normal faults implies an extensional or transtensional tectonic regime in the Mesozoic. Several authors have reported evidence for a Mesozoic extensional event elsewhere in the region. Early Cretaceous extension and transtension are well documented in a broad east-west zone in south central and southeast Mongolia, and northeast China (e.g., Traynor and Sladen, 1995; Webb *et al.*, 1999; Johnson *et al.*, 2001). Upper Jurassic continental deposits are interbedded with basalt in the north-western Gobi Altai in western Mongolia (Shuvalov, 1969). Evidence for transtension within the Junggar Basin and Tien Shan during the late Permian-early Triassic is reported by Allen *et al.* (1995), however one or more Jurassic contractional events apparently followed (Vincent and Allen, 2001; Dumitru *et al.*, 2001). Likewise, Mesozoic extension in western Mongolia has been suspected (e.g. Sjostrom, 1997), but not previously established. However, within the Altai region there is now increasing evidence for Mesozoic extension. Cunningham *et al.* (1996a) reported structural evidence for a major pre-Cenozoic extensional event within the crystalline core of the high Altai west of the Dzereg Basin. Cenozoic thrust faults with pre-Cenozoic extensional histories were documented at two locations in ranges 130 km north of the Dzereg Basin by Cunningham *et al.* (2002). Sjostrom (1997) discussed the Mesozoic sedimentation of the Dzereg region and noted that the preserved sedimentary record is compatible with either a compressional foreland basin setting or extensional basin setting. Together, these results and our combined structural and stratigraphic data

permit the interpretation that Mesozoic extensional tectonism led to the initial development of the Dzereg Basin. This has potential implications for future work in the region, because it extends the previously reported zones of possible Mesozoic extension both west and north into western Mongolia. If widespread fault reactivation is present within both the Altai range and other flanking basins, this has important implications for understanding mechanisms of intracontinental mountain building in the region and the overall structural controls on the distribution of Cenozoic basins. These remain open questions and further work is needed to fully establish the extent of Mesozoic extension in western Mongolia.

### 3.9 Conclusions

In this study, we present new detailed sedimentary and structural data including geological maps and stratigraphic sections for the Dzereg Basin, western Mongolia. The Dzereg Basin is interpreted to have undergone a two-stage history based on differences between the Mesozoic and Cenozoic stratigraphy, palaeocurrent data and the geometry of structures within the basin. Mesozoic sediments are found within the modern basin, but not in bordering ranges suggesting that the modern Dzereg Basin is an inherited older depocentre. Palaeocurrent measurements indicate that Jurassic and Cretaceous sediments were supplied from distant sources in the northwest and southeast by rivers that flowed parallel to faults observed in the basin today, suggesting that these faults may have originated as Mesozoic structures (Sjostrom, 1997). The geometry of faults and folds within the basin and the distribution of Mesozoic sediments leads us to believe that the major faults may be inverted Mesozoic normal faults, and that prior to the onset of compression during the Miocene, the Dzereg Basin was controlled by an extensional or transtensional tectonic regime.

The Cenozoic stage of basin development began in the Oligocene and continues to the present. The basin is sandwiched between two actively forming transpressional mountain ranges which occur at the termination zones of major dextral strike-slip fault systems. Cenozoic sedimentation is dominated by coarse alluvial fan material shed from these ranges. The mountains are bounded by outwardly propagating thrust faults which deform the basin margins whereas within the basin, active folding and thrust faulting occur within two deforming belts on either side. The basin is actively closing, but is also receiving eroded material from adjacent ranges and uplifted deformed strata within the basin. This makes for a complex interplay between uplift, erosion and sedimentation. Two unconformities occur within the Cenozoic section. Modern sediments are deposited behind uplifted ridges of Cretaceous and Neogene strata and major ephemeral river systems, which have incised through the actively deforming belts, feed large alluvial fans in the basin centre.

The Dzereg Basin provides a rare window into the early stages of basin inversion and destruction in an intracontinental transpressional setting. Continued growth of the Altai will lead to further inversion and uplift of the basin sediments and result in erosion and redeposition of these sediments progressively closer to the basin centre. These competing processes of uplift, erosion, sedimentation and depocentre migration lead to a complex facies architecture which changes through time. Transpressional basins along modern transform boundaries, such as the Ventura Basin in southern California, may also have experienced an earlier history similar to that observed in the Dzereg Basin. For example, the Ventura Basin also contains folded and thrust stratigraphy, uplifted basement blocks along its margins, and multiple pulses of sedimentation, erosion and depocentre migration (Yeats *et al.*, 1994). Thus, the Dzereg Basin is a useful early-stage analogue for



workers interested in understanding the temporal and spatial evolution of other modern and ancient transpressional basins that are preserved in more advanced phases of development.

## Chapter 4

### Stratigraphy of the Dariv and Shargyn basins

#### 4.1 Introduction

Field data were collected within the Dariv and Shargyn basins during summer 2001 (Fig. 4.1). The region was divided into 8 areas, each containing exposures of the Mesozoic and Cenozoic sedimentary fill (Fig. 4.2). Each area was examined in detail and the stratigraphy correlated, as far as is possible, both with the other seven areas and with the Dzereg Basin to the north (Fig. 4.3). Exposure is inevitably associated with deformation related to late Cenozoic uplift of the Altai range. The fieldwork focussed on areas of unstudied exposure in order to maximise the volume of new data collected during the season. This study therefore provides a large volume of new data and also incorporates sedimentary logs and other sedimentological data that Sjöström *et al.* (2001) recorded from the Dariv Section (area 7, Fig. 4.2). The stratigraphy of the Dariv Basin is described from the oldest sediments upward. Palaeontological data used to constrain the stratigraphy are shown in Appendix 1. Each formation is first described at its type (best) locality and the lateral variation between sections is then discussed.

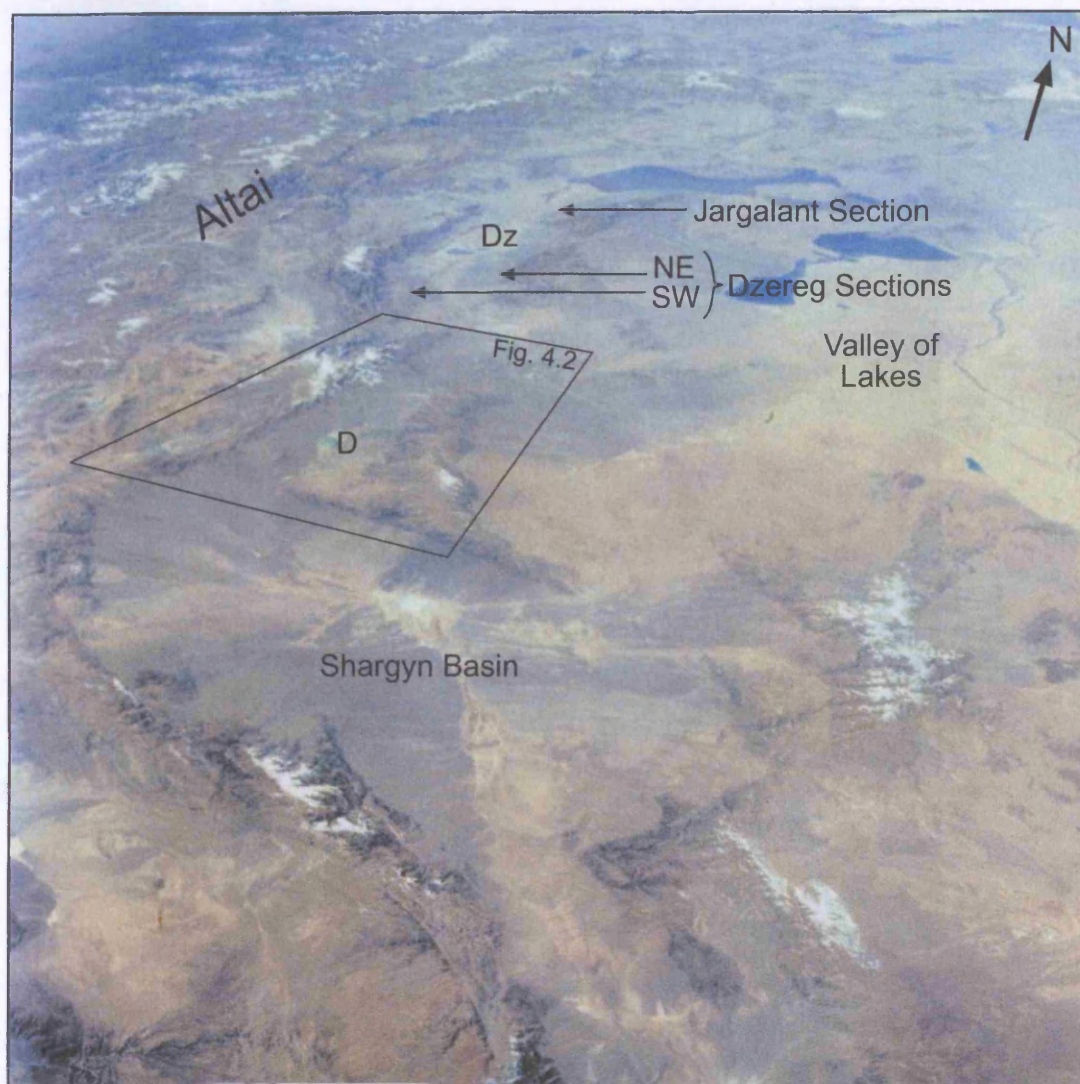


**Figure 4.1** – Oblique shuttle view of the Altai region. The study area comprises three basins on the eastern margin of the Altai. D - Dariv Basin, Dz Dzereg Basin. Note the location of the Jargalant Section and Dzereg Sections in the Dzereg Basin. The area covered in Fig. 4.2 is shown. Scale varies in photo, base width is approximately 300 Km. Image courtesy of Earth Sciences and Image Analysis Laboratory, NASA Johnson Space Centre (<http://eol.jsc.nasa.gov>).

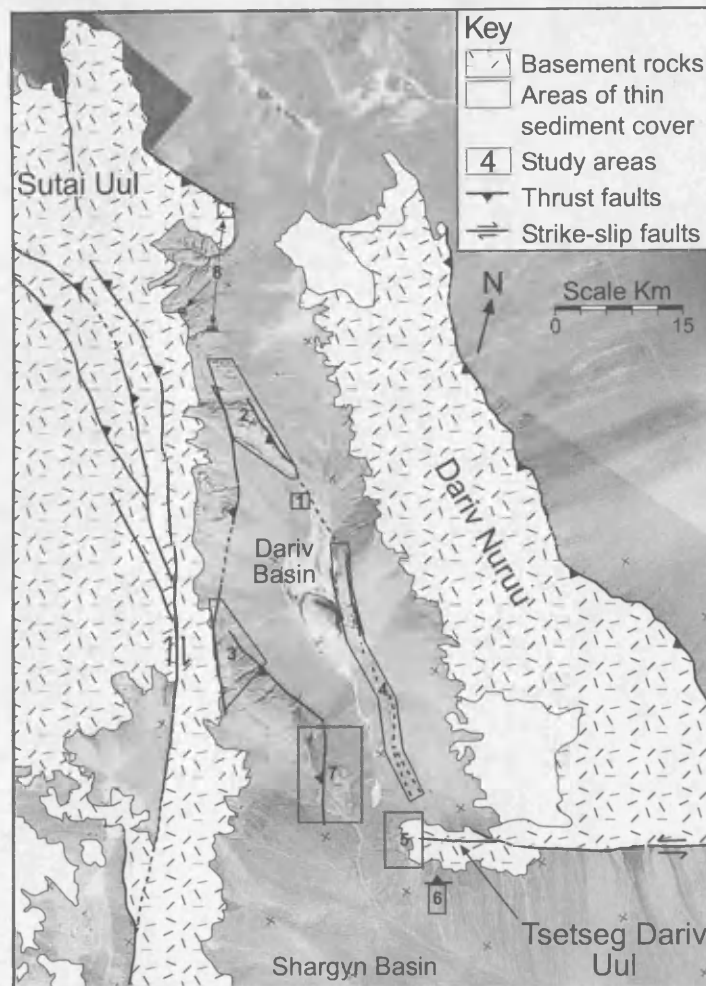
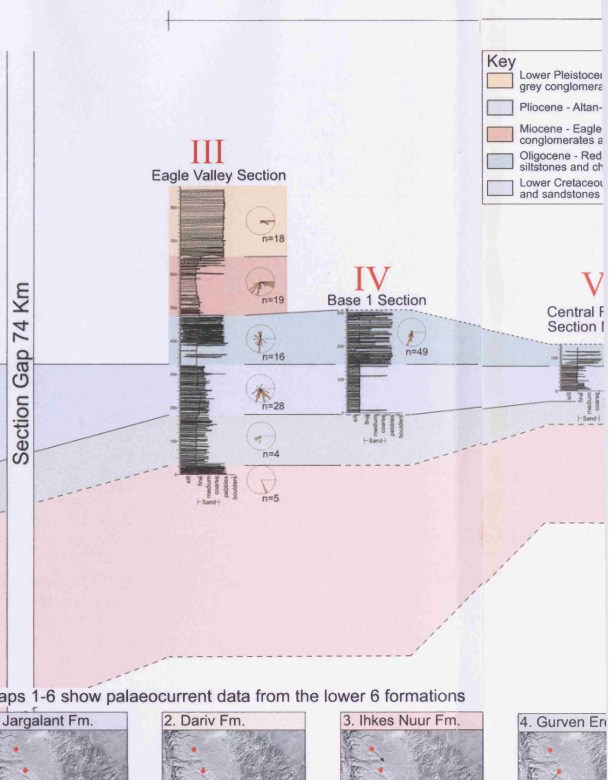
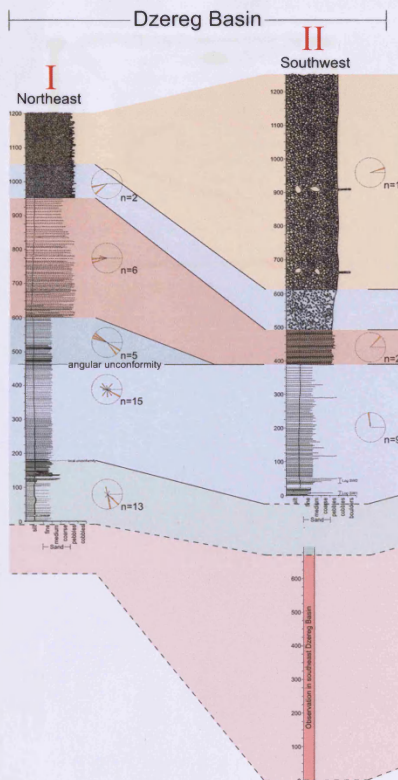


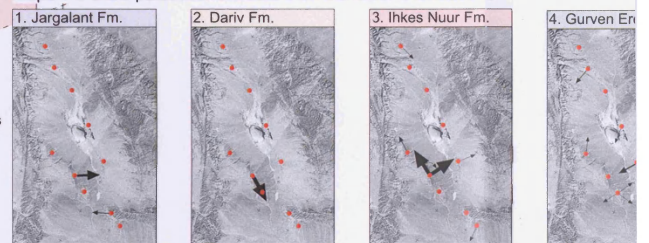
**Figure 4.2** – Interpreted Kosmos satellite image showing the 8 study areas within the Dariv and Shargyn Basins. 1 = Base 1 Section, 2 = North Foreberg area (contains the East Ridge Section, North Canyon Section & Eagle Valley Section), 3 = Green Valley Section, 4 = Central Ridge area (Contains the Central Ridge Section (north) & Central Ridge Section (south)), 5 = Radio Mast Section, 6 = Shargyn Section, 7 = Southern Foreberg area (contains the Dariv Section & Sandstorm Section) and 8 = Sutai Flanking Sections. Major structures that uplift mountain ranges and bound active ridges within the basin are also shown. Uul = Mountain, Nuruu = Range.

**Figure 4.3** – Correlation panel showing generalised stratigraphic sections from the Dzereg, Dariv and Shargyn basins, Section VIII, the Dariv Section is taken from Sjostrom, 2001. Inset map shows the location of sections. Formation names largely correspond to Devjatkin (1981) with the exception of the Red Hill and Eagle Valley Formations which are new. Correlation is based on biostratigraphic data (listed in appendix 1), field mapping of formations and major changes in lithology. The direction of measured palaeocurrent is shown on sections and on 6 inset maps. Loose-leaf copy in appendix 3.





Maps 1-6 show palaeocurrent data from the lower 6 formations



Key to paleocurrent maps

- n = <5
- n = 6-15
- n = 16-25
- n = 26-35
- n = >36

Key

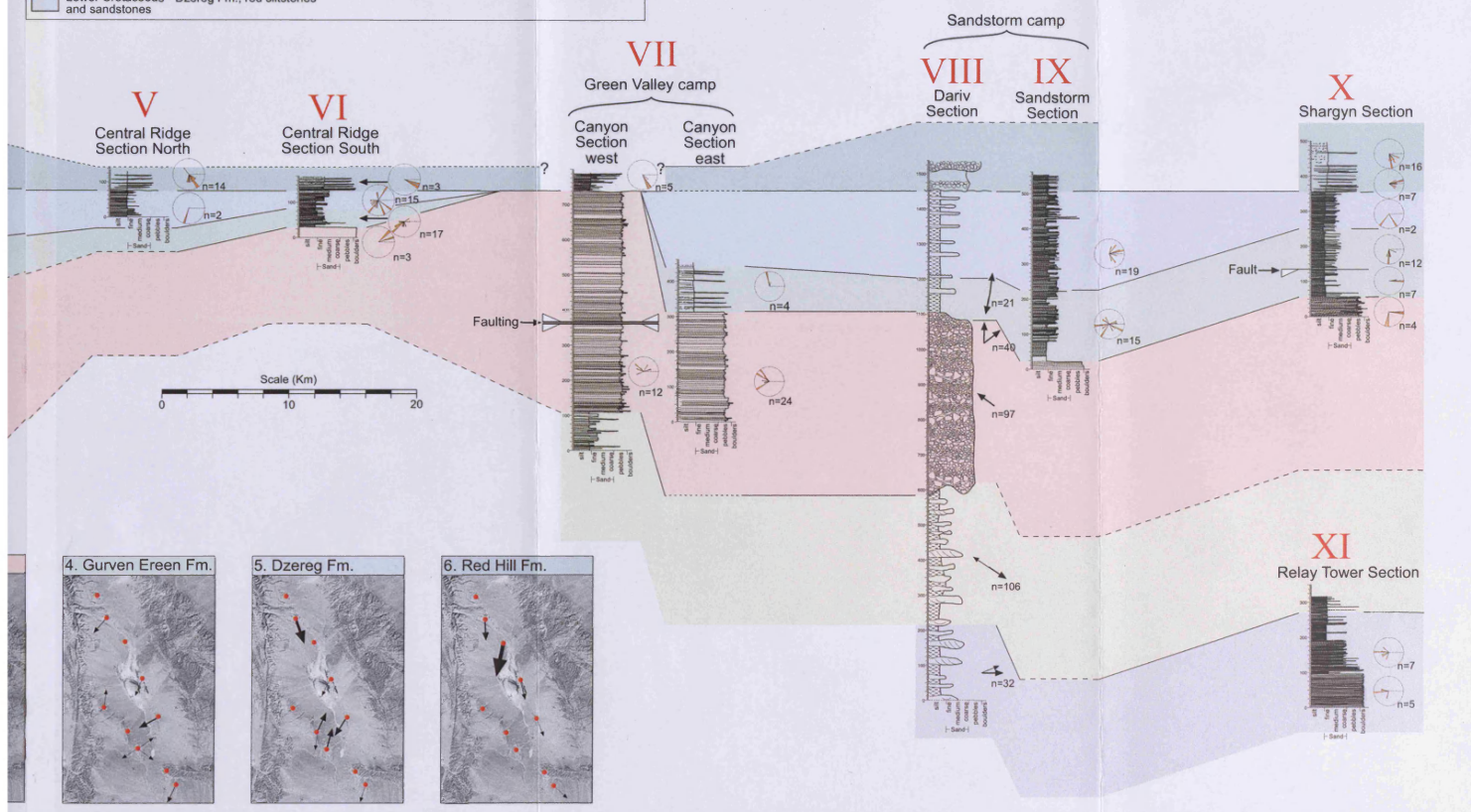
- Lower Pleistocene grey conglomerates
- Pliocene - Altan
- Miocene - Eagle conglomerates and sandstones
- Oligocene - Red siltstones and clays
- Lower Cretaceous and sandstones



# Dariv Basin

# Shargyn Basin

<b>Key</b> Lower Pleistocene - Goshu Fm., massive grey conglomerates Pliocene - Altan-Teel Suite, yellow conglomerates Miocene - Eagle Valley Fm. (Oshin suite), channelised conglomerates and grey siltstone Oligocene - Red Hill Fm. (Beger Suite), red siltstones and channelised sandstones Lower Cretaceous - Dzereg Fm., red siltstones and sandstones	Lower Cretaceous - Gurven Ereen Fm., grey siltstone and fine sandstone Upper Jurassic/Lower Cretaceous - Ihkes Nuur Fm., matrix supported conglomerate Upper Jurassic - Dariv Fm., channelised sandstone and red siltstone Middle Jurassic - Jargalant Fm., channelised green sandstone and siltstone
---	--



## 4.2 Mesozoic Stratigraphy

### 4.2.1 Previous work

Mesozoic strata exposed in the Dariv and Shargyn basins have been documented during several earlier studies. The regional stratigraphy published in Devjatkin (1981) includes data collected from the Dariv Section within the Dariv Basin during numerous Russian expeditions (e.g. Devjatkin *et al.*, 1975; khosbayer, 1979; Rasnitsyn, 1985). Devjatkin (1981) includes a basic description of each formation and lists biostratigraphic constraints on their age. Recent work within the Dariv Basin has built on the regional stratigraphy to produce detailed facies analysis and environmental interpretations for the Dariv Section (e.g. Graham *et al.*, 1997; Sjostrom *et al.*, 2001). This PhD represents the first study of the remaining Mesozoic-Cenozoic sedimentary sections exposed within the Dariv Basin.

### 4.2.2 Jargalant Formation - Middle Jurassic

The Jargalant Formation onlaps Palaeozoic strata and is >300 m thick. The formation has a characteristic green colour and fines upward from basal cobble conglomerate beds into interbedded sandstone and siltstone beds. The Jargalant Formation's upper contact with the overlying Dariv Formation is conformable and is defined by a sharp green/grey to red colour change. The formation name is after Devjatkin *et al.* (1981).

#### 4.2.2.1 DESCRIPTION

The greatest thickness of Jargalant Formation sediments in the Dariv Basin is poorly exposed along the northern flanks of Tsetseg Dariv Uul (Little Dariv Range; area 5, Fig. 4.2). The middle-upper Jargalant Formation is, however, best exposed at the Dariv Section (area 7, Fig. 4.2). Within Tsetseg Dariv Uul, the Jargalant Formation is mainly in tectonic contact with basement rocks along sinistral strike-slip faults that uplift the range (Fig. 4.4). However, the formation is observed to onlap Palaeozoic sediments and intrusive igneous rocks in exposures along the eastern flanks of the range. The basal contact of the Jargalant Formation is not exposed in the Dariv Section, where the formation is in tectonic contact with Cretaceous sediments (Fig. 4.5). The entire Jargalant Formation is also well-exposed outside the field area, in the Jargalant Section from the northern Dzereg Basin (Fig. 4.1), and is reported to be 1180 m thick (Sjostrom *et al.*, 2001). However, in the Dariv Basin, the Jargalant Formation is estimated to be only 300-400 m thick, based on this field study. The formation comprises 6 facies (AF, BC, C, D, EF and EC in table 4.1), and is divided into two members.

#### ***Type locality – The Radio Mast Section:***

##### *Tsetseg Uul Member*

The Tsetseg Uul Member onlaps Palaeozoic basement and is dominated by cobble conglomerate beds. The Member's upper contact is marked by a decrease in mean grainsize from cobble conglomerate to sandstone with isolated conglomerate channels. The Member is a new subdivision of the Jargalant Formation and is named after Tsetseg Dariv Uul.

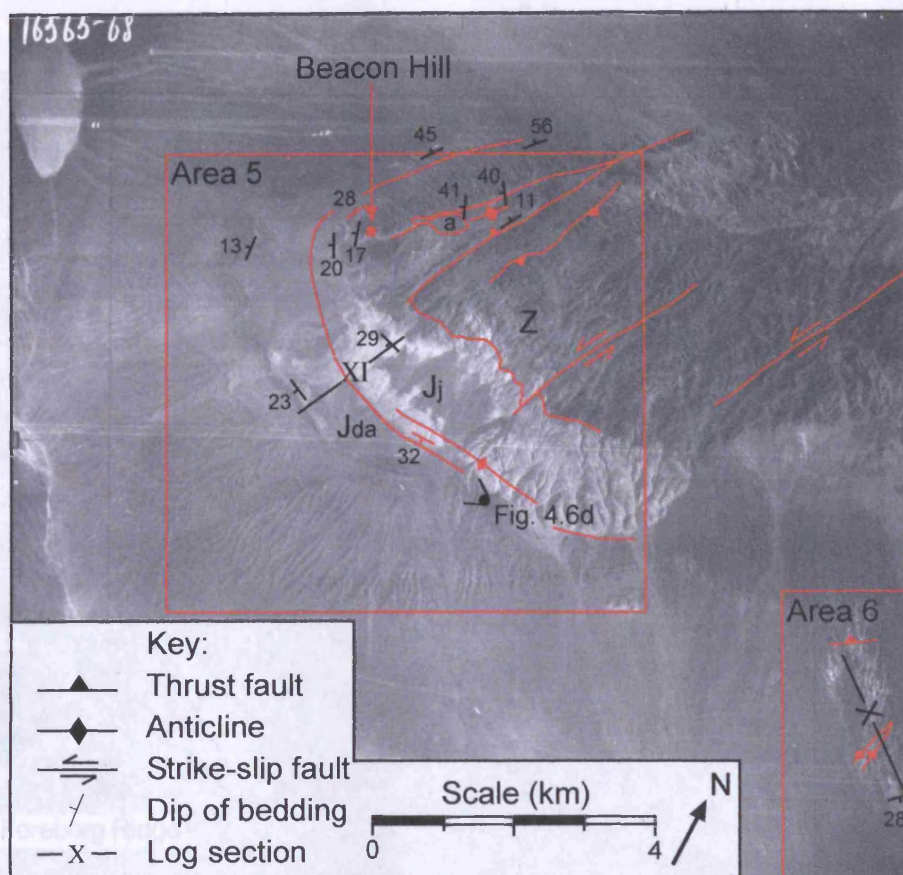


**Figure 4.4** – Aerial photograph and interpretation for areas 5 & 6 showing the location of the Shargyn Section (X), the Radio Mast Section (XI) and the relationship between the Jargalant Formation (Jj) and the Palaeozoic basement rocks (Z). The upper contact of the Jargalant Formation with the Dariv Formation (Jda) is also shown along with the location of Fig. 4.6d. (a) defines an area of coal outcrop.

Figure 4.5 – Aerial photograph and interpretation for area 7 (Fig. 4.2). The location of the Dariv Section (VII) and Sandstorm Section (IX) are shown, along with structures that uplift the ridges and define the Mesozoic and Cenozoic basin fill. Note the two dome structures and the presence of both igneous and metamorphic rocks that uplift the South Foreberg Ridge. Viewpoints for photographs Fig. 4.6a, 4.6b, 4.6c & 4.6d are shown.



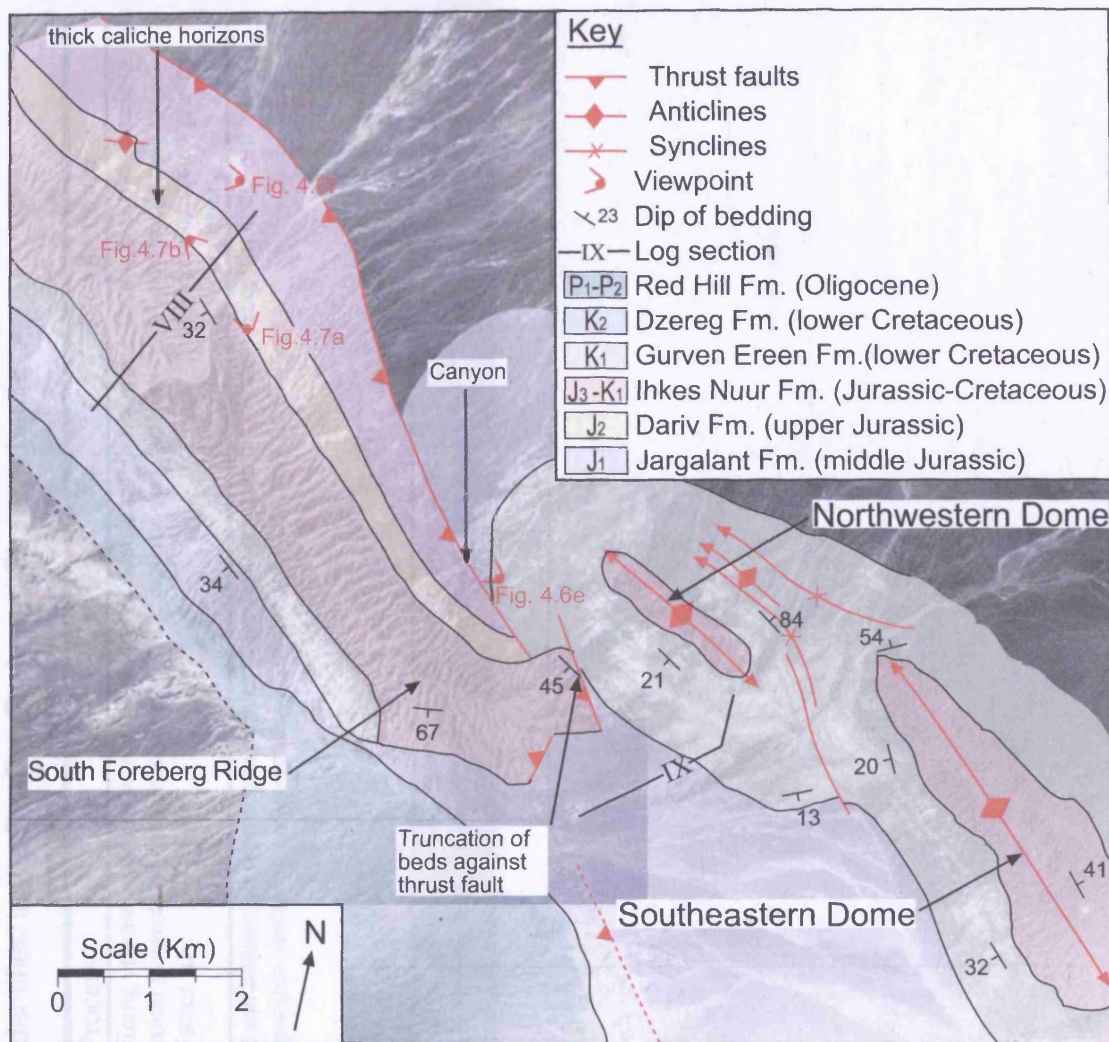


**Figure 4.5** – Aerial photograph and interpretation for area 7 (Fig. 4.2). The location of the Dariv Section (VIII) and Sandstorm Section (IX) are shown, along with structures that uplift the ridges and deform the Mesozoic and Cenozoic basin fill. Note the two dome structures and the truncation of beds against thrust faults that uplift the South Foreberg Ridge. Viewpoints for photographs Figs. 4.6e, 4.6f, 4.7a & 4.7b are shown.

Table 4.1 – Facies chart for major stratigraphic units identified in the Dzereg, Dariv and Shargyn basins.

Facies	Description	Process	Interpretation
AC	Erosive base. Laterally extensive pebble sheets, massive or upward fining, clast supported and <60 cm thick. Occasional lamination or cross-stratification.	Fining upward indicates waning flow during deposition and lateral extent suggests a broad unconfined flow. Usually associated with Facies AF.	Coarse sheetflood deposit. Massive beds may be hyperconcentrated gravity flow deposits.
AF	Sharp, often erosive base. Occasional basal pebble/granule lag overlain by a fining upward sandstone succession. Some/all of a characteristic vertical sequence of sedimentary structures: Laminar, planar or trough-cross stratification, laminae, massive sandstone. Upper surface may be rippled. Associated with facies EF/EC.	Basal lamination representing upper phase flow overlain by fining upwards sandstone and structures characteristic of waning flow.	Sheetflood deposit.
BC	Massive clast-supported cobble/pebble conglomerate with some interbedded sandstone. Laterally extensive <3 m thick. Rare normal grading. Interbedded with facies AF.	Lateral migration of a cobble dominated channel system. Reworking of sedimentary structures and little preservation of overbank material (Facies AF and EF).	Deposits of a coarse bedload braided river system on a fluvial or alluvial fan.
BF	Massive laterally extensive pebble conglomerate and sandstone sheets with many internal erosion surfaces. Abundant imbrication and cross-stratification and occasional normal grading.	Variable clast size and complex internal structure results from the migration of channel macroforms within a braided gravel-bed river system.	Deposits of a braided river system.
C	15-30 cm thick pebble conglomerate with minor erosive bases and rare cross-stratification. Grade laterally into coarse sandstone. No internal erosion surfaces.	Coarse sediment deposited over the floodplain during a flood event. Slightly channelised base indicated more confined flow than facies AF and AC.	Crevasse splay deposit.
D	Well-defined channels containing clast supported pebbles (rarely cobbles) that fine up between internal erosion surfaces. Interbedded with sandstone sheets. Cross-stratification, lamination and deformation of underlying strata are common. Occasional silt (facies EF) drapes.	Bedload gravel and sand transport in a fluvial system with variable discharge. Gravel and sandstone bodies record the migration of bedforms. Intermittent siltstone (facies EF) horizons indicate flow was ephemeral.	Deposits of an ephemeral, sinuous mixed-load river. Massive beds may represent hyperconcentrated flood gravels.
EF	Intermittently laminated siltstones and rare mudstones. Containing organic material. Large colour variations.	Slow setting of silt from suspension after inundation of the floodplain. Primary lamination is commonly reworked by bioturbation and rooting. Colour variation records hydromorphic processes in action on the floodplain.	Overbank deposits.
EC	Massive silt-rich sandstone or sand-rich siltstone sheets often containing matrix-supported granules.	Deposition either by (1) transport of clay within fluvial systems as sand-grade aggregates (Nanson <i>et al.</i> , 1988; Talbot <i>et al.</i> , 1994), where post depositional breakdown of the aggregates produces a matrix supported sand rich siltstone (2) muddy debris flow (3) reworking of interbedded sandstone and siltstone by bioturbation. These options cannot be distinguished without microscopic analysis of the sediment.	Overbank deposits or debrites.
F	Lenticular sand sheets containing extensive cross-stratification that are laterally extensive over 100's m. > 1 m high foresets are mantled with pebbles and granules with occasional pebble sheets.	Migration of sand-bed channel. Cross-stratification represents both the migration of 3D bedforms and preservation of bank attached foresets resulting in a broad range of measured palaeocurrent.	Deposits of a high sinuosity sand bed river system.
G	Coarsening upward clast supported granule/pebble or pebble/cobble conglomerate.	Deposit of a wet or hyperconcentrated debris flow from which the matrix drained after deposition.	Hyperconcentrated gravity flow deposits.
H	Pebbles and granules supported in a fine sand or siltstone matrix. Massive or coarsening upward.	Cohesive debris flow in which large grains are carried by a dense matrix.	Cohesive debris flow deposit.
I	Sandstone dominated sheets that fine upward from an occasionally pebbly base and contain structures indicating waning flow. Dish and pillar structures or laminations form the upper part of beds. Massive beds are rare and contain evidence of burrowing. Commonly interbedded with lacustrine fines (Facies J & K).	Fining upward with a structure indicative of waning flow suggests the influx of coarse sediment into a lake as an individual flood event. This facies represents sheetflood facies AF entering a lake.	Deposits of a sheetflood entering a lake.
J	Very well laminated siltstone and claystone often showing fine variations between lamina. Individual laminations have a large lateral extent in good exposure. Can be associated with gypsum horizons.	Slow settling of silt or clay particles from suspension in the water column. Background sedimentation with the variation in lamination picking out periodic changes in climate or water column composition. Lack of bioturbation put down to anoxic bottom waters or elevated salinity. Gypsum horizons are precipitated from concentrated water, water concentration varies.	Lacustrine deposits recording conditions hostile to burrowing benthic organisms.
K	Massive siltstone and claystone, occasionally micritic. Sometimes associated with gypsum horizons.	Reworked lacustrine sediments often associated with gypsum. Lamination removed by either sub-aqueous burrowing – suggesting conditions supported benthic life or sub aerial exposure, often difficult to establish which. Gypsum deposited during concentration of water by evaporation.	Lacustrine deposits reworked by burrowing organisms or hydromorphic processes.
Facies association L	LA Coarsening upwards interbedded sandstone and laminated, massive or bioturbated siltstone. Sand beds have sharp planar bases.	Distal influence of prograding fluvial system into lacustrine environment. Preservation of lamination implies anoxic conditions. Bioturbated or massive siltstones suggest oxic conditions.	Prodelta deposits.
	LB Massive or coarsening upward sandstone with low-angle planar lamination or cross-stratification. Commonly affected by small-scale soft sediment deformation e.g. dish and pillar structures and minor slumping.	Deposition of sandstone over the delta surface. Slumping and dish and pillar structures form due to loading of saturated prodelta sediments.	Delta front deposits.
	LC Large (>1 m) trough cross-stratified sandstone beds with erosive bases, often with lag surfaces and occasional siltstone drapes.	The migration of mouth bars close to the mouth of the fluvial system. Silt drapes suggest periodic pauses in fluvial input, possibly seasonal.	Mouth bar deposits.
	LD Ripple cross-stratified sandstone with a coarse lag surface, commonly bioturbated.	Reworking of abandoned delta surface by wind derived currents into ripples etc. Lag surface results from continual reworking of sediment and winnowing of coarse fraction. Bioturbation affects the surface if it is exposed for extended periods.	Reworked delta top deposits.
	LE Erosive based conglomerate sheets and interbedded fine sediment (Facies EF). Commonly hard and resistant to erosion due to intensive caliche formation.	Sub aerial deposits on the delta top. Laterally extensive channels reflect channel migration and the extensive carbonate concretion indicate long-term exposure and non-deposition.	Delta top deposits.
M	Micritic limestone containing ostracods and gastropods.	Deposition of calcium carbonate in a temporary lake environment.	Temporary lake deposits.



The oldest exposed sediments are texturally mature, clast-supported, green-grey, cobble conglomerate beds with a poorly sorted green/yellow sandstone matrix (facies BC). The clast assemblage is dominated by diorite, granite and fine-grained grey limestone, along with subordinate intraclasts of green conglomerate. Individual beds are up to 3 m thick and generally massive, some with normal grading. Bedding surfaces can be difficult to identify in some exposures, however, they are commonly associated with thin (<15 cm) sandstone layers that are usually massive, but occasionally contain trough cross-stratification or laminae (facies AF). The conglomerate-dominated Tsetseg Uul Member fines upward slightly and becomes yellow-green. Thick, green, basal conglomerates are also reported in the Jargalant Section (Sjostrom *et al.*, 2001).

#### *Relay Tower Member*

The basal contact of the Relay Tower Member is conformable with the underlying Tsetseg Member and is marked by a decrease in mean clast size from cobble conglomerate to sandstone with conglomerate channels and a corresponding colour change from green to white/grey. The Relay Tower Member fines upward and comprises interbedded sandstone, siltstone and conglomerate beds. The Members upper contact is conformable with the overlying Dariv Formation and is marked by a colour change from green to red. The Relay Tower Member is a new sub division of the Jargalant Formation and is named after a radio relay station located on the type section.

A fining upward succession overlies the massive green conglomerate. The basal succession is dominated by grey-white sandstone beds that weather into distinctive slabs (Fig. 4.6a, b) and obscure much of the formation. Rare, green, channelised, cobble-dominated conglomerate bodies (facies D), up to 1 m thick



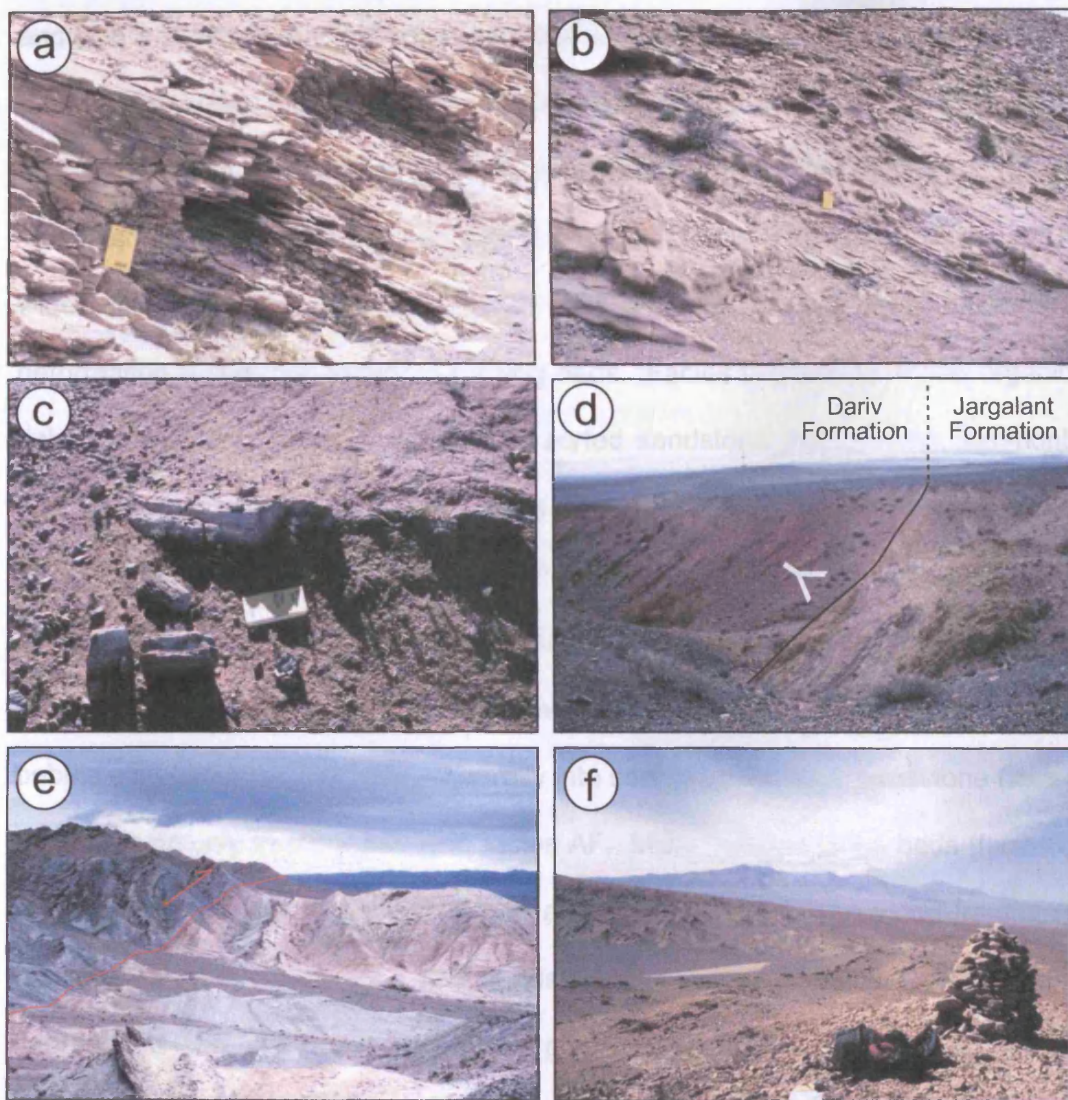


**Figure 4.6a & b** - Photographs a and b show good exposures of the sandstone and pebble conglomerates of the central Jargalant Formation. **4.6c** - 14 cm diameter wood fragments within the upper Jargalant Formation in area 5 (Fig. 4.2). **4.6d** - The gradational upper contact between the grey/yellow Jargalant Formation and the overlying red Dariv Formation. The location of this photograph is shown in figure 4.4. **4.6e** - The Middle Jurassic Jargalant Formation (grey/green) thrust over Cretaceous red/blue beds. The location of this photograph is shown on figure 4.5. **4.6f** - The Jargalant Formation at the Dariv Section. Note the change from yellow/white sandstone slabs in the foreground to dominantly green silt beds in the midground. Sutai Uul (Fig. 4.2) is in the background. The location of this photograph is shown on figure 4.5.

siltstones of the Jargalant Formation have a gradational contact with the red beds of the Dariv Formation. Further exposures to the north of Tsingling Pass and preserve a gradational contact with the red beds (facies EF), thin conglomerate shows facies

and with a lateral extent <10 m are isolated within the sandstone beds at the base of the Relay Tower Member. These bodies contain clast-supported, subrounded to rounded pebbles and cobbles that fine upward between internal erosion surfaces. The majority of facies D beds comprise small channels (<30 cm thick and <4 m wide) containing poorly sorted pebbles and granules. Localised soft-sediment deformation is common in the underlying beds. Facies D channels incise organic-rich, medium to coarse-grained, poorly sorted sandstone beds, which commonly contain granules and occasional pebbles (facies AF). Individual beds are 8-30 cm thick, and may fine upward. Facies AF sandstone occasionally contains trough cross-stratification, generally at the base, which is then overlain by massive or laminated beds. Thin (<20 cm) erosive sheets of poorly sorted, subrounded pebble conglomerate, that grade laterally into coarse pebble-rich sandstone (facies C), are commonly interbedded with facies AF. Many conglomerate beds (facies C and D) contain intra-basinal sandstone and siltstone clasts, and wood fragments are also common (Fig. 4.6c). The sandstone and pebble conglomerate beds are interbedded with laterally discontinuous grey-brown, red and, occasionally, purple sand-rich siltstone beds (facies EC).

The formation fines upward and facies D channels become smaller and pebble dominated with height before abruptly disappearing. Sandstone facies AF is increasingly silt rich, with less common cross-stratification. The Relay Tower Section is dominated by interbedded green/grey siltstones (facies EF). The upper contact with the overlying Dariv Formation is exposed in one small stream section (Fig. 4.4 & 4.6d). The yellow/grey sandstones interbedded with grey-green siltstones of the Jargalant Formation have a gradational contact with the red beds of the Dariv Formation. Patchy exposures to the north of Tsetseg Dariv Uul preserve green-grey siltstone beds (facies EF), thin conglomerate sheets (facies

C) and sandstone beds (facies AF) that represent the upper part of the formation. Thin coal seams were observed to the east of Beacon Hill (Fig. 4.4), although their exact position within the Jargalant Formation is unclear. Coal seams are reported from the upper Jargalant Section in the Dzereg Basin (Sjostrom *et al.*, 2001).

***Additional exposures of the Jargalant Formation:***

The middle-upper part of the Jargalant Formation is exposed in area 7, both in and around the Dariv Section (Fig. 4.5). The oldest strata can be seen in patchy exposures east of the Dariv Section and in a canyon where the basal thrust is exposed (Fig. 4.5 & 4.6e). Log VIII (Fig. 4.3) records the well-exposed, upper part of the formation in the Dariv Section (Fig. 4.6f). In the canyon (Fig. 4.5), the central part of the formation is comparable to that seen in area 5. It comprises green, sand rich, siltstone beds (facies EC) and granular, fining upward sandstone beds (facies AF) interbedded with erosive based conglomerate sheets (facies C). These beds are incised by channelised pebble conglomerates (facies D) that rapidly die out upwards. Conglomerate facies C and D initially comprise approximately 50% of the succession. Exposure is poor up to the base of the Dariv Section, however, green siltstones and sandstone beds dominate the stratigraphy. The base of the Dariv Section (Log VIII, Fig. 4.3) comprises mainly white-grey, organic rich sandstone (facies AF, Fig. 4.6f) that fine upward. Interbedded with the sandstone are poorly exposed green, grey and occasionally white siltstone beds (facies EF). Facies EF, green siltstones increasingly dominate the Dariv Section. It is interbedded with yellow-green commonly cross-stratified sandstone lenses over hundreds of metres long (facies F). The upper contact with the red beds of the overlying Dariv Formation is again gradational. Detailed logs of

the upper part of the Jargalant Formation at the Dariv and Jargalant Sections are found in Sjöström *et al.* (2001).

*Summary:*

Sjöström *et al.* (2001) report a dominant palaeocurrent direction to the east-northeast based on trough axis measurements, although their imbrication readings tend towards the east. Palaeocurrent indicators were rare in poor exposure at Tsetseg Dariv Uul and show great variation. However, a general westerly trend was established (Fig. 4.3). This unit is considered to be Lower and Middle Jurassic on the basis of ostracods and plant remnants (Devjatkin *et al.*, 1975; appendix 1). The contact of the Jargalant Formation with the overlying Dariv Formation is conformable.

#### 4.2.2.2 INTERPRETATION

*Tsetseg Uul Member*

The basal conglomerate contains clasts of a green pebble conglomerate. This indicates that some of the material is reworked from an older conglomerate source, and so the well-rounded nature of the clasts may, therefore, be inherited and not necessarily indicative of extensive transport. The remainder of the clasts comprise basalt, diorite and grey limestone, all of which are widespread Palaeozoic basement lithologies, and consequently cannot provide additional information about the source region. The large clast size and good sorting of the conglomerate beds (facies BC) indicate fluvial transport. Few sedimentary structures were observed in these massive erosive-based conglomerate sheets. These beds are difficult to interpret in isolation. However, the preservation of a few sandstone beds (facies AF) between the erosive conglomerate sheets provides

further information. Facies AF commonly fines upward and is predominantly massive, but occasionally contains trough cross-stratification, representing the migration of 3D dunes, and discontinuous laminae, which can represent either upper-phase flow or settling from suspension. In facies AF, discontinuous laminae locally drape the irregular contact with underlying trough cross-stratified sandstone suggesting that they settled from suspension when bedform migration ceased. Sandstone layers between conglomerate sheets suggest periodic flood events that overtopped the channel margins and deposited over the floodplain. Despite limited preservation, the observed structures and upward fining are characteristic of waning-flow in sheetflood deposits (e.g. Hardie *et al.*, 1978; Hartley *et al.*, 1992; Miall, 1996). Massive or upward-fining conglomerate bodies (facies BC), with little preservation of overbank fines, are characteristic of a braided stream-dominated fluvial, or alluvial fan setting (e.g. Nemec & Postma, 1993). Lateral migration of multiple channels over a wide area has reworked sedimentary structures leaving only massive conglomerate sheets preserved. The Tsetseg Uul Member is, therefore, interpreted to represent a cobble dominated, braided river system.

#### *Relay Tower Member*

The Relay Tower Member fines upward in sections from areas 5 and 7, although some differences exist between the two. The base of the member contains well-defined channelised conglomerates (facies D) that represent a significant change in fluvial style from the braided stream system that dominated the Tsetseg Uul Member. The presence of internal erosion surfaces suggests facies D channel fills are longer-lived, more aggradational features. The cobble-dominated facies D channels are large, rare, and seen only at the base of the Relay Tower Member in area 5. They are interpreted to record major channels



that were short lived relative to the system that deposited the fining upward succession. They perhaps record a transitional stage between facies BC and the smaller, pebble-rich facies D channels that dominate the lower part of the member (especially the Dariv Section). The channels incise pebble conglomerate, sandstone and siltstone beds (facies AF, C EC & EF) that are interpreted as floodplain deposits. The channel fill deposits are, therefore, interpreted as deposits from low sinuosity gravel-bed rivers with extensive preservation of overbank deposits. The erosive based, thin conglomerate sheets (facies C), that thin and grade into pebbly sandstone beds over a few metres laterally, record cut and fill during individual weakly confined floods. These sheets are interpreted as crevasse splay flood deposits (e.g. Miall, 1996). The better exposure in the Relay Tower Member clearly shows that facies AF fines upward and contains structures indicative of waning flow. The beds each preserve part, or all, of a vertical progression 'from cross-stratified sandstone beds to massive, then laminated, sandstone beds that is characteristic of sheetflood deposition (e.g. Tunbridge, 1981; Nemec & Steel, 1984; Young, 1993). Rapid deposition of the basal sandstone beds is indicated by the presence of matrix-supported coarse grains where cross-stratification is absent. Siltstone beds (facies EF) that overlie sandstone beds record the final, slow, settling of silt from suspension following a flood event. The limited preservation of siltstone layers is ascribed to their easy erodability by the next flood. Facies EC contains matrix-supported granules and coarse sand grains. This can be interpreted as either the deposits of a debris flow, or an overbank flood carrying silt as sand size aggregates which degrade after deposition, leaving sand and granules apparently matrix-supported (e.g. Nanson *et al.*, 1986, 1988). It is difficult to distinguish between the alternate origins without detailed analysis of the sediment microstructure, however, given the proximity of

the fluvial channels, facies EC siltstones were most likely deposited as sand size aggregates. Siltstones and mudstone intra-clasts are common in facies D channel fills. The colour variation from grey/green to white and, rarely, red siltstones and sandstone beds, within the overbank deposits, may record fluctuations in the water table resulting in alternating of anoxic and oxic conditions within the floodplain sediment between flood events (e.g. Retallack, 1988).

As the Relay Tower Member continues to fine upward, facies D dies out and conglomerate is present only as less confined, more sheet-like bodies (facies C), deposited by crevasse splays. This suggests that a channel must have remained active nearby at this time. The high degree of basal erosion below facies C layers appears to relate to mean grainsize, with greater erosional relief associated with a coarser sediment load. The central part of the Member is dominated by upward fining sandstone beds, representative of sheet flood deposition (facies AF). The relative volume of coarse versus fine sediment can be interpreted as either fluctuations in the intensity of individual flood events, in which case the overall fining upwards character of the succession would represent an increasingly distal location, or a temporal decrease in the competence of the system.

The upper part of the Relay Tower Member is better exposed in area 7, where it is dominated by green/grey siltstones (facies EF) with interbedded cross-stratified sandstones (facies F). The sandstones are lenticular over 100's m and Sjöström *et al.* (2001) interpreted these as the deposits of a moderate to high sinuosity, suspension dominated fluvial system. This is consistent with the interpretation presented here, although a sandstone-dominated system appears to have persisted in area 5.

## Summary

Throughout the Jargalant Formation, the abundance of plant debris and organic fragments suggests a well-vegetated environment, which, when combined with the evidence for a long-lived, coarse bedload fluvial system, suggests an environment that contrasts with that of the modern day Dariv Basin. Asia was probably considerably wetter in the Middle Jurassic than it is today, with a diminished monsoonal climate, despite the ongoing break up of Pangea (Parrish & Curtis, 1982; McKnight *et al.*, 1990; Keller & Hendrix, 1997). While the most intense rainfall may not have penetrated as far inland as the Dariv Basin, seasonal rainfall must have been higher than it is at the present day. The limited palaeoclimatological data that exists for Mongolia (Keller & Hendrix, 1997; Devjatkin, 1970), and a comparison with adjacent parts of China (McKnight *et al.*, 1990), suggests that in the Jurassic there was a marked increase in aridity from east to west across Mongolia. Despite this systematic geographic change, rainfall models predict a relatively wet period for the Dariv Basin, although it seems likely that rainfall was declining throughout the Jurassic (Keller & Hendrix, 1997). The Relay Tower Member is interpreted as recording a river flowing through a well-vegetated floodplain. Exposure is limited to two sections but a fluvial-dominated low angle fan system is suggested from the data. In area 5, sediments were derived from the east (data from this study) and in area 7, sediments were derived from the west (Sjostrom *et al.*, 2001). The opposing palaeocurrent indicators suggest that sediment was transported into a depression between the two sections (Fig. 4.3). The stratigraphy documented in the Jargalant Section of the Dzereg Basin suggests this depression had a north-south trend. Some of the variation in measured palaeocurrents may result from deformation and block rotation during

uplift of Tsetseg Dariv Uul, which cannot be properly quantified or corrected for here.

The upward fining trend of the Jargalant Formation is interpreted as recording a diminution of the source area, this simultaneously reducing both the sediment supply and the drainage gradient (and therefore transport competence) of the fluvial systems. A reduction in rainfall related to climate change might produce a similar signal, but the large quantity of silt and clay grade sediment (relative to the present) suggests a humid climate promoted active chemical weathering in the source area (e.g. Hardie *et al.*, 1978). In the absence of a change in base level, fan systems respond to source area diminution by retreating into their drainage basins as relief becomes less pronounced (Harvey, pers. com. 2003). An increasingly distal succession will be recorded at any given location on the fan surface as the fan onlaps the catchment area.

#### 4.2.3 Dariv Formation – Upper Jurassic

The Dariv Formation overlies a conformable basal contact with the underlying Jargalant Formation, defined by a colour change from green to red, and is 390 m thick. The formation fines upward and is dominated by red siltstone incised by sandstone channels. The Dariv Formation's upper contact with the overlying Ihkes Nuur Formation is locally scoured, but generally conformable and is defined by a sharp increase in mean grainsize from siltstone to cobble conglomerate. The formation name is after Devjatkin *et al.* (1981).

##### 4.2.3.1 DESCRIPTION

The Dariv Formation is well-exposed only in the Dariv Section (Fig. 4.5 & 4.7a). The formation fines upward from medium-grained sandstone (facies F) and sand-rich siltstones (facies EC) into interbedded red siltstones and mudstone beds

(facies EF). Individual beds are laterally continuous over 100 m. Facies F comprises massive and planar or trough cross-stratified, poorly sorted sandstone that overlies minor erosive channelised bases, with rare well-rounded pebble conglomerate lags. Foresets within facies F are commonly mantled by layers of granules and coarse grains. The channels incise sandy siltstones (facies EC) and siltstones (facies EF) that contain abundant plant material and are commonly pedoturbated. As the formation fines upward, sandstones (facies F) become finer and less well confined before dying out completely. Correspondingly, sand-rich siltstones (facies EC) also die out upwards and the upper part of the succession comprises soft red or red/brown siltstones and mudstones (facies EF). Caliche beds are increasingly common upward and two unusually well developed caliche horizons are visible as white bands on aerial photographs (Fig. 4.7b). Two, metre-scale micrite horizons are reported in Graham *et al.* (1997), but these were not observed in this study. Limited exposure in area 5, the Radio Mast Section (Fig. 4.2 & 4.4), comprises soft red and brown siltstones (facies EF) with interbedded sandstones (facies F).

### *Summary*

Palaeocurrent indicators from this formation suggest transport from the northwest (Fig. 4.3; Sjöström *et al.*, 2001). The formation is Upper Jurassic based on fresh water pelecypods (Khosbayer, 1973) and an Upper Jurassic sauropod (Graham *et al.*, 1997).

#### 4.2.3.2 INTERPRETATION

The Dariv Formation has been extensively studied (Khosbayer, 1973; Graham *et al.*, 1997; Sjöström *et al.*, 2001) and is interpreted as the deposits of a shallow, sinuous, sand-bed river system with mud-dominated overbank deposits,

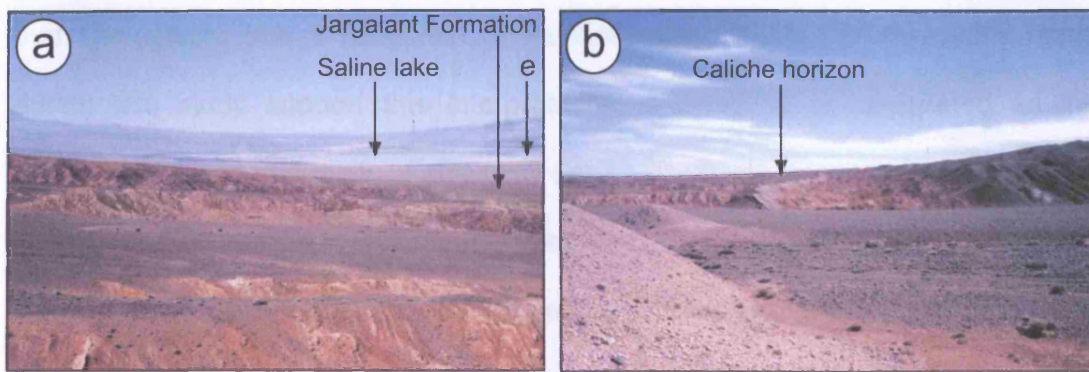


**Figure 4.7a** - View north across the Dariv (a) Formation red beds, with the green rocks of the Jargalant Formation visible on the right hand side. The shallow saline lake in the centre of the Dariv Basin is visible in the distance. Note the white evaporite deposits on its margins (e). **4.7b** - View south across the Dariv (a) Formation showing one of two major caliche horizons visible on aerial photographs (Fig. 4.5).

beds is the upper part of the formation, composed of a thin-bedded, light-colored, silty sandstone on the north side (Fig. 4.7a, b).

#### Sedimentation

The Dariv Basin is a large, shallow, evaporitic depression, in which the sedimentary rocks are primarily composed of silty sandstone and siltstone. The basin is bounded by the Jargalant Formation to the north and the Dariv Formation to the south. The basin is filled with a thick sequence of red beds, which are composed of alternating layers of sandstone and siltstone. The red beds are deposited in a series of cycles, each representing a period of sedimentation. The cycles are separated by thin layers of white evaporite deposits, which are formed by the evaporation of saline water. The evaporite deposits are visible as white, flat areas on the margins of the basin (Fig. 4.7a, e). The basin is also characterized by the presence of caliche horizons, which are layers of hardened, white, crystalline material. These horizons are formed by the precipitation of calcium carbonate from saline water. The caliche horizons are visible as distinct, light-colored layers within the red beds (Fig. 4.7b). The basin is situated in a region of high evaporation, which is responsible for the formation of the evaporite deposits and the caliche horizons. The basin is also a source of salt, which is used for various purposes, including the production of salt brine and the extraction of other minerals. The basin is a significant geological feature, and its study provides valuable information about the processes of sedimentation and evaporation in arid environments.



that fine-upward into a floodplain or mudflat environment. Observations made during this study support this interpretation, with facies F interpreted as the deposits of fluvial channels. Facies EC sand rich siltstones are again interpreted as deposits of sand size aggregates (see discussion page 76). Facies EF fine siltstone beds were deposited during overbank floods and any primary lamination has most likely been reworked by vegetation and bioturbation; plant debris is common and extensive pedoturbation suggests a well vegetated floodplain. Well-developed caliche horizons suggest long periods of non-deposition and exposure of the floodplain to weathering processes. In contrast, the metre-scale micrite beds in the upper part of the formation represent deposition in a short-lived playa lake system that developed on the floodplain (Graham *et al.*, 1997).

#### SUMMARY

The predominant red colour suggests a seasonally wet climate, in which iron minerals (predominantly haematite) dissolved during wet periods and precipitated during dry periods (e.g. Parrish, 1993). A dominant northwest derived palaeocurrent is axial to the northwest-southeast trending depression identified in the Jargalant Formation suggesting that the two formations have coincident depocentres. The Dariv Formation is interpreted as the deposits of a river system that flowed along the axis of this depression. The only section through the Dariv Formation is located in the basin centre. It is probable that alluvial fan sedimentation continued along the basin margins, although there is no direct evidence for this. These alluvial fans would be grouped lithostratigraphically with the overlying conglomeratic Ihkes Nuur Formation, and biostratigraphic data do suggest some overlap in the ages of the two formations.

#### 4.2.4 Ihkes Nuur Formation (Upper Jurassic to Lower Cretaceous)

The Ihkes Nuur Formation overlies a conformable basal contact with the underlying Dariv Formation defined by a change in mean grainsize from siltstone to cobble conglomerate. The formation is up to 600 m thick and is dominated by red pebble/cobble/boulder conglomerate beds that form laterally extensive sheets. The Ihkes Nuur Formation's upper contact varies around the basin. A gradational contact was documented in the southwest but slight angular unconformities were observed in the north and east. The contact is defined in all cases by a sharp colour change from red to grey corresponding to a decrease in mean clast size from cobble conglomerate to siltstone interbedded with fine sandstone. The formation name is after Devjatkin *et al.* (1981).

##### 4.2.4.1 DESCRIPTION

The Ihkes Nuur Formation is exposed within the Dariv Basin (areas 2, 3 and 7, Fig. 4.2), in the Shargyn Section (area 6, Fig. 4.2) and also in the southern Dzereg Basin (Fig. 4.1 & 4.3). The formation is best exposed in the South Foreberg Ridge (Fig. 4.5) where, in two canyon sections (areas 3 and 7, Fig. 4.2), over 600 m of well-bedded conglomerate are present. Seven facies are represented (AC, AF, BC, BF, G, H, and EF in table 4.1), but conglomerate facies AC and BF are predominant. Systematic variations in the proportions of each facies are identified across the basin.

##### ***Type locality – The Dariv Section***

In the Dariv Section (Fig. 4.5) angular, clast-supported and predominantly massive red conglomerate beds (facies BF) comprise 70% of the section. Beds are 30-100 cm thick with sharp, commonly erosive, basal contacts that can be

traced laterally over a few 10's m. Clast size ranges from 1 cm to 100 cm, although individual beds are generally well sorted. Clast imbrication is common and some facies BF beds fine upward. Inversely graded, matrix-supported pebble, occasionally cobble, conglomerate beds (Facies G) are observed throughout the section, and contain occasional outsized isolated clasts (<110 cm). The two conglomerate facies are interbedded with texturally and mineralogically immature, medium-grained sandstone beds (Facies AF) that contain granules and are occasionally trough cross-stratified. Rare beds, comprising pebbles and granules supported in a fine-sandstone or siltstone matrix (Facies H), are present throughout the section.

#### *Additional exposures of the Ihkes Nuur Formation*

The Green Valley Section is 6 km along strike from the Dariv Section (area 3, Fig. 4.2 & 4.8a) and exposes a different facies architecture. Individual beds have a greater lateral extent than in the Dariv Section and this predominantly grey succession coarsens upward. The succession contains a greater proportion of fine sediment, especially in its basal part, and clast-supported pebble conglomerate sheets (Facies AC) dominate. Facies AC is commonly massive, but occasionally contains laminae defined by minor fine/coarse grain size variations on a 2-3 cm scale. Major changes in clast size, combined with planar erosive bases, define bedding surfaces on a 2-25 cm scale and beds commonly fine upward. The clast assemblage is dominated by granite, diorite, volcanic lithologies and minor intrabasinal clasts, including well-rounded sandstone and siltstones. Intrabasinal clasts are especially common at the base of Facies AC. Coarsening upward, clast-supported conglomerate beds (Facies G), along with matrix-supported pebble conglomerate beds (Facies H), are interbedded with facies AC. The abundant



**Figure 4.8a** – Photograph showing conglomerates of the Ikkes Nuur Formation in the Green Valley Section (area 3, Fig. 4.2). **4.8b** – Photograph showing dessication cracks in faces EF within the Ikkes Nuur Formation, Green Valley Section.

finer material is dominated by texturally and mineralogically immature, grey sandstone beds, that commonly contain granules (Facies AF). Silt drapes (Facies EF), not observed in the Dariv Section (area 7), are common in area 3 and contain desiccation structures at several horizons (Fig. 4.8b). The mean clast size of facies AC conglomerates increases upward and individual beds become thicker with occasional cross-stratification. Siltstones (facies EF) become less common upward, but occasional thin siltstone drapes remain throughout the section. Facies G inversely graded conglomerate sheets become increasingly abundant upward, again associated with outsize boulders. Within the section, the dip of bedding is variable over a range of approximately 10 degrees.

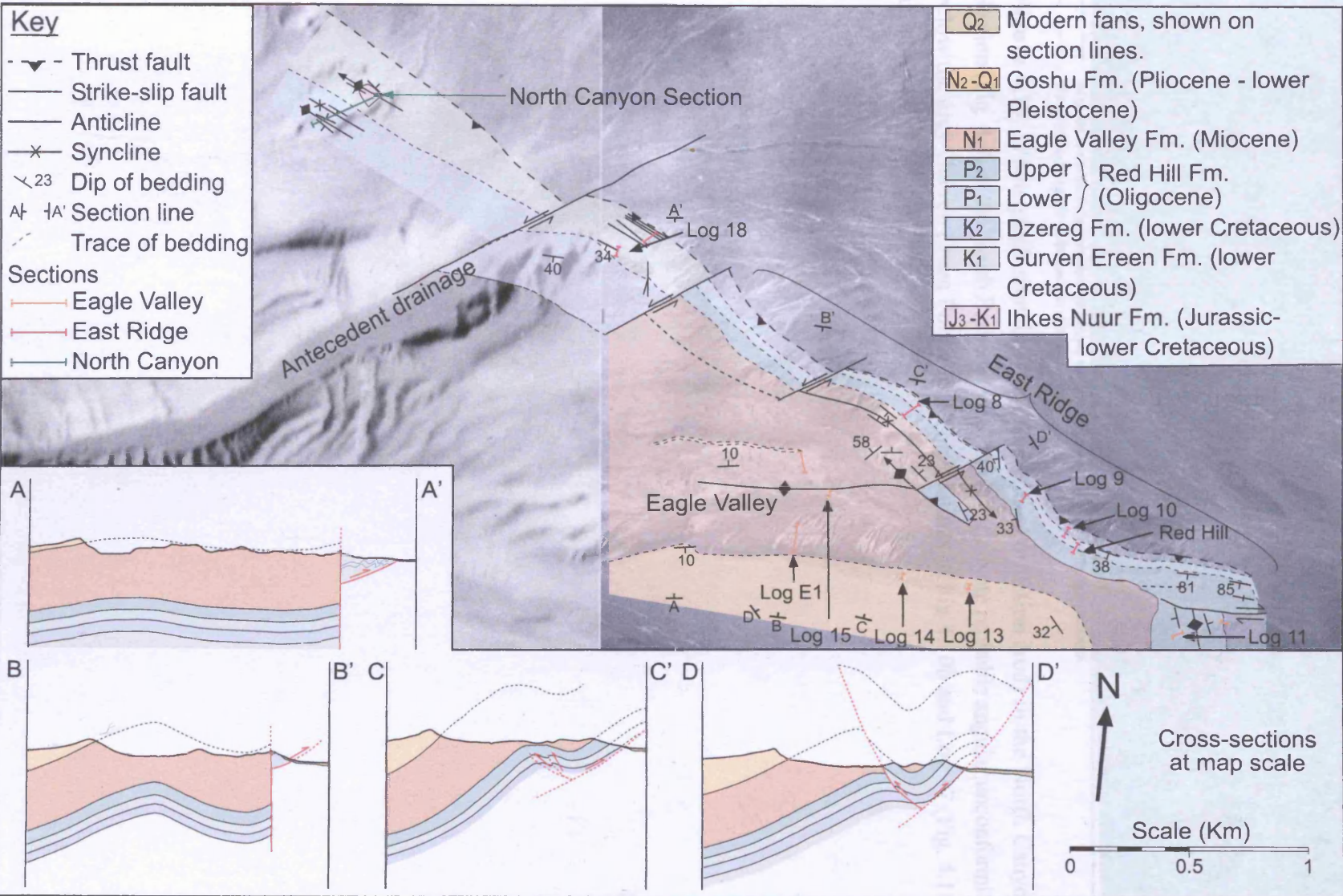
In the North Canyon Section of the north Foreberg (Fig. 4.9), the Ihkes Nuur Formation is exposed in a large canyon (Fig 4.10a & b) and is illustrated by log 17 (Fig. 4.11a & b). This section is dominated by facies AC, a clast-supported conglomerate, but is significantly finer than those documented in areas 3 and 7. Clast size ranges from 2–5 cm, with occasional larger cobbles and rare boulders. Massive, matrix-supported, granule and pebble conglomerate beds (facies H) are more common than elsewhere. Fine sediments are dominated by massive or poorly laminated sandstone (facies AF) and some silt-rich sandstone beds (facies EC). Sediment at the base of log 17 (Fig. 4.11a) is grey, but rapidly becomes redder upward. Beds are well sorted with sharp, slightly erosive contacts and are laterally extensive over 40 m exposure.

Exposure of the Ihkes Nuur Formation is limited elsewhere in the Dariv Basin. In area 4 (Fig. 4.2), on the eastern flank of the Central Ridge (Fig. 4.12),

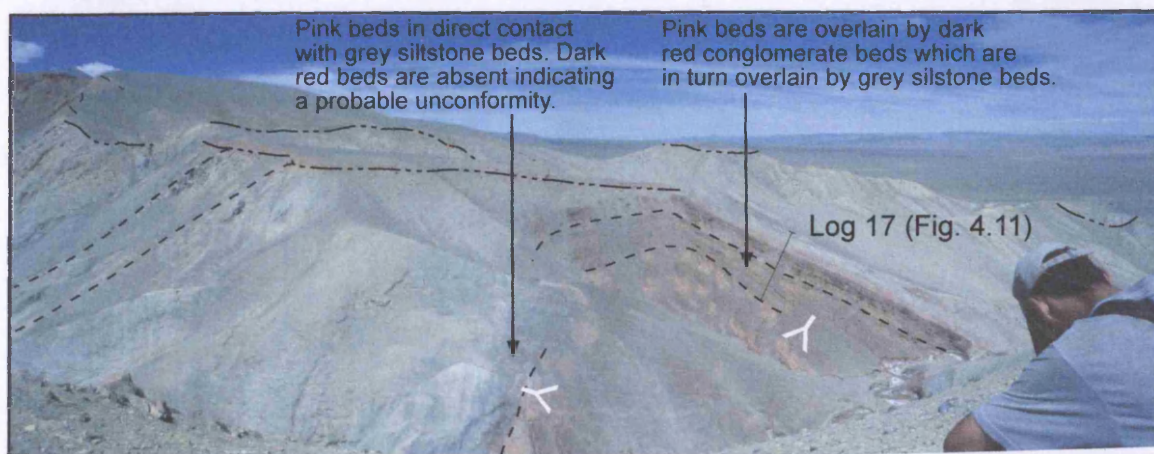
---

**Figure 4.9** (following page) – Aerial photograph and interpretation for the North Foreberg (area 2, Fig. 4.2) showing the different sections studied, the structures that uplift the ridge and locations mentioned in the text.









— — — — Angular unconformity between Mesozoic sediments and Holocene alluvial fan deposits.  
 - - - - Trace of bedding within Mesozoic strata.

**Figure 4.10** - Photograph showing the Ihkes Nuur Formation (red) in the North Canyon Section (Fig. 4.9) of the North Forberg (area 2, Fig. 4.2). Note probable angular unconformity below the grey Gurven Ereen Formation. The locations of Fig 4.10b and Log 17 (Fig. 4.11) are shown.

Figure 4.11a - Log 17 from the Ihkes Nuur Formation in the North Canyon Section (Fig. 4.9). Key to sedimentary logs on following page.





**Figure 4.11b - Key for sedimentary logs**

	Laminated sediments
	Cross-stratification
	Irregular laminations
	Laminated clay in silt
	Asymmetric ripples
	Pebble lag surfaces
	Clast supported conglomerate
	Matrix supported conglomerate
	Climbing ripples
	Convolute bedding
	Loading structures
	Bioturbation
	Water escape structures
^	Gypsum
org	organic matter

**Key to lithologies**

	Conglomerate
	Sandstone
	Siltstone/ mudstone
	Limestone

**Caliche development**

- ① Minor dissipated nodules
- ②
- ③ Isolated nodules forming distinct horizons
- ④
- ⑤ Hard carbonate cement >15 cm thick

Note that the numbering of caliche shown on the logs is the author's own system and does not correspond with the stages presented by Machette (1985) or Kraus & Brown (1988).

**Facies key**

AF	Fine sheetflood deposit
AC	Coarse sheetflood deposit
C	Crevasse splay deposit
D	Ephemeral river deposit
EF	Fine overbank deposit
EC	Coarse overbank deposit
G	Debrite
H	Cohesive debris flow
I	Deposit of sheetflood entering a lake
J	laminated lacustrine deposits
K	Bioturbated lacustrine deposits
LA	Prodelta deposits
LB	Delta front deposits
LC	Mouth bars deposits
LD	Reworked delta top deposits
LE	Delta top deposits
M	Lacustrine limestone deposition

**Sediment colour codes**

(Sediments are red in the absence of a qualifying letter)

gy	- grey
g	- green
y	- yellow
o	- orange
b	- brown
w	- white

**Figure 4.12 - Aerial photograph and interpretation of the Central Ridge of the Dniepr Basin. Structures that uplift the ridge and the location of the Central Ridge Sections (north V and south V) are shown.**

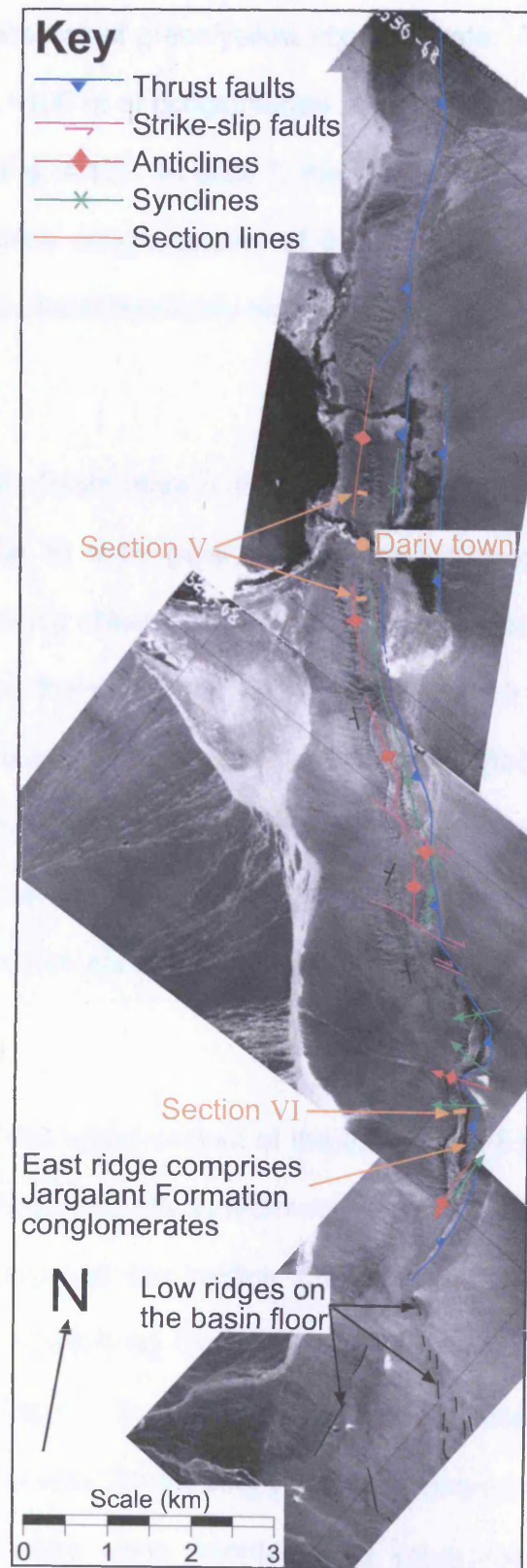


**Figure 4.12** – Aerial photograph and interpretation of the Central Ridge in the Dariv Basin. Structures that uplift the ridge and the location of the Central Ridge Sections (north) V and (south) VI are shown.



there are a few exposures of green/yellow conglomerate. The topography in area 4 is consistent with <100 m of conglomerate forming the resistant eastern flank of the Central Ridge (Fig. 4.12). In area 7, the two prominent domes (Fig. 4.5) are interpreted to comprise conglomerates of the Ihkes Nuur Formation, based on limited exposure, the characteristically high topography, and the overlying strata.

### *The Shargyn Basin*

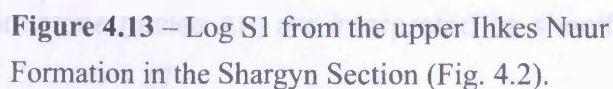
In the Shargyn Basin (area 6, Fig. 4.2), exposure is limited and comprises well bedded, angular to subangular, clast-supported conglomerate (facies AC) similar to the succession observed in area 7. Facies AC beds are 30-60 cm thick and clast size ranges from 5-50 cm. In Log S1 (Fig. 4.13), the finer sediment is dominated by matrix-supported pebble conglomerate (facies H). The section contains a small proportion of fine, silt-rich, red sandstone (facies EC). Above 13 m on Log S1 several metres of green/yellow conglomerate (Facies AC & G) characterise the top of the section.

### *Summary*

The nature of the upper contact of the Ihkes Nuur Formation varies around the basin. The contact is locally conformable in area 2 (18.7 m on log 17, Fig. 4.11), but a photograph of the section (Fig. 4.10) shows a probable angular unconformity with the overlying Gurven Ereen Formation. In area 7 the upper contact is conformable. In areas 4 and 6 the contact appears to be disconformable, and in area 3 onlapping younger sediments obscure it.

Palaeocurrent data were recorded from imbricated pebbles and cross-stratified sets and are shown in figure 4.3. Sjöström *et al.* (2001) report palaeoflow to the southeast at the base of the Ihkes Nuur Formation in the Dariv Section (not observed in this study), abruptly changing to a consistent northerly flow (Fig. 4.3).

Response	Percentage
Agree with similar subgroups within other basins	85





In the Green Valley (area 3, Fig. 4.2), abundant imbricated pebbles indicate a consistent north-northwest transport direction, whereas, in the North Foreberg and Shargyn Section (areas 2 and 6, Fig. 4.2), rarer examples of imbricated pebbles suggest south-eastward flow. The Ihkes Nuur Formation is not dated within the Dariv Basin. An Upper Jurassic – Lower Cretaceous age is assigned, based on stratigraphic position and a comparison with similar outcrops within other basins (Khosbayar, 1973).

#### 4.2.4.2 INTERPRETATION

The similarities in each studied section lead to the interpretation that they all record the same type of depositional system. Variations in the distribution of facies across the Dariv and Shargyn basins, therefore, reflect relative proximity to their source area and permit interpretation of the geometry of depositional bodies.

##### *Type locality – The Dariv Section*

The structureless clast-supported conglomerate beds, that dominate the formation, are difficult to interpret in terms of depositional environment. They commonly record deposition via fluvial processes, either streamfloods/sheetfloods (e.g. Harvey, 1988) or braided fluvial systems (e.g. Nemec & Postma, 1993). The association observed in the Dariv Section (area 7, Fig. 4.2) of massive, laterally discontinuous, conglomerate sheets, with abundant imbricated clasts (Facies BF), rare normally graded beds (Facies AC) and the limited preservation of fine material is characteristic of a proximal fluvial-dominated alluvial fan (e.g. Nemec & Postma, 1993; Harvey, 1988). Facies BF conglomerate beds are interpreted as the deposits of migrating channel bars within a braided river system (e.g. Nemec & Postma, 1993). The upward fining, laterally extensive, clast-supported conglomerate (facies AC) and sandstone (facies AF) are interpreted as sheetflood

deposits from unconfined flows across the fan surface (see Jargalant Formation, page 74). The upward coarsening clast-supported conglomerates (Facies G) are interpreted as the deposits of hyperconcentrated gravity flows (e.g. Miall, 1996) in which the matrix drains from the body following deposition leaving the characteristic coarsening upward profile in clast support (e.g. Ryang & Chough, 1997). Matrix-supported pebbles and granules (Facies H) are a minor component of the Dariv Section and represent the deposits of infrequent cohesive debris flows that may result from reworking of the fan surface during rainstorm events (e.g. Gloppen & Steel, 1981; Whipple & Dunne, 1992). The coarse, angular clasts, relatively thick beds and weakly channelised fluvial system suggest that the Dariv Section records a proximal position on a fluvial-dominated alluvial fan. Palaeocurrent data indicate that the fan system was prograding to the north, and variation in palaeocurrent data probably relates to avulsion of the major distributary network across the fan over time. The south-directed palaeoflow in the basal Dariv Section (Sjostrom *et al.*, 2001) may relate to reworking of the toe of a prograding alluvial fan by the axial drainage system documented in the Dariv Formation.

#### *Additional exposures of the Ihkes Nuur Formation*

The other sections within the Dariv and Shargyn basins are interpreted to represent part of the alluvial fan system documented in the Dariv Section, or a similar alluvial fan system. The Green Valley Section (area 3) is located 6 km northeast along strike from the Dariv Section (area 7, Fig. 4.2) and contains many facies that represent the same depositional processes. However, overall clast size is much smaller and individual beds are more laterally continuous in area 3 than in area 7. This, combined with the northwest-north trending palaeocurrent data, suggests area 3 was in a more distal position within the fan system relative to area

7. The thin, laterally extensive beds observed at area 3 are interpreted to have been deposited downslope of the channel system documented in area 7 by unconfined flows (e.g. Whipple & Dunne, 1992). Facies AC is again interpreted to represent deposition from periodic sheetflood events sourced from the upper fan, with the overlying siltstone beds (facies EF) recording slow settling from suspension following a flood event (see prior discussion page 74). Rip up clasts of siltstone (facies EF) are commonly preserved above the basal erosive contacts of facies AC. Matrix-supported debris flow deposits (facies H) are also more common in area 3. Thinner facies H beds may result from reworking of the fan surface, possibly by rainwash processes (e.g. Nemec & Postma, 1993). However, thicker layers are interpreted to result from streamflow processes active in the catchment area and transported to the lower fan via the channel system observed in area 7.

The overall coarsening upward trend of the formation in area 3 is interpreted to represent northward progradation of the fan system. The observed along-strike variation in dip and the variable orientation of measured palaeocurrents are interpreted to reflect depositional lobes on the fan surface. Such lobes are seen on active fans today (e.g. Harvey *et al.*, 2003) where they influence the transport and distribution of sediment over the fan surface. No palaeosols were observed and this suggests that the fan was not abandoned and exposed for long periods. Possible evidence for exposure of area 7 sediments is suggested by their red colour, compared to the grey dominated area 3. Red staining is again tentatively interpreted to indicate a seasonally wet-dry climate (e.g. Parrish, 1993). The upper parts of an alluvial fan are commonly zones of incision and bypass therefore exposure of surfaces is expected.

Exposure in the North Foreberg (Log 17, Fig. 4.11) again represents the distal deposits of an alluvial fan. Facies AC clast-supported granule

conglomerates are interpreted to be the distal deposits of the coarse sheetflood deposits observed elsewhere.. Deposits of cohesive debris flows (facies H), are relatively common. Palaeocurrent data indicate transport to the southeast suggesting that these deposits relate to a second alluvial fan system sourced in the northwest.

## THE SHARGYN BASIN

The Shargyn Section (area 6) lies between the Dariv Section and Green Valley Section (areas 7 and 3) in terms of relative proximity to source. The mean grainsize is smaller and beds are thinner than the proximal deposits observed in the Dariv Section, but with a lower proportion of interbedded facies EF siltstones than in the Green Valley Section. The Shargyn Section also contains a greater proportion of debris flow deposits (Facies H) than is seen elsewhere. This section is interpreted to represent a similar type of fan system to areas 7 and 3 but is not the same fan given the southerly palaeocurrent and the greater predominance of debris flow deposits. The discoloured yellow/green top is interpreted to represent a period of non-deposition and alteration of this surface prior to deposition of the overlying formation. The same interpretation is made for the small Central Ridge Section (south) exposures (area 4).

### *Summary*

A large fan system prograded northwards into the Dariv Basin in response to a new sediment source from the southwest, while elsewhere in the basin smaller fans were sourced from existing uplifted areas. These deposits represent a major change in both the sediment yield of the source area and depositional style.

#### 4.2.5 Gurven Ereen Formation – Lower Cretaceous

The Gurven Ereen Formation overlies a locally unconformable basal contact with the underlying Ihkes Nuur Formation defined by a marked decrease in mean grainsize from cobble conglomerate to siltstone and a corresponding colour change from red to grey. The formation is up to 200 m thick and dominated by grey siltstone and claystone with occasional fine sandstone sheets. The Gurven Ereen Formation's upper contact is conformable with the overlying Dzereg (Zerik) Formation and is defined by a colour change from grey to red. The formation name is after Devjatkin *et al.* (1981).

##### 4.2.5.1 DESCRIPTION

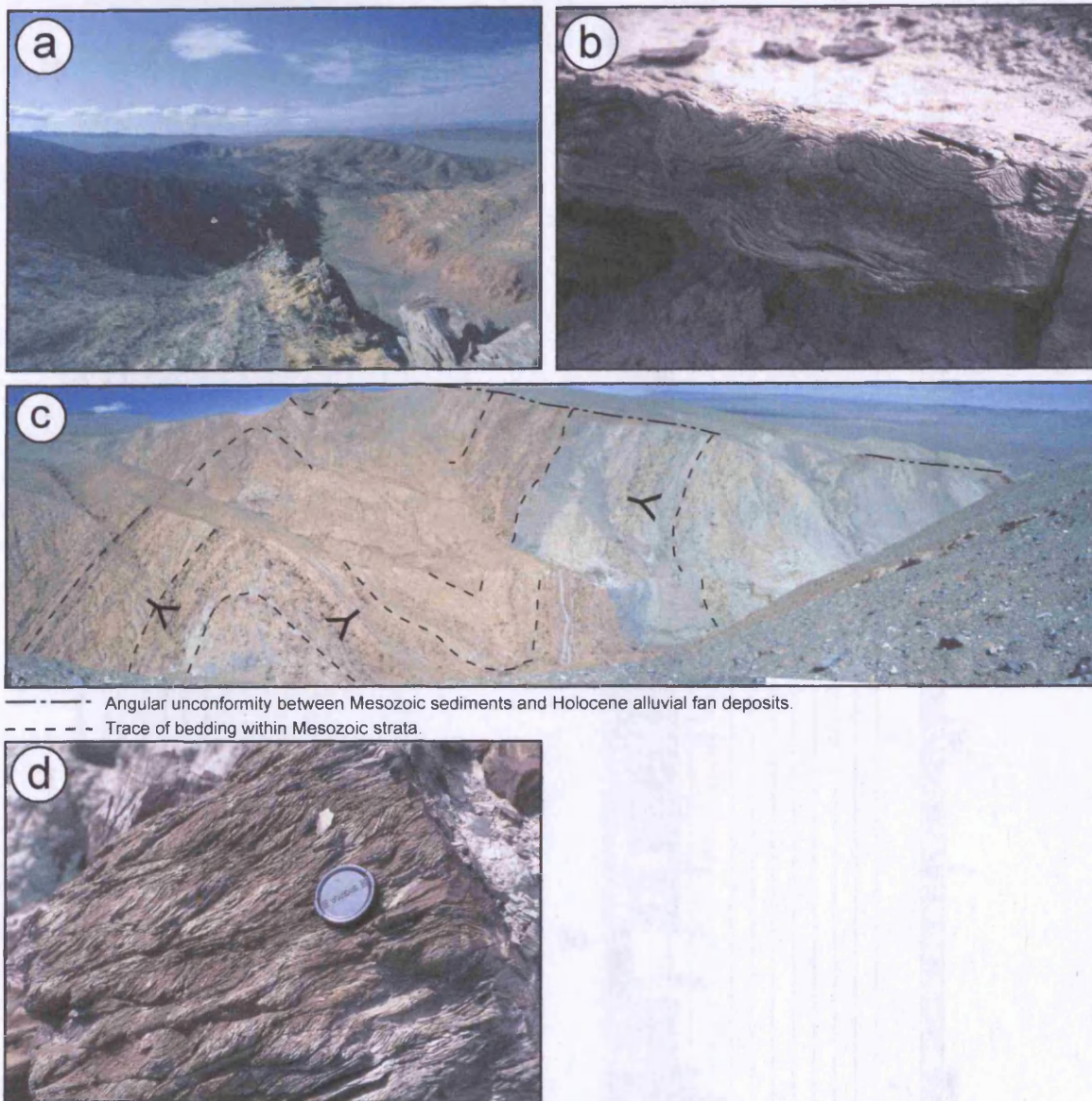
The Gurven Ereen Formation was studied at five localities within the Dariv Basin (areas 1, 2, 3, 4 and 7, Fig. 4.2), as well as in the Shargyn Section. Two sections from the southwest and southeast of the Dzereg Basin (Fig. 4.1) are described by Howard *et al.* (2003).

##### ***Type locality – The Central Ridge Section (south)***

The type locality for the Gurven Ereen Formation is seen in the Central Ridge Section (south), where the formation is 50 m thick (Fig. 4.12 & 4.14a). Log VI (Fig. 4.15) documents the upper 45.3 m of the fine-grained succession, which is dominated by grey siltstones and sandstones and comprises 6 facies (AC, AF, EF, I, J and K in table 1). This section is divided into two members:

---

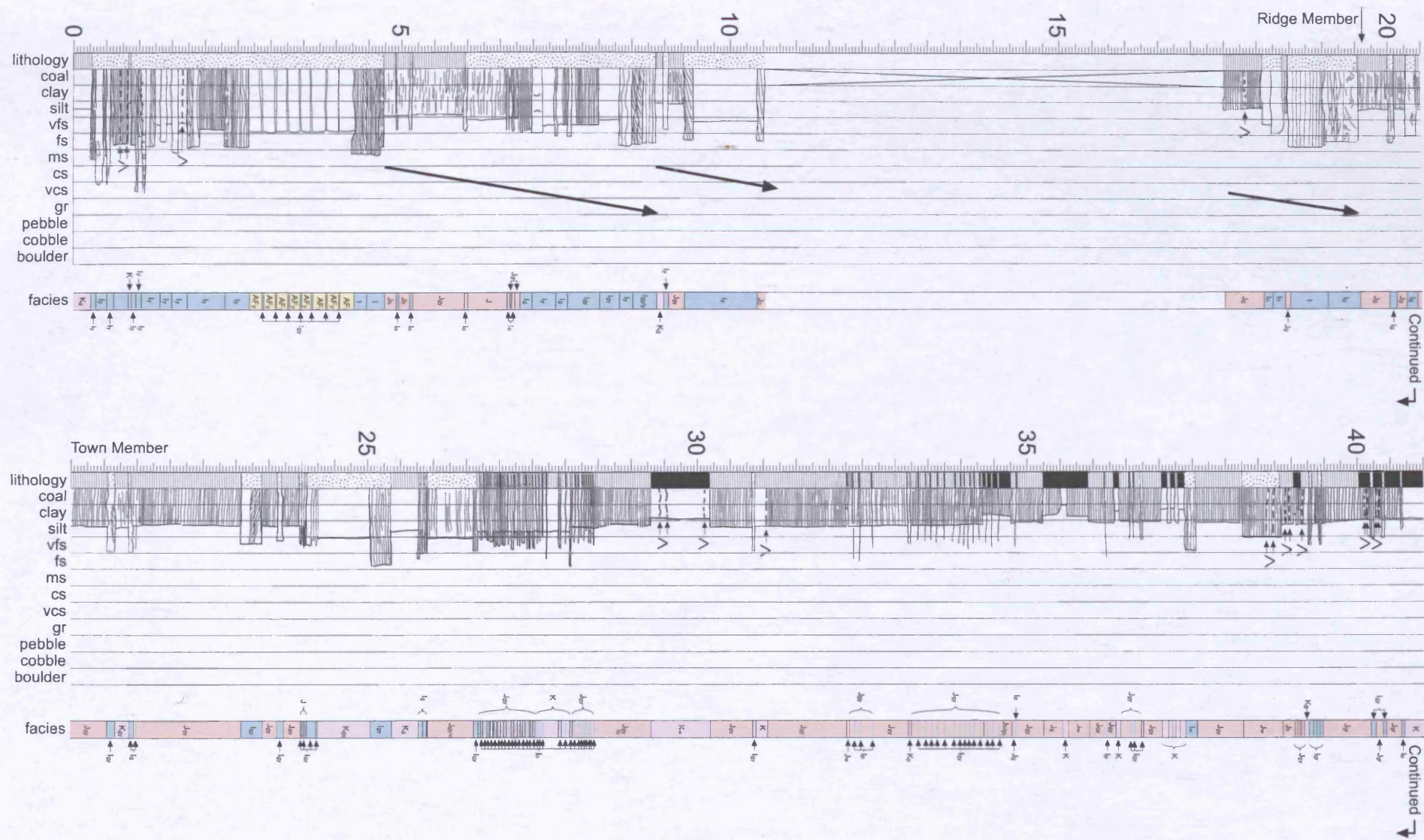
**Figure 4.15** (follows Fig. 4.14) – Log VI from the Central Ridge Section (south) showing the Gurven Ereen, Dzereg and Red Hill Formations.

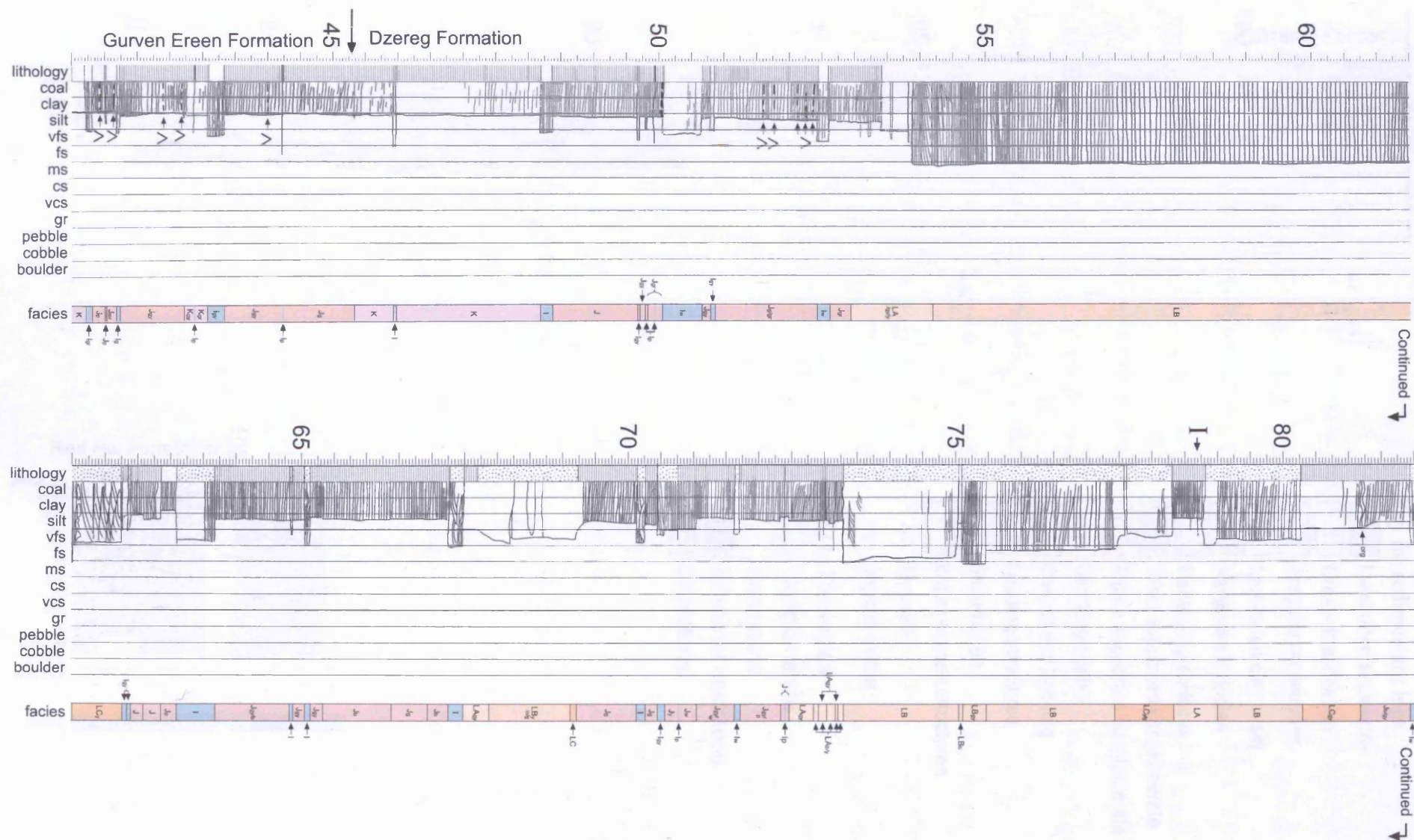


**Figure 4.14a** – View south down the Central Ridge Section (south) showing general exposure of the grey Gurven Ereen Formation sediments and the overlying Dzereg Formation (red base). This section's lower part is shown in figure 4.10a. **4.14b** - Soft sediment deformation in facies I, in the Gurven Ereen Formation, Central Ridge Section (south). **4.14c** - View north showing the exposures in the North Foreberg Section. The grey unit is the Gurven Ereen Formation, the overlying Dzereg Formation is red. The folds are on the upper plate of the North Foreberg thrust (Fig. 4.9). **4.14d** - Climbing ripple cross-stratification in a fine to medium-grained sandstone in the Gurven Ereen Formation, East Ridge Section. Current direction is to the left/

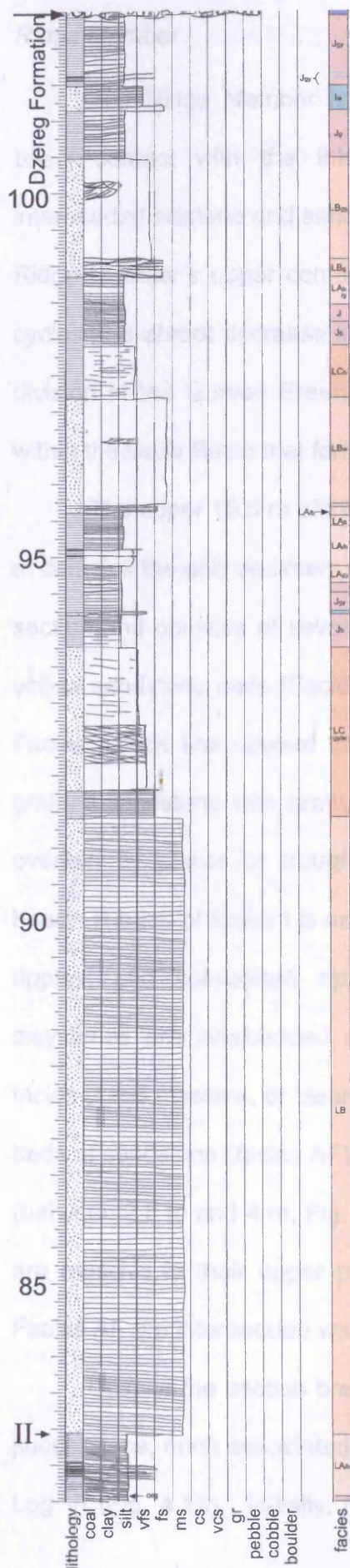
Figure 4.15 - Log V1 from the Central Ridge Section (south) showing the Gurven Ereen, Dzereg and Red Hill Formations.











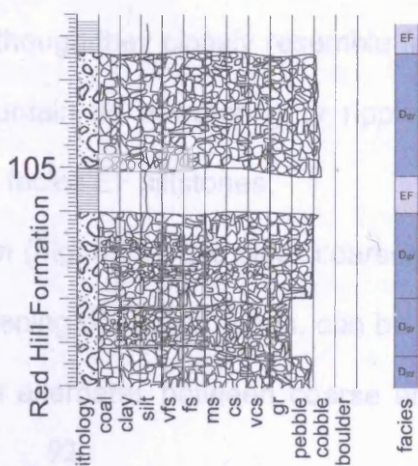
Continued

### Key for sedimentary logs

- Laminated sediments
- Cross-stratification
- Irregular laminations
- Laminated clay in silt
- Asymmetric ripples
- Pebble lag surfaces
- Clast supported conglomerate
- Matrix supported conglomerate
- Climbing ripples
- Convolute bedding
- Loading structures
- Bioturbation
- Water escape structures
- Gypsum
- organic matter

### Key to lithologies

- Conglomerate
- Sandstone
- Siltstone/ mudstone
- Limestone



### *Ridge Member*

The Ridge Member is 24 m thick, and overlies a locally unconformable basal contact with the Ihkes Nuur Formation. The formation comprises interbedded siltstone and sandstone beds defining coarsening upward cycles. The Ridge Member's upper contact is defined by the top of the coarsening upwards cycles and abrupt decrease in mean grainsize. The Ridge Member is a new subdivision of the Gurven Ereen Formation and is named after the prominent ridge within the Dariv Basin that forms its type section.

The upper 19.5 m of the Ridge Member are recorded in log VI. The basal 5 m contains the only sediment coarser than medium-grained sandstone in the entire section and consists of several initially centimetre scale, fine-to medium-grained, yellow sandstone beds (Facies I) that are laterally extensive over 10's to 100's m. Facies I beds fine upward from a coarse basal lag, comprising a soft, medium-grained sandstone with granules, or matrix-supported pebbles. This basal lag is overlain by planar or trough cross-stratified, occasionally massive, sandstone beds. The top of facies I is usually well laminated, but locally includes symmetrical ripples, and convoluted ripples (Fig. 4.14b). Multicoloured siltstones and claystones are interbedded with facies I. Laminated siltstone beds represent facies J and massive, or clearly bioturbated siltstones are facies K. Fining upward beds of sandstone (facies AF) form an interval near the base of the Ridge Member (between 2.5 m and 4 m, Fig. 4.15). Although they closely resemble facies I, they are massive in their upper part and contain no dewatering or ripple structures. Facies AF are interbedded with massive facies EF siltstones.

Despite the section break at 10 m (Fig. 4.15), two clear coarsening upward successions, each associated with thickening of Facies I beds, can be identified in Log VI (Fig. 4.15). Initially, the section alternates between coarse and fine with



facies I overlying facies K, grain size then stabilises with facies AF beds dominating up to 4 m (log VI). The member then abruptly fines, before coarsening upward to 9 m (Log VI) from siltstones (Facies J) to fine sandstone (facies I). The base of a third possible coarsening up succession is truncated by the section gap and the member finally coarsens up to its top at 19.5 m log VI. Throughout the member, hard, orange, very fine-grained sandstone horizons, <5 cm thick, are observed within facies I; these are characteristic of this formation. Bedding surfaces within the member are sharp and planar, with erosion only recorded beneath the coarsest beds at the base of Facies I. Gypsum horizons are present and are interbedded with both facies K and I.

#### *Town Member*

The Town Member has a conformable basal contact with the Ridge Member which is defined by a decrease in mean grain size from sandstone to siltstone. The Town Member is dominated by grey siltstone with occasional fine sandstone beds. The upper contact of the Town Member is conformable with the overlying Dzereg Formation and is marked by an abrupt colour change from grey to red. The Town Member is a new sub division of the Gurven Ereen Formation and is named after the small town around which good exposure may be found.

The almost exclusively grey Town Member (19.5 m to 45.3 m, log VI, Fig. 4.15) is significantly finer than the Ridge Member. The Town Member fines upward slightly and is dominated by laminated, micaceous siltstones and clay beds (facies J), that become increasingly red above 36 m, log VI. Facies J again contains distinctive hard, orange and purple sandstone sheets that are <3 mm thick. Massive siltstones and claystone beds (facies K) are interbedded with facies J and, although facies K beds represent a small percentage of the total section,



they occur throughout the member and reach 40 cm thick. Intermittent laminated or cross-stratified micaceous sandstone beds (facies I), generally <30 cm thick and laterally extensive over 10's m with minor thickness variation, are interbedded with facies J. As the Town Member becomes progressively finer, facies I sandstone beds become laminated and very fine-grained. Layers of fibrous gypsum (<3 mm thick) occur throughout the Town Member within facies J and K.

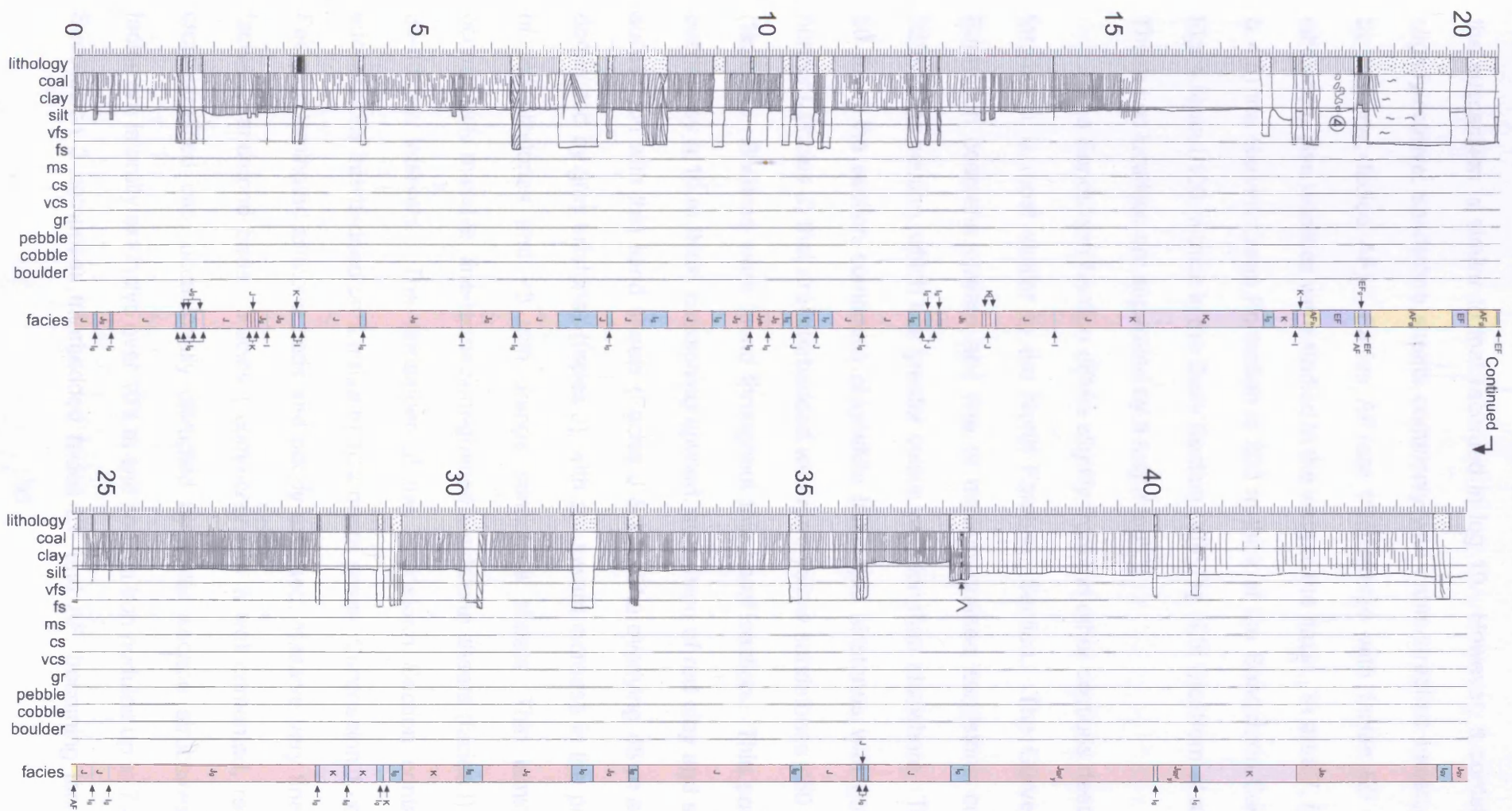
#### *Additional exposures of the Gurven Ereen Formation*

Elsewhere in the Dariv Basin, two good exposures of the Gurven Ereen Formation were documented in area 2 (the North Foreberg), where the formation is 150 m thick. Figure 4.14c illustrates exposure in the North Canyon Section (Fig. 4.9) and Log 10 (Fig. 4.16) records a 44.5 m section measured in the East Ridge Section (Fig. 4.9).

Log 10 documents a similar stratigraphy to that described in The Town Member, dominated by grey and red laminated siltstones interbedded with yellow/brown clay (facies J). The thin orange and purple horizons are again present throughout this section. Facies I sandstones, interbedded with facies J siltstones, contain excellent examples of climbing ripples (base of Log 10, Fig. 4.14d). Massive multicoloured siltstone beds (facies K) are more common within this section, but gypsum is apparently less common. A notable difference is the presence of a well-developed caliche horizon (18.3 m, Fig. 4.16) below a well bioturbated, fining upward sandstone bed that contains vertical burrows 2-5 cm long (Facies AF). Facies AF forms the thickest sandstone beds seen in this section. Exposure in the North Canyon Section (Fig. 4.9 and 4.14c) is good and

---

**Figure 4.16** (following page) – Log 10 from the East Ridge Section of the North Foreberg (area 2, Fig. 4.2). Log 10 is located on Fig. 4.9.



the succession is similar to that recorded in log 10. However, it contains more slightly-erosive, sandstone sheets commonly with cross-stratified bases, overlain by laminae (facies AF). Facies AF are interbedded with facies EF massive siltstones. Two localities were studied in the west of the basin. In area 7, (Fig. 4.2 & 4.5) the Gurven Ereen Formation is 200 m thick at the Sandstorm Section (IX, Fig. 4.5) and 100 m thick in the Dariv Section (XIII, Fig. 4.5, Sjöström *et al.*, 2001). These two localities are separated by a major fault.

The Sandstorm Section differs slightly from the other sections described so far, but it is most similar to the North Foreberg Section. The Gurven Ereen Formation coarsens upward and fine to medium-grained sandstone comprises 32% of the section, which has greater colour variation than elsewhere. The basal 50 m of the section comprises grey/white laminated siltstones with gold/yellow horizons (facies J) that are interbedded with rare, yellow sandstones <30 cm thick (facies I). Bivalves were found throughout this basal section. This package is overlain by a 10 m thick, coarsening upward, succession of red clay and siltstones succession with thin sand sheets (Facies J & K). The overlying 48 m are again dominated by grey siltstones (facies J), with an upward increase in the proportion of red siltstones and <3 mm orange sandstone sheets. Thin laminated or occasionally massive, fine-to medium-grained sandstone sheets (facies I) occur at 30-50 cm intervals. The remainder of the Sandstorm Section contains two successions interbedded on a metre to 10's metre scale. Succession 1 comprises Facies J laminated siltstone beds and poorly exposed, massive very fine-grained facies I sandstone beds. Facies I commonly has a well-cemented, red, ripple cross-stratified cap, occasionally disrupted by water escape structures. Both facies are laterally extensive over 10's m and contain iron nodules up to 7 cm long. Succession 2 comprises interbedded facies EF and AF, becoming increasingly

common upward. Facies EF is massive or poorly laminated grey/green, grey/blue or red siltstones. Fining upward sandstone beds (facies AF) have a cross-stratified base and massive or laminated top and lack dewatering structures and ripples. A single caliche horizon is present at 85 m within facies EF.

The Dariv Section comprises approximately 200 m of siltstones overlying a gradational contact with the Ihkes Nuur Formation (Section VIII, Fig. 4.3). It comprises predominantly well-laminated, grey/green siltstones (facies J) and massive siltstones and silt-rich sandstone (facies K), interbedded with centimetre-scale sandstone intervals (facies I). Facies I sandstone beds containing ripple cross-laminae and planar-laminae occur mainly towards the top of the formation. At the base of the unit, in the transition zone, red siltstones (facies J) and cross-stratified sandstones (facies I) are interbedded with grey conglomerate sheets that are in turn overlain by fining upward, occasionally cross-stratified sandstone, (facies AC) and grey siltstones (facies EF). Abundant wood debris and occasional pyrite crystals were found within this section.

#### *The Shargyn Basin*

In the Shargyn Section (area 6), the Gurven Ereen Formation is disrupted by faults but at least 195 m of well-exposed, siltstones and occasional sandstones were documented. The basal part of the section is poorly exposed and overlies a disconformable contact with the Ihkes Nuur Formation. The section is dominated by laminated siltstones interbedded with clay (facies J), containing rare, 3-5 cm thick, facies I sandstones, as seen elsewhere. Facies AF sandstone beds sometimes preserve casts of desiccation structures in their base and asymmetric ripples on their upper surface. Clasts become increasingly rounded upward and include angular quartz and intrusive rocks (granite and diorite). Up section, there

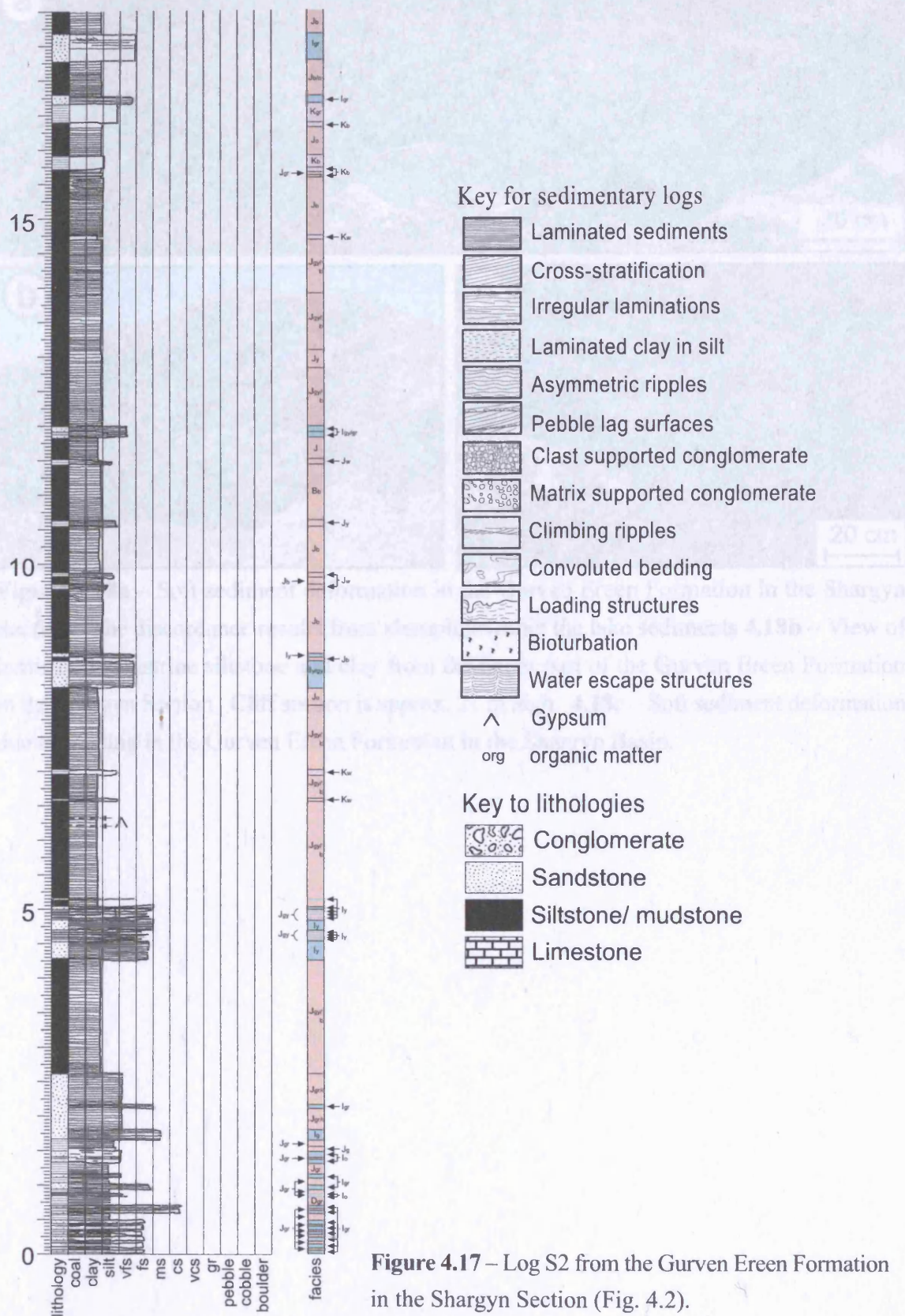
is increasing colour variation in the facies J and K siltstones which include grey, brown, yellow and some green beds (Log S2, Fig. 4.17). Facies I sandstone sheets become thicker (<15 cm) and occasionally have a basal pebble lag. The sandstone sheets become increasingly common upward and eventually occur every 1-3 m. The lower part of the Shargyn Section is comparable with the Ridge Member in the Central Ridge Section, south (log VI, Fig. 4.15)

Exposure is excellent in the upper part of the Shargyn Section. Laminated grey and yellow siltstones and clay (facies J, Fig. 4.18a, b) are again interbedded with very fine-to fine-grained, laminated sandstone beds <10 cm thick, (facies I). Localised internal deformation is present, commonly affecting only individual beds or thin intervals (Fig. 4.18a, c). The section becomes increasingly sand-rich upward. Massive, fine-grained, red weathering sandstones, <70 cm thick, with slightly erosive bases (15 cm over distances of 1 m) are present (facies AF). Iron-stained horizons also become increasingly common within the siltstones and clay intervals. Channelised scours, up to 60 cm deep are filled with horizontally laminated siltstones and are seen at several horizons. A small log through the upper part of the Shargyn Section is shown in log S3 (Fig 4.19).

### *Summary*

As in the other formations, palaeocurrent directions vary around the basin. In the Central Ridge Section and the North Foreberg area, flow was dominantly from the northeast. In the Shargyn Section, palaeoflow was initially from the west but palaeoflow indicators show a gradual change to a northeast source. In the Dariv and Sandstorm Section, data were rather variable, however the combined unidirectional data show flow predominantly to the northeast (Fig. 4.3). The





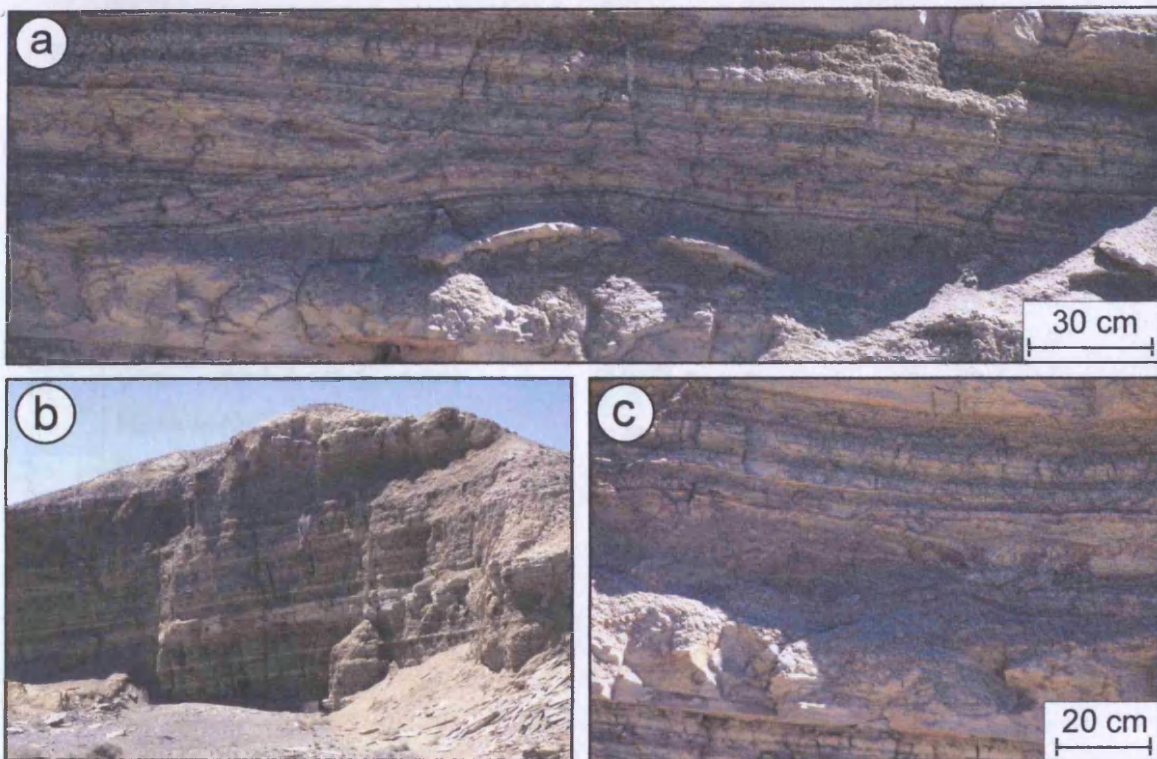


**Figure 4.18a** – Soft sediment deformation in the Gurven Ereen Formation in the Shargyn Section. The discordance results from slumping within the lake sediments **4.18b** – View of laminated lacustrine siltstone and clay from the upper part of the Gurven Ereen Formation in the Shargyn Section. Cliff section is approx. 21 m high. **4.18c** – Soft sediment deformation due to loading in the Gurven Ereen Formation in the Shargyn Basin.





contact between the Gurven Ereen Formation and the overlying Dzereg Formation is conformable.

The Gurven Ereen Formation in the Dariv Basin is of latest Jurassic – Lower Cretaceous age on the basis of biostratigraphic data (appendix 1) from insects, molluscs, ostracods, fish and phyllopods (Devjatkin et al., 1975) and a small ornithischian dinosaur (Khosbayer, 1973).

#### 4.2.5.2 INTERPRETATION

A lacustrine environment is interpreted from the various exposures of the Gurven Ereen Formation. The differences observed in the 5 localities record and reflect different aspects of the evolving depositional system within the Dariv Basin.

##### *Type locality – The Central Ridge Section (south)*

The Ridge Member, from the basal Central Ridge Section (south), is significantly coarser than the overlying Town Member. Only at the base of log VI are massive siltstone beds (Facies K) exposed. Facies K siltstone beds are interpreted to have settled from suspension and contain fossils, such as bivalves and gastropods, typical of a lacustrine environment. Bioturbation destroyed the primary laminae and this implies oxygenated conditions within the lake waters and lake floor sediments at the time of deposition. Facies K is overlain by a coarsening upward succession of facies I sandstone beds. Facies I beds fine upward and contain sedimentary structures which, as discussed in the Ihkes Nuur Formation (page 86), are characteristic of sheetflood deposits. Dewatering structures, wave ripples and interbedded facies K siltstones, suggest periodic sheetfloods entered a shallow lake and were reworked by waves (e.g. Hardie et al., 1978). The coarsening upward succession represents the advance of a sheetflood-dominated alluvial system into the lake. The basal succession recorded in Log VI is overlain

by facies AF which fines upward and contains the same structures as facies I, however, the absence of wave ripples and presence of a well-cemented red top suggests subaerial exposure on the floodplain. The coarsening upward successions observed in Log VI indicate lake level fluctuations that kept the shoreline close to the section line throughout deposition of the Ridge Member. The section is comparable to the nearshore lacustrine facies described by Link & Osborne (1978). The thin laterally extensive gypsum horizons, observed at several levels within these coarsening upwards successions, represent the precipitation of selenitic gypsum from the water column (e.g. Sanz *et al.*, 1994). The presence of gypsum, in association with the abrupt progradation of sandstone facies, suggests rapid alluvial deposition was linked to periods of lake level fall, when hypersaline lake water developed after evaporation.

In contrast to the Ridge Member, the Town Member is dominated by well-laminated grey siltstones and claystone (facies J), with many typically lacustrine fossils, that record the suspension fallout of fine sediment from the water column. This style of sedimentation is dominant in lakes that lack an external supply of coarse sediment. Thick successions of <1 mm thick laminae indicate an absence of burrowing benthic organisms and may reflect high salinity, as interpreted from deposits of laterally extensive selenitic gypsum. Elevated salinities can limit benthic life (Gierlowski-Kordesch & Rust, 1994). However, no thick evaporite deposits occur and, therefore, the gypsum horizons may reflect only brief periods of hypersalinity within the lake that were unlikely to prevent the development of benthos at other times. A diverse fossil assemblage has been recovered, indicating lake waters were able to support life, but the lake bed may have been poorly oxygenated. Surface waters would have developed elevated salinities during periods of evaporation and, in lakes only a few metres deep, high salinity



waters have been observed to sink producing a density stratified water column (Smoot & Lowenstein, 1991). Any density stratification would prevent mixing of the water column and produce lakebed anoxia. The lake may have been meromictic but, because many modern groups of bioturbators were absent in the Late Jurassic-Early Cretaceous, even seasonal anoxia could lead to a sediment water interface devoid of life and bioturbation (Olsen, 1991). The dominance of facies J in all of the sections examined indicates that anoxia was persistent in the bottom waters of an open lake environment. In this density stratified saline lake, the bioturbated siltstones (facies K) of the Ridge Member are interpreted to represent either shallow-water deposition proximal to the palaeo-shoreline and therefore above the density stratified anoxic zone, or a period of mixing in the water column that introduced oxygen to the lake bed. Shallow-water deposition is most likely, but the influx of a sheetflood would disturb and possibly mix the water column and so oxygenated conditions may result from a combination of processes.

The upward fining of the Town Member is interpreted to represent increasingly distal sedimentation away from the lake margin environment recorded by the Ridge Member. It is likely that lake level rose significantly following deposition of the Ridge Member, and continued to rise throughout the deposition of the Town Member. Facies K massive siltstones and claystones present throughout the section are again interpreted to represent reworking of the initially laminated sediment by benthic organisms. Therefore, any bottom water/sediment anoxia was periodically disturbed. Three >50 cm thick facies K intervals may represent prolonged periods of bioturbation, unfortunately no relative time periods can be fully established because bioturbation can also affect sediment deposited during anoxia once oxygenated conditions are re-established. The gypsum horizons are commonly associated with the massive layers and this is interesting

because it suggests water column mixing is better during times of increased evaporation. This is logical because if there were continuous sinking of dense saline surface waters produced through evaporation (e.g. in times of rapid evaporation) there would be an effective transfer of oxygen to the lakebed (e.g. Hardie *et al.*, 1978). Rapid evaporation associated with facies K siltstones is further supported by the presence of thicker (and therefore closer to the lake margin) sheetflood deposits (facies I) overlying many of the facies K massive siltstones. This interpretation suggests that density stratification was stable only when the influx of freshwater matched or exceeded surface evaporation. The Town Member is characterised by laminated siltstones, therefore a stable density stratified lake was the dominant depositional environment. There are no subaerial deposits within the Town Member.

#### *Additional exposures of the Gurven Ereen Formation*

Changes in the area submerged by the lake can be determined using the sedimentary record preserved in the other sections. The section shown in Log 10 (Fig. 4.16) is in an intermediate location between the Ridge and Town members (Fig. 4.9). In this location, lacustrine siltstones (facies J) are interbedded with sheetflood deposits (facies I) that occur throughout the section and are slightly coarser than those in the Town Member. The section between 15-22 m in log 10 records an important change, where laminated lacustrine siltstones (facies J) are overlain by massive bioturbated siltstones (facies K). The bioturbated siltstones are interpreted as shallow-water and shoreline proximal deposits based on the presence of overlying sheetflood deposits (facies I). Above the sheetflood deposit, a well-developed caliche horizon in siltstones indicates a significant period of subaerial exposure. Facies AF subaerial sheetflood deposits above the caliche

horizon have themselves been extensively pedoturbated and are overlain by lacustrine siltstones (facies J). This succession represents a significant and long-lived fall in lake level. The remainder of the section records lacustrine deposition. The exposure 2.5 km along strike in the North Canyon Section (Fig. 4.9) is similar to log 10, but represents an increasingly lake shore proximal area with several intervals of subaerial sheetflood sandstone (facies AF) and siltstone deposits (facies EF). These subaerial sediments are interbedded with a lacustrine succession suggesting a fluctuating lake level. An initial lake level fall is represented by a concentration of facies I within the fine-grained lake sediments dominated by facies J and K, this is overlain by subaerial sheetflood deposits. A rise in lake level is marked by the superposition of lacustrine siltstones on a subaerially exposed surface. This fluctuating lake margin suggests the North Canyon Section lies close to the lake's maximum northern extent.

In the southern Dariv Basin, the Dariv Section records the initial lacustrine transgression across the coarse-grained alluvial fan system represented by the Ihkes Nuur Formation. Lacustrine flooding is represented by an upward coarsening series of subaqueous and subaerial sand and conglomerate beds (facies I, AF and AC), similar to those seen in the Ridge Member (Log VI, Fig. 4.15). Above the lake margin deposits, lacustrine facies, J and K, alternate with thin sheetflood sandstone deposits recording open water lacustrine sedimentation. This succession is comparable to Log 10 (Fig. 16) and the Town Member (Log VI) in the north and east of the basin. Sjöström *et al.* (2001) state that the shallow-water environment recorded in the Dariv Section represents deposition in a predominantly oxygenated lake with only intermittent periods of anoxia. The greater proportion of massive siltstones (facies K) and the abundant sand grains observed in this study suggests a more nearshore location than in logs 10 and VI,

which in part supports this interpretation. There is, however, ample evidence for extended periods of anoxia, including well-preserved fossils and the presence of pyrite within the laminated green siltstones. Sand grains present within the siltstones may have been transported to the lake via aeolian or fluvial processes.

The lower part of the Sandstorm Section is dominated by lacustrine siltstones (facies J), although the basal contact with the Ihkes Nuur Formation is not seen (Fig. 4.5). Based on observations in the other locations, a succession with interbedded subaerial and subaqueous facies is predicted. The exposed succession is initially dominated by fine-grained lacustrine sediments (facies K & J), but subaqueous sheetflood deposits (facies I), and then subaerial sheetflood deposits (facies AF), become increasingly important. The caliche horizon provides evidence for long-term subaerial exposure and is consistent with progressively more subaerial deposition. Lacustrine sediments represent a small proportion of the overall section and, therefore, this area was located close to the most southerly extent of the Latest Jurassic-Lower Cretaceous Dariv Basin lake.

### *The Shargyn Basin*

The Gurven Ereen Formation records the first evidence for the separation of the Dariv Basin from the Shargyn Basin. The Shargyn Section records a lake environment similar to that interpreted from the Dariv sections. However, area 7 in the Dariv Basin records shoreline deposition, therefore the Shargyn deposits are interpreted as recording a separate second lake. This is also consistent with southerly palaeoflow indicators within the Shargyn Section. The formation is characterised by laminated and dominantly grey siltstones, that record almost exclusively deep-water sedimentation with bottom water anoxia and limited sand input (facies J). Towards the top of the formation yellow sandstone beds,

associated with deformation structures in the underlying siltstones, become more common (Fig. 4.18a, b & c) and are interpreted as sheetflood deposits (facies I). Load structures beneath sandstone beds are common, however, some structures suggest minor slumping occurred (Fig. 4.18a). Erosive flows are suggested by the sharp bases cutting across deformed laminae. The increasingly coarse sediment indicates a progressively more source proximal position that is interpreted to represent the southward progradation of the shoreline.

### *Summary*

Fine-grained facies within the Gurven Ereen Formation preserve a wide range of colours. Predominantly grey sandstone beds are interpreted as distal anoxic deposits (facies J), however, small amounts of red sediment occur within these beds. Colour variations in lacustrine sediments can result from a range of external and internal processes. The green/grey versus red/orange colours generally represent the oxidation state of iron within the system and consequently red coloration is not common within facies J. The presence of red colouration may indicate a period of oxidising conditions on the lakebed, or simply an iron-rich horizon that was oxidized during uplift. Relative carbonate content can also be important and can produce a range of yellow-white beds. Colour variations, however, predominantly reflect trace element chemistry (Turner, 1980). The colour variation in subaerial deposits (facies EF) from the Sandstorm Section results from hydromorphic processes on the floodplain (e.g. Retallack, 1988). The dominant grey and blue siltstone beds are interpreted as gley soils, which formed in a water saturated soil horizon close to the lake shore.

The Cretaceous climate in Mongolia is generally accepted to have been more arid than the Jurassic, and Cretaceous aeolian deposits are reported in



eastern Mongolia (Fastovsky *et al.*, 1997). Climate models also predict low rainfall (Parrish *et al.*, 1982). In this study, an arid climate is supported by the occurrence of gypsum layers which indicate intense evaporation. The formation of extensive perennial saline lakes does require a significant input of fresh water which, in the Dariv Basin, was probably delivered via a river. Although no exposure of Gurven Ereen Formation fluvial sediments was seen in the Dariv Basin, an axial river is present in the Dzereg Basin at this time (Howard *et al.*, 2003). The Dzereg river flowed to the south and may have supplied water to the Dariv Basin lake.

This interpretation for the Gurven Ereen Formation implies that the base of the formation is not time equivalent across the basin. Initially, during Ridge Member deposition, a lake existed in areas 1,2 and 4 defining the basin centre. Sheetflood sedimentation around the basin margin, for example, on the alluvial fans in area 7, was coeval with lacustrine sedimentation and would be lithostratigraphically grouped with the Ihkes Nuur Formation. The absence of fossils in the coarse facies prevents a biostratigraphic correlation. The Town Member represents the expansion of the lake through time, as the marginal alluvial fans were progressively flooded.

#### 4.2.6 Dzereg (Zerik) Formation – (Lower Cretaceous)

The Dzereg (Zerik) Formation overlies a conformable basal contact with the underlying Gurven Ereen Formation defined by a marked colour change from grey to red. The formation is up to 250 m thick and dominated by red siltstone and claystone interbedded with coarsening upward sandstone intervals. The Dzereg (Zerik) Formation's upper contact is a (locally angular) unconformity overlain by Cenozoic strata. The formation name is after Devjatkin *et al.* (1981) however the

translation Dzereg is in common use in western literature rather than their original translation Zerk.

#### 4.2.6.1 DESCRIPTION

The Dzereg Formation is exposed at 5 locations within the Dariv Basin (areas 1, 2, 4, 5 and 7, Fig. 4.2) and is also exposed in the Dzereg Basin (Howard *et al.*, 2003) and in the Shargyn Section (area 6, Fig. 4.2).

##### ***Type locality – The Central Ridge Section (south)***

The 57 m thick, Central Ridge Section (south) represents the type locality for this formation and provides excellent exposure of both the vertical and lateral extent of individual horizons (Fig. 4.14a). Log VI (Fig. 4.15, between 45.5-102.5 m) documents the entire formation, which is dominated by red siltstones and sandstones, and overlies a conformable basal contact with the dominantly grey Town Member of the Gurven Ereen Formation. The sharp grey/green to red colour change across this contact is very distinctive and was recognised in sections from the three basins. The formation comprises nine facies (J, K, I, LA, LB, LC, LD, LE and EF in Table 4.1).

The Dzereg Formation is generally coarser than the Gurven Ereen Formation, but the basal 7 m is dominated by initially red, then grey/green, brown and occasionally white, micaceous siltstones and claystone, with intermittent lamination (facies K). Thin red and grey, laminated, or massive sandstone sheets, occasionally with dish-and-pillar structures (facies I), are interbedded with facies K. Gypsum horizons were observed only in this basal part of the section, concentrated around 52 m (Log VI, Fig. 4.15).

The upper part of the Dzereg Formation is dominated by the coarsening upward facies association L which comprises 5 facies (LA, LB, LC, LD and LE,

Table 4.1). Facies association L forms broad sheets, which thin laterally, and preserved sedimentary structures vary across exposures. The maximum thickness of an individual unit varies from 8.5 m at 83 m height (Log VI, Fig. 4.15) to <2 m towards the top of the section. The thickest units of facies association L units are the most laterally persistent and can be traced for  $\leq 800$  m. However, thinner units are much less extensive. Facies LA forms the base of the association, and coarsens upward. It is dominated by massive siltstone and sandstone beds that are generally red or brown and contain clear signs of bioturbation, occasional lamination is preserved. Blue mottling, black organic lenses, numerous hard red nodules and clasts of siltstone are commonly present within the thicker and coarser sandstone beds near the top of facies LA. Facies LB invariably represents the greatest proportion of facies association L sediment. In Log VI, Facies LB consists of micaceous, medium-grained red sandstone dominated by parallel low-angle planar cross-stratification. Small slumps (Fig. 4.20a) that offset beds are common within the basal part of facies LB and water escape structures were observed. The thickest facies association L bodies recorded in log VI (at 59 m and 83 m) were only studied near their margins and, therefore, do not record all the variations in sedimentary structure observed towards the centre of these sediment bodies. In the central area of these lens shaped units facies LB is erosively truncated by facies LC. Facies LC coarsens upward and is dominated by <1.5 m thick cross-stratified sandstone beds (Fig. 4.20b). Thin siltstone drapes are occasionally preserved on foresets within facies LC and organic matter, e.g. charcoal, is common, occasionally exposed as extensive thin sheets. Near the margins of these bodies facies LD overlies facies LB and, in log VI, facies LD tends to be slightly finer than the underlying facies LB beds. Facies LD commonly contains fine or very fine-grained sandstone with ripple cross-lamination and,

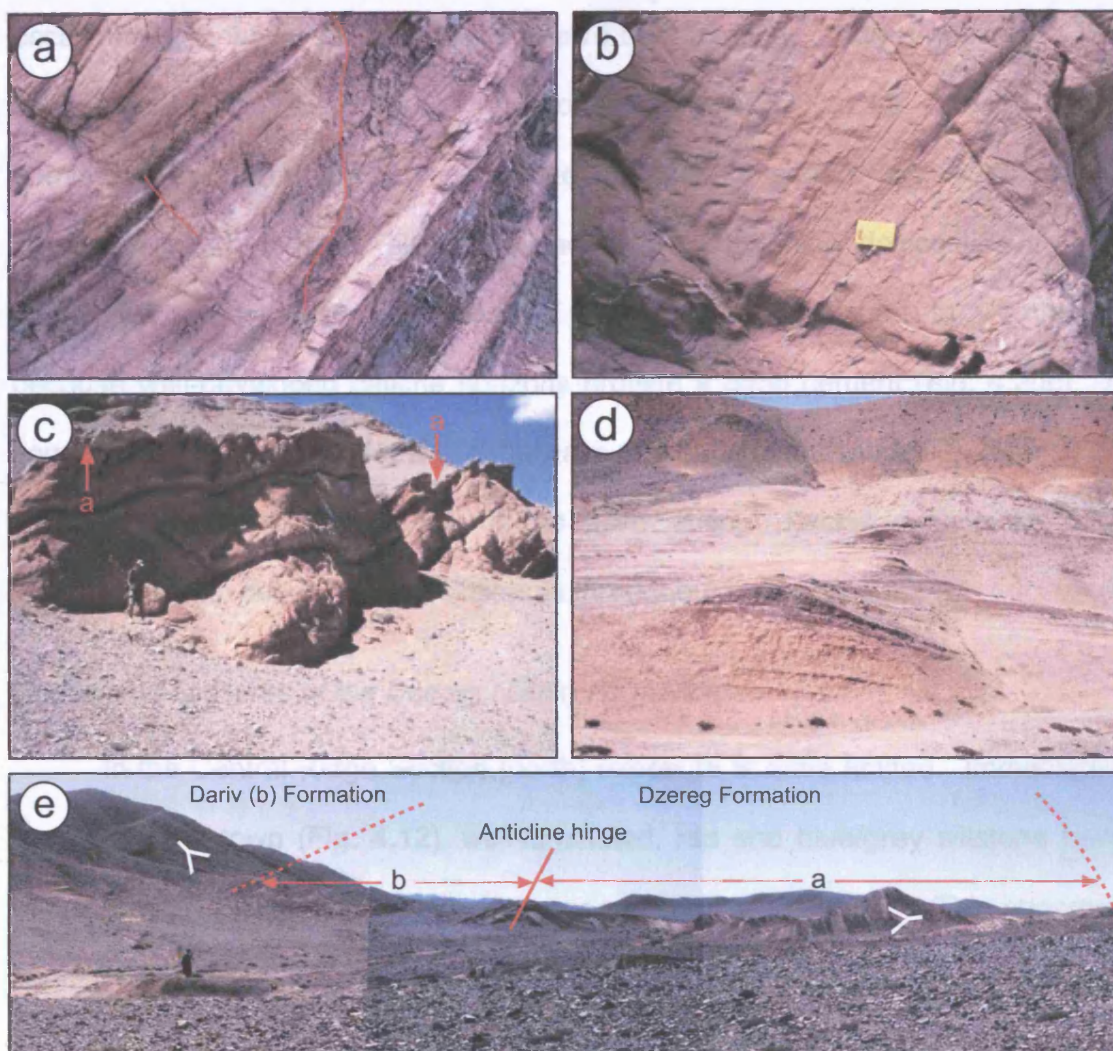


**Figure 4.20a** – Facies LA and LB in the Central Ridge Section (south). Note slump offsets in the basal part of LB (in red). **4.20b** – Low angle cross-stratification in facies LB medium grained sandstones interpreted to have been deposited on a delta front. **4.20c** – View of facies association L inferred to represent the central part of a delta. Note resistant caliche-cemented conglomerate facies LE (a) at the top. **4.20d** – Lacustrine sediments in the Central Ridge Section (north). **4.20e** – Exposure in the Central Ridge Section (north) showing structure within the ridge and lacustrine sediments. Note thickness of sediments differ on each side of the valley; this lies below the erosive base of the Cenozoic sediments.

section.

The formation is exposed at two locations in the North Foothills (Fig. 4.9); the North Canyon Section (Fig. 4.14c) and the East Ridge Section (Fig. 4.21a). In the North Canyon Section exposure is good, comprising dominantly red well-bedded sandstone and siltstones. The siltstones are soft with occasional laminar

occasionally, a basal lag surface. Facies LD commonly grades into facies LE, although there may be a direct transition from facies LC to LE. Facies LE is dominated by coarse-grained sandstone and pebble sheets and is commonly interbedded with massive siltstones (facies EF) containing desiccation cracks. Facies LE sandstones and facies EF siltstones are resistant to weathering because well-developed caliche horizons provide a good cement (Fig. 4.20c). A complete transition from LA-LE is not always present and facies LA and LB may be the only representatives of this facies association. Facies association L is interbedded with facies J and K siltstones throughout the section.

#### *Additional exposures of the Dzereg (Zerik) Formation*

In the Central Ridge Section (north) exposure is more limited. Immediately south of Dariv town (Fig. 4.12), well-laminated, red and blue/grey siltstone beds (facies J), commonly associated with loose gypsum, are exposed. Thin sheets of sandstone and pebble conglomerate (facies association L) are interbedded with facies J. Further south (Fig. 4.12 & 4.20d, e) better exposure reveals grey, grey/blue and, rarely, red siltstones with interbedded sandstone sheets (facies LA). In the best exposure, the siltstones are thinly colour-banded (facies J) and several preserved burrows were observed, although siltstones are generally massive (facies K). In these poor exposures, less sandstone was observed than at the Central Ridge Section (south), with no complete examples of facies association L seen.

The formation is exposed at two locations in the North Foreberg (Fig. 4.9); the North Canyon Section (Fig. 4.14c) and the East Ridge Section (Fig. 4.21a). In the North Canyon Section exposure is good, comprising dominantly red well-bedded sandstone and siltstones. The siltstones are soft with occasional laminae



and rare grey/blue horizons (facies EF). The sandstones are well cemented and commonly form spherical nodules up to 50 cm in diameter. Sandstones fine upward and are generally laminated although they may occasionally be ripple cross-laminated (facies AF). Extensive weathering and steep exposures largely prevent the measurement of palaeocurrent indicators. To the south, in the East Ridge Section, the sandstone sheets (facies AF) become less important. Red, sand-rich siltstone beds (facies EC) dominate the succession, but these soft sediments are more poorly exposed. The massive pedoturbated siltstones coarsen up section and contain occasional granules. In better exposures root systems and moderately developed caliche are present. Within the facies EC siltstone beds, rare, channelised and clast-supported conglomerates (facies D) are observed north of the Red Hill (Fig. 4.9). The pebbles in the conglomerate are well rounded and well sorted with low mineralogical maturity. Clast types include granitic, volcanic and metamorphic lithologies with some intrabasinal sandstone clasts. The largest channel is an exceptional 6 m wide and 2 m deep, filled with laminated sandstone and conglomerate. Most conglomerates are <20 cm thick and a few metres wide.

Exposures in the North Foreberg correlate well with the Base 1 Section (Fig. 4.2 & 4.3), where the  $\geq 145$  m thick succession comprises moderately exposed red/brown and, rarely, white or blue/grey clay-rich pedoturbated siltstones with well-developed caliche horizons (Log 1, Fig. 4.22 & 4.21b). Exposure quality is reduced by the presence of swelling clay. Root casts were observed in some beds. Conglomerate beds (facies D) are rare in this section and only one thin lens is recorded in Log 1. Where observed they form thin channelised units

---

**Figure 4.22** (following page) – Log base 1 from the Base 1 Section (area 1 Fig. 4.2) Showing the Red Hill Formation.

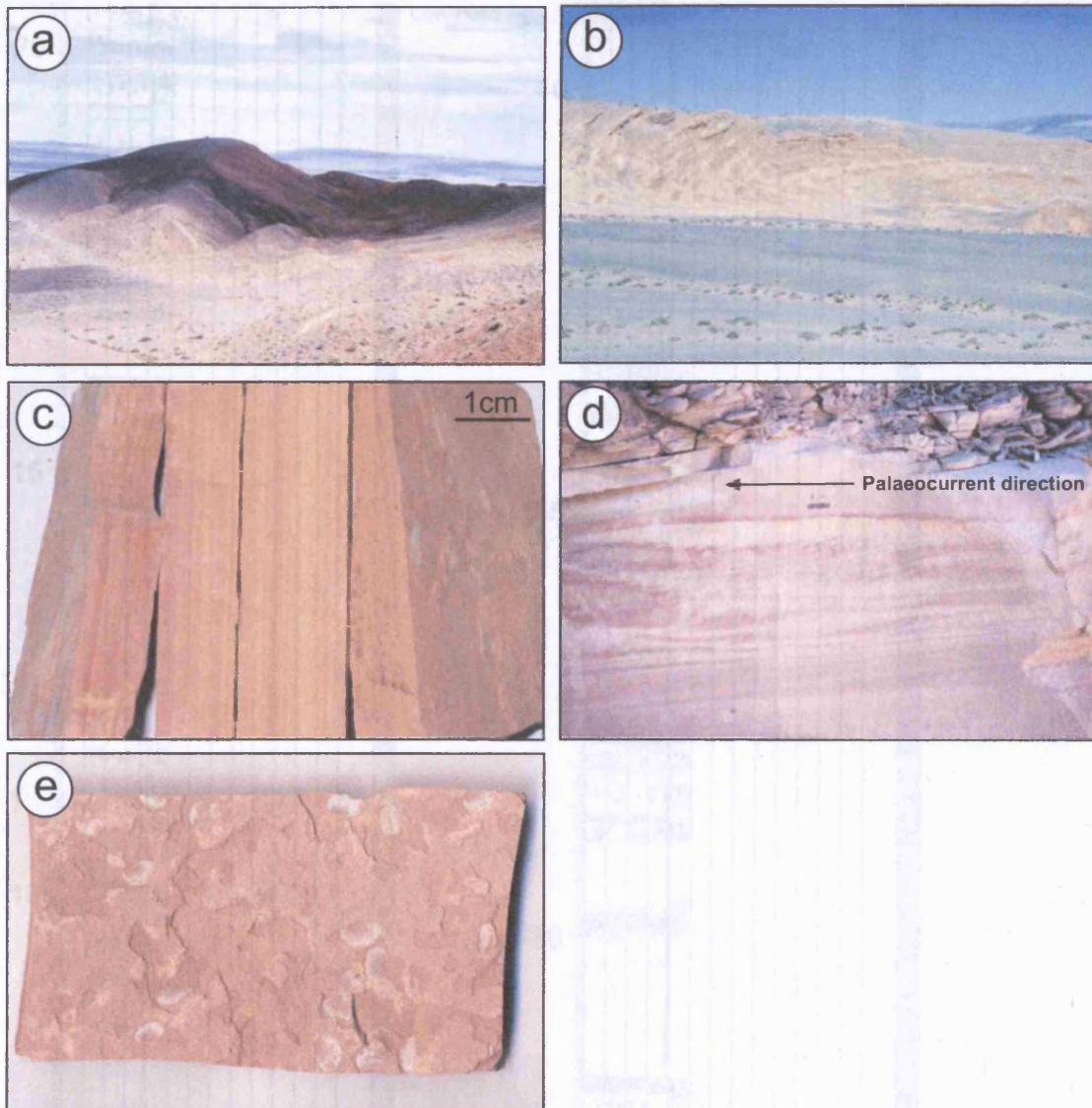
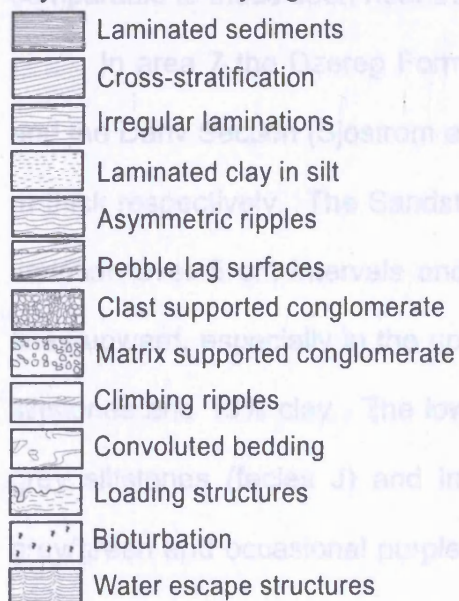


**Figure 4.21a** – View south down the East Ridge Section, towards the Red Hill (located on Fig. 14), showing red beds of the Dzereg Formation overlying grey beds of the Gurven Ereen Formation. **4.21b** – View north across the Base 1 Section showing soft red/brown siltstones in the Dzereg Formation. The more resistant beds (greater relief) contain caliche. **4.21c** – Very fine parallel lamination from the Dzereg Formation in the Shargyn Section interpreted to record the slow settling of silt and clay in a lacustrine environment. **4.21d** – Climbing ripple lamination in a facies I sandstone bed in the Dzereg Formation in the Shargyn Section interpreted as the deposits of a rare sheetflood event which transported sandstone into the lacustrine environment. **4.21e** – Death assemblage of lacustrine bivalves from the Dzereg Formation in the Shargyn Section.





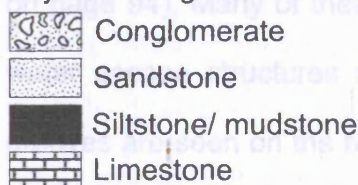
### Key for sedimentary logs



^ Gypsum

org organic matter

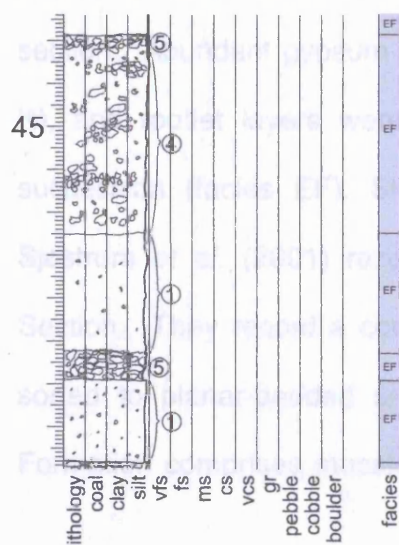
### Key to lithologies



### Caliche development

- ① Minor dissipated nodules
- ②
- ③ Isolated nodules forming distinct horizons
- ④
- ⑤ Hard carbonate cement >15 cm thick

Note that the numbering of caliche shown on the logs is the author's own system and does not correspond with the stages presented by Machette (1985) or Kraus & Brown (1988).



comparable to those seen near the Red Hill locality (Fig. 4.9)

In area 7 the Dzereg Formation is exposed in both the Sandstorm Section and the Dariv Section (Sjostrom *et al.*, 2001) where the formation is 280 m and 250 m thick respectively. The Sandstorm Section exposure is characterised by colour variation over 5 cm intervals and clast size changes up section. The formation fines-upward, especially in the upper 100 m, and comprises 23% sandstone, 58% siltstones and 19% clay. The lower formation is dominated by laminated red and grey siltstones (facies J) and intermittent sandstones (facies I) with rare blue, grey/green and occasional purple horizons. The facies I sandstones are primarily soft and poorly exposed, but commonly have a hard, laminated, occasionally planar-or trough cross-stratified, red-weathered cap (identical to those described on page 94). Many of these structures have been disturbed by weathering and/or water escape structures so they are poor palaeocurrent indicators. Distinctive grooves are seen on the base of some sandstone units. Rare intervals of erosive-based channelised sandstone (facies D) associated with massive or poorly laminated siltstones (facies EF) are present within the section. The central section is dominated by red and blue/grey siltstones (facies J & K) and sandstones (facies I). The upper section is dominantly grey/blue and red with a minor purple, yellow and green component. There is significantly less sandstone toward the top of the section. Abundant gypsum is associated with some siltstones beds (facies J and K), and rootlet layers were identified in several horizons near the top of the succession (facies EF). Siltstone beds are commonly mottled blue and red. Sjostrom *et al.* (2001) recorded 350 m of the Dzereg Formation at the Dariv Section. They record a conformable basal contact marked by a 3 m thick well-sorted to planar-bedded sandstone. Above this basal sandstone the Dzereg Formation comprises massive, light grey or yellow siltstones and mudstone beds



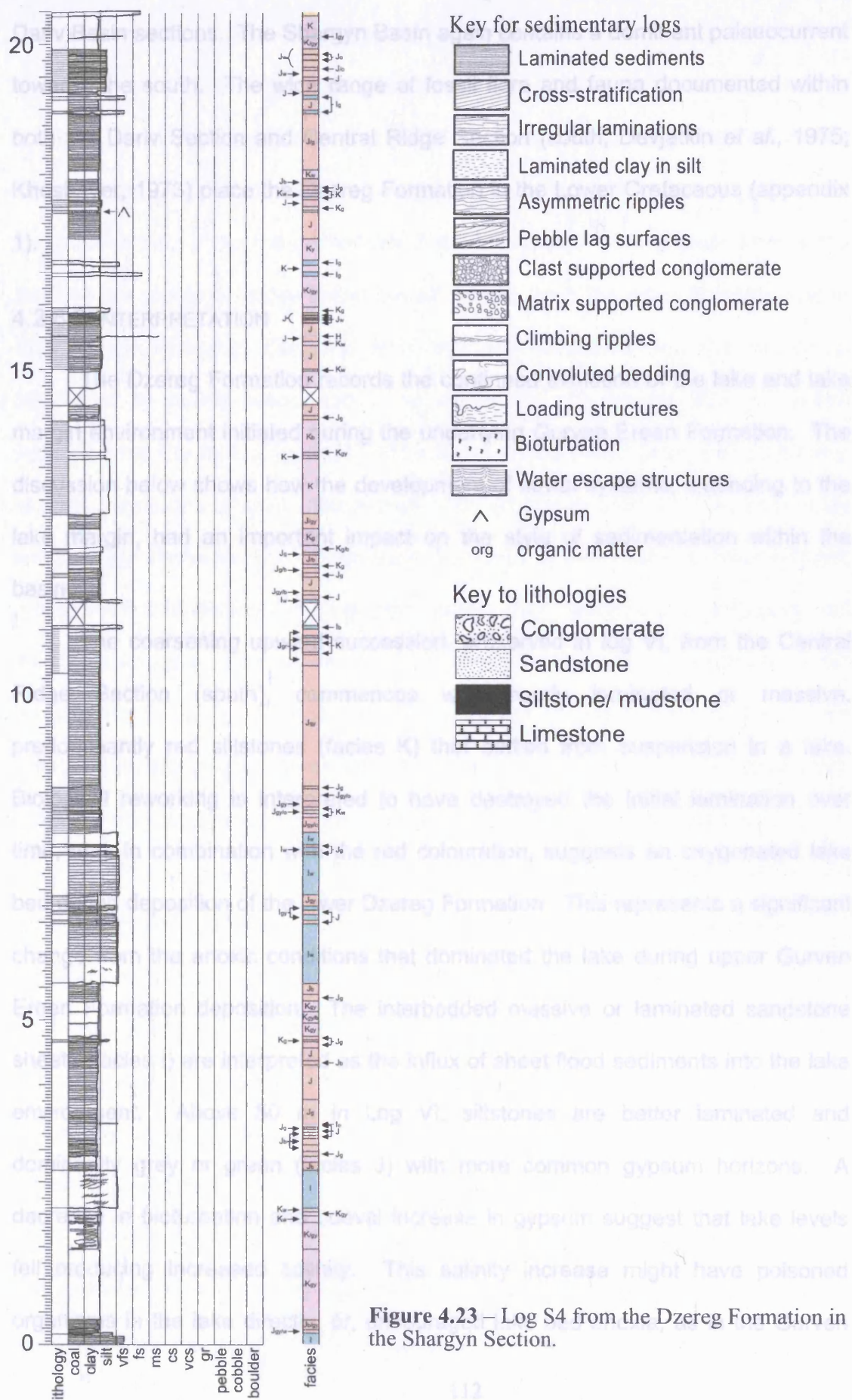
(facies K) with common gypsum horizons, especially towards the top of the section. The siltstones are predominantly well bedded, and have yielded a wide range of fossil material and plant remains, including one tree stump apparently preserved *in situ*. Occasional metre-scale sandstone beds contain ripple cross-lamination and trough cross-stratification (facies LC). The sandstones also contain planar lamination, convolute bedding and occasional desiccated surfaces (facies LB). Channel filling sandstone (facies D) is present, sometimes overlying facies association L.

### *The Shargyn Basin*

In the Shargyn Basin, 107 m of the Dzereg Formation has a conformable contact with the Gurven Ereen Formation, that is again marked by an abrupt colour change from grey to red. Log S4 (Fig. 4.23) records 21 m at the base of the section. This section is dominated by red, occasionally green/yellow, thin parallel-laminated siltstones (Fig. 4.21c) and rare claystone (facies J), with more massive blue-grey (facies K) horizons. Metre-scale slump deposits are present, particularly within blue/grey beds. The sandstone beds are fine-grained, well laminated and preserved in thin horizons <3 cm thick. Sandstone beds become thicker upward with occasional 30-40 cm thick beds concentrated near the top of the formation (facies I). Ripple and dune cross-lamination is preserved in the thicker sandstone beds (Fig. 4.21d), with symmetrical ripples in their upper part. Bivalves were found in sandstones throughout the formation (Fig. 4.21e).

### *Summary*

Palaeocurrent data for the whole formation are shown on figure 4.3. Palaeoflow directions were similar to the underlying Gurven Ereen Formation with flow towards the centre on the present day Dariv Basin recorded in each of the



Dariv Basin sections. The Shargyn Basin again contains a dominant palaeocurrent towards the south. The wide range of fossil flora and fauna documented within both the Dariv Section and Central Ridge Section (south; Devjatkin *et al.*, 1975; Khosbayer, 1973) place the Dzereg Formation in the Lower Cretaceous (appendix 1).

#### 4.2.6.2 INTERPRETATION

The Dzereg Formation records the continued evolution of the lake and lake margin environment initiated during the underlying Gurven Ereen Formation. The discussion below shows how the development of fluvial systems, extending to the lake margin, had an important impact on the style of sedimentation within the basin.

The coarsening upward succession, preserved in log VI, from the Central Ridge Section (south), commences with poorly laminated or massive, predominantly red siltstones (facies K) that settled from suspension in a lake. Biological reworking is interpreted to have destroyed the initial lamination over time, and, in combination with the red colouration, suggests an oxygenated lake bed during deposition of the lower Dzereg Formation. This represents a significant change from the anoxic conditions that dominated the lake during upper Gurven Ereen Formation deposition. The interbedded massive or laminated sandstone sheets (facies I) are interpreted as the influx of sheet flood sediments into the lake environment. Above 50 m in Log VI, siltstones are better laminated and dominantly grey or green (facies J) with more common gypsum horizons. A decrease in bioturbation and coeval increase in gypsum suggest that lake levels fell producing increased salinity. This salinity increase might have poisoned organisms in the lake directly, or, encouraged lake bed anoxia, as in the Gurven

Ereen Formation, by the sinking of dense saline water and production of a stratified water column. Thick evaporite deposits are not present, therefore hypersaline conditions were not maintained, if reached at all, and the density-stratified anoxia model is again preferred. Lakebed anoxia is also supported by the well preserved fossils seen throughout the section which are interpreted to have lived either at the shallow lake margins, above saline bottom waters, or in the water column. Above 52.5 m, the siltstones (facies J & K) are less abundant and the section is dominated by facies association L, which records the progradation of coarse sediment into the lake (Fig. 4.24). The basal association comprises coarsening upward sandstone sheets interbedded with siltstones that are both generally bioturbated. These sediments represent deposition in a pro-delta environment and record the first fluvial input into the Dariv Basin. The presence of bioturbation, and the increasingly red colouration, suggests either shallow-water deposition, above the saline layer or, more likely, that fluvial input was driving circulation of the water column and reducing or removing the anoxia, at least locally. The coarsening upward profile indicates progradation of the deltaic system into the lake.

Facies LA is overlain by facies LB and LC. Facies LB is interpreted as the sand-dominated delta front. On the margins of the delta, sand was deposited in low-angle sheets across the delta surface and small-scale slumping in the delta front was common. Slumps developed when large quantities of sand were deposited on wet uncompacted siltstones. Disrupted bedding at the base of facies LB provide evidence for rapid dewatering. Close to the river mouth, mouth bars formed and migrated producing large scale planar-sets with erosive bases (Facies LC). Thin silt drapes on the bedding planes and foresets of facies LC indicate calm periods when silt settled from suspension, and this suggests pauses in fluvial input that may have resulted from seasonal flow variations. Facies LD and LE

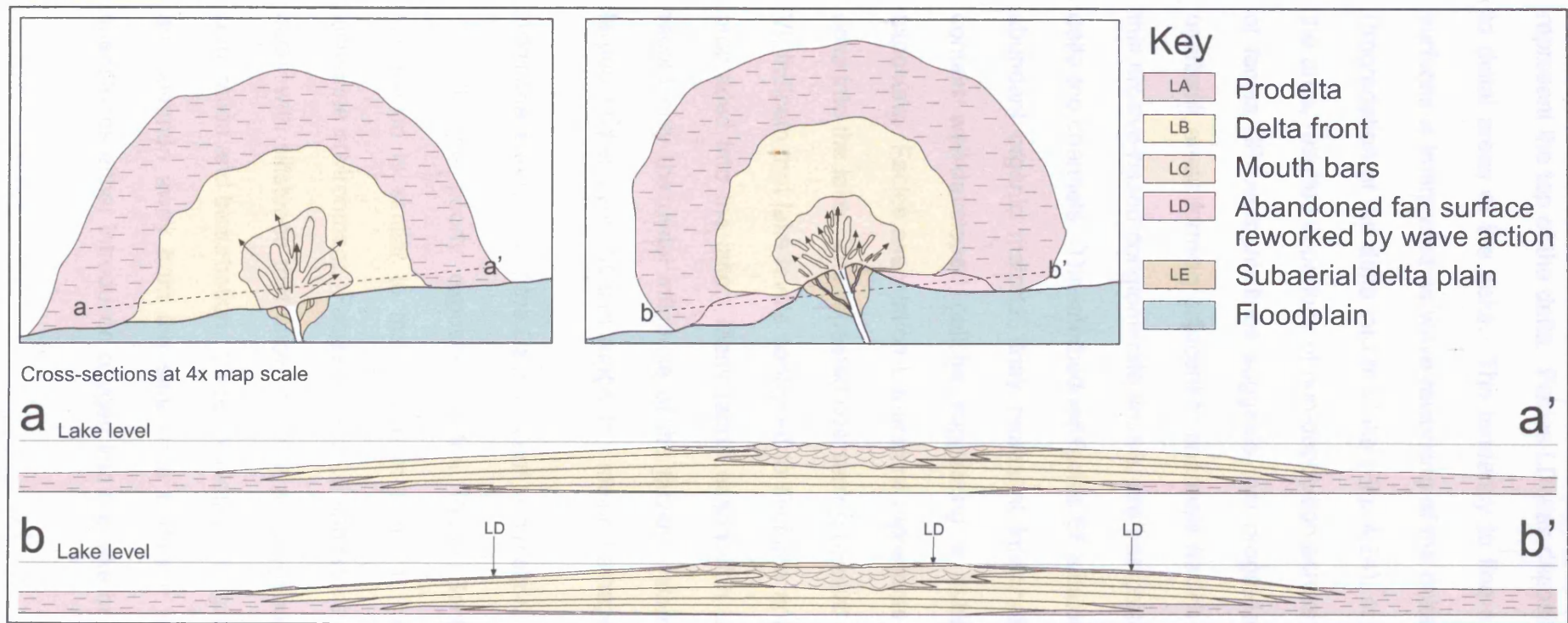


**Figure 4.24** - Map and section through a theoretical delta to explain the distribution of facies within facies association L in the Dzereg Formation.



represent the top of the delta. Facies LD was deposited over facies LB in the mid to distal areas of the delta. The tendency to fine slightly with abundant rippled surfaces is interpreted as wave reworking of the delta top following abandonment. Progradation of the delta into the lake (Fig. 4.24), or channel avulsion away from the area, resulted in periods of non-deposition across the delta top. The presence of facies EF overbank fines suggests that progradation of the delta resulted in overbank areas forming adjacent to channels (facies LE). Facies LE, comprising thin erosive-based conglomerate sheets, are interpreted to represent the subaerial delta top channels. The interbedded facies EF siltstones are massive and contain abundant organic material, they represent interchannel overbank deposits and contain well-developed caliche suggesting a substantial period of subaerial exposure. Facies association L therefore represents the progradation of a sandy delta into the lake. The repeated coarsening upward successions, recorded in log VI, indicate that lake levels continued to fluctuate and that large and small deltas prograded into the lake. Many facies association L bodies are incomplete and record only the distal influence of the fluvial system. The lateral extent of the largest bodies over 100's m suggests a major drainage source.

#### *Additional exposures of the Dzereg (Zerik) Formation*

In the poorly exposed Central Ridge Section (north), the preserved succession is similar to that shown in Log V1, but represents a more distal lacustrine environment. Facies LA and LB sandstone bodies within this section co-occur with siltstones that show signs of an oxygenated environment in their red colouration and bioturbation. Since well-laminated grey green siltstones (Facies J) are common away from the sandstone bodies it is possible that the influx of sheetfloods either introduced oxygen into the lake or disturbed the stratified water

column. The absence of a complete succession from LA-LE in facies association L sandstone bodies suggests a more distal position relative to fluvial input than Log VI. However, this does not necessarily require deeper water, it may just represent a section of the lake margin away from fluvial input.

In the northern Dariv Basin, the North Canyon Section exposes an entirely terrestrial succession comprising fine EF and EC siltstones beds interbedded with facies AF sandstones, interpreted to represent overbank fines deposited across the floodplain during sheetflood events. Facies AC, however, comprises granules and coarse sandstone supported in a siltstone matrix. This can either be interpreted as a fine-grained debris flow or as the deposits of silt transported as sand size aggregates (e.g. Nanson *et al.*, 1986, 1988; see discussion page 76). Given the association with facies EC, facies AC is considered more likely to represent disassociated sand size aggregates. The overall depositional environment is interpreted as a sheetflood-dominated, low gradient alluvial fan system. The dominant red colour of the sediment, supports subaerial exposure and suggests a seasonal wet and dry climate (e.g. Parrish, 1993). Grey horizons are interpreted to represent gleysols that form in saturated soil horizons.

The East Ridge and Base 1 Sections show very similar depositional environments. Both are dominated by facies EC and EF fine-grained sediments interpreted to be deposited on a subaerial alluvial plain, which preserved root casts and organic fragments indicate was vegetated. In the Base 1 Section, there are well-developed caliche horizons which are absent in the East Ridge Section, which contains more channelised conglomerate and sandstone bodies (facies D). The generally poorly exposed conglomerate bodies are isolated within the fine sediment and are interpreted as the deposits of a low sinuosity stream. These appear to be short-lived channels because bodies are confined to certain horizons

and are interpreted as dominantly cut and fill deposits, with only one major multistorey channel deposit observed. Facies D channels are interpreted to record base level (i.e. lake level) fall, which resulted in periods of fluvial incision in an otherwise distal fan or floodplain setting. An increase in caliche horizons towards the basin centre is consistent with an increasingly distal environment undergoing long periods of non-deposition. Palaeocurrents are consistently from the north, but no channel system was observed within the North Canyon Section. This absence may be due to the confinement of the fluvial system in a fan head trench cut in response to a fall in lake level; any such confined channel has a low presentation potential.

In the southern Dariv Basin, two sections record mixed lacustrine and subaerial deposition. In the Dariv Section, Sjöström *et al.* (2001) report predominantly massive pale cream and yellow siltstones, which they interpret as deposits from an oxic lacustrine environment. There is still, however, a proportion of laminated siltstones (facies J) and widespread well preserved fossils, which suggest periodic anoxia at the sediment/water interface. Sandstone bodies (facies association L) are interpreted as the deposits of fringing deltas and this supports Sjöström *et al.*'s (2001) interpretations. The periods of oxic deposition may, therefore, be explained as circulation of the water column proximal to the influx of fluvial systems. Where conglomerate channels are associated with the top of facies association L (facies LE) they are interpreted to represent the subaerial channels of the delta top. Occasional isolated conglomerate channels are observed within the lacustrine sediments which suggests incision and deposition following a lake level fall.

The Sandstorm Section is dominated by lacustrine sediments (facies J and K) with characteristics that suggest fluctuating anoxic and oxic periods. Erosive-

based, fining upward sheetflood sandstone beds (facies I) are again interbedded with the lacustrine siltstones. Periods of channel deposition, interpreted as incision due to base level change, appear to be more prolonged in this area and thick overbank deposits with preserved root systems are seen (facies EF). The fine-grained upper 100 m of the section lacks channels and comprises interbedded siltstones with gypsum horizons (facies J and K), that represent lacustrine deposition, alternating with root-penetrated and caliche horizons (facies EF), suggesting floodplain sedimentation. The overall environment is interpreted as a lake margin subject to minor lake level fluctuations. Facies EF and K are difficult to separate in exposure because both are massive. The absence of sandstone suggests a change in the transport system bringing sediment from the south. The overall fining upward trend may represent the degradation of the hinterland or a change in the transport competence of the system related to climate/ tectonic change.

### *The Shargyn Basin*

In the Shargyn Basin, the Dzereg Formation represents a wholly lacustrine environment with some subaqueous sheetfloods. The section is dominated by red sediments that are interpreted to indicate a predominantly oxic lakebed.

### *Summary*

The Dzereg Formation represents the continued evolution of a lacustrine environment with a surrounding floodplain dominated by overbank deposition from sandstone and pebble conglomerate channels. Palaeocurrent data indicate sediment supply from each basin margin throughout the deposition of the formation. The basinwide, grey to red colour change at the base of the formation

may be coeval across the basin and, if so, preserves a basin wide oxic event. This is the only basinwide event identified.

## 4.3 Cenozoic Sediments

### 4.3.1 Introduction

Uplift of ranges adjacent to the Dariv Basin began in the Oligocene and sediment eroded from these ranges dominates Cenozoic basin stratigraphy. The observed stratigraphy is comparable across the flanking basins, but most of it can only be correlated within individual basins. The Cenozoic deposits overlie a regional unconformity related to a Palaeogene peneplanation event, recognised throughout the region (Devjatkin *et al.*, 1975). This unconformity is angular in the Central Ridge Section (north; Fig. 4.20e), however, the dip of bedding differs only slightly across the unconformity suggesting only minor tilting of strata prior to peneplanation. Erosive contacts are also observed in the North Foreberg and the Central Ridge Section (south) where an angular contact is suspected, but not proven. Cenozoic sediments are poorly exposed within the Dariv Basin and are considerably thinner than the Mesozoic deposits.

### 4.3.2 Previous work

Cenozoic strata in the Dariv Basin have not been documented in detail during previous studies, and post- Cretaceous sediments are grouped together as Palaeogene on the geological map of Togtoh & Baatarhuyag (1991), despite being differentiated by them elsewhere. This study identifies Cenozoic formations and ascribes ages based on lithological comparison with the stratigraphy of surrounding basins (Devjatkin, 1981; Howard *et al.*, 2003), stratigraphic relationships within the Dariv Basin, and limited faunal evidence. The Cenozoic



ages remain less well constrained than Mesozoic ages, but this study represents an improvement on previous work.

#### 4.3.3 Red Hill Formation - Oligocene (Beger Suite)

The Red Hill Formation overlies a regional unconformity surface related to a Palaeogene peneplanation event. Where the unconformity is not angular, the basal contact with the Dzereg (Zerik) Formation is recognised by an increase in mean grainsize from interbedded siltstone and sandstone to pebble conglomerate channels. The formation is up to 150 m thick and dominated by channelised grey conglomerates interbedded with laterally extensive dark red siltstone and sandstone beds. The Red Hill Formation's upper contact is gradational with the overlying Eagle Valley Formation and is defined by the transition from the uppermost grey conglomerate bed into a thick succession of multicoloured siltstone beds. The formation is named after a prominent hill on the eastern flank of the North Foreberg where good sections of this formation may be found. The Red Hill Formation is a new formation equivalent to the Beger Suite of Devjatkin *et al.* (1981).

##### 4.3.3.1 DESCRIPTION

The Red Hill Formation is exposed at four localities within the Dariv Basin, the East Ridge Section, the Central Ridge Sections (north and south) and the Base 1 Section (areas 1, 2 and 4, Fig. 4.2), the formation is also seen in the Dzereg Basin (Howard *et al.*, 2003) and in the Shargyn Section (area 6, Fig. 4.2). The formation fines upward and comprises seven facies, AC, AF, C, D, EF, EC, and H in table 4.1.

### ***Type Locality – The Base 1 Section***

The 160 m thick, Base 1 Section is the type locality for the Red Hill Formation (Fig. 4.25a). It is dominated by well-exposed channelised conglomerate and sandstone beds (facies D; Fig. 4.25b & c), interbedded with red and brown siltstones (facies EF and EC) and is recorded on log 4 (Fig. 4.26).

Facies D has an erosive channelised base, commonly overlain by a coarse pebble or cobble lag, containing soft-state deformed siltstone clasts (Fig. 4.27a). The channel fill contains numerous internal erosion surfaces (Fig. 4.25b, c) that separate lenses of carbonate-cemented, texturally and mineralogically immature, coarse sediment. White/grey, clast-supported, pebble conglomerate or granule beds with a coarse-grained sand matrix dominate facies D. The conglomerates generally appear crudely stratified, but are occasionally laminated or planar cross-stratified. Matrix-supported granule and, rarely, pebble conglomerates grade both vertically and laterally into yellow sandstone (Fig. 4.27b) that is commonly laminated or contains low-angle planar cross-stratification (Fig. 4.27c). Between major internal erosion surfaces, beds are arranged in upward-fining associations rarely capped by thin siltstone beds (facies EF). Facies D channels >1 m thick extend 40-50 m laterally and are spaced at <10 m intervals vertically. The dominant clasts are quartz, feldspar and volcanic lithics.

Facies D channels incise poorly exposed, red/brown (rarely blue/grey or white) siltstone beds (facies EF and EC). Facies EF siltstones are clay-rich and predominantly massive; they contain angular blocky beds, sometimes with clay-coated cutans, that exhibit slickensides. Extensive rooting is preserved as grey casts within the red siltstone beds (Fig. 4.27d). Several distinctive grey/white

---

**Figure 4.26** (follows Fig. 4.25) – Log 4 from the Base 1 Section (area 1 Fig 4.2) showing the Eagle Valley Formation.

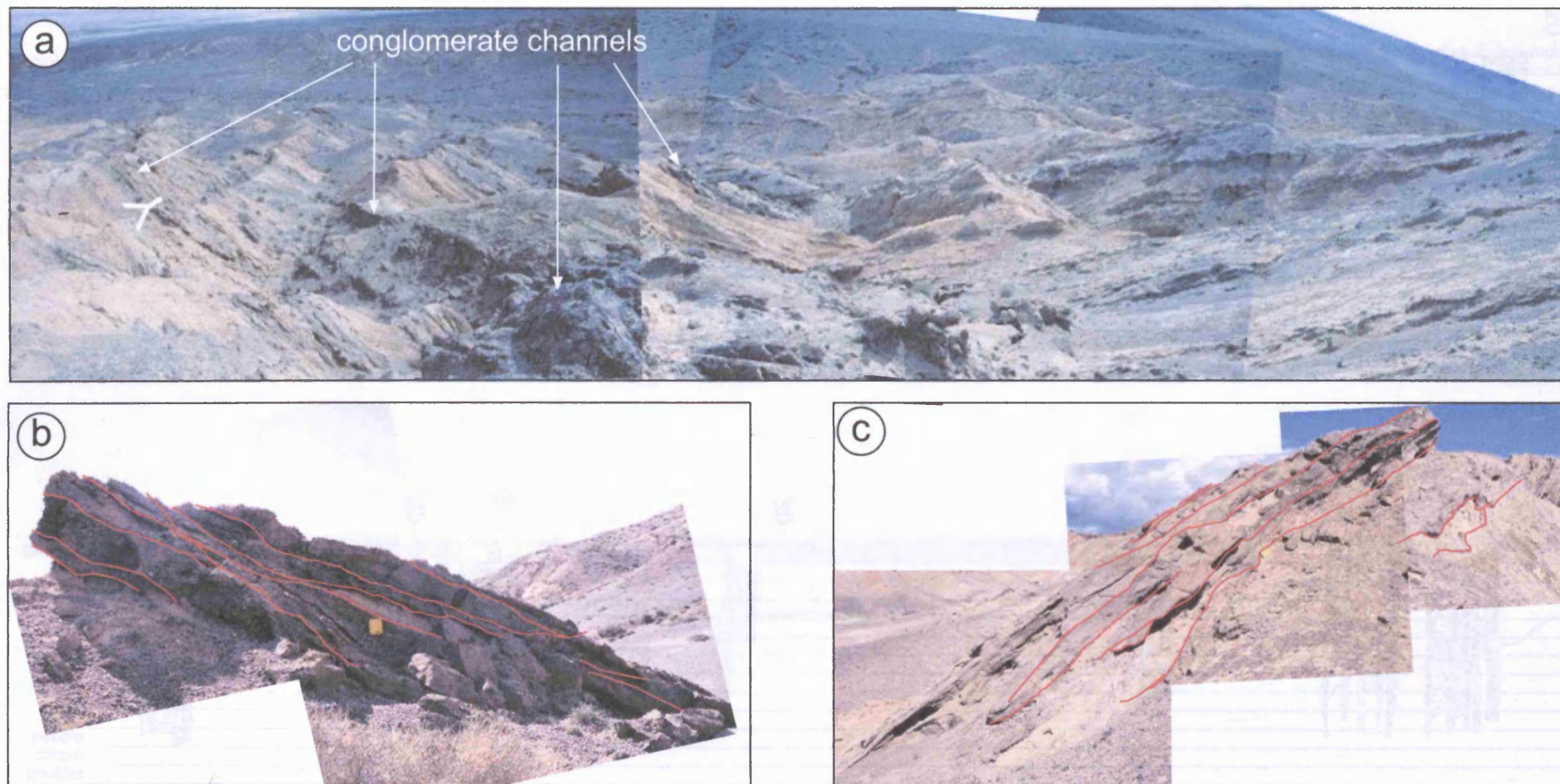
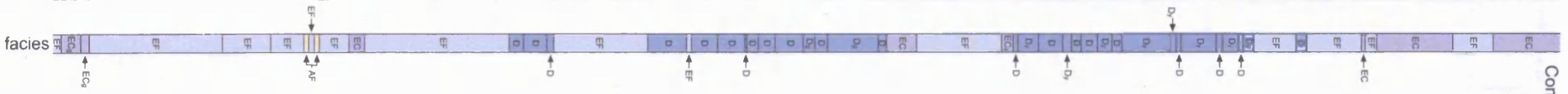
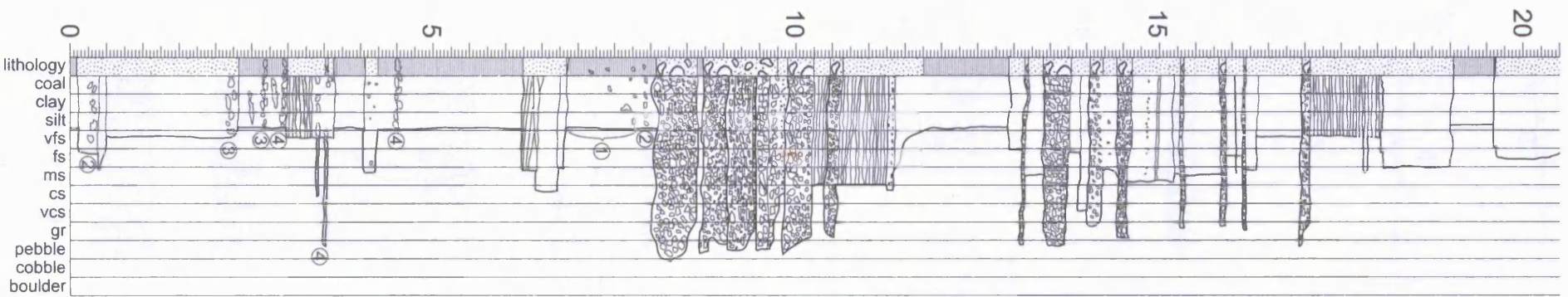
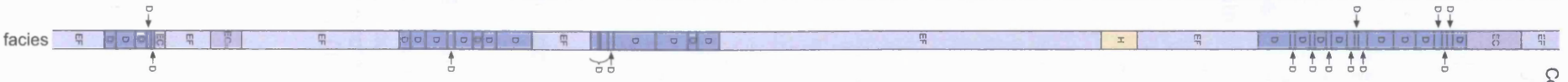
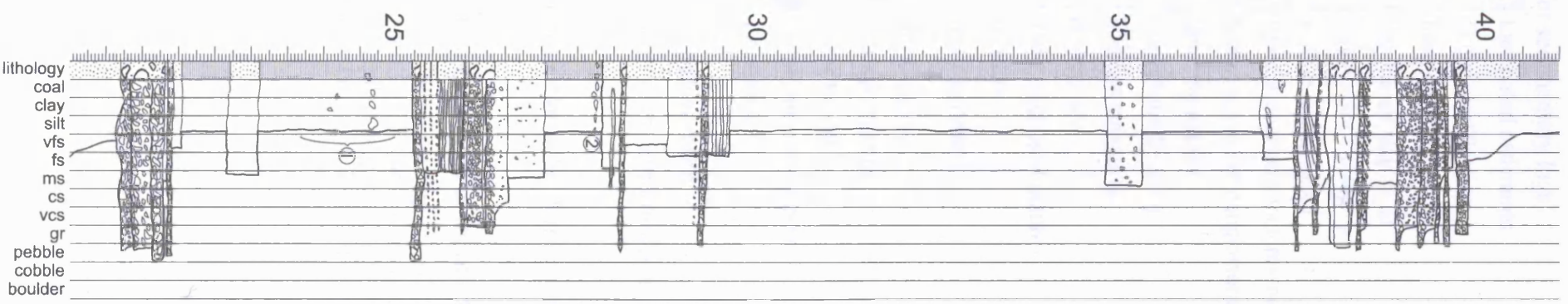


**Figure 4.25a** – View to the west of the Base 1 section (area 1, Fig. 4.2) showing the channelised conglomerate bodies (facies D) within yellow/brown siltstone beds (facies EF). **4.25b & c** – Figures b and c show photographs and interpretation of a facies D channel body with a multi-stage fill. Internal erosion surfaces are picked out in red. Red Hill Formation, Base 1 Section (area 1, Fig. 4.2).

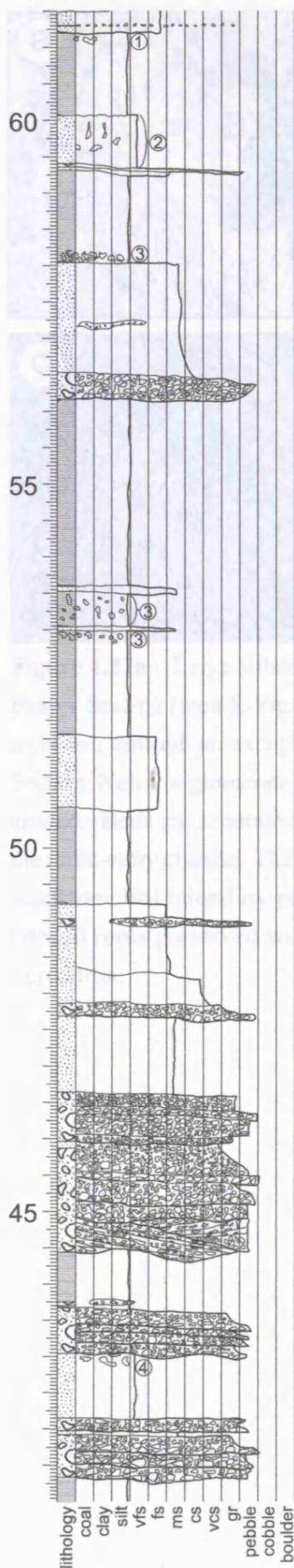


Continued →



Continued →





### Key for sedimentary logs

- Laminated sediments
- Cross-stratification
- Irregular laminations
- Laminated clay in silt
- Asymmetric ripples
- Pebble lag surfaces
- Clast supported conglomerate
- Matrix supported conglomerate
- Climbing ripples
- Convoluted bedding
- Loading structures
- Bioturbation
- Water escape structures
- Gypsum
- organic matter

### Key to lithologies

- Conglomerate
- Sandstone
- Siltstone/ mudstone
- Limestone

### Caliche development

- ① Minor dissipated nodules
- ②
- ③ Isolated nodules forming distinct horizons
- ④
- ⑤ Hard carbonate cement >15 cm thick

Note that the numbering of caliche shown on the logs is the author's own system and does not correspond with the stages presented by Machette (1985) or Kraus & Brown (1988).



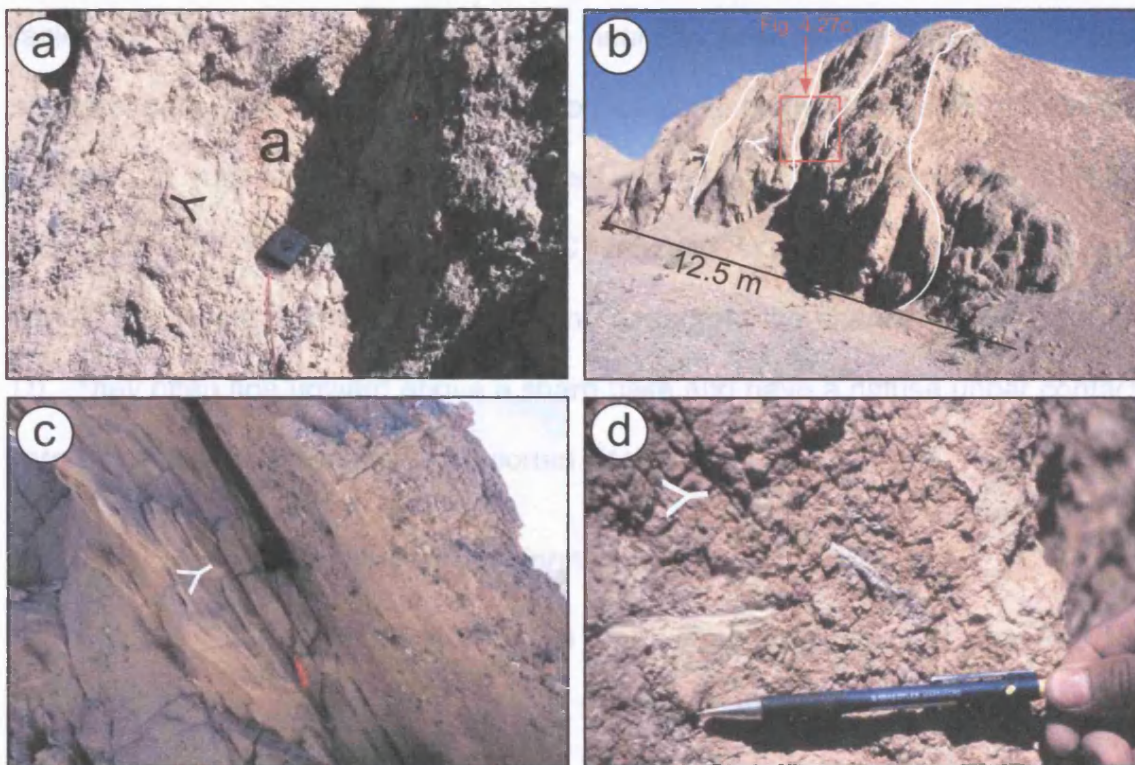


**Figure 4.27a** – Large siltstone rip-up clast (a) in the basal part of a conglomerate bed in the Base 1 Section (area 1, Fig. 4.2). Compass clinometer is 7 cm long. **4.27b** – View showing a section through an exceptionally thick multi-story channel (Facies D) within the Base 1 Section. Note conglomerate stands out as ribs whereas siltstone and sandstone are more easily eroded. Beds are separated by internal erosion surfaces (white lines). **4.27c** – Close up of the multi-story channel. The succession youngs to the right, note the low-angle cross-stratified sandstone bed bound by pebble conglomerate beds. Red whistle is 5 cm long. **4.27d** – Gleyed roots preserved within a red siltstone bed in the Base 1 Section of the Dariv (b) Formation.

the channel bodies (Facies D) become isolated within facies BC and E+ beds. Log 8 records the strike equivalent of Log 5 to the north (Fig. 4.9). Here conglomerate beds dominate, although most lacking well-defined channelized bases observed in log 5 and the Base 1 Section, and instead take the form of sheets which commonly fine upward and contain laminae (Facies AC & C). Facies C, pebble conglomerate beds overlie a localized or full-scale, contain no internal erosion surfaces and pinch out laterally. Facies AC, fine upward-fining pebble/granule conglomerate beds, have a

Figure 4.18 (Following page) – Log 8 from the East Ridge Section of the North Foreberg (area 2 Fig. 4.1) showing the Eagle Valley Formation.

facies EF siltstone horizons were seen near the base of the formation. Some siltstone beds contain a large proportion of sand grains (facies EC). Caliche horizons, in varied stages of development, are present within facies EF and EC throughout the formation. Facies AC, laterally extensive conglomerate and sandstone sheets extend into the siltstone beds from the channel margins (facies D). They often fine upward above a sharp base and have a diffuse upper contact; rarely, these sheets are matrix-supported (facies H).

#### *Additional exposures of the Red Hill Formation*

In the East Ridge Section of the North Foreberg (Fig. 4.9), the Red Hill Formation is 150 m thick. Logs 8 and 9 (Figs. 4.28 & 4.29) record the section which shows marked lateral variation over 2 km. Log 8 is located just north of Red Hill (Fig. 4.9) and is characterised by white/grey pebble and granule conglomerate channels (facies D, Fig. 4.30a & 4.30b) incising red and brown siltstones (facies EF & EC). It is very similar to the Base 1 Section. At the base of log 8 there is less siltstone (facies EF & EC), relative to the Base 1 Section, and channels commonly incise each other. The proportion of siltstone increases up-section and the channel bodies (facies D) become isolated within facies EC and EF beds. Log 9 records the strike equivalent of Log 8 to the north (Fig. 4.9). Here conglomerate beds dominate, although most lack the well-defined channelised bases observed in log 8 and the Base 1 Section, and instead take the form of sheets which commonly fine upward and contain laminae (facies AC & C). Facies C, pebble conglomerate beds overlie a localised basal scour, contain no internal erosion surfaces and pinch out laterally. Facies AC, upward-fining pebble/granule conglomerate beds, have a

---

**Figure 4.28** (Following page) – Log 8 from the East Ridge Section of the North Foreberg (area 2 Fig. 4.2) showing the Eagle Valley Formation.











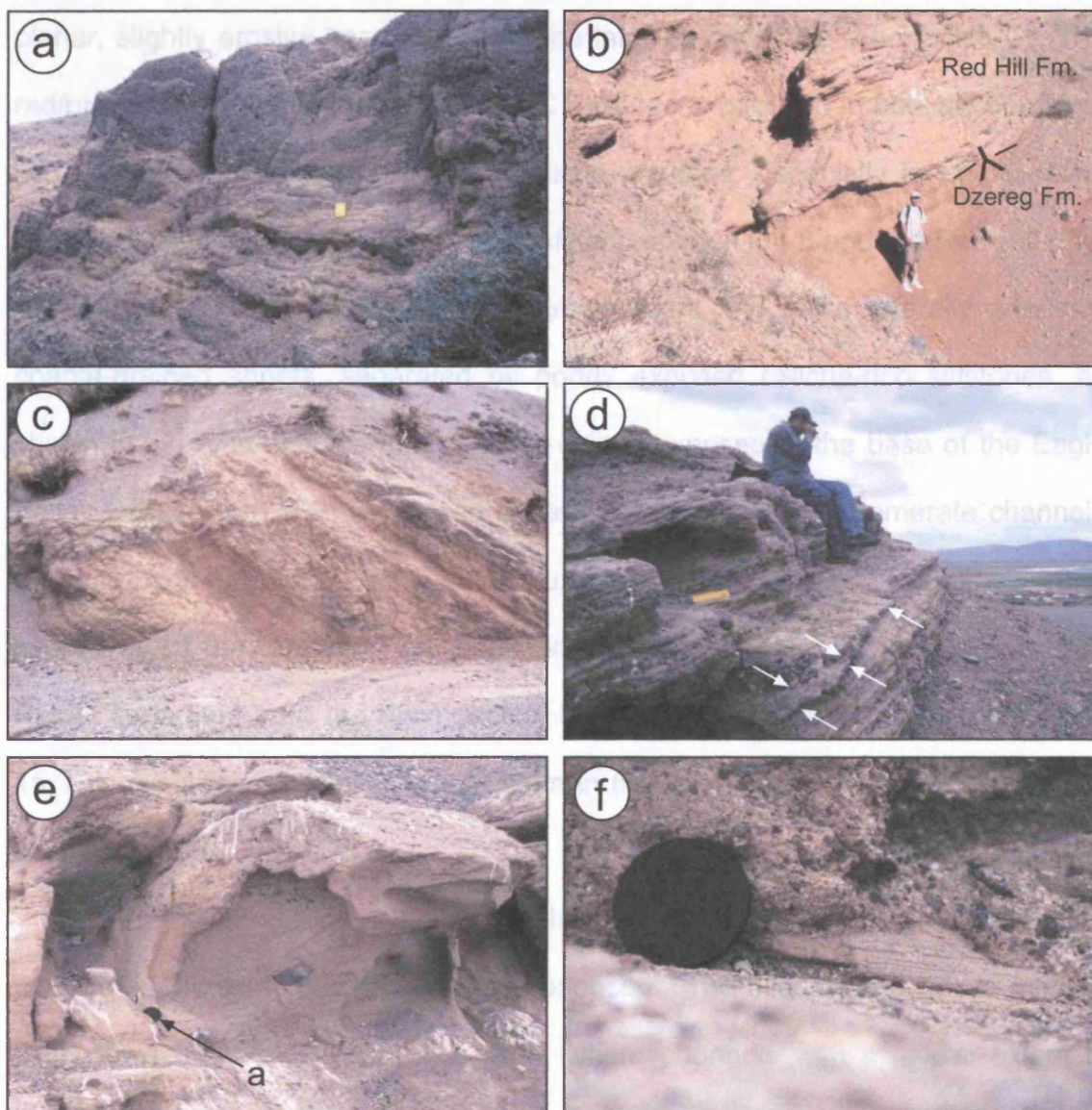


**Figure 4.30a** - Laterally extensive pebble conglomerate channels in the East Ridge Section, North Foreberg area. **4.30b** – Basal contact of the Red Hill Formation with the Cretaceous red beds of the Dzereg Formation. Note deep scours at the base of the channel and the foresets within the channel that record the migration of channel macroforms. **4.30c** – Interbedded sandstone and conglomerate in the upper Red Hill Formation within the Eagle Valley. **4.30d** – Channelised conglomerate body just north of Dariv town (in background). Note thin conglomerate beds with erosive scours. Scours picked out by white arrows. The green area behind Dariv town is a salt marsh around the central lake. **4.30e** – Close up of channelised conglomerate. Note the varied inclination of foresets and the interbedded pebble and sandstone dominated beds. Isolated large clasts are present within the sandstone beds. The lens cap (a) is 7 cm across. **4.30f** - Close-up of an erosive basal contact showing remnants of a planar laminated sandstone below. Conglomerate carbonate cemented and hard. loam, where red to grey-blue colour banding was observed. The Red Hill Formation is also poorly exposed in the Central Ridge Section (South) where

planar, slightly erosive base and are more laterally extensive than facies C. The red/brown siltstone beds (facies EF & EC) are poorly exposed in both sections, but contain moderate to well-developed caliche horizons, especially in Log 9. The facies D channel bodies are laterally confined between log 8 and the Red Hill (Fig. 4.9). Southeast of the Red Hill, a similar trend into more laterally-extensive coarse-grained sheets, separated by poorly exposed caliche-rich siltstones, as shown in log 9, is observed. The same unit is exposed at the base of the Eagle Valley Section (Fig. 4.9) where red siltstone and red/grey conglomerate channels are interbedded in the valley floor (Log 11, Fig 4.31; Fig. 4.30c). Further exposures of the formation are seen at the eastern extent of the Eagle Valley Ridge, separated from the main section by faulting. The stratigraphy there (Log. 15, Fig. 4.31) is very similar to that seen in the Base 1 Section, which is located along strike (Fig. 4.9).

In the Central Ridge Section (north), only the facies D carbonate cemented, white/grey conglomeratic channels are exposed. The best examples are seen in Dariv town (Fig. 4.12 & 4.30d, e, & f), where channels with a lateral extent in excess of 25 m are present at 4-8 m intervals. They again contain pebble conglomerate interbedded with coarse-grained sandstone beds that are laminated or, more commonly, low angle planar cross-stratified. The laminae are defined by coarse-fine grainsize variations and sediment packages fine-upward between internal erosion surfaces. Toward the channel margins, structures are poorly preserved and many beds appear massive. The mean grain-size is 1-2 cm, with occasional large clasts, <30 cm in size (Fig. 4.30e). The fine-grained sandstone and siltstone beds that separate these channels are poorly exposed south of Dariv town, where red to grey-blue colour banding was observed. The Red Hill Formation is also poorly exposed in the Central Ridge Section (South) where





similar carbonate-cemented pebble conglomerate channels are interbedded with poorly exposed siltstone beds (top of Log V1, Fig. 4.15). Along-strike variations in the distribution of coarse bodies are present with the coarsest and best-defined channel bodies (facies D) in the Log V1 section (Fig. 4.10 & 4.15) and more diffuse sheet-like bodies (facies C and AC) observed to the north and south. The Red Hill Formation is not exposed in the east of the Dariv Basin where it is obscured by recent deposits.

### *The Shargyn Basin*

In the Shargyn Basin the Red Hill Formation is at least 145 m thick and is comparable to the sections observed elsewhere (Fig. 4.3, Section X). The channels are smaller and range from 2 to 10 m wide, with the maximum incision observed being 1 m. They also lack the multiple internal erosion surfaces seen elsewhere, commonly having one or two stage fills. The channel fill again comprises pebble/granule conglomerate and sandstone beds (facies D). The clast composition reflects the basement lithologies and large blocks of reworked caliche along with soft sandstone and siltstone intra-clasts are also seen. At the channel margins thin granule and pebble rich sheets (facies AF) extend into the siltstone beds (facies EF). Facies EF beds are poorly exposed, but contain well-developed caliche that rarely forms distinct horizons, rather it is distributed throughout the siltstone beds.

### *Summary*

Palaeocurrent data from the Red Hill Formation are shown on figure 4.3 and show a southerly trend within the Dariv Basin and a south-easterly trend in the Shargyn Section. The greatest scatter is seen in the North Foreberg locality, although a general southerly trend was identified. This formation is dated as

Oligocene based on geological mapping by Zaitsev *et al.* (1978) and comparison with the stratigraphy of adjacent basins (Devjatkin *et al.*, 1981). The Red Hill Formation has a conformable upper contact with the Eagle Valley Formation.

#### 4.3.3.2 INTERPRETATION

##### ***Type Locality – The Base 1 Section***

The Red Hill Formation represents the first sediment pulse from the newly uplifting Altai range. Facies D comprises thick channelised conglomerate bodies with several internal erosion surfaces and is interpreted to represent a long-lived, stable, fluvial channel. Between internal erosion surfaces, fining-upward packages record the migration of both gravel and sand bedforms within the channel.

The conglomerate beds are interpreted to record three different components of the active channel system. Truly massive conglomerate beds are rare and are interpreted as lag deposits introduced into the stream as a “slug” of coarse sediment resulting from, for example, upstream bar erosion and subsequently deposited in a zone of shallowing or flow expansion (e.g. Hoey, 1992; Miall, 1996). Massive beds within channel systems may also be interpreted as debris flow deposits resulting from bank collapse (e.g. Turner & Munro, 1987; Wizevich, 1992; Miall, 1996). However, the coincident occurrence of most massive beds with major channel scours, combined with the lack of post-depositional reworking by later stream flow, suggest they represent the traction load of rare high-stage flow events.

Low-angle horizontal and cross-stratified conglomerate beds are interpreted as the deposits of downstream lengthening, stratified gravel sheets (e.g. Miall, 1996), also called longitudinal bars. These mesoforms suggest rapid gravel transport and that aggradation is subordinate to downstream migration. They may



fine or coarsen upward dependant on variations in stream power or sediment load (Miall, 1996). Cross-stratified conglomerate bodies record the presence of a different type of gravel mesoform, in which vertical accretion dominates, this creates a downstream avalanche face resulting in the formation of a cross-bedded transverse bedform (Miall, 1996), also called a transverse bar. The sandstone horizons also contain structures representing the migration of different channel bedforms. Horizontally bedded sandstone intervals indicate unconfined flow with planar and trough-cross-stratified sandstone beds recording the migration of 2D and 3D dunes respectively (Ashley, 1990). From their vertical and lateral relationships, the channel mesoforms were combined into larger macroforms, e.g. channel bars. The exact geometry of the macroforms cannot be well constrained in 2D exposure, however some suggestions can be made. The recognition of low-angle stratification with dips perpendicular to the channel margin in some sections, suggests the evolution of bank-attached structures that accreted as the river migrated. The dominance of gravel mesoforms suggests the presence of mid channel bars, and consequently a degree of channel braiding, at least during low stage flow (Miall, 1996). The thin beds suggest shallow water and the interbedding of varied clast sizes, including siltstone within the channels indicates a widely variable flow regime. Also upward-fining sediment packages suggest repeated cycles of incision and aggradation. The thickest channels show 7 cycles. The fluvial system is interpreted as a shallow, slightly sinuous, mixed load, ephemeral stream with a degree of low stage braiding introduced by the mid-channel mesoforms. The sinuosity is not resolved in the palaeocurrent data so may have been slight, but it is supported by the presence of bank attached bars.

Surrounding the channels are facies EF and EC siltstones interpreted as overbank fines, deposited during waning flood events. Facies EF siltstones are

rarely laminated and have been widely pedoturbated. The most mature horizons represent palaeosols of which four types were identified. The most common contain visible peds, which are angular and blocky (USDA soil survey classification) occasionally with clay-coated cutans, which show extensive slickenside development. This clay coating is a characteristic of soils that are below the water table for some part of the year (e.g. Retallack, 1988). Other beds with high clay content show expansion related structures not clearly restricted to ped surfaces, that result from compression of the interped voids. The preserved root horizons (Fig. 4.27d) provide further information; they are grey within red siltstones which indicates reducing conditions in predominantly oxic sediment. This may have two causes, a) they may preserve the rhizosphere around the living plant root, or b) they may represent anaerobic microbial decay of organic material soon after burial (e.g. Retallack, 1988). These palaeosols correspond to weakly developed inceptisols, or where clay is more concentrated vertisols, on the revised USDA tables presented by Retallack (1988). They are vertisols in the palaeosol system of Mack *et al.* (1993).

The second group of palaeosols were pedoturbated and contained calcic glaebules distributed throughout, they indicate a well-drained alkaline soil (e.g. Retallack, 1988) and were particularly common in the Shargyn Basin. These soils are moderately-developed aridisols with stage II carbonate accumulation (revised USDA tables, Retallack, 1988), or calcic vertisols in the system of Mack *et al.* (1993).

The third palaeosol type contains a well-developed caliche horizon and was present in all sections. These horizons record stage III or IV caliche development (e.g. Machette, 1985) in a moderate, occasionally strongly developed arid soil

(revised USDA tables, Retallack, 1988), or calcisol horizons in the system of Mack *et al.* (1993).

A fourth soil type, comprising a homogenous grey/blue siltstone, is rare. It is interpreted to have formed where the vadose zone was water saturated (e.g. Turner, 1980). They are gleysols in the system of Mack *et al.* (1993). No equivalent USDA soil exists because such soils are rarely observed at present. Gleysols are associated with clay-coated peds. Such extensive soil development within the overbank deposits suggests extended periods of non-deposition over the floodplain.

#### *Additional exposures of the Red Hill Formation*

The relationship between overbank facies C, AF, EF and EC and the channel bodies (facies D) is best seen in the East Ridge Section (Fig. 4.9) and the Central Ridge Section (south; Fig. 4.12). In these sections channel-bodies (facies D) accrete vertically, and grade laterally, into thinner sheet-like bodies (Facies AC & C) interbedded with siltstone beds (facies AF & AC, Log 9, Fig. 4.29). Facies C are upward-fining channelised sandstone and pebble sheets that fine laterally. The absence of internal erosion surfaces indicates a cut and fill style evolution, characteristic of a single event. Facies C beds are interpreted as crevasse splay deposits sourced from a major channel (facies D). Palaeocurrent readings from facies C beds are responsible for the scatter in palaeocurrent data measured in the North Foreberg locality. Interbedded with facies C are upward-fining, granule and sandstone sheets with minor erosive bases (facies AC), also seen in the Shargyn Section. These are interpreted as overbank sheetflood events, deposited when the river overtopped its bank and flowed as broad sheets over the floodplain (e.g. Williams, 1971; Hardie *et al.*, 1978; Miall, 1996). Crevasse splay deposits (facies

C) were not observed within the Base 1 Section, however, sand dominated overbank sheetflood deposits (facies AF) were present.

#### SUMMARY

The palaeosols, combined with the fluvial sediments, allow some suggestion of climate to be deduced. Parrish (1993) suggests that red sediments indicate a seasonally wet floodplain environment with repeated dissolution and precipitation of iron minerals onto grain surfaces. However, Turner's (1980) argument that the oxidation state is often set, not at deposition, but during early diagenesis remains convincing, so care must be taken in using sediment colour as a proxy for climate. Furthermore, sediment colour often relates more to the local water table than the regional climate, and may vary laterally over a palaeosol horizon, or pedofacies (Turner, 1980; Kraus & Brown, 1988). Turner (1980) defines two red bed associations that permit basic climate interpretation, the Red Hill Formation sediments fall into his "desert evaporite red bed association". An arid climate is also implied by the interpreted ephemeral river system and the abundant caliche horizons. Mack & James (1994) link their palaeosol groups to climate on a global scale. The Red Hill Formation deposits fall into their dry subtropical zone, with <100 cm/yr precipitation and seasonally variable temperature (hot summers and cool winters). This dry subtropical interpretation corresponds well with climate models for the Oligocene (Parrish *et al.*, 1982). The limited gleysols and evidence for a periodic high water table at the base of the formation are interpreted to represent periodic swamps developed on the floodplain (Farrell, 1987). Limited vegetation is indicated by the widespread distribution of facies across the basin floor. The depositional environment is interpreted to be semi arid/arid with limited vegetation cover. This environment is comparable to the present day basin.

No significant variation exists between the Dariv Basin sections, although in the Shargyn Section, facies D channels are finer and contain fewer reactivation surfaces. This, combined with the reworked caliche and intrabasinal sediment, suggests that it may lie in a more distal setting. The similar stratigraphy and uniform palaeocurrent suggests that these deposits represent a fluvial system that flowed south through the Dariv Basin into the Shargyn Basin. The recorded change in palaeocurrent orientation in the Shargyn Section suggests that the Shargyn basin has been a major basin throughout the Cenozoic. This interpretation suggests that, following the regional peneplanation event, the Dariv and Shargyn basins were again linked during the Oligocene. It also implies that Sutai Uul was not a major sediment source during this period; the possible reasons for this are discussed later (section 5.4, the synthesis of Cenozoic Basin evolution, page 166). The upward-fining trend of this formation reflects a change either in the source area or in the transport competency of the system. It is not possible to state with certainty which is correct, based on these data.

#### 4.3.4 Eagle Valley Formation - Miocene

The Eagle Valley Formation overlies a conformable contact with the underlying Red Hill Formation, defined by a gradational change from grey conglomerate interbedded with dark red siltstone to a thick succession of multicoloured siltstone beds. The Eagle Valley Formation is up to 180 m thick and dominated multicoloured siltstone beds. The Eagle Valley Formation's upper contact comprises a slight angular unconformity with the overlying Goshu Formation and is recognised by a sharp transition from siltstone to the grey pebble/cobble conglomerate sheets. The Eagle Valley Formation is named after a prominent valley within the North Foreberg where the formation is well exposed.



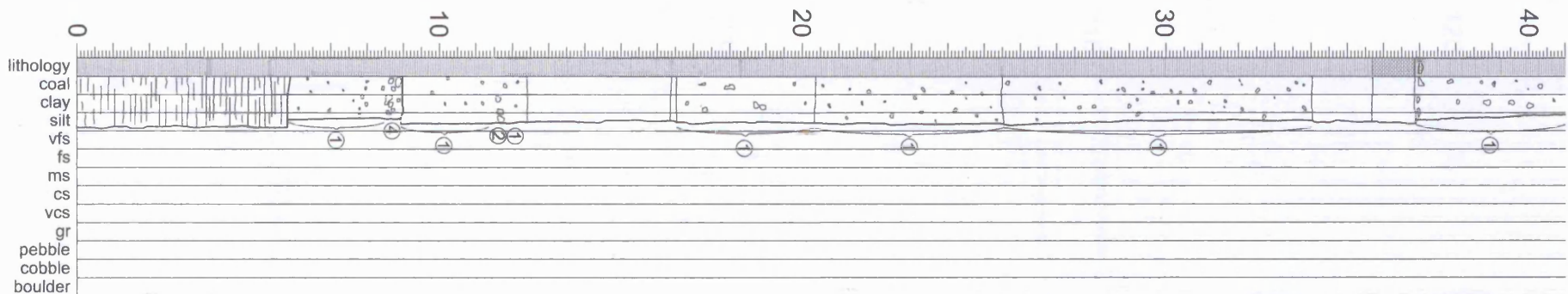
The Eagle Valley Formation is a new formation and is equivalent to the Oshin Suite of Devjatkin *et al.* (1981).

#### 4.3.4.1 DESCRIPTION

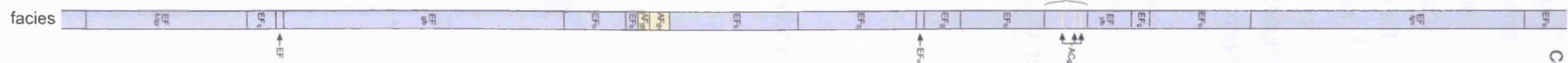
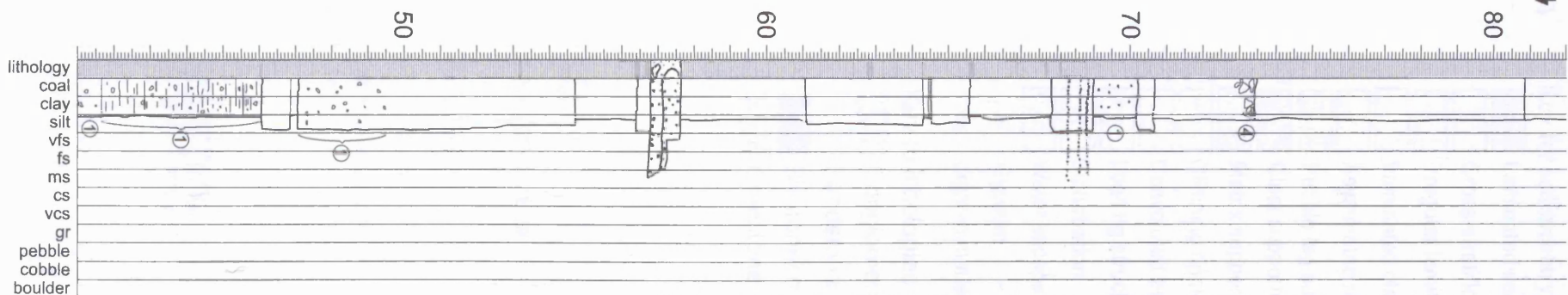
The Eagle Valley Formation is 175 m thick and well exposed only in the Eagle Valley and East Ridge Sections of the North Foreberg locality (area 2, Fig 4.2 & 4.9). Poor exposure was studied in the Shargyn Section (area 6, Fig 4.2). Log E1 (Fig. 4.32) records 133 m of the Eagle Valley Section that is dominated by massive siltstone (facies EF) with rare, coarse-grained beds (facies AC and C), which become more common up section. The siltstone beds (facies EF) are soft, and consequently poorly exposed, and colour variation is used to define bedding (Fig. 4.33a, b & c). Grey, blue-grey, brown and red beds are present, but there is no systematic distribution of colour through the section. Weakly developed caliche nodules and concretions are common throughout log E1, becoming increasingly well-developed upward where they are associated with root casts. At 36 m on log E1 a hard, white micritic limestone (facies M) contains *Plenabis Sensulata* and ostracods, a second limestone horizon occurs below log E1. Thin massive siltstone beds that lack caliche (facies K) are associated with the limestone beds (facies M). Facies EC is a massive, sand-rich siltstone supporting grains up to coarse-sand grade; it is present at two horizons (68-71 m and 108-117 m log E1, Fig. 4.32) where it is associated with coarse facies AC and C respectively. Coarse facies are rare in the basal 125 m of the section but, where seen, comprise commonly thin (<50 cm) sand (occasionally pebble) sheets with minor erosive bases (facies AC) that are laterally extensive over 10's of metres. Siltstone

---

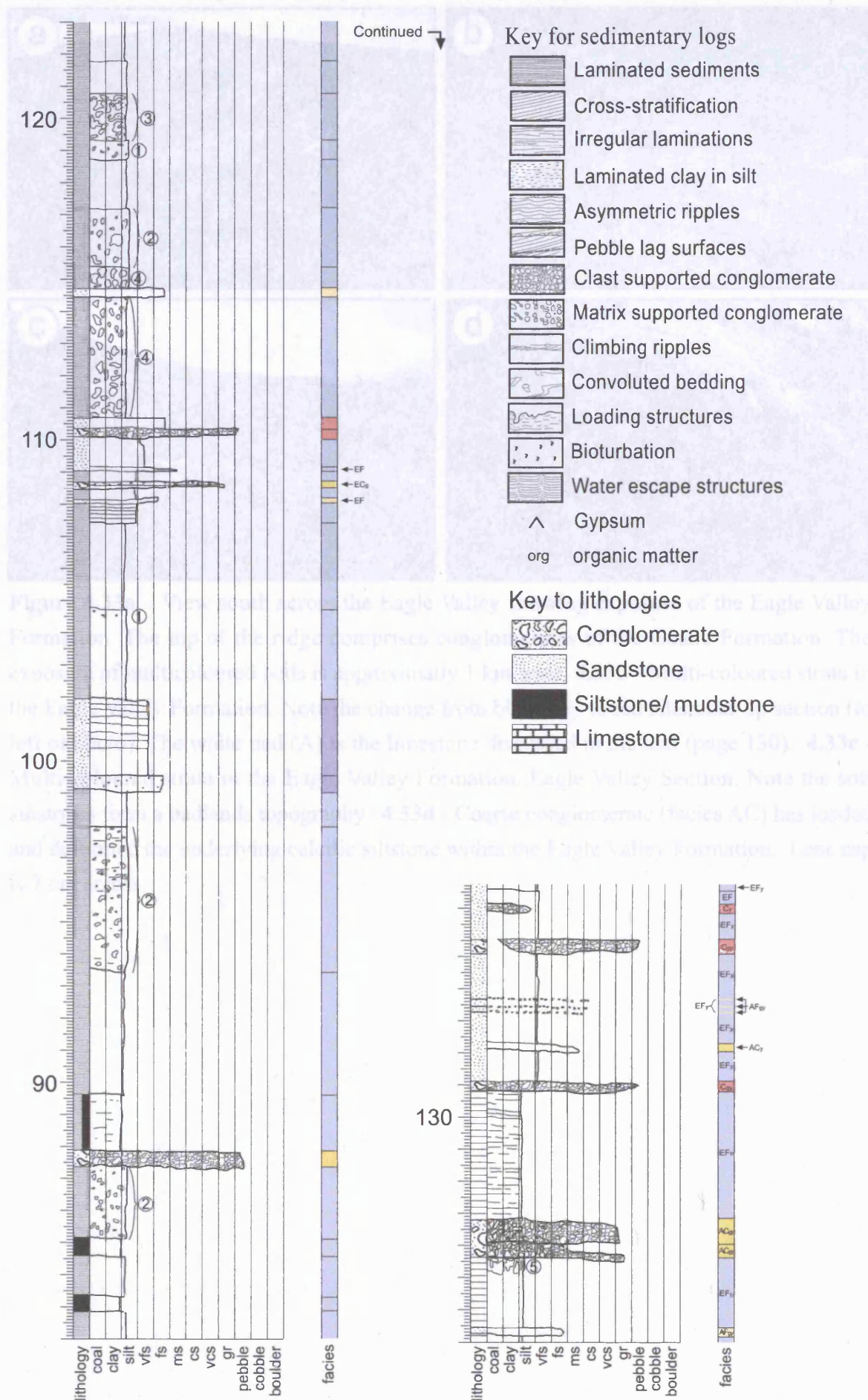
**Figure 4.32** (following page) – Log E1 from the Eagle Valley Section of the North Foreberg (area 2 Fig 4.2) showing the Eagle Valley Formation.



Continued →



Continued →





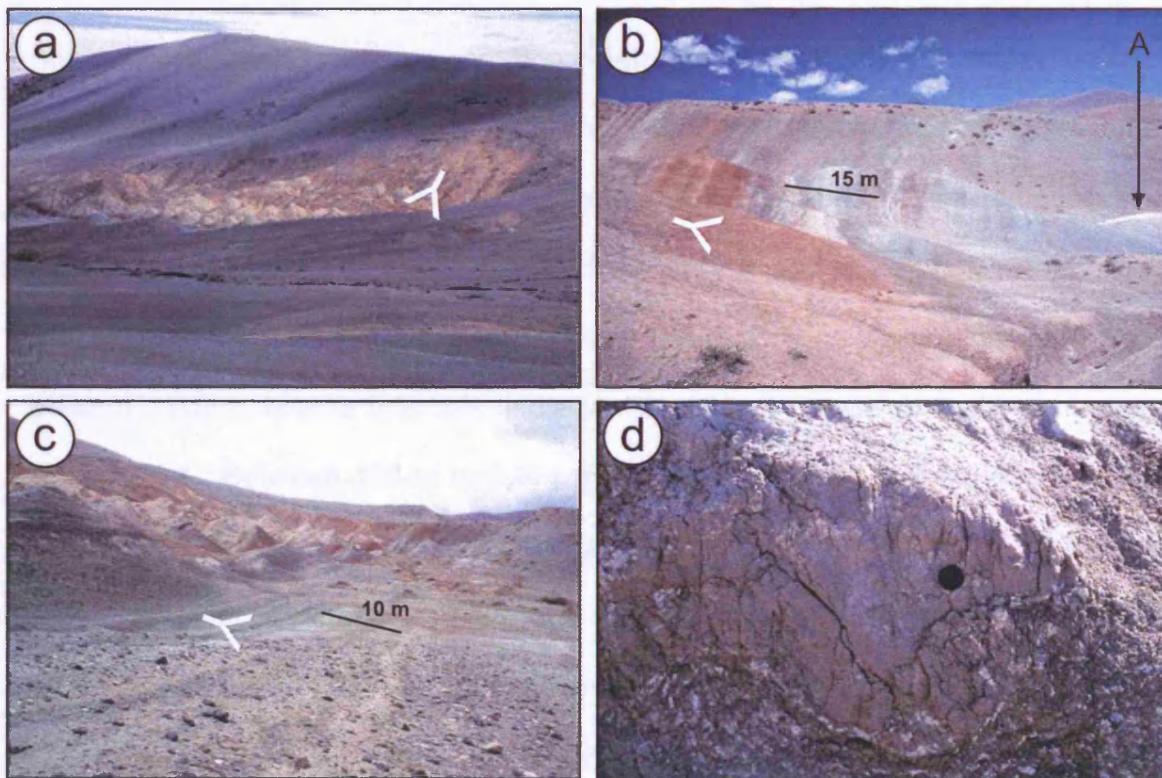


**Figure 4.33a** – View south across the Eagle Valley showing exposure of the Eagle Valley Formation. The top of the ridge comprises conglomerates of the Goshu Formation. The exposure of multicoloured beds is approximately 1 km wide. **4.33b** - Multi-coloured strata in the Eagle Valley Formation. Note the change from blue/grey to red siltstones up section (to left of photo). The white bed (A) is the limestone discussed in the text (page 130). **4.33c** - Multi-coloured strata in the Eagle Valley Formation, Eagle Valley Section. Note the soft siltstones form a badlands topography. **4.33d** - Coarse conglomerate (facies AC) has loaded and deformed the underlying calcitic siltstone within the Eagle Valley Formation. Lens cap is 7 cm across.

horizons below facies AC are commonly deformed (Fig. 4.33d). Towards the top of Log E1, facies C clast-supported, angular pebble and granule conglomerate beds, with an erosive channelised base become common. Clast compositions include granite, quartz, gneiss, volcanic clasts, schists and phyllite, with a matrix of fine yellow sandstone. Intrabasinal siltstone and reworked caliche blocks are also present. Within coarse intervals, individual beds and groups of beds commonly fine upward. Between 108 m and 111 m (log E1) four upward-fining paired beds are recorded. Above 125 m the stratigraphy is dominated by facies C beds that are <50 cm thick which both thin and fine laterally over a few meters. The channels are surrounded by a yellow/brown silt-rich sandstone facies EC. The lower part of the Eagle Valley Formation is recorded in the East Ridge Section (above 72 m, Log 8, Fig. 4.28). It is similar to the Eagle Valley Section, but with greater caliche development.

#### *The Shargyn Basin*

In the Shargyn Section, soft, red siltstones, containing well-developed caliche horizons, are poorly exposed. Siltstone beds containing coarse-grained sandstone and granules with occasional pebbles (facies EC) become more common upward. At the top of the section, there is an influx of granules and pebbles into all horizons, some of which become clast-supported (Facies H). The Eagle Valley Formation is Miocene based on fossils found in limestone horizons and palynology results from samples within the succession. It is equivalent to the Oshin suite (Devjatkin, 1981).

#### 4.3.4.2 INTERPRETATION

The fine-grained Eagle Valley Formation records an unexpected pause in coarse sedimentation during the early Miocene, a time when uplift of adjacent



ranges is thought to have been rapid (Cunningham *et al.*, 2003). The siltstone beds (facies EF), which contain traces of bedding, carbonate concretions and commonly appear pedoturbated, are interpreted as overbank floodplain deposits from a distal fluvial source (see also Red Hill Formation interpretation, page 124). The colour variations observed (Logs 8 (Fig. 4.28) and E1 (Fig. 4.32) & photographs Fig. 4.33a, b & c) are striking, but difficult to interpret with certainty. They range from red/brown siltstones that are indicative of an oxidising environment to drab grey, grey/green and grey/blue horizons that are characteristic of reducing conditions (e.g. Truc, 1978; Miall, 1996). This section also contains many mottled beds indicative of fluctuating redox conditions (e.g. Turner, 1980) and care must be taken when interpreting climate from the colour of sediments (See Red Hill Formation interpretation, page 124). Caliche is present in many beds and is characteristic of arid climates (e.g. Retallack, 1988; Miall, 1996). The majority of soil horizons contain diffuse caliche, they are classified as calcic-vertisols in the system of Mack *et al.* (1993), this is further refined to gleyed calcitic-vertisols when colour indicates reducing conditions. Where the caliche is developed only to stage I or II (Table 1, appendix 2), they are classified as inceptisols in the USDA table (Table 2 appendix 2, Retallack, 1988). It is unusual to see drab colours, interpreted to represent periods with high water table and, possibly, periodic swamp development, associated with caliche, which is indicative of an arid climate. This caliche may have been precipitated around the root systems of vegetation during evapotranspiration, or have formed later as the soil dried out. The overall climatic interpretation is a continuation of the arid conditions recorded in the Red Hill Formation, which corresponds with the climate models for the period (e.g. Parrish *et al.*, 1993). The two micritic limestone beds (facies M) are <1 m thick and are interpreted to represent lakes that developed on the

floodplain. The presence of ostracods and the vertical thickness of these deposits suggest the lakes persisted for a considerable period. Facies EC siltstones contain sand grains and occasional granules that have several possible sources. Sand may have been deposited as thin sheets within the siltstones that were then mixed during pedoturbation, however the palaeosols are not advanced, and intact sand sheets were not observed, despite investigating several laminated horizons. Grains may be the deposits of fine-grained debris flows or the siltstone may have been transported as sand size aggregates (e.g. Rust & Nanson, 1989; see discussion page 76). The most likely source of sand is via reworking of peds from up dip slope surfaces that were transported along with sand grains during flood events.

The formation becomes significantly coarser upward and contains pebble and granule conglomerate horizons (facies AC) and siltstones with well-developed caliche horizons. Facies AC laterally extensive, upward-fining sandstone sheets are again interpreted as the distal deposits of sheetfloods (e.g. Williams, 1971; Tunbridge, 1981; See discussion page 86). Facies C, weakly-channelised conglomerate bodies dominate the upper part of the formation and grade laterally into sandstone and siltstone. These are again interpreted as crevasse splay deposits (see discussion page 126). It is not possible to estimate the proximity of the feeder channels because the thickness of crevasse splay deposits also relates to the dimensions of the source channel. The absence of significant coarse input into the East Ridge Section, and the development of extensive calcisol horizons there (based on the system of Mack *et al.*, 1993), suggests deposition in a more distal location relative to the sediment source. Palaeocurrent data show a degree of scatter in this formation, which is expected in crevasse splay and sheetflood deposits, but a general southeasterly trend was established. This corresponds

with a source area in the north and suggests significant sediment that was derived from Sutai Uul finally reached the Dariv Basin during the later Miocene. The cause of the delay between uplift and deposition is discussed in chapter 5.4 (the synthesis of Cenozoic basin evolution).

#### *The Shargyn Basin*

In the Shargyn Section the upward-coarsening floodplain siltstones (facies EC) suggest either an increasingly proximal position to, or an increase in the bedload competence of, the source river. Both are probable during movement along the Tonhil fault or uplift of Dariv Nuruu. Uplift of Dariv Nuruu is interpreted to have separated the two basins at this time.

### 4.3.5 The Goshu Formation - Pliocene to Lower Pleistocene

The Goshu Formation overlies a basal unconformity with the underlying Eagle Valley Formation, defined by a sharp change from multicoloured siltstones to grey pebble/cobble conglomerate. The formation is dominated by laterally extensive conglomerate sheets and is up to 190 m thick. The Goshu Formation's upper contact is not seen within the Dariv Basin. The formation name is after Devjatkin *et al.* (1981).

#### 4.3.5.1 DESCRIPTION

The Goshu Formation is exposed only in the Eagle Valley Section (Fig. 4.9), where it is at least 200 m thick (Fig. 4.34). It overlies a slight angular unconformity with the underlying stratigraphy and comprises almost exclusively conglomeratic facies as shown on logs 13 and 14 (Fig. 4.35 & 4.36). The dominant facies are clast-supported, grey, granule and pebble conglomerate beds with a yellow sandstone matrix (facies AC). Facies AC is texturally and mineralogically

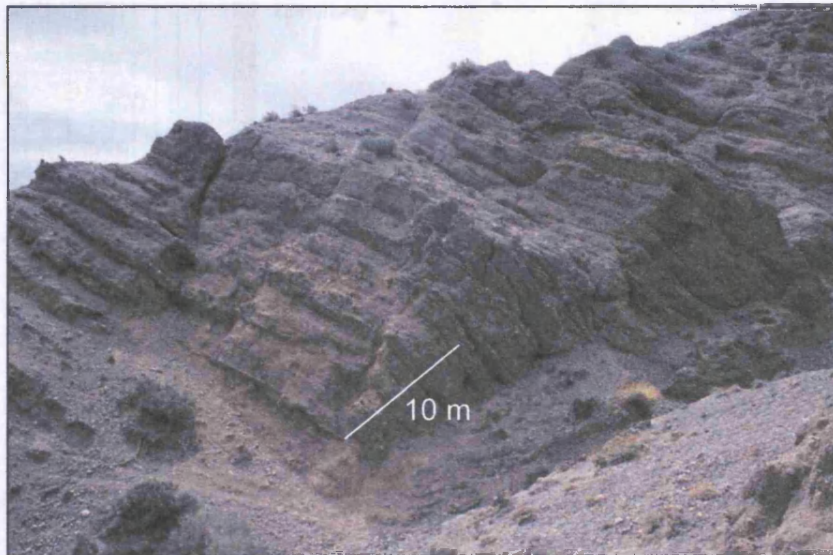


**Figure 4.34** - Typical section of the Goshu Formation (Pliocene to Lower Pleistocene). Note the laterally extensive conglomerate beds with little fine material (yellow) preserved between them.





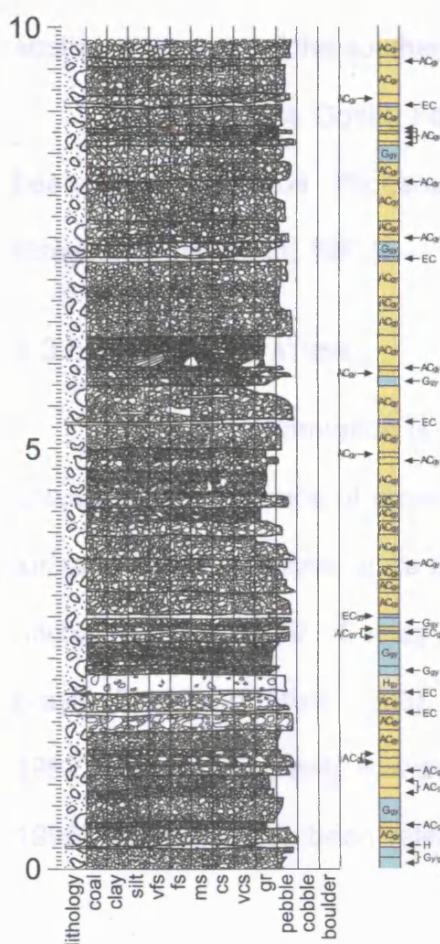
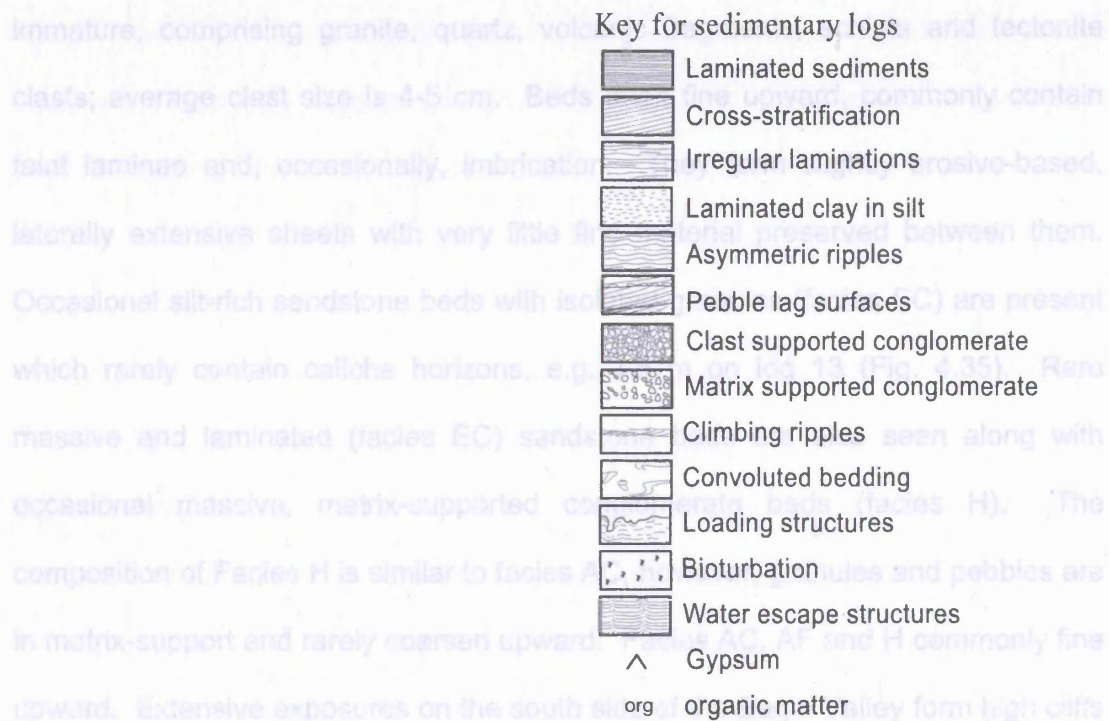


**Figure 4.36** – Log 14 from the Goshu Formation in the Eagle Valley Section (Fig. 4.9).

immature, comprising granite, quartz, volcanic fragments, schists and tectonite clasts; average clast size is 4-5 cm. Beds often fine upward, commonly contain faint laminae and, occasionally, imbrication. They form slightly erosive-based, laterally extensive sheets with very little fine material preserved between them. Occasional silt-rich sandstone beds with isolated granules (facies EC) are present which rarely contain caliche horizons, e.g. 1.5 m on log 13 (Fig. 4.35). Rare massive and laminated (facies EC) sandstone beds are also seen along with occasional massive, matrix-supported conglomerate beds (facies H). The composition of Facies H is similar to facies AC, however, granules and pebbles are in matrix-support and rarely coarsen upward. Facies AC, AF and H commonly fine upward. Extensive exposures on the south side of the Eagle Valley form high cliffs with little apparent variation up section, although most of the section is inaccessible. The formation fines and thins to the east and is not exposed in the south-eastern end of the southern ridge (Fig. 4.9).

The age of the Goshu Formation in the Dariv Basin is unknown, but it has been inferred to be Pliocene-Early Pleistocene, based on similar deposits elsewhere (Devjatkin, 1981).

#### 4.3.5.2 INTERPRETATION

The Goshu Formation is dominated by facies AC beds that commonly fine upward. The presence of cross-stratification and occasional imbrication indicates turbulent flow conditions, while the thin, laterally extensive bed geometry indicates unconfined sheet flow. Facies AC is interpreted as the deposits of cohesionless gravity flows (e.g. Miall, 1996), or sheetflood traction gravels (e.g. Hartley *et al.*, 1992). These are gravity flow deposits with a sediment concentration <40% (Miall, 1996) that have also been referred to as high-density turbulent flows (Postma &

Roep, 1985) when concentration is <30%. They are interbedded with rare facies H beds which comprise pebbles and granules supported in a siltstone or sandstone matrix. Facies H beds occasionally coarsen upward and are interpreted as the deposits of a debris flow, in which intergranular dispersion forces produce inverse grading. Within the fine sediments (facies EC), that are interpreted as overbank deposits, weakly developed palaeosols with stage II carbonate accumulation (USDA Scheme - Retallack, 1988) have developed. These represent calcic-protosols in the scheme of Mack *et al.* (1993). The section is interpreted as the deposits of a sheetflood dominated alluvial fan prograding to the east. Progradation is implied by the wedge shaped geometry of the conglomerate and the basinward fining exposure. The East Ridge Section contains no alluvial fan sediment and is interpreted to record the margins of the alluvial fan system. The formation is interpreted to record deposition from the Sutai Range source area, which initiated during the Miocene.

#### 4.3.6 Undifferentiated Cenozoic Sediments

##### 4.3.6.1 DESCRIPTION

Sediments of Plio-Pleistocene age are poorly exposed in the Green Valley Section where they are both undated and isolated from the older stratigraphy of the basin. These deposits are described briefly for completeness. In the Green Valley area (area 2, Fig. 4.2) subhorizontal, red/orange siltstone beds (facies EF), often with well-developed caliche horizons, onlap the ridge formed by Ihkes Nuur Formation conglomerate. They appear massive in badland style exposure (Fig 4.37a). The exposure coarsens upward with increasingly sand-rich red siltstone beds and fine sandstones (facies AF). Lenses and horizons of red-brown, granule and pebble conglomerate with a fine sand matrix also become increasingly



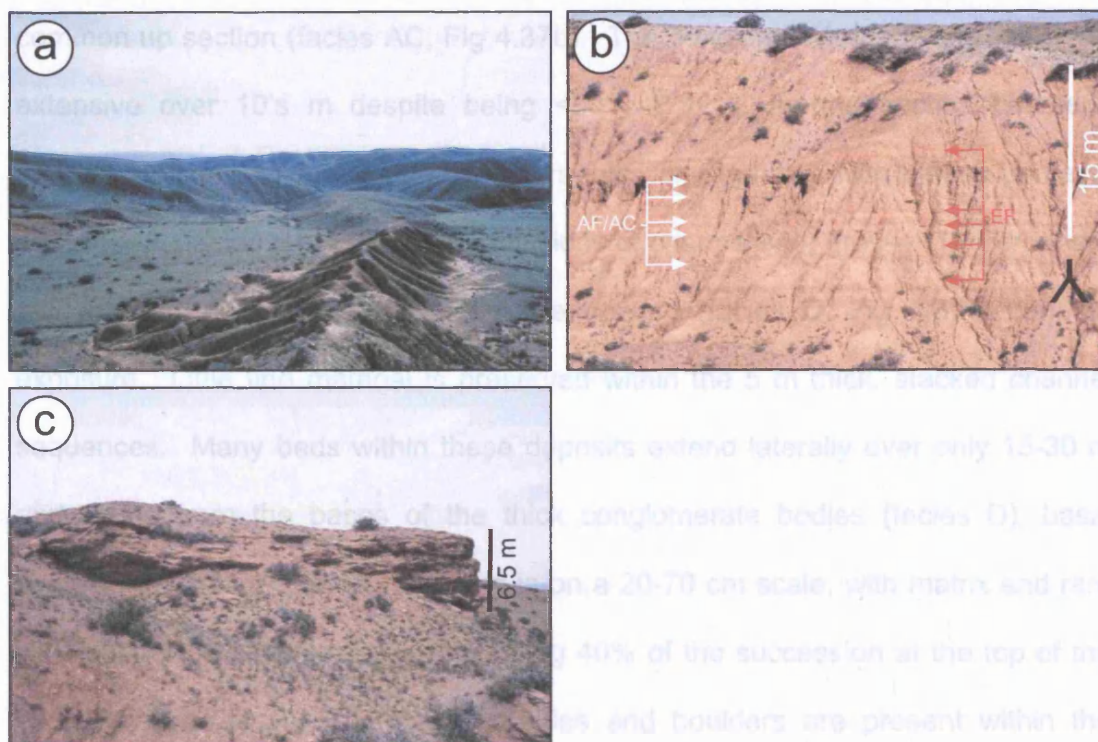


**Figure 4.37a** – Badland exposure of the undifferentiated Cenozoic strata. The ridge in the background is the Ihkes Nuur Formation conglomerate in the Southern Foreberg. The canyon that incises the ridge is visible. **4.37b** – Horizontal stratification in the undifferentiated Cenozoic deposits. The stratigraphy comprises sheetflood sandstone and conglomerate (facies AF and AC) interbedded with overbank siltstone (facies EF). **4.37c** – Carbonate cemented channel conglomerate in the upper part of the undifferentiated Cenozoic strata

These deposits record a fluvial system that post-dated the initial uplift of the South Foreberg ridge which they onlap. The base of the section is dominated by facies AF and AC interbedded with fine-grained floodplain deposits (facies EF and EC). The presence of poorly developed caliche (term from Mack *et al.*, 1993) suggests periods of inactivity on the floodplain. Facies AF and AC are again interpreted as sheetflood deposits of differing magnitudes (see discussion on page 86). In combination, these facies are interpreted as the deposits of a small alluvial fan that built eastwards from the uplifting Tonalil Mountain to the west until it was dammed by the thrust edge to the east. The exposure then becomes increasingly dominated by facies H matrix-supported conglomerates, which are interpreted as

common up section (facies AC, Fig 4.37b). The conglomerate bodies are laterally extensive over 10's m despite being <50 cm thick. As the section coarsens upward, horizons of matrix-supported granules and pebbles with diffuse contacts are present (facies H). Stacked successions of channelised, grey-white, carbonate cemented, conglomerate that often fine upward (facies D, Fig 4.37c) cap the exposure. Little fine material is preserved within the 5 m thick, stacked channel sequences. Many beds within these deposits extend laterally over only 15-30 m and, aside from the bases of the thick conglomerate bodies (facies D), basal contacts are mainly planar. Bedding is on a 20-70 cm scale, with matrix and rare clast-supported conglomerate comprising 40% of the succession at the top of the exposure (Facies AC & H), rare cobbles and boulders are present within the conglomerate. Clast lithologies are granite, quartz, metamorphic and volcanic lithologies and tectonites. The dip of strata increases toward the mountain front where the formation is in faulted contact with Devonian strata.

#### 4.3.6.2 INTERPRETATION

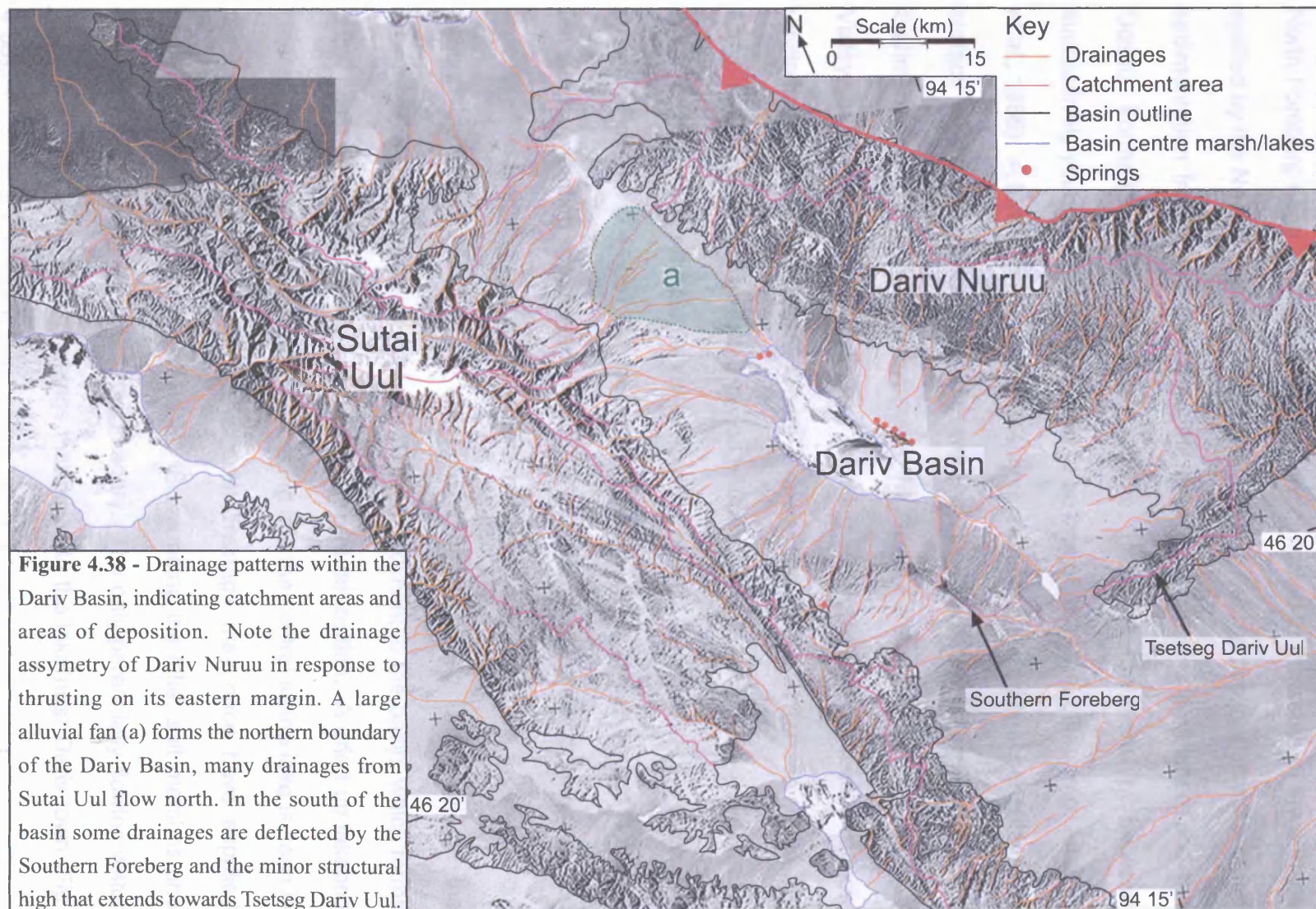
These deposits record a fluvial system that post-dated the initial uplift of the South Foreberg ridge which they onlap. The base of the section is dominated by facies AF and AC interbedded with fine-grained floodplain deposits (facies EF and EC). The presence of poorly developed calcisols (term from Mack *et al.*, 1993) suggests periods of inactivity on the floodplain. Facies AF and AC are again interpreted as sheetflood deposits of differing magnitudes (see discussion on page 86). In combination, these facies are interpreted as the deposits of a small alluvial fan that built eastwards from the uplifting Tonhil Nuruu to the west until it was dammed by the thrust ridge to the east. The exposure then becomes increasingly dominated by facies H matrix-supported conglomerates, which are interpreted as



the deposits of hyperconcentrated gravity flows (e.g. Miall, 1996). These flows are interpreted to have built up against the thrust ridge until they overtopped it. The presence of thin drapes of fan sediment on top of the South Foreberg Ridge provides some evidence for this. At this point, channelised conglomerate bodies (facies D) begin to occur. The stacked conglomerate bodies (facies D) comprise thin beds (<50 cm) suggesting a shallow, stable channel system (see discussion on page 75). The channels are well confined within their overbank sediment and contain few structures that record the migration of channel macroforms. The streams represent small, relatively straight systems, with limited accommodation, which resulted in only the basal lag being preserved. These channels are interpreted to have allowed sediment to bypass over the thrust ridge and into the basin centre. Fluvial incision eventually backcut through the ridge and into the onlapping sediments, producing the canyon we see today. The soft sediment that ponded behind the ridge is now being eroded and redeposited basinward of the thrust ridge. These deposits must postdate uplift of the South Foreberg and, although they are of similar style to the Eagle Valley Formation sediments, they are tentatively ascribed to the Plio-Pleistocene.

#### 4.3.7 Quaternary deposits

The Dariv Basin has a centripetal drainage pattern and Pleistocene-recent sedimentation is dominated by alluvial fans that flank each basin margin and drain directly into the small saline lake at the basin centre. The western and northern margins of the Dariv Basin supply large quantities of coarse sediment to the basin (Fig 4.38). In the north, a structural high which forms a drainage divide has developed between two forebergs (Fig 4.38). In the area south of the North Foreberg a second large fan is derived from a smaller drainage on the east flanks





of Sutai Uul. The fan onlaps an angular unconformity with the Eagle Valley Section and Base 1 Section so must, at least in its later part, postdate uplift of the North Foreberg ridge. Recent drainages are deflected to the south of the surface uplifted by the North Foreberg. There has probably been a continuous influx of fan sedimentation from Sutai Uul since the two main canyons developed and the Goshu Formation was deposited. The geometric relationship between successively younger fans is interpreted to be one of rotational offlap (e.g. Anadón *et al.*, 1986). A further gravel lag, probably representing the original peneplanation surface is exposed throughout the west of the North Foreberg (Fig 4.39a). Sediment from Sutai Uul now bypasses the North Foreberg while, in the Eagle Valley, headward erosion continues, resulting in erosion of the basin fill now uplifted above the basin floor. There is an abandoned river terrace within the canyon interpreted to represent a period of uplift in the foreberg (Fig 4.39b) and a small fan feeding into the Eagle Valley from the north is truncated by the axial river system (Figs. 4.9 & 4.39b). On the western margin of the basin, several faults cut fan surfaces leading to localised incision. In the Southern Foreberg, only a limited amount of sediment is deposited behind the thrust ridge because 5 canyons cut through the ridge. Minor fans are derived from Tsetseg Dariv Uul but the remainder of Dariv Nuruu supplies only limited sediment to the basin, which forms a low angle gravel fan with no indication of recent deposition. A dried up lakebed crossed by an inactive axial drainage feeding into the central saline lake is seen in the south of the Dariv Basin. This axial drainage may once have supplied sediment south into the Shargyn Basin. Surrounding the lake, salt marshes and evaporate deposits are visible on the imagery. The only perennially flowing water within the Dariv Basin is from springs that flow into the lake near Dariv town (Fig. 4.38).



**Figure 4.39a** – View south across the basin centre from the top of the East Ridge in the North Foreberg (Fig. 4.9). Note the surface of the ridge is draped by uplifted fan material which mantles uplifted topography across the basin. **4.39b** - View northeast across the Eagle Valley in the North Foreberg area (Fig. 4.9). Photographer is standing on the conglomerates of the Goshu Formation. The Eagle Valley is in the foreground with the East Ridge in the midground. Dariv Nuruu is in on the skyline. Note the ongoing incision in the Eagle Valley and terrace formation. Note the alluvial fan entering the valley from the north, which is truncated, by the ephemeral stream course (marked by the arrows). The multicolored sediments of the Dariv (c) Formation can be seen within the basin. Field of view is 4.5 km.





## Chapter 5

### The Structural Evolution of the Dariv and Shargyn basins

#### 5.1 Introduction

The basement geology of western Mongolia comprises Palaeozoic subduction accretion belts and arc/back-arc complexes that accreted between cratonic blocks in Siberia, China and central Mongolia (Chen & Jahn, 2002; Badarch *et al.*, 2002; Windley *et al.*, 2002). Progressive terrane accretion resulted in the development of a basement structural grain defined by regional foliation and fault trends. In the Altai, this structural anisotropy is oriented northwest-southeast and generally dips northeast. This basement fabric has exerted a strong influence on all later deformation within the region.

The modern Dariv Basin is influenced by many active structures that bound the basin and internally deform it. The Mesozoic and Cenozoic sedimentary fill is consequently uplifted and exposed in deforming zones around the basin. Exposed sedimentary strata and the broad distribution of active structures suggest that the Dariv Basin may have a more complex history than the Dzereg Basin. This history is further complicated by the position of the Dariv Basin in an area of conjugate strike-slip faulting (Tapponnier & Molnar, 1979; Schlupp, 1996) at the intersection between the Altai and Gobi Altai ranges. The Altai is uplifted by thrust displacements linked to dextral strike-slip faults, and the Gobi Altai is uplifted by thrust displacements linked to sinistral strike-slip faults (Fig. 5.1).

This field-based study combines information about basin structures and exposed strata (chapter 4) in order to understand the Dariv Basin evolution. Faults are generally unexposed, but the geometry of folded strata and tilted surfaces



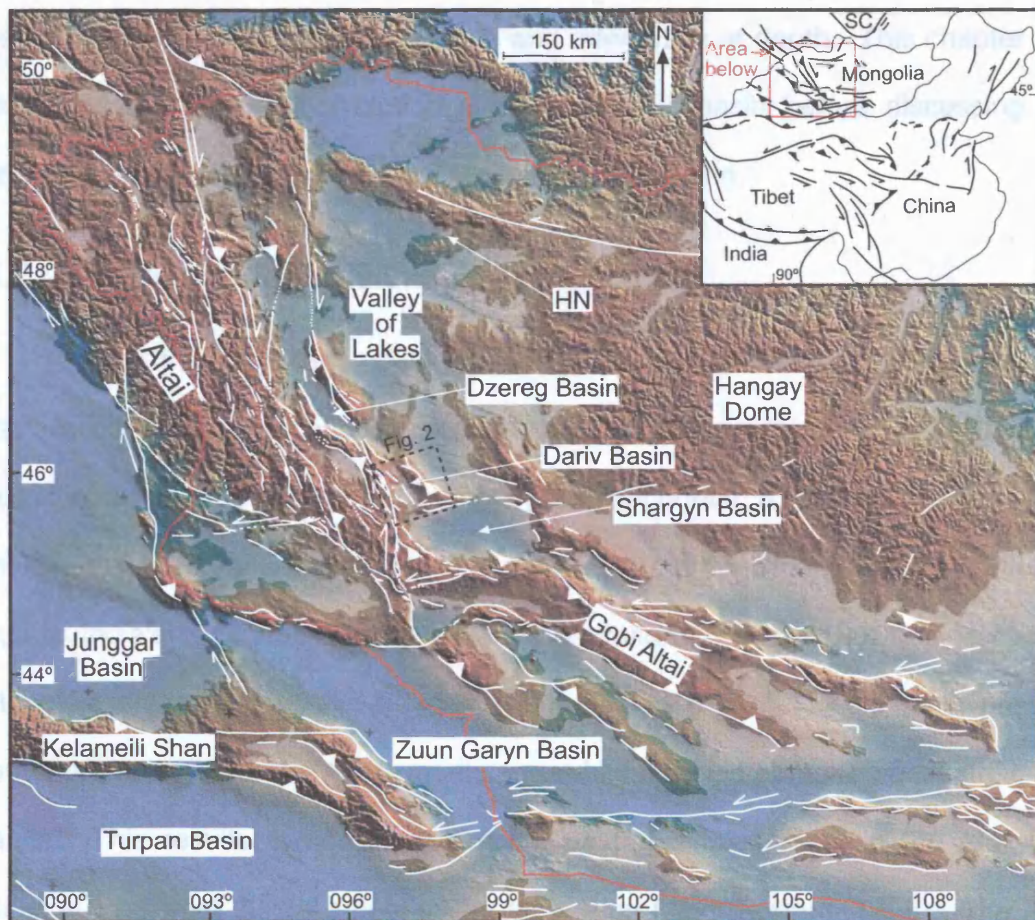


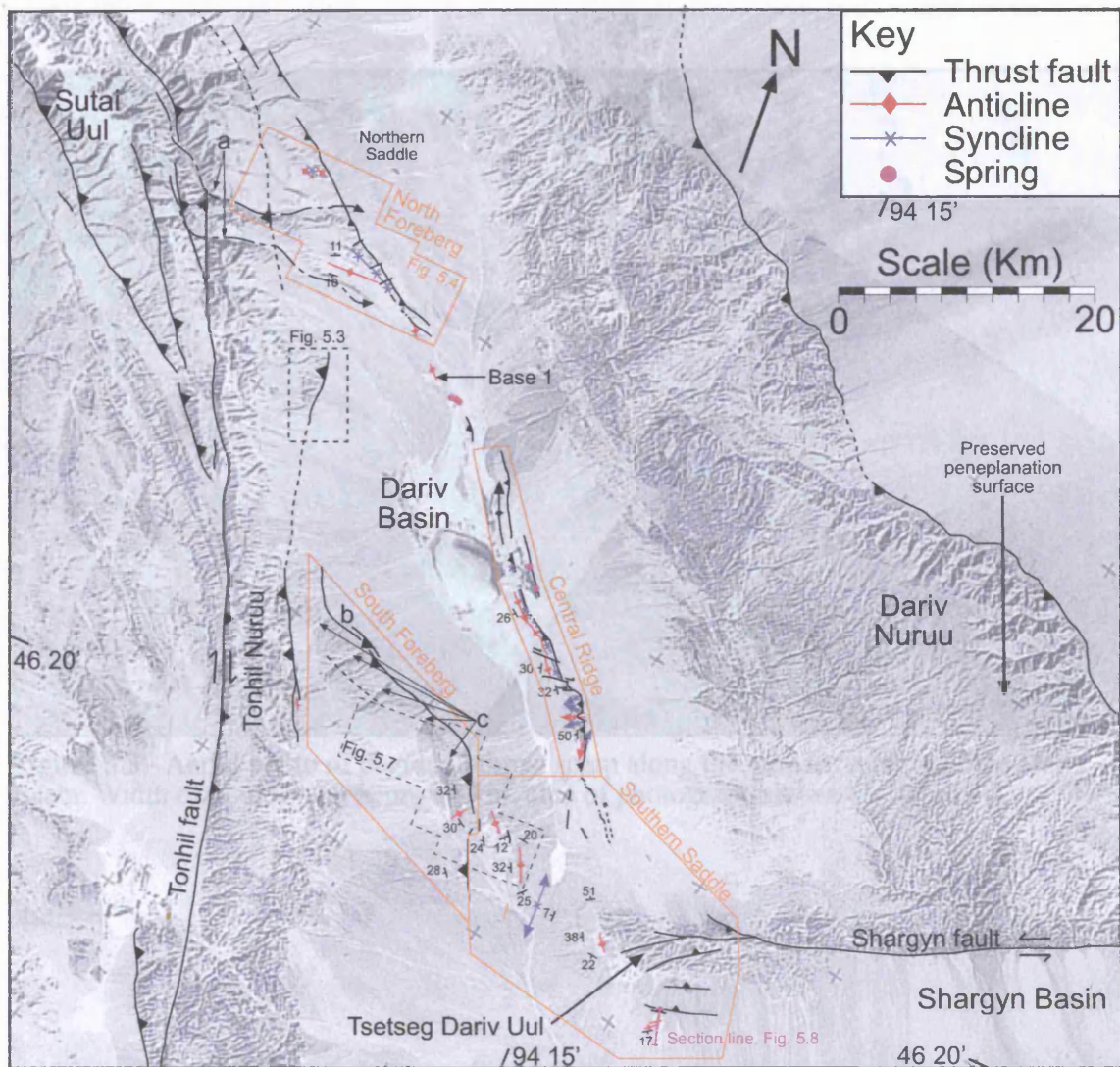
**Figure 5.1** - Digital elevation model showing western Mongolia and adjacent parts of China and Russia. Sedimentary basins are shown in pale tones. Major Cenozoic thrust and strike-slip faults are also shown (Cunningham, 1998). Note the contrast between the dextral transpression in the Altai and the sinistral transpression in the Gobi Altai. Location of three studied basins is shown as well as area covered by Fig. 5.2. Inset map shows major Cenozoic faults within Asia. SC = Siberian Craton, HN = Hyargas Nuur.

symmetric basin structures with outward directed thrusting at the margins (Fig. 5.2). Both the Altai and Gobi Altai are active as indicated by the recent earthquakes (Balanyan et al., 1993) and tectonic geomorphology (Cunningham et al., 1994; Balanyan et al., 2003). Many ranges are bound by fresh fault scarps along their fronts (Fig. 5.3).

permits interpretation of their presence and orientation at depth. This chapter first describes the structural evolution of the Cenozoic basin before discussing the probable structure of the precursor Mesozoic Dariv Basin.

## 5.2 Cenozoic Basin Structure

Since the Oligocene, deformation within western Mongolia is believed to have occurred in response to far-field stresses derived from the Indo-Eurasian collision over 2500 km to the south-west (Tapponnier & Molnar, 1979). The maximum horizontal compressive stress in western Mongolia is oriented northeast due to India's continued north-eastward indentation (Zoback, 1992). The central Mongolia craton, under the Hangay Dome region (Fig. 5.1) acts as a passive indenter, forcing lateral displacements around its margins along regional strike-slip faults. This results in northwest-directed dextral displacement in the Altai and sinistral east-west displacement in the Gobi Altai (Cunningham, 1998). The Altai range is also undergoing anticlockwise rotation relative to the applied stress (Bayasgalan *et al.*, 1999b). Ranges within the Altai represent discrete transpressional uplifts and thrust ridges, linked to regional strike-slip fault systems (Cunningham *et al.*, 1996a, 2002, 2003). Many individual ranges comprise asymmetric flower structures with outward directed thrusting at their margins (Fig. 5.2). Both the Altai and Gobi Altai are active as indicated by historical seismicity (Baljinnyam *et al.*, 1993) and tectonic geomorphology (Cunningham *et al.*, 1996a, b, 2003). Many ranges are bound by fresh fault scarps along their fronts (Fig. 5.3).





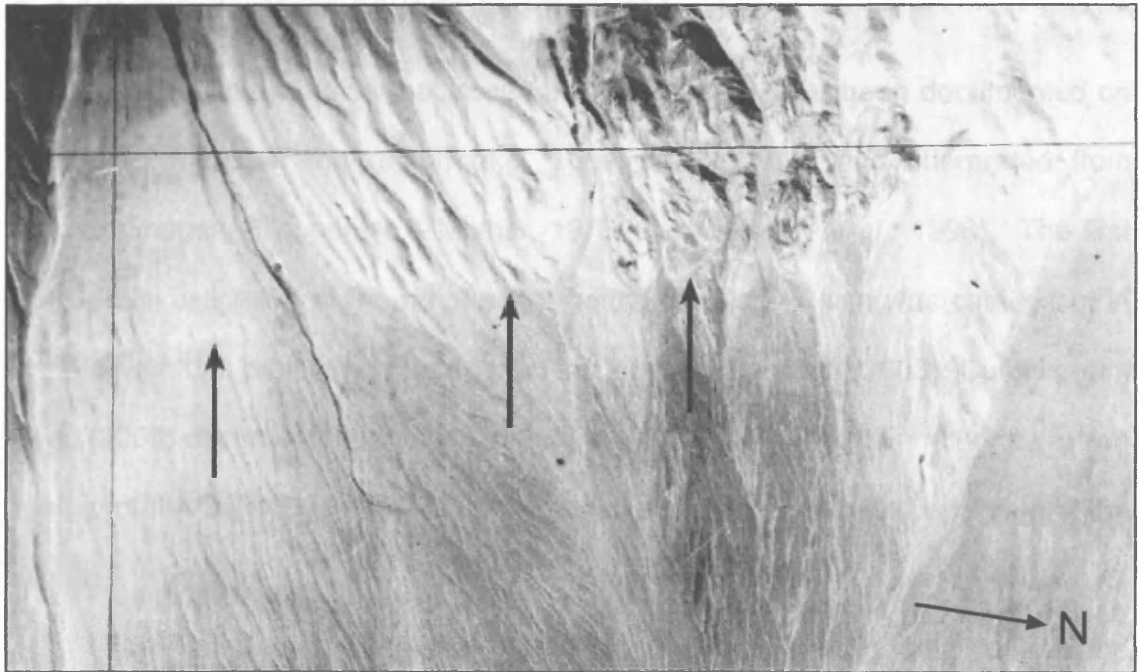


**Figure 5.3** - Aerial photo of degraded thrust scarp along the western margin of the Dariv Basin. Width of photograph approx 4 km, area of photograph shown on figure 4.2.

### 5.2.1 External (basin bounding) structures

The faults and folds that bound the Dariv Basin have been documented on geological maps of the region (e.g. Tomurtogoo, 1999) and interpreted from satellite imagery (Tapponier & Molnar, 1979; Cunningham *et al.*, 1996). The first detailed investigation of the ranges that bound the Dariv Basin was carried out in parallel with this project and is reported in Cunningham *et al.*, (2003). Cunningham *et al.*, (2003) document the internal structure of the Sutai range on the northwestern margin of the Dariv Basin and present models for the initiation and evolution of the range.

The Tonhil fault, a regionally important dextral strike-slip fault, controls the western margin of the Dariv Basin (Fig. 5.2). Relief along this fault (Tonhil Nuruu) is low in the south where strike-slip motion dominates, but increases to the north as the fault curves westward, culminating in the Sutai Massif. The Sutai Massif, including the highest peak in the region, Sutai Uul (4090 m) is a restraining bend uplifted at a stepover zone between two segments of the Tonhil fault (Cunningham *et al.*, 2003). The internal structure of the range comprises an asymmetric flower structure with most uplift accommodated by thrusting in the centre and on the south-western side. In the Dzereg Basin, (Fig. 5.1), the earliest Cenozoic sediment is derived from Sutai Uul, suggesting that it was the initial locus of rejuvenated uplift in the region (Howard *et al.*, 2003). The flat summit plateau on Sutai Uul, and other peaks within the region (e.g. Dariv Nuruu, Fig. 5.2), is a preserved Palaeogene peneplanation surface recognised throughout the region (Devjatkin *et al.*, 1975). Tonhil Nuruu is asymmetric with the major thrust component directed toward the west. Eastward directed thrusts are also present cutting alluvial surfaces and uplifting basement blocks within the Dariv Basin (Fig. 5.3).



In contrast, the eastern Dariv Basin margin is inactive and sediments onlap the western, gently tilted flank of Dariv Nuruu. Dariv Nuruu is uplifted by a thrust fault on its eastern margin (Fig. 5.2), but there is no evidence for Cenozoic deformation within the range. The range's asymmetry is clearly expressed in the modern drainage distribution, with short steep channels in the east/northeast and longer, sinuous channels draining towards the west/southwest. The southern Dariv range front is sharply defined by a major, active sinistral fault, the Shargyn fault. This fault extends westwards into the Dariv Basin where it splays and curves northwest as it approaches the Tonhil Fault (Fig. 5.2). Tsetseg Dariv Uul (Little Dariv Mountain), which forms the southern margin of the Dariv Basin, is uplifted at this splay zone along the Shargyn fault.

Low uplifted "saddles" bound both the southern and northern margins of the Dariv Basin and effectively leave it perched above the Shargyn Basin to the southeast and the Valley of Lakes to the north (Fig. 5.1). The geology underlying the saddles is poorly exposed. The Northern Saddle formed where the Sutai and Dariv ranges are closest and lies adjacent to a zone of internal deformation within the basin (Fig. 5.2). The Southern Saddle contains structures indicative of east-west compression and appears to result from interaction between the Tonhil fault and the Shargyn fault (Fig. 5.2).

### 5.2.2 Internal Basin Structures

This PhD represents the first detailed study of intrabasinal deformation within the Dariv Basin. The Dariv Basin is dominated by alluvial fans that extend outward from adjacent ranges onto a gravel plain that forms the basin floor. Within the basin, four structural domains are identified: the North and South Forebergs, the Central Ridge and the Southern Saddle (Fig. 5.2). These domains may be

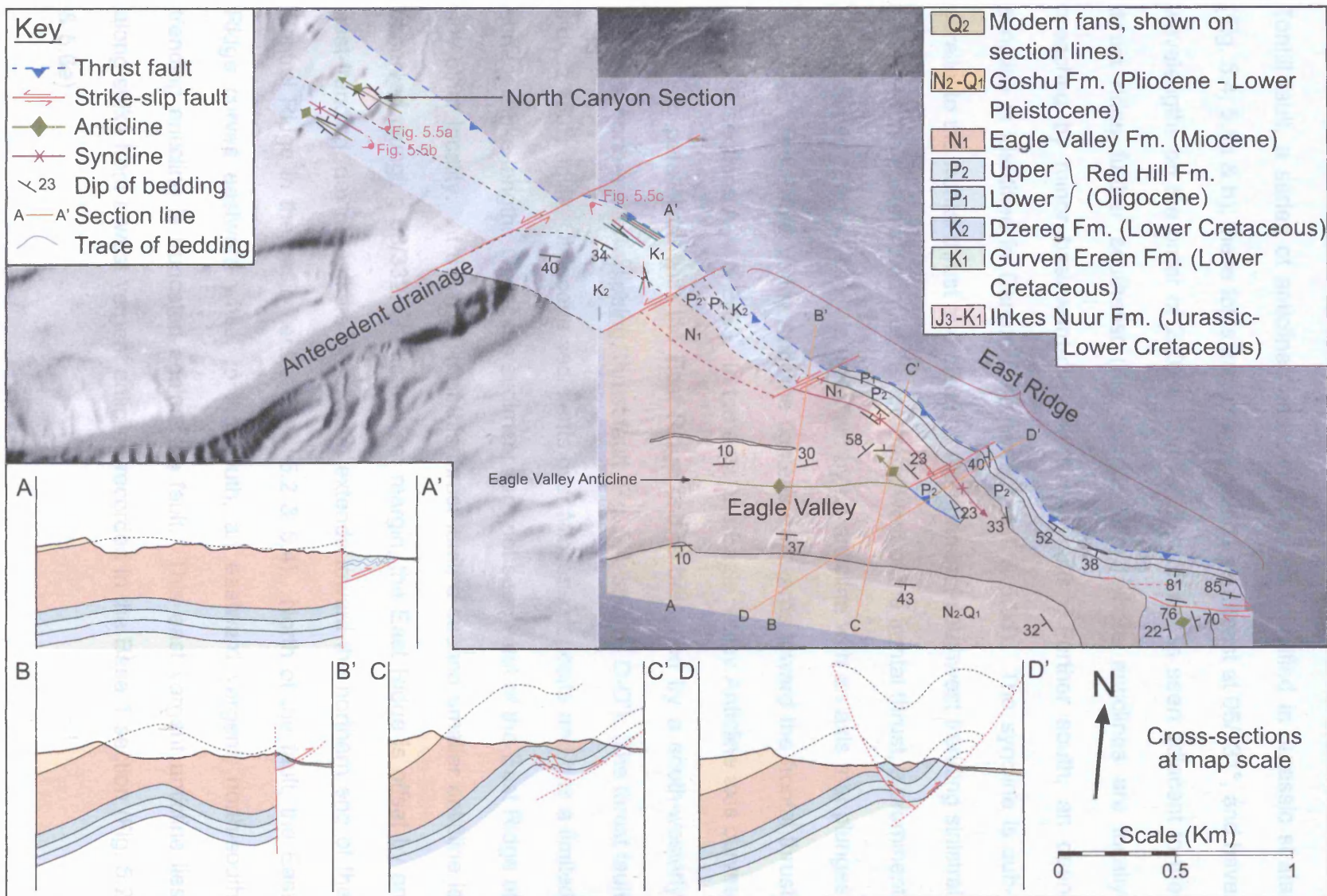
structurally linked and appear to define a rhomboid of active deformation adjacent to the Tonhil fault (Fig. 5.2). The linked areas between structural domains are poorly exposed, and underlying structures must be inferred from deformation in the overlying sediment (no borehole or seismic data exist). Because the eastern margin of the basin is inactive, the eastern tectonic margin of the Dariv Basin is defined by the Central Ridge and, consequently, the active basin is considerably smaller than the complete area of modern sedimentary deposits.

#### 5.2.2.1 THE NORTH AND SOUTH FOREBERGS

Forebergs are thrust-bound ridges that form within sedimentary basins, adjacent to a through-going strike-slip or thrust fault that uplifts the bounding range (e.g. the Tonhil fault). They are observed within transpressional tectonic settings and are reported in the Gobi Altai by Bayasgalan *et al.* (1999a). Two forebergs project into the Dariv Basin from the west (Fig. 5.2). The North Foreberg is the more structurally complex and contains better exposures of its internal geology (Fig. 5.4). Its frontal ridge, the East Ridge (Fig. 5.4), trends approximately 20° to the Tonhil fault and is bound on its northeast side by a basinward-directed thrust fault. The thrust itself is unexposed, however its presence is inferred from the uplift of the ridge relative to the basin floor, the asymmetric topography of the ridge and the westerly tilt of strata adjacent to the front. Exposed strata young to the southwest, with Jurassic sediments of the Ihkes Nuur Formation seen only in the North Canyon Section (Fig. 5.4). The East Ridge is offset by 4 northeast-orientated (065°) sinistral strike-slip faults. These faults are identified by

---

**Figure 5.4** (following page) – Aerial photograph of the North Foreberg overlain by geological map showing the distribution of major stratigraphic units and structures referred to in the text. Note how strata exposed adjacent to the northeast-directed frontal thrust become younger toward the southeast. Location of Figs. 5.5a, b & c are shown.



stratigraphic offsets. Widespread folding and minor faulting is present to the southwest of the frontal thrust. In the north-western North Foreberg, near to the Tonhil fault, a series of anticlines and synclines are identified in Jurassic strata (Fig. 5.4, 5.5a & b); these folds are upright, plunge southeast at  $06/131^{\circ}$ , and have wavelengths on the order of 200 m. Similar tight folding is seen adjacent to the thrust ridge further southeast (Fig. 5.4 & 5.5c), where anticlines are locally breached by minor basinward-directed thrust faults. Further south, an open syncline is identified in Cenozoic strata (Fig. 5.4 & 5.5d). The syncline is sub-parallel to the frontal thrust and offset by the northeast-southwest trending sinistral faults. At the eastern extent of the foreberg, west of the frontal thrust, a prominent valley named "Eagle Valley" is underlain by an anticline with an axis that plunges  $10/101^{\circ}$ E. The Eagle Valley Anticline tightens eastwards toward the frontal thrust (Fig. 5.4, sections A-A' & B-B'). In the east, the Eagle Valley Anticline axis curves south into parallelism with the East Ridge and is breached by a south-westerly directed, north-easterly dipping, thrust fault (Fig. 5.4, section D-D'). The thrust fault strikes  $150^{\circ}$ , uplifts Oligocene sediments over Miocene deposits and has a limited surface strike-length. Oligocene sediments are not seen west of the East Ridge at any other locality. At the margin of this thrust fault, a second smaller anticline is observed plunging  $58/332^{\circ}$ . At its eastern margin, the East Ridge is offset by an east-trending, dextral strike-slip fault that extends toward the northern end of the Central Ridge in the basin centre (Figs. 5.2 & 5.4). North of the fault, the East Ridge curves eastward while, to the south, an eastward vergent, north-south trending anticline is truncated against the fault. This east vergent anticline lies along strike from a west vergent anticline recorded in the Base 1 section (Fig. 5.2 & 5.6a).



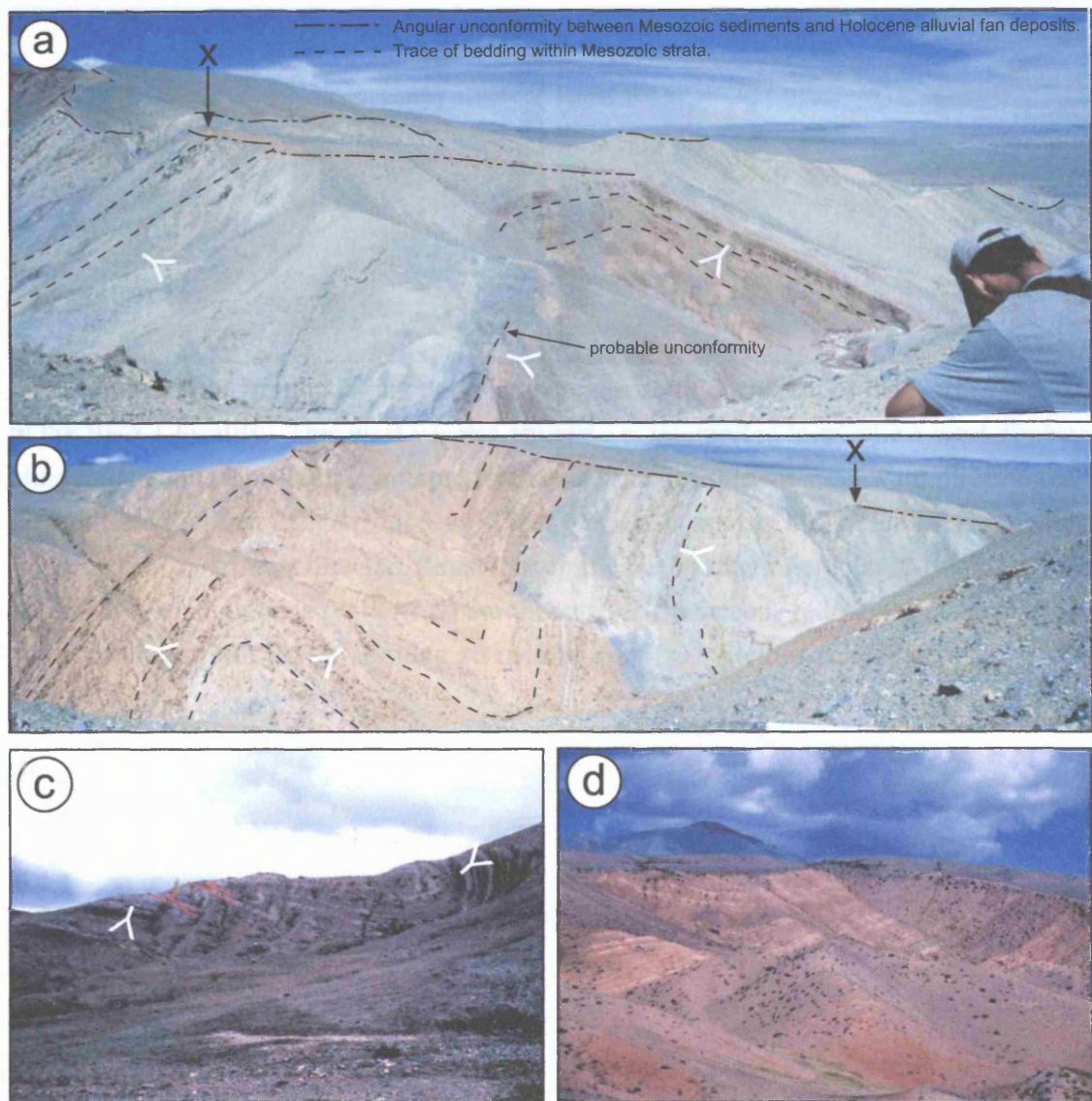


**Figure 5.5a & b** - View north across the North Canyon Section (Fig. 5.4) showing exposed basin stratigraphy in the North Foreberg. X indicates the same location in a and b. In photograph a, the red unit is the Jurassic Ihkes Nuur Formation; the overlying units are the Cretaceous Gurven Ereen Formation (grey) and the Dzereg Formation (red, photograph b). **5.5c** - View south down the East Ridge showing asymmetric east verging folds in the Cretaceous Dzereg (Dzerik) Formation. Some fold hinges are locally broken by east directed thrust faults. The major frontal thrust is unexposed, but lies left of the picture. **5.5d** - View northwest up the East Ridge showing the major syncline to the west of the frontal thrust.



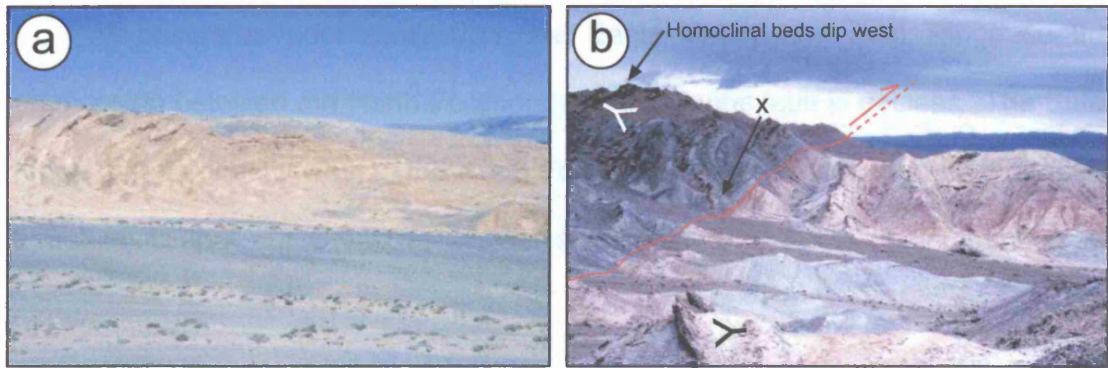


**Figure 5.6a** - Photograph looking north showing the southern extent of the North Foreberg in the Base 1 locality. This west vergent anticline is interpreted to overlie a west directed blind thrust fault. This fault is interpreted to be a back thrust to the basinward directed fault that uplifted the East Ridge (Fig. 5.4). Field of view is approx 800m. **5.6b** - Photograph showing the frontal, east directed, thrust that uplifts the Southern Foreberg. Middle Jurassic Jargalant Formation beds (dark grey) are thrust over Cretaceous red/pale grey beds. Beds curve southeast into the fault along steep fold axes (x). Field of view is approx 1 km.

Exposure is poor away from the Eagle Valley and East Ridge so the relationship between the North Foreberg and the Tonhil fault is unclear. The Sutai range margin directly west of the North Foreberg contains a series of east directed thrust faults that cut Cenozoic alluvial sediments (Fig. 5.3, Cunningham *et al.*, 2003).

The Southern Foreberg is less well exposed and has a less complex internal structure, comprising an elongate ridge trending 40° to the Tonhil fault (Fig. 5.2 & 5.7). The ridge is bound by an east directed thrust fault on its east and north-eastern side. This thrust emplaces lower Jurassic (Jargalant Formation) sediments onto Cretaceous sediments of the Gurven Ereen and Dzereg Formations (Fig. 5.6b). The internal structure of the foreberg contains a homoclinal section dipping 30° west. In the northwest part of the South Foreberg, close to the Tonhil fault, a pair of northeast-directed frontal thrusts that repeat stratigraphic units were identified (Fig. 5.2). In contrast to the Northern Foreberg, the Southern Foreberg is transected by a series of five antecedent drainages that transport sediment into the Dariv Basin centre (Fig. 5.2). Close to the pronounced kink in the ridge, small scale open folds that plunge 30/295 were identified (x on Fig 5.6b). The Foreberg is truncated in the east by a series of northwest-southeast faults that separate the South Foreberg from the adjacent southern saddle area (Fig. 5.7).

#### 5.2.2.2 THE SOUTHERN SADDLE DOMAIN

The geology of this area is poorly exposed, but it links the Southern Foreberg/Tonhil fault with a deforming belt associated with the sinistral Shargyn fault (Fig. 5.2). In the west of the domain, two low ridges of uplifted Mesozoic sediment lie immediately adjacent to the Southern Foreberg. These ridges form

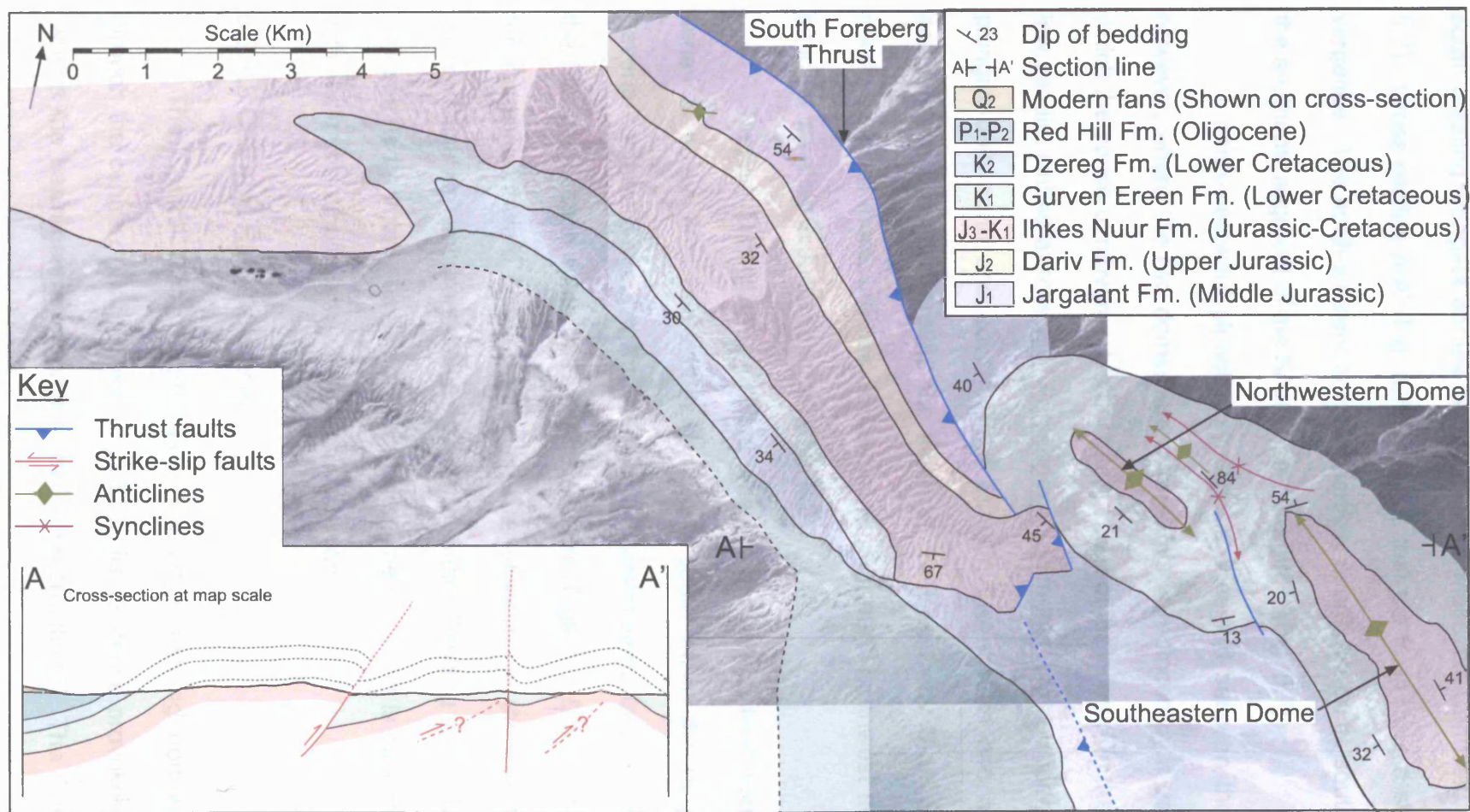


**Figure 5.7** - Aerial photograph of the South Foreberg overlain by geological map showing the distribution of stratigraphic units and geological structures. The foreberg is truncated at its eastern end by a series of north-south trending faults. East of these faults lie two dome structures.

the core of northwest-southeast trending anticlines that plunge both north and south creating elongate domes that deform the Mesozoic-Cenozoic basin fill (Fig. 5.7). Cross-section A-A' (Fig. 5.7) indicates that the folds have a slight eastward vergence. The north-western dome is partially overthrust on its southwest side by the southeast segment of the South Foreberg thrust (Fig. 5.7).

A north-westward plunging syncline is observed between the two domes, however, where the two domes are closest this is replaced by a vertical fault on which the sense of movement is uncertain. East of the domes, in the centre of the low saddle, limited exposure of Palaeogene sediments form an open syncline that plunges both north and south (Fig. 5.2). On the eastern end of the saddle, sediments are uplifted around the flanks of Tsetseg Dariv Uul. Structures are poorly exposed there, but one southwest vergent north-northwest trending domal anticline is visible in Jurassic strata (Fig. 5.2).

Tsetseg Dariv Uul is uplifted where the Shargyn fault separates into a series of splays that curve both north and south within the range (Fig. 5.2). Several southward-directed thrust faults and asymmetric folds were identified in the Shargyn section south of Tsetseg Dariv Uul (Figs. 5.2 & 5.8). To the north of the range, northward directed thrusting was observed in the basement. These faults define an apparent flower structure within Tsetseg Dariv Uul with uplift concentrated primarily on its southern side. The mountain is essentially a pop-up with sediments dipping away from it on each side.

#### 5.2.2.3 CENTRAL RIDGE SECTION

The Central Ridge comprises a low ridge trending northwest-southeast through the centre of Dariv Basin (Fig. 5.2). Its existence provokes the question "why is the basin centre undergoing active deformation?" The Central Ridge is

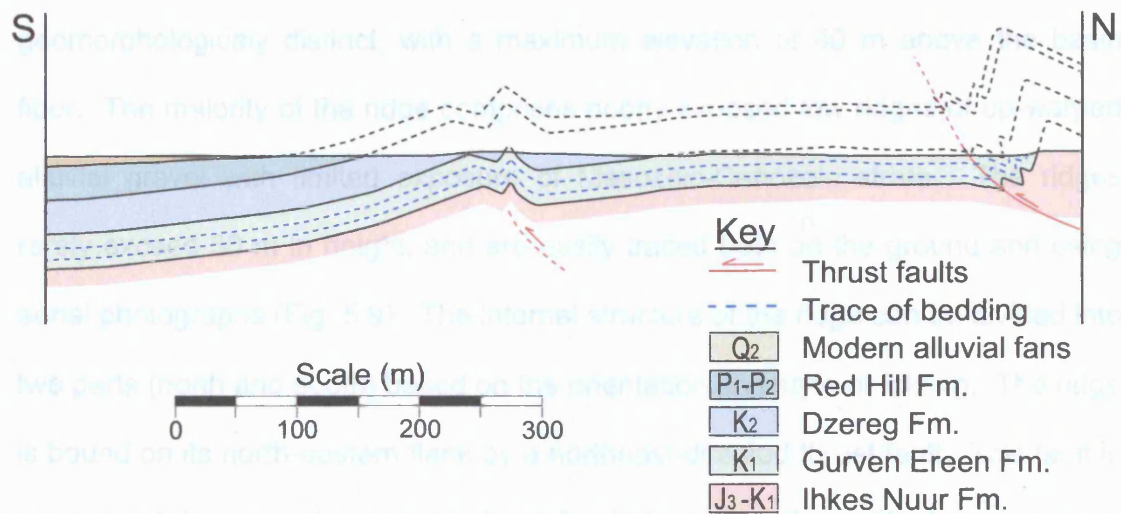


**Figure 5.8** - Cross-section through sediments exposed in the northern Shargyn Basin, adjacent to Tsetseg Dariv Uul. The section line is shown in Fig. 5.2. Note the south directed thrust fault at the north end and the southward vergent fold with possible blind thrust below.



geomorphologically distinct, with a maximum elevation of 40 m above the basin floor. The majority of the ridge comprises poorly exposed low ridges of up-warped alluvial gravel with limited exposure of Mesozoic-Cenozoic strata. The ridges rarely exceed 30 m in height, and are easily traced both on the ground and using aerial photographs (Fig. 5.9). The internal structure of the ridge can be divided into two parts (north and south) based on the orientation and style of folding. The ridge is bound on its north-eastern flank by a northeast-directed thrust fault. This fault is unexposed, however its presence is probable based on the uplifted exposures of deeper basin stratigraphy and asymmetric, east vergent, folds. The presence of springs around Dariv town provides further evidence for a fault rupture at the surface. The thrust fault appears segmented and slightly sinuous in the northern part of the ridge (Fig. 5.9). To the west of the fault, in the northern area, an anticline-syncline pair verges eastward. These folds are oriented sub-parallel to the thrust, plunge gently in opposing directions and have slightly sinuous crest lines. In the southern part of the Central Ridge, the exposed stratigraphic section is homoclinal, dipping and younging to the west. The ridge is offset by three northwest-southeast oriented, dextral strike-slip faults. South of these faults, tight folds deform the section. In one location, two folds form an S-shape in plan view (Fig. 5.10a & b), whereas other folds form tight box structures. This zone of complex folding comprises the highest elevations of the Central Ridge. At the northern margin of the Central Ridge, low gravel ridges trend towards the north and northwest. Those ridges trending northwest align with a series of springs, and beyond, link with the southern end of the North Foreberg (Fig. 5.2 & 5.9). South of the Central Ridge, a splay of low ridges (Fig. 5.9 & 5.10c) curves toward Tsetseg Dariv Uul; these ridges lack exposures of basin stratigraphy.

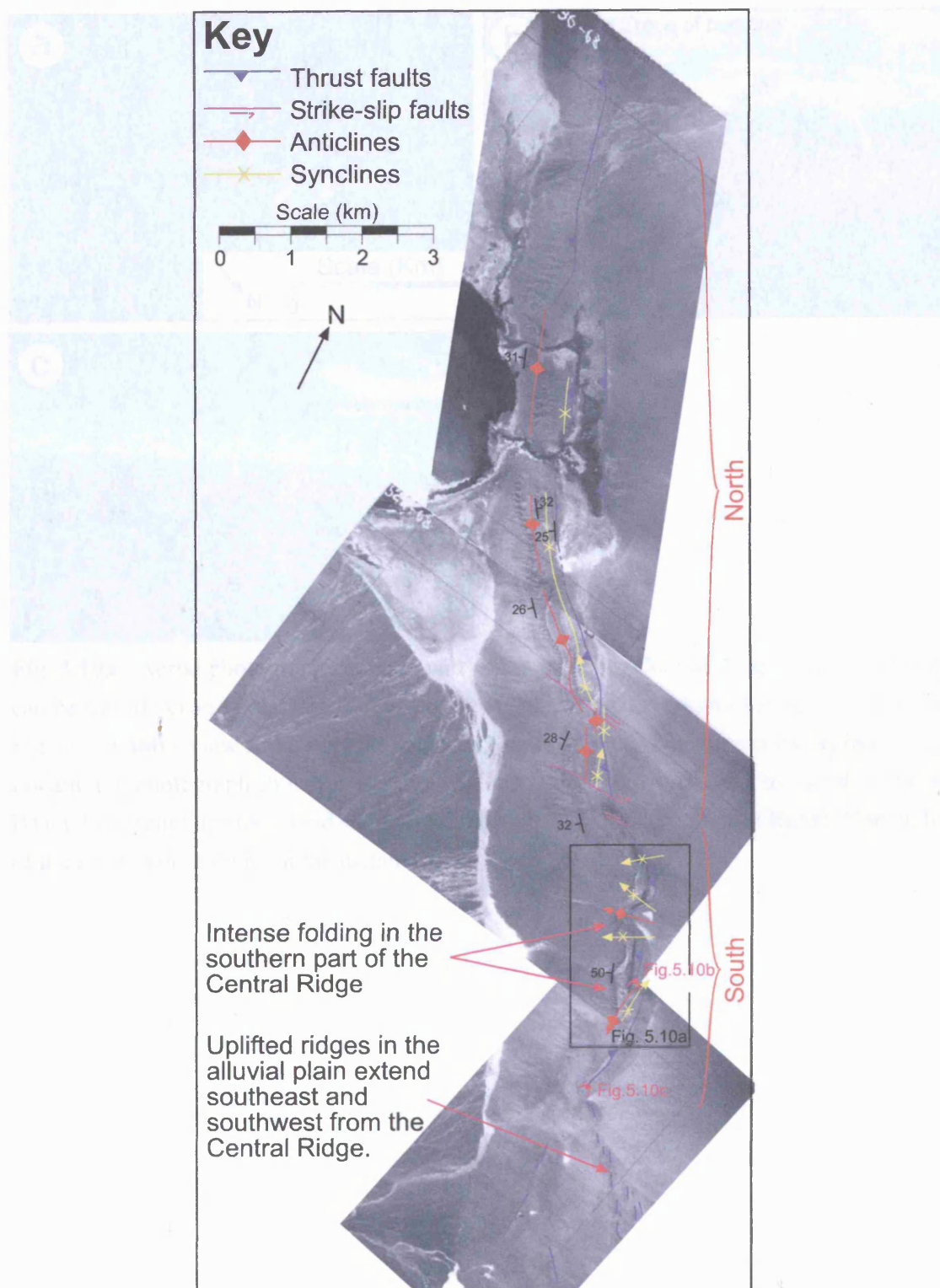


**Figure 5.9** - Aerial photograph mosaic and interpretation of the Central Ridge domain of the Dariv Basin. Thrust faults that uplift the ridge, folds and location of photographs Figs. 5.10a, b & c are shown.

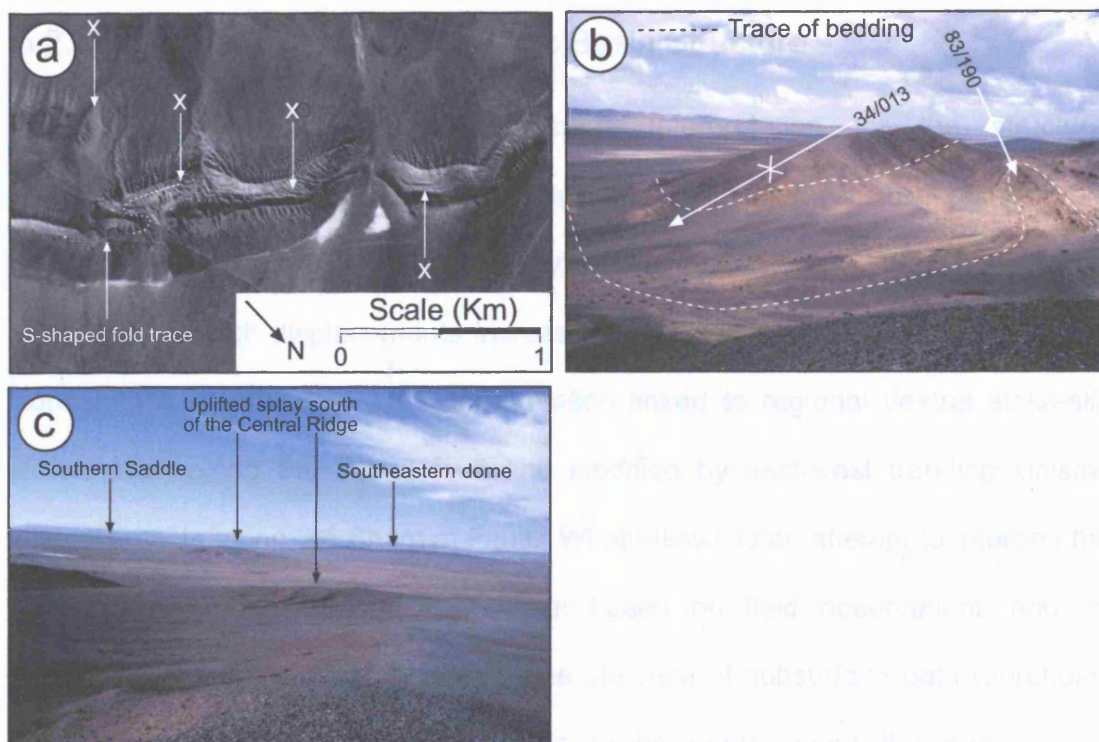


**Fig. 5.10a** - Aerial photograph showing part of the southern Central Ridge. Individual beds can be traced (x) and crest lines act as proxies for bedding. Location of image is shown on Fig. 5.9. **5.10b** - View south over the southern Central Ridge. The ridge contains tight folds. Location of photograph shown in Fig. 5.9. **5.10c** - View southeast across the southern Dariv Basin. Low relief uplifts extend southwest and southeast from the Central Ridge. Note uplift of the southeastern dome in the distance.



### 5.2.3 Interpretation of the Cenozoic Basin Structure

Figure 5.11 shows a three-stage interpretation for the structural development of the Cenozoic Dariv Basin. The four major structural domains are believed to have initially been distinct deformation zones that increasingly interacted as fault displacements increased and folds developed. Together they constitute a rhomboid of active deformation linked to regional dextral strike-slip deformation along the Tonhil fault and modified by east-west trending sinistral displacements along the Shargyn Fault. What follows is an attempt to interpret the Cenozoic evolution of the Dariv Basin based on field observations and an understanding of structural geology. The absence of subsurface data (boreholes or seismic lines) requires assumptions to be made about the geometry of structures and nature of structural linkages at depth. The developmental model also assumes that vertical axis block rotations occur adjacent to strike-slip faults as is reported in other strike-slip settings (e.g. Cobbold & Davy, 1988; England and Molnar, 1990; Bayasgalan *et al.*, 1999b; Thomas *et al.*, 2002). The northeast-directed maximum horizontal stress is assumed to have been constant throughout the mid-late Cenozoic because the driving force is thought to be the continuous north-eastward indentation of India into Asia. The timing of fault and fold development is not well constrained and, while the model fits available data, it represents a non-unique solution for some parts. Another assumption is that existing faults may be reactivated and inverted during a later stage of basin evolution (e.g. Holdsworth *et al.*, 1997).

### 5.2.3.1 STAGE 1 - INITIATION (FIG. 5.11)

#### *The North and South Foreberg*

The two forebergs recognised within the Dariv Basin represent an outward progression of contractional deformation away from the Sutai Uul restraining bend and the transpressional zone associated with the Tonhil fault. Forebergs can vary in both their internal structure and geomorphology (Bayasgalan *et al.*, 1999a), but the two within the Dariv Basin are similar to one another.

The initial growth of both forebergs is interpreted to have been relatively simple. The first surface expression of an incipient foreberg is a low ridge in the alluvial plain recording the influence of a fault propagation anticline over a blind, basinward-directed, thrust fault. The thrust faults eventually broke through the anticline and reached the surface (Fig. 5.11, stage 1). The initial uplift is interpreted to have been at the mountain front (i.e. north-western) end of the present day forebergs because this is where the oldest basin sediments are exposed (in the North Foreberg) and where relief across the ridge is greatest. Progressive along-strike growth to the southeast is associated with younging of the exposed basin strata in the North Foreberg, and decreasing topographic expression of the ridge. In the North Foreberg, a series of sinistral, strike-slip faults offset the ridge and compartmentalised strain. The origin of these structures is unclear. They may have formed at an early stage as primary faults antithetic to the Tonhil fault, or during progressive shortening and clockwise rotation of the North Foreberg at a later stage.

The presence of canyons incising through the frontal ridges in both

---

**Figure 5.11** (following 3 pages) – Three stage evolutionary model for the Cenozoic Dariv Basin. EVA = Eagle Valley Anticline.



## The structural evolution of the Dariv Basin

### Stage 1 - Initiation

- \* Eastward vergent thrusts and thrust tip anticlines form.
- \* Deformation is confined to five distinct areas (labelled).

Outward directed thrusting into the Dariv Basin as the Sutai Uul restraining bend develops along the Tonhil fault and its step over zone.

The North Foreberg initially develops as a basinward vergent thrust ridge propagating south under a thrust tip anticline. The southwest oriented sinistral strike-slip faults are antithetic to the main Tonhil fault.

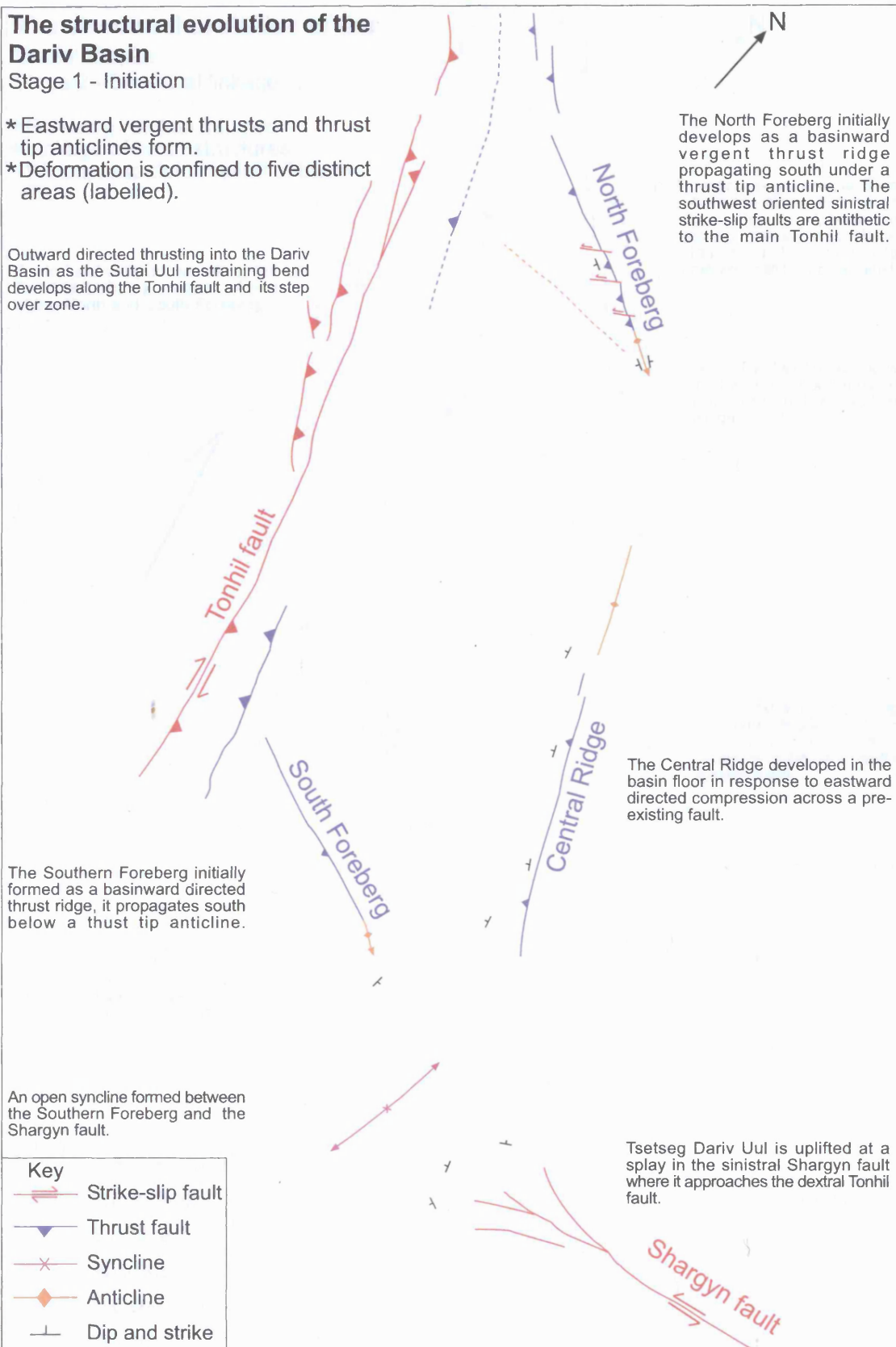
The Southern Foreberg initially formed as a basinward directed thrust ridge, it propagates south below a thrust tip anticline.

The Central Ridge developed in the basin floor in response to eastward directed compression across a pre-existing fault.

An open syncline formed between the Southern Foreberg and the Shargyn fault.

Tsetseg Dariv Uul is uplifted at a splay in the sinistral Shargyn fault where it approaches the dextral Tonhil fault.

Key	
	Strike-slip fault
	Thrust fault
	Syncline
	Anticline
	Dip and strike



## The structural evolution of the Dariv Basin

### Stage 2 - Structural linkage

- \* Foreberg rotation initiated.
- \* Linkage of basin structures.
- \* Widespread deformation of basin fill.

Dextral strike-slip motion along the Tonhil fault initiates clockwise rotation of the North and South Forebergs.

An anticline-syncline pair form behind the North Forebergs frontal thrust. Continued foreberg rotation causes these folds to rotate towards parallelism with the frontal thrust.

Dextral strike-slip faulting is interpreted to link the North Foreberg to the Central Ridge.

Minor dextral motion along the Central Ridge may have produced the gentle curvature of the thrust fault's surface trace.

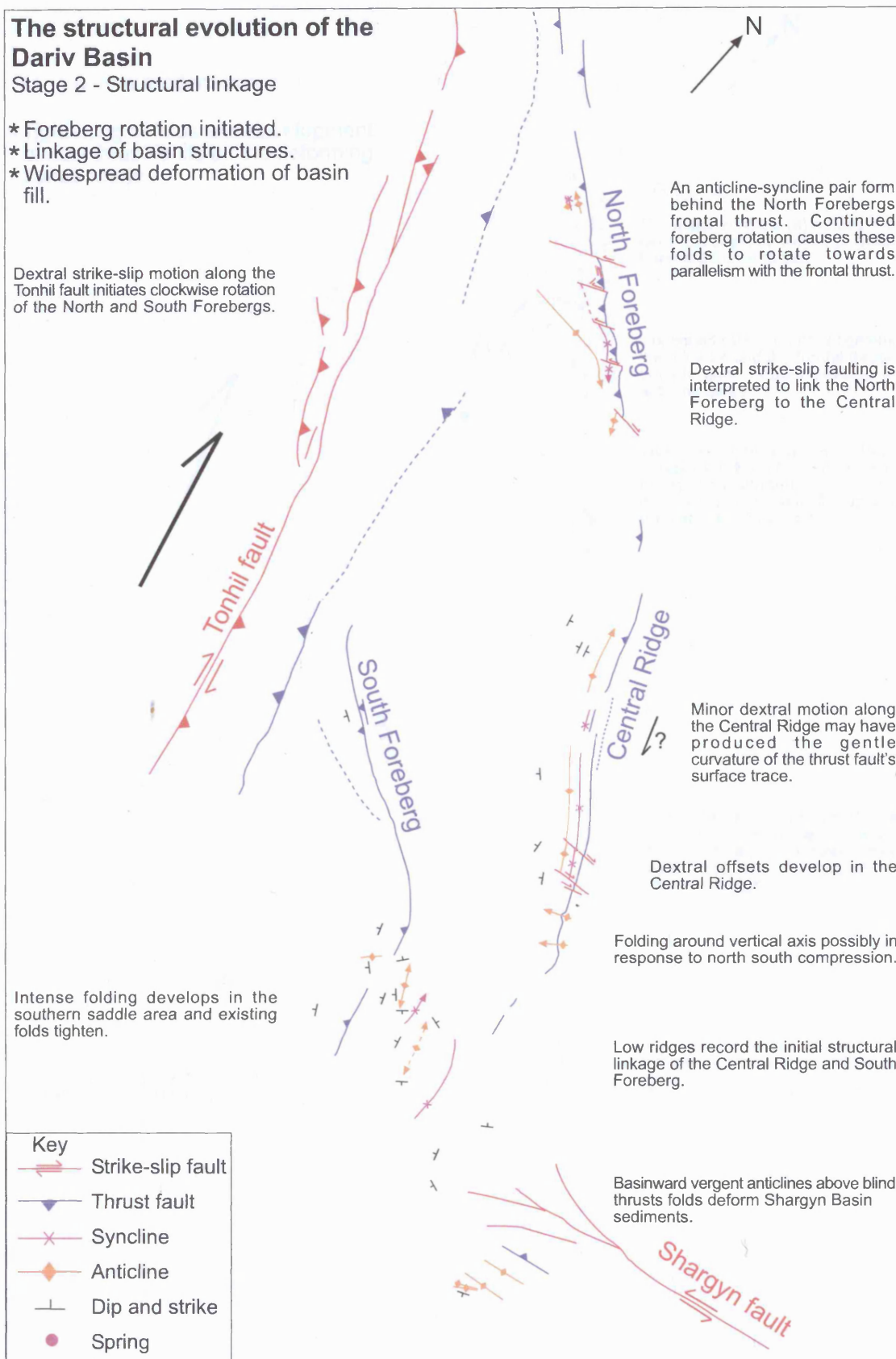
Dextral offsets develop in the Central Ridge.

Folding around vertical axis possibly in response to north south compression.

Low ridges record the initial structural linkage of the Central Ridge and South Foreberg.

Basinward vergent anticlines above blind thrusts folds deform Shargyn Basin sediments.

Key	
	Strike-slip fault
	Thrust fault
	Syncline
	Anticline
	Dip and strike
	Spring

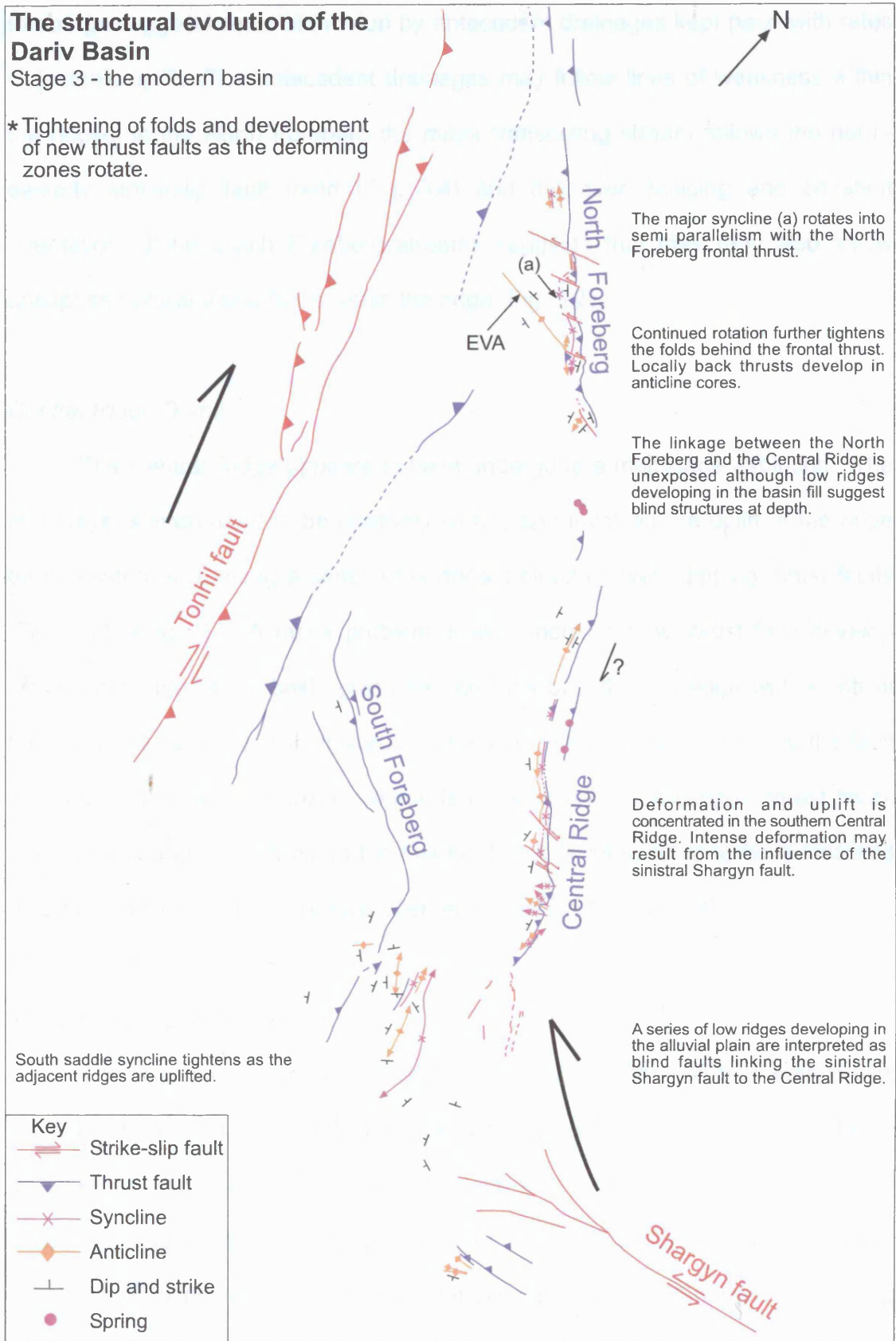


PAGE  
CONTAINS  
PEN/PENCIL  
MARKS

## The structural evolution of the Dariv Basin

Stage 3 - the modern basin

\* Tightening of folds and development of new thrust faults as the deforming zones rotate.



because this is present-day,  
you could add dip valves  
and Adams phase valves

forebergs suggests rates of incision by antecedent drainages kept pace with rates of tectonic uplift. The antecedent drainages may follow lines of weakness within the ridges; in the North Foreberg the major transecting stream follows the north-easterly strike-slip fault trend (Fig. 5.4) and the even spacing and constant orientation of the South Foreberg streams suggests that they may also follow unexposed crosscutting faults within the ridge (Fig. 5.2).

### *Central Ridge Domain*

The Central Ridge appears to have undergone a multistage evolution. The first stage is interpreted to be relatively simple and involved the uplift of the ridge on its eastern side along a series of northeast directed, west dipping thrust faults (Fig. 5.11, stage 1). A major problem is why should a new thrust fault develop within the centre of the basin given the absence of a thrust wedge with a critical taper to the west within Tonhil Nuruu? The most likely explanation is that the fault is a reactivated older Mesozoic normal fault (or possibly a Mesozoic thrust fault). This initial phase of uplift along the Central Ridge is interpreted to be a localised response to the regional northeast-directed maximum horizontal stress.

### *The Southern Saddle Domain*

The area between the Southern Foreberg and the Shargyn fault system was probably inactive during the initial stages of basin deformation. This interpretation is based on the low relief of tectonic ridges in this area compared with other domains, suggesting that they are younger features or the product of smaller contractional displacements. The rate of movement along the Shargyn fault during this period is impossible to quantify. The spatial relationship and linkage between the sinistral Shargyn fault and the dextral Tonhil fault increases the structural



complexity of the evolving Dariv Basin. The conjugate geometrical relationship between these faults was recognised by Tapponnier & Molnar (1979) and Schlupp (1996), but no discussion of their interaction was attempted. Initial deformation along the Shargyn fault is limited to the uplift and tilting of proximal sedimentary rocks away from the evolving Tsetseg Dariv Uul. This limited tilting produced an open syncline between the evolving Southern Foreberg and Tsetseg Dariv Uul, at the southern margin of the basin.

#### 5.2.3.2 STAGE 2 - STRUCTURAL LINKAGE (FIG 5.11)

During stage 2 of Cenozoic Dariv Basin evolution (Fig. 5.11b), the evolving structural domains link forming a rhomboid of active deformation (Fig. 5.12). Dextral motion along the Tonhil fault and the evolving restraining bend at Sutai Uul is coupled to deformation within the Dariv Basin. The simple rhomboid model is complicated by the influence of the Shargyn sinistral fault in the south of the basin.

##### *The North and South Forebergs*

Block rotation of the forebergs relative to the Tonhil fault is interpreted as a response to differential rates of thrusting along the strike-length of the frontal thrust. Thrust initiation occurred along the northwest fault segment proximal to the Tonhil fault with which it is partially linked. This resulted in more rapid thrust propagation there and, consequently, clockwise rotation of the ridge. Such block rotations are expected in transpressional settings wherever a thrust fault with a gradient of displacement away from a linked strike-slip fault exists (Bayasgalan *et al.*, 1999b). Figure 5.13 shows a simple triangular model representing the North Foreberg. The model indicates shortening in the north and southeast where folds parallel to the frontal thrust are documented. It also explains the geometry of the Eagle Valley Anticline, which records the interplay between contractional folding

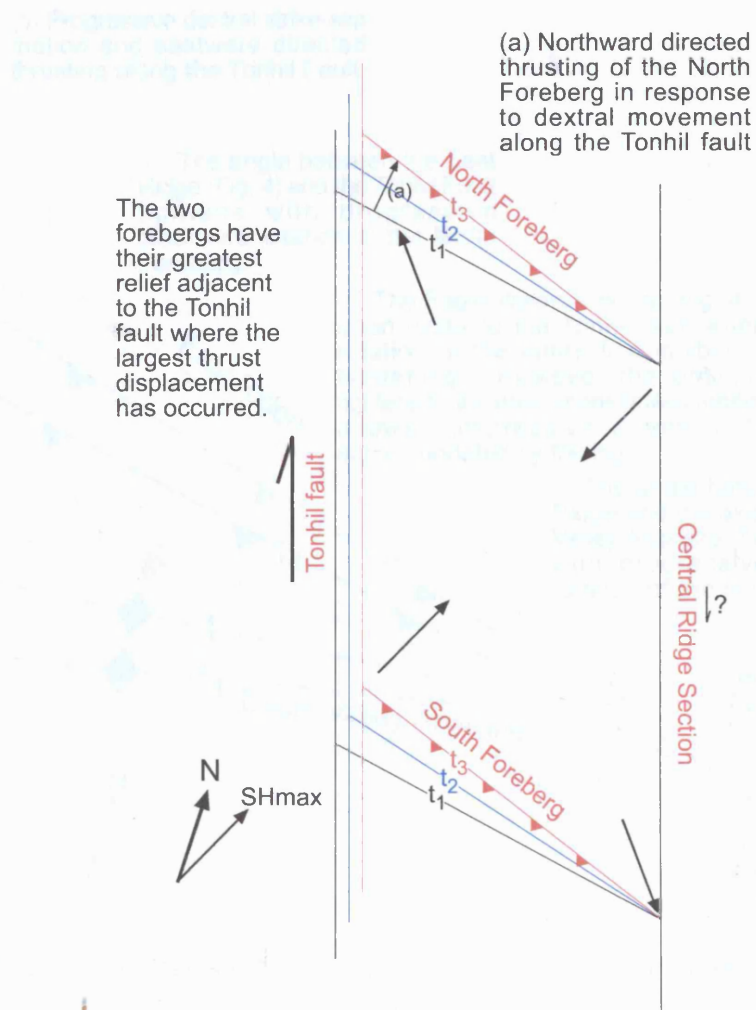


**Figure 5.12** - Conjugate fault model driven by northeast SHmax. Progressive rotation drives contraction in triangular zones (forebergs). This model predicts some of the features observed, however the real basin is complicated by the influence of the sinistral Shargyn Fault in the southeast.  $t_1$ -3 indicate progressive stages of deformation.

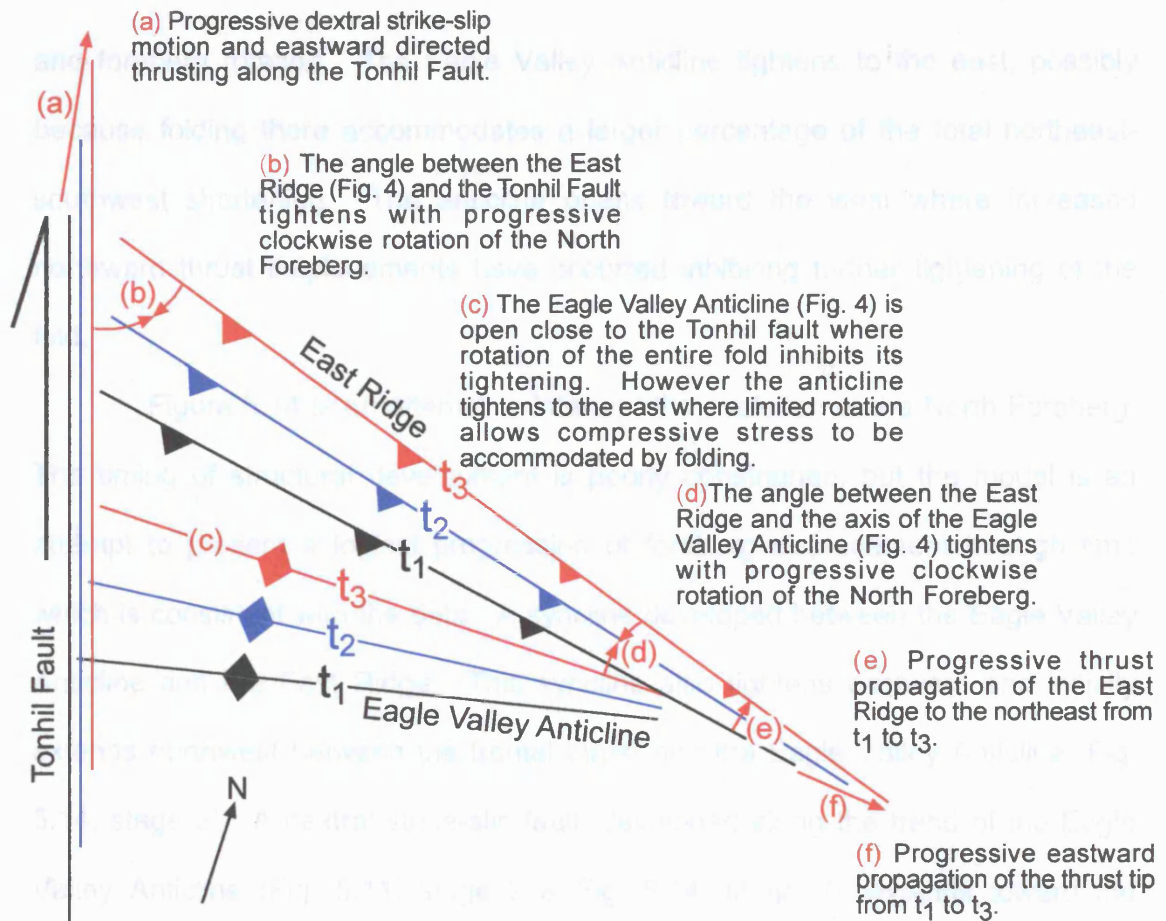
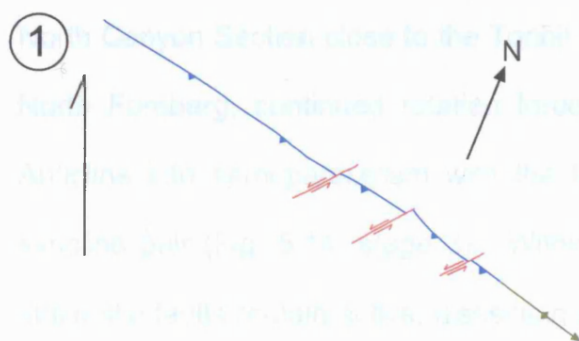


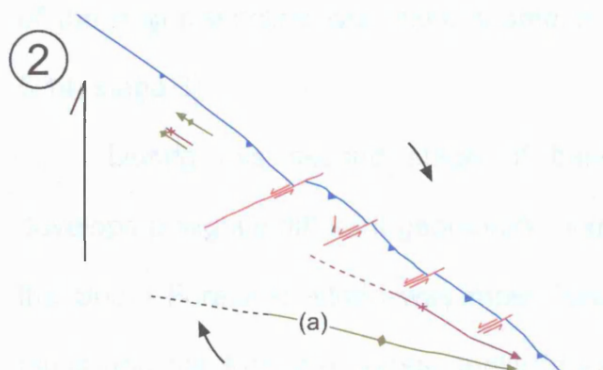
**Figure 5.13** - Figure shows three stage, progressive evolution of the North Foreberg taking into account north-east directed shortening and clockwise rotation adjacent to the Tonhil dextral strike-slip fault. Note the effect that clockwise rotation has on the angles (b) and (d) between the areas of uplift.  $t_1$ -3 indicate increasingly advanced stages of deformation.

and foreberg rotation. The Eagle Valley Anticline tightens to the east, possibly because folding there accommodates a larger percentage of the total northeast-southwest shortening. The anticline opens toward the west where increased northward thrust displacements have occurred inhibiting further tightening of the fold.

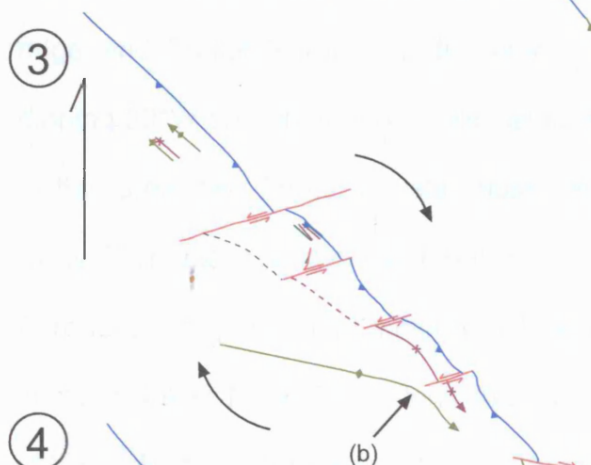
Figure 5.14 is an attempt to interpret the evolution of the North Foreberg. The timing of structural development is poorly constrained, but the model is an attempt to present a logical progression of foreberg displacement through time which is consistent with the data. A syncline developed between the Eagle Valley Anticline and the East Ridge. This syncline also tightens eastward and initially extends northwest between the frontal thrust and the Eagle Valley Anticline (Fig. 5.14, stage 2). A dextral strike-slip fault, developed along the trend of the Eagle Valley Anticline (Fig. 5.11, stage 2 & Fig. 5.14, stage 3), extends toward the Central Ridge, and offsets the East Ridge. It is likely that the eastern tip of the North Foreberg and the northwest tip of the Central Ridge migrated towards each other until faults linked at depth allowing further contractional displacements in the southern part of the North Foreberg to be accommodated instead by displacements in the northern part of the Central Ridge. This linkage prevented further southeasterly growth of the North Foreberg and left the anticlines south of the dextral fault inactive (Fig. 5.14, stage 4). The eastward vergent anticline observed at the south-eastern margin of the North Foreberg (Fig. 5.4) is interpreted to overlie the east directed thrust fault that uplifted the North Foreberg. The westerly vergence of the Base 1 anticline (Fig. 5.6b) is unexplained; it may overlie an unexposed back thrust behind the east directed frontal thrust fault. The structural linkage of the Central Ridge and North Foreberg is coincident with ongoing clockwise rotation and tightening of thrust parallel folds in the area of the



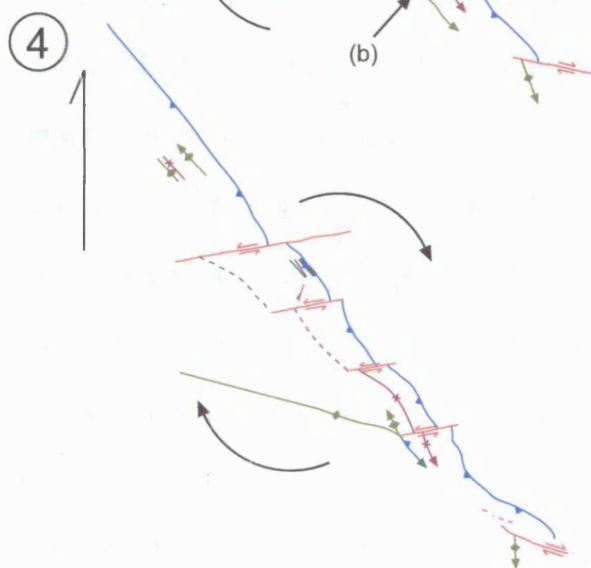
Stage 1. Basinward directed thrust faulting initiates uplift of the North Foreberg which grows southeastwards under a thrust tip anticline. The origin of the left-lateral strike-slip faults is unclear. They may be primary structures antithetic to the Tonhil fault, or they could have formed later in response to clockwise rotation of the North Foreberg.



Stage 2. Uplift and along-strike growth of the ridge southeastwards continues as dextral motion along the Tonhil fault leads to anticlockwise rotation of the North Foreberg. The Eagle Valley Anticline (a) begins to form and a syncline forms between it and the frontal thrust.



Stage 3. The developing North Foreberg is linked to the Central Ridge by a dextral strike-slip fault that cuts the thrust tip anticline. Clockwise rotation of the North Foreberg continues and intense folding develops behind the frontal thrust. In the south, deformation is focused where the major fold hinges merge and curve.



Stage 4. Offset across the southeasternmost dextral fault increases. The rotation of the Eagle Valley Anticline leads to localised thrusting and exposure of deeper sediments. Tilted Quaternary terraces suggest that the Eagle Valley Anticline remains active at the present day.

**Figure 5.14** - A four stage interpretation for the evolution of the North Foreberg based on the actual geometry of structures seen in the field and the implications of the models shown in Figs. 5.12 & 5.13.



North Canyon Section close to the Tonhil Fault (Figs. 5.2 & 5.4). In the east of the North Foreberg, continued rotation forces the eastern end of the Eagle Valley Anticline into semi-parallelism with the frontal thrust and tightens the anticline-syncline pair (Fig. 5.14, stage 3). Within the North Foreberg, antithetic sinistral strike-slip faults remain active, dissecting and accommodating vertical axis rotation of the major syncline with axial segments sub-parallel to the frontal thrust (Fig. 5.14, stage 3).

During this second stage of basin evolution, the Southern Foreberg develops a slightly different geomorphic expression to the North Foreberg. Within the South Foreberg, strain was most likely accommodated on the frontal thrust faults and the foreberg consequently lacks an uplifted area between the frontal ridge and Tonhil Nuruu. Sedimentary strata within the ridge are homoclinally dipping 30°W and overlapped by alluvial fans derived from Tonhil Nuruu to the west. In this area, two frontal thrusts cause repetition of the Jurassic Ihkes Nuur and Dariv Formations within the foreberg. West of these thrusts, within the South Foreberg ridge, abundant minor thrust faults are associated with an increase in the Jurassic Ihkes Nuur Formations thickness. These structures are interpreted as oblique-slip back thrusts that formed during progressive block rotation. The angle between the Southern Foreberg and Tonhil Nuruu becomes more acute to the east, away from Tonhil Nuruu (Fig. 5.2). A flexure in the foreberg ridge (point A, Fig. 5.2) is interpreted to be the combined result of dextral shearing of the western basin margin and the influence of the Shargyn fault that causes local east-west compression at its western tip. The south-eastern end of the Southern Foreberg is truncated by a series of northwest-southeast trending thrust and oblique-slip faults that form the boundary with the adjacent southern saddle domain (Fig. 5.7). These

north-eastward-directed thrusts are interpreted to accommodate stresses derived from east-west compression between the Tonhil and Shargyn fault systems.

#### *Southern Saddle Domain*

The Northern and Southern domes deform Mesozoic strata adjacent to the Southern Foreberg (Fig. 5.7) and may be fault propagation anticlines above a segmented blind thrust fault. Togtoh *et al.* (1991) connected the northwest-southeast trending faults with thrust faults southeast of Tsetseg Dariv Uul, however field evidence for this linkage was not found and this interpretation is considered unlikely. The strain accommodated across the flower structure interpreted to underlie Tsetseg Dariv Uul, combined with the thrusts in the west, represent the termination of the Shargyn fault against the Tonhil Fault deforming zone. The broad topographic low that extends between these areas of active deformation contains a poorly exposed syncline (Fig. 5.11b, stage 2). This syncline may have tightened in response to east-west directed shortening between the actively uplifting Tsetseg Dariv Uul and the North and South Domes.

#### *Central Ridge Domain*

Strain is accommodated in the Central Ridge by tightening of folding behind the frontal thrust in the north, and the formation of open, vertical axis folds that produce a sinuous crest line (Fig. 5.11b). This sinuosity may be due to the linkage of a series of initially distinct fault segments to form a through-going fault or, following structural linkage of the North Foreberg and Central Ridge, a component of strike-slip motion away from the developing restraining bend at Sutai Uul may have been accommodated by a pre-existing north-south striking fault within the basin centre.

### 5.2.3.3 STAGE 3 RECENT – FUTURE (FIG. 5.11)

Deformation during the third stage of Dariv Basin evolution is dominated by tightening and rotation of existing structures in response to continued dextral motion along the Tonhil fault and ongoing northeast-southwest directed shortening. Few new structures developed, although previously blind thrust faults have broken the surface.

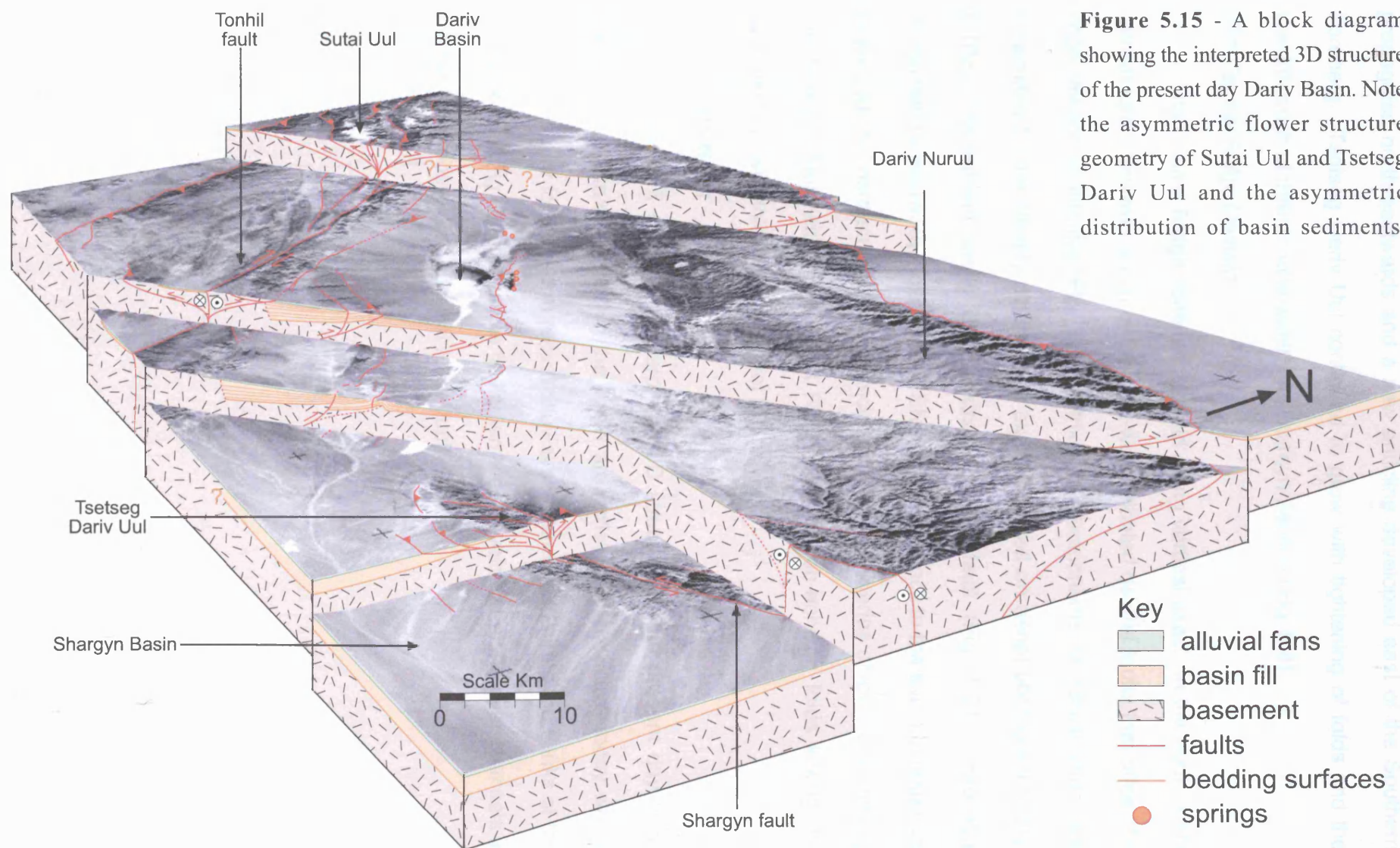
#### *The North and South Forebergs*

Figure 5.14, stage 4, represents the final stages of North Foreberg evolution. Continued clockwise rotation has tightened structures in the northwest that run parallel to the East Ridge. In the east, the Eagle Valley anticline continued to rotate into parallelism with the frontal thrust until it was locally broken by a back-thrust that emplaced Oligocene sediments (Dariv B Formation) over Miocene sediments (Dariv C Formation). Anticlines formed at either end of the thrust fault's surface trace and overlie the fault at depth. To the northwest, the anticline splays off the trend of the Eagle Valley Anticline and extends northwest, parallel to the frontal thrust below the East Ridge. This minor fold is shown in Fig. 5.4, section C-C'. The dextral strike-slip fault at the southeast end of the Eagle Valley continued to offset the original foreberg structure; its dextral sense of motion is interpreted from the geometry of adjacent sedimentary units (Fig. 5.4).

In the Southern Foreberg, strain continued to be accommodated by frontal thrusting and clockwise block rotation. No new structures were developed during this stage of basin growth.

#### *The Southern Saddle domain*

As uplift of the two domes continued, they became increasingly proximal. At their closest point, locally intense folding is associated with a minor vertical fault (Fig. 5.7). Other folds in the area extended northward as the major thrusts



**Figure 5.15** - A block diagram showing the interpreted 3D structure of the present day Dariv Basin. Note the asymmetric flower structure geometry of Sutai Uul and Tsetseg Dariv Uul and the asymmetric distribution of basin sediments.

propagated north-eastwards and a new anticline developed east of the Southern Foreberg. Tsetseg Dariv Uul continued to grow with tightening of folds and the breakthrough of thrust faults within the Shargyn Section (Fig. 5.8).

#### *The Central Ridge Domain*

The Central Ridge continued to fold along vertical axes. In the north, folds remain open, however south of the east-west oriented dextral faults that offset the ridge, folding is intense (Fig. 5.9). Strike-slip components of displacement are suggested by the steeply dipping fold axes observed on aerial photographs (Fig. 5.10a). Movement along the sinistral Shargyn fault (Fig. 5.2) is probably dominated by eastward motion of the Shargyn Basin block to the south in response to the regional northeast directed principle stress. The series of low ridges linking the Shargyn fault with the Central Ridge may be en-echelon folds linking the Shargyn fault with folds in the Central Ridge.

#### *The Modern Basin*

Figure 5.15 shows the interpreted 3D structure of the present day Dariv Basin. Some structures within the basin are believed to be active today where thrust faults and folds deform recent alluvial sediments e.g. along the flanks of the Tonhil Nuruu (Fig. 5.3). Multiple fluvial terraces developed along river channels in the North Foreberg also suggest recent uplift.



## 5.3 Mesozoic Basin Evolution

A thick, laterally extensive Mesozoic sedimentary succession records the early history of the Dariv Basin. However, Mesozoic structures in the Dariv Basin are overprinted by Cenozoic faulting and folding making interpretation of the Mesozoic basin structure difficult. Two evolutionary models for the Mesozoic Dariv Basin, which fit available structural and stratigraphic field data, are presented. Neither of these models can be proved in the absence of subsurface data (seismic or borehole) because the geometry of structures at depth remains uncertain.

### 5.3.1 Regional Mesozoic tectonics

The tectonic setting of Mesozoic basin development along the northeast flanks of the Altai is poorly constrained. Sjöström *et al.* (2001) base a discussion of Mesozoic basin formation on widely spaced sections from Dariv and Dzereg basins and the northern Valley of Lakes and suggest a flexural foreland basin existed west of a palaeo-Altai. Conversely Howard *et al.* (2003) suggest an extensional (possibly transtensional) setting based on fieldwork in the Dzereg Basin (Chapter 3).

Southwest of the Altai, crustal shortening occurred in the Tien Shan and Bei Shan region during the late Palaeozoic, in response to multiple collision events further to the south (Allen & Vincent, 1997). The Tien Shan was a positive topographic feature throughout the Mesozoic (Zhang *et al.*, 1984; Allen & Vincent, 1997; Vincent & Allen, 2001), and periodic uplifts produced sediment pulses recorded in adjacent basins (Hendrix *et al.*, 1992). Vincent and Allen (2001) report strong evidence for multiple Mesozoic compressional uplifts within the Kelameili

Shan 275 km to the south west of the study area. The existence of a thrust Mesozoic palaeo-Altai with a foreland basin on its eastern margin is suggested by Sjöström *et al.* (2001), however structural evidence for Mesozoic shortening within the proposed range is lacking (Cunningham *et al.*, 1996a). In addition, apatite fission-track data show no evidence for significant Mesozoic uplift and exhumation (D. Seward, pers. comm., 2003). Thus there is limited evidence for Mesozoic mountain building in the Mongolian Altai, however relict topography from Palaeozoic orogenic events may have been present. Sjöström *et al.* (2001) further suggest a west vergent, compressional palaeo-Hangay range to the east of the Dariv Basin during the lower-middle Jurassic, however no evidence for Mesozoic contractional structures in the range is given (Fig. 5.16). Thomas *et al.* (2002) invoke a sharp variation in structural style between the Junggar and Altai domains corresponding to major faults or fault zones to explain variations in block rotations during the Cenozoic. It is possible that structural partitioning along these major structures may have inhibited compressional uplift of the Altai in the Mesozoic.

In contrast, southern and eastern Mongolia and north-eastern China are dominated by a broad belt of late Jurassic and Cretaceous extension/transension (Traynor & Sladen, 1995; Webb *et al.*, 1999; Johnson *et al.*, 2001; Meng, 2003). Upper Jurassic continental deposits are interbedded with basalt in the north-western Gobi Altai (Fig. 5.1; Shuvalov, 1969). Within the Altai, there is some evidence to suggest that Mesozoic extension affected the region. Cunningham *et al.* (1996a) reported structural evidence for a major pre-Cenozoic extensional event within the crystalline core of the high Altai west of the study area. Cenozoic thrust faults with pre-Cenozoic extensional histories were documented at two locations in ranges 130 km north of the study area by Cunningham *et al.* (2003). Evidence for Mesozoic normal faulting within the neighbouring Dzereg Basin has

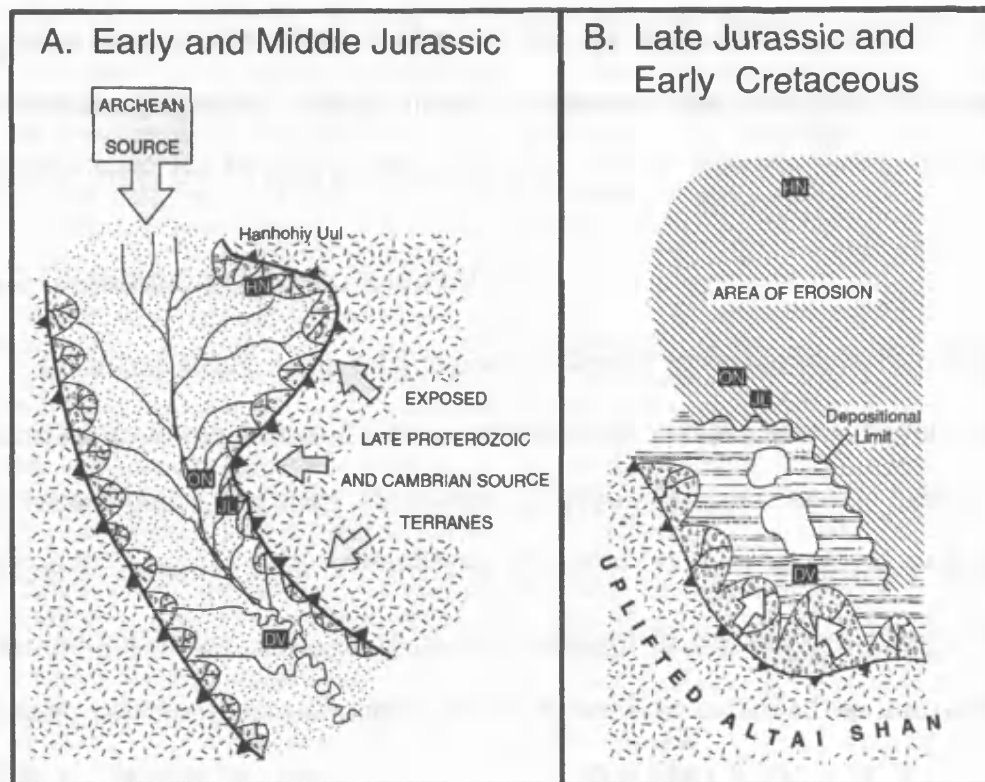


**Figure 5.16** - Model showing contractional foreland setting for the Mesozoic Dariv Basin from Sjöström *et al.* (2001). HN = Hyargas Nuur, ON = Oshin Nuur, JL = Jargalant Locality, DV = Dariv Section

also been documented (Howard *et al.*, 2003). Sjostrom (1997), while favouring a compressional foreland setting, does not discount the possibility of Mesozoic extension within the Dzereg and Dariv basins.

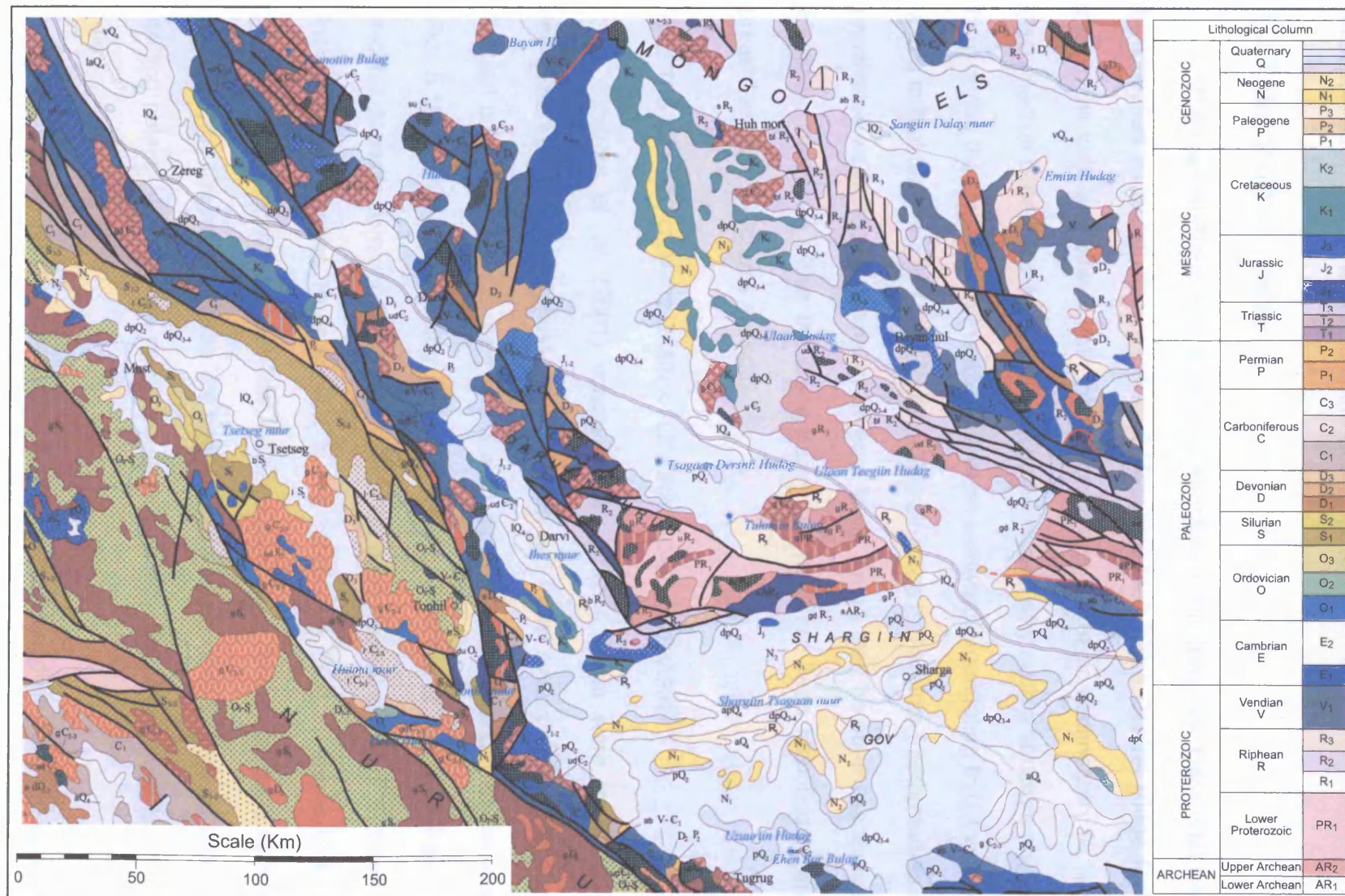
### 5.3.2 Distribution of Mesozoic sediment

Mesozoic strata in the Altai region are limited to an elongate belt along the eastern flanks of the Altai and Gobi Altai coincident with the active modern basins. One recent geological map (Tomurtogoo, 1999) indicates some Jurassic and Cretaceous sediment east of Dariv Nuruu (Fig. 5.17). No Mesozoic sediment is preserved within the interiors of ranges adjacent to the modern basins and, if Mesozoic sediment were deposited in the areas now occupied by the ranges, it should be present in some places today. Complete erosion of any uplifted Mesozoic sediment is unlikely because the amount of uplift and exhumation, based on the presence of a preserved late Cretaceous peneplain, is only 2 km maximum and generally much less. The limited distribution of Mesozoic sediment therefore suggests the existence of distinct Mesozoic depocentres.

Mesozoic strata within the Dariv Basin show marked lateral thickness variations (see chapter 4; Fig. 4.3). The basin fill is highly asymmetric, thinning to the east, e.g. the Dzereg Formation thins by 80% over 10 km between the Sjostrom Section and the Central Ridge Section (south; Fig. 4.3). Jurassic strata have a greater lateral extent than the overlying formations and have more uniform thickness; they are the only sediments exposed within Tsetseg Dariv Uul. Mesozoic strata are not exposed east of the Central Ridge Section (Fig. 5.2),

---

**Figure 5.17** (following page) – Geological map of the southern Altai showing previously mapped sedimentary units and basement rocks particularly the exposures of Jurassic sediment to the east of Dariv Nuruu. Reproduced from Tomurtogoo (1999).





however extrapolation of the thinning sediment wedge to the east suggests that the Mesozoic basin margin lay close to the Central Ridge.

### 5.3.3 Mesozoic structures

The Central Ridge fault is the only structure within the Dariv Basin that can be identified as a probable reactivated Mesozoic fault. The Central Ridge fault dips to the west and offsets both the Mesozoic and Cenozoic sedimentary fill. As discussed on page 12, there appears to be no reason why such a structure should form during the Cenozoic in the absence of an eastward propagating thrust wedge with a critical taper within Tonhil Nuruu. This structure is therefore interpreted as a reactivated west-dipping normal or reverse fault. There may be other reactivated Mesozoic structures within the Dariv Basin that have not been identified or are present as blind structures at depth.

#### WAS THE MESOZOIC DARIV BASIN A FLEXURAL FORELAND BASIN?

Sjostrom *et. al.* (2001) conclude that Jurassic strata were most likely deposited in a flexural foreland basin between two thrust bound ranges, an east directed palaeo-Altai in the west and a west directed palaeo-Hangay to the east (Fig. 5.16). This interpretation is based on the absence of the interstratified volcanic deposits common in rift basins, and the broad lateral extent of sediments (including the Hyargas Nuur section in the north, Fig. 5.1). Limited vitrinite reflection data suggest low heat flow, further supporting a flexural foreland setting. The overlying Cretaceous strata are interpreted as being derived from an actively uplifting palaeo-Altai with the proposed palaeo-Hangay becoming inactive by this time.

Evidence for Mesozoic mountain building in the Mongolian Altai and Hangay is limited. However, there is clear evidence for Mesozoic uplift of the Kelameili

Shan 275 km to the southwest (Fig. 5.1; Vincent & Allen, 2001). If a palaeo-Altai were present, perhaps located within the Chinese Altai, a compressional model may explain the features observed within the Dariv Basin. Complete erosion of Mesozoic strata from the interior of Dariv Nuruu is unlikely, so preserved strata indicate deposition in a narrow asymmetric trough at least 20 km wide. This is narrow for a simple flexural foreland basin (Allen & Allen, 1990). Sjostrom *et al.* (2001) compare the basin to Laramide, or broken foreland types, in which discrete depocentres are separated by basement-cored uplifts. Sjostrom *et al.* (2001) speculate that such basement uplifts existed, although they do not provide any specific examples. Limitations in their regional model result from examination of a single stratigraphic section within each basin and the assumption that unit thickness variations and palaeocurrent trends are regionally constant. Palaeocurrent data and unit thickness variation within the Dariv Basin, recorded during this study, require a local sediment source at the eastern margin of the basin. This source could be a basement cored uplift within a compressional Laramide style setting. These data, and the presence of Mesozoic sediment to the east of Dariv Uul (Fig. 5.17, Tomurtogoo, 1999) suggest at least 2 smaller basins existed in the area between the Altai and Hangay ranges. This contrasts with the single broad basin suggested by Sjostrom (Fig. 5.16). A Laramide style compressional model (Fig. 5.18) implies many Mesozoic faults are reactivated, perhaps explaining the absence of relic Mesozoic faults within the Dariv Basin. Figure 5.18a shows basement-cored ranges uplifted along eastward-directed thrust faults within an incipient foreland basin east of the proposed palaeo-Altai. Jurassic strata are deposited in flexural troughs between these basement cored uplifts and onlap their tilted western flanks. Palaeocurrent data show that the upward fining alluvial conglomerates and sandstones of the Jurassic Jargalant



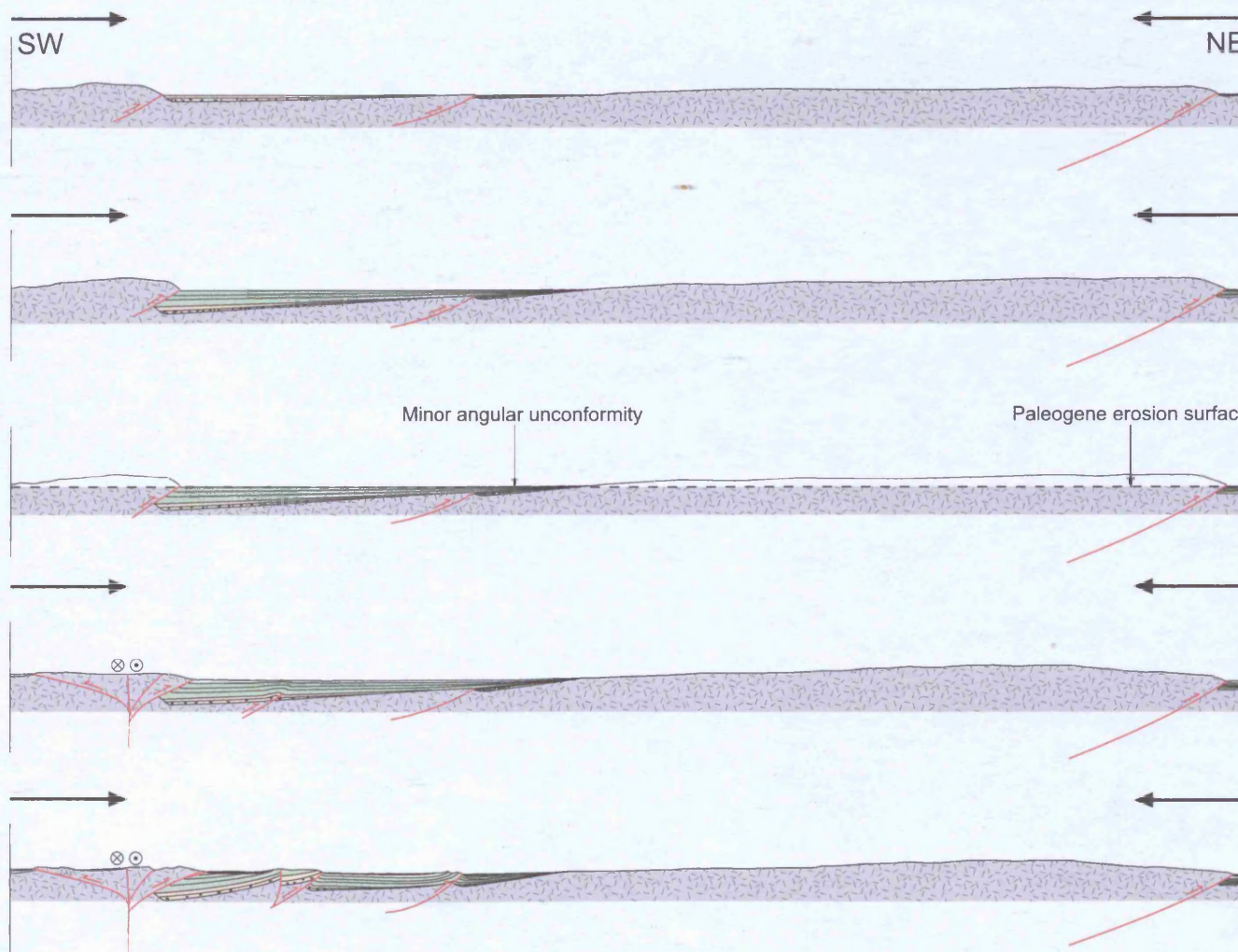
Formation (Fig. 4.3) were derived from adjacent ranges with an increasingly axial trend identified in the Cretaceous Dariv Formation fluvial sandstones. An eastward-directed thrust fault is interpreted within the basin based on comparable Jurassic strata in the southeast and southwest of the Dariv Basin and the great thickness of Jurassic strata in Tsetseg Dariv Uul (despite their absence from the Central Ridge Section). The cobble conglomerate observed in the southeast of the basin (Tsetseg Uul Member) may have ponded against this palaeo-Central Ridge (Fig. 5.18a). Laramide-style basins are commonly bound by opposing basinward-

directed thrust faults, however, examples with an asymmetric geometry comparable to Fig. 5.18 are reported (Dickinson *et al.*, 1988). These examples are all axial basins in the terminology of Dickinson *et al.* (1988) and provide local areas of sediment storage in the upper reaches of an evolving drainage system. Axial basins link with perimeter basins further from the advancing thrust wedge. There is no record of Mesozoic sediment within the Valley of Lakes aside from that shown on Fig. 5.17, but this area may contain buried deposits of Mesozoic perimeter basins, now covered by younger strata. Exposed strata indicate that the Dariv and northwest Shargyn basin were linked during the Jurassic.

Cretaceous strata are observed in all sections, including the Central Ridge, consequently, either the Central Ridge fault became inactive by this time, or the rate of sedimentation exceeded uplift on this fault (Fig. 5.18b). Palaeoflow data

---

**Figure 5.18** (following page) – Cross-sections showing a compressional model for the evolution of the Dariv Basin A) Regional compression uplifts a palaeo-Altai range to the west creating a Laramide style broken foreland basin. B) Compression continues and sediment eroded from uplifted ranges is deposited in adjacent basins. C) Tectonic quiescence and regional peneplanation in the Palaeogene. D) Transpressional uplift of Dariv Nuruu and Sutai Uul along reactivated older faults begins in the Oligocene. Cenozoic sediment is derived from adjacent ranges. E) Ongoing transpression results in intrabasinal deformation by foreberg evolution and uplift of the Central Ridge. This deformation causes uplift and erosion of the basin fill and its redeposition downslope.



a) Jurassic - Onset of compression. Foreland basin contains basement cored uplifts of Laramide type.

b) Cretaceous - Continued compression and sedimentation from adjacent ranges.

c) Paleogene - Regional peneplanation event.

d) Miocene - Renewed Compression leading to uplift of ranges and reactivation of Mesozoic structures.

e) Present day - Ongoing compression uplifts intrabasinal structures.

#### Key

- |                            |                      |                     |
|----------------------------|----------------------|---------------------|
| Holocene fan conglomerates | Cretaceous sediments | Paleozoic sediments |
| Cenozoic sediments         | Jurassic basement    |                     |



from the Ihkes Nuur Formation conglomerate in the west of the basin indicate flow from the south, which Sjöström *et al.* (2001) interpret as being derived from uplifted ranges in the south (Fig. 5.16). The model of Sjöström *et al.* (2001) therefore suggests a coarser, more proximal conglomerate dominated fill in the Shargyn Basin to the south, which is not supported by the data presented here. In the Shargyn Section (Fig. 4.3) palaeocurrents within the Ihkes Nuur Formation trend south and the formation is less coarse than the Shargyn Section overall. An alternative model better supported by these data is that a fluvial system entered the Dariv Basin along its southwest flank, possibly linking two Laramide type basins, via a fault stepover zone or other topographic low.

Largely conglomeratic alluvial and fluvial strata characterise the stratigraphy of axial basins (Dickinson *et al.*, 1988), but such basins lack both the fining upward trend and extensive lacustrine deposits observed in the Cretaceous Dariv Basin. Palaeoflow data from the Cretaceous strata of the Dariv Basin (Gurven Ereen and Dzereg Formations) indicate an internally drained basin. Corresponding southerly or westerly flow within the north-western Shargyn Basin suggests that it was separated, at least periodically, from the Dariv Basin during the Cretaceous. Partially interconnected basins with internally drained saline lakes are a common feature in ponded basins (Dickinson *et al.*, 1988). Ponded basins develop in proximal positions relative to the advancing thrust wedge, and the Dariv Basin may have evolved from an axial to a ponded type over time as the proposed thrust wedge migrated eastward. Fig. 5.18c shows the geometry of sediments during the Palaeogene peneplanation event. While this corresponds with the observed stratigraphy, the lateral thickness variation within the basin remains large for a small flexural basin. The absence of Mesozoic folds, thrust faults and tilted strata beneath the Oligocene unconformity provides the strongest argument against a



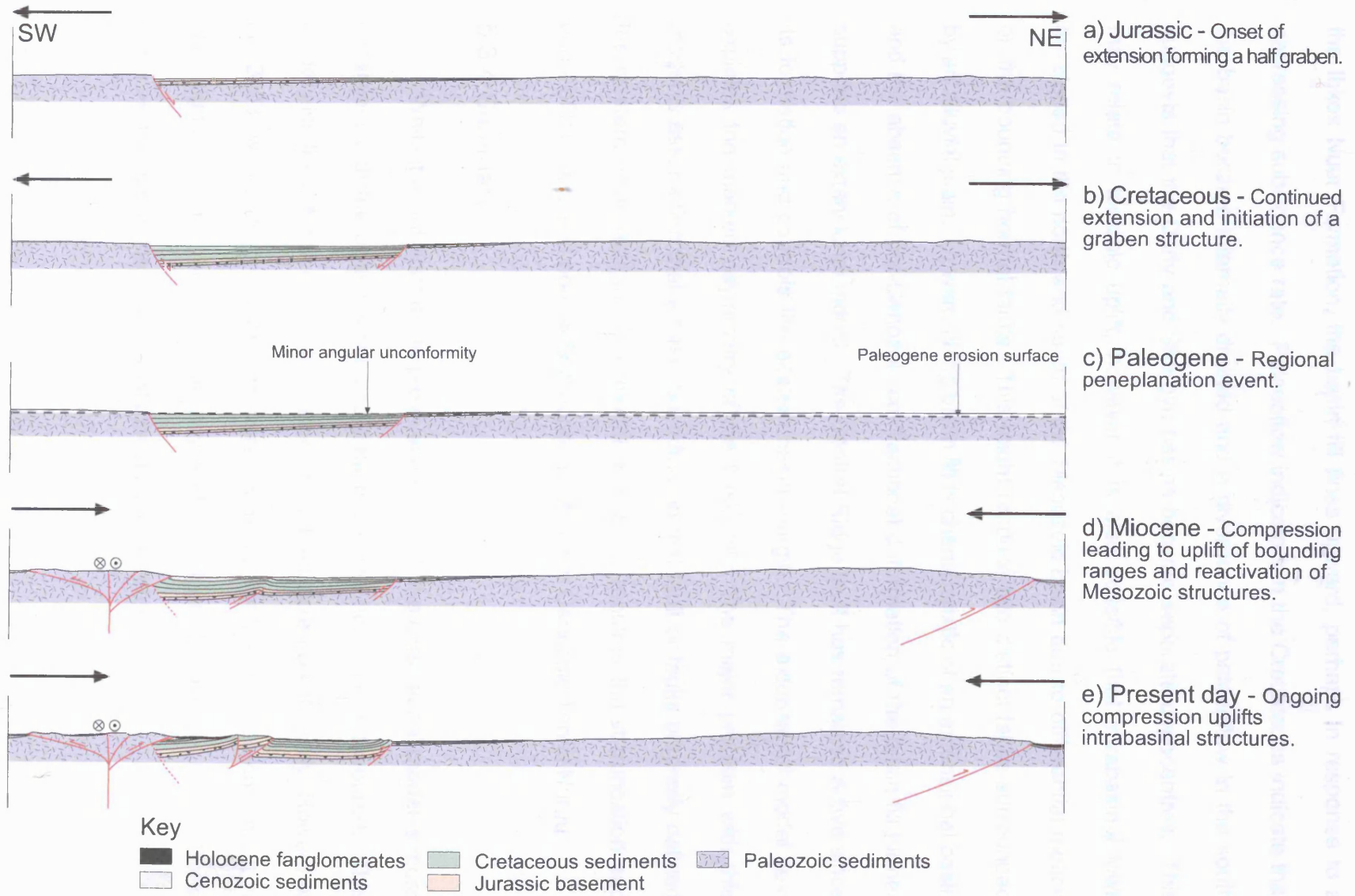
Laramide style contractional basin. Contractional deformation, similar to that seen in the modern Dariv Basin, would be expected in Mesozoic strata deposited within a basin bound by active thrust faults. This is nowhere recorded within the Dariv or Shargyn basins.

#### DOES THE MESOZOIC DARIV BASIN RECORD AN EXTENSIONAL BASIN?

Mesozoic extension resulting in the formation of an elongate northwest-southeast graben provides an alternative model for the Dariv Basin (Fig. 5.19). Initially, a half-graben develops bound on the southwest side by an east dipping normal fault, which itself follows the basement grain (Fig. 5.19b). The bounding fault is not interpreted as a continuous structure, but as a system of normal faults trending northwest toward the Dzereg Basin forming an elongate trough. This half-graben contains an axial fluvial system flowing toward the north adjacent to the main bounding fault in the west. In the east of the basin, sediment derived from the hanging wall flows west down the dip slope to join the axial system. Extension continues during the Cretaceous and a westerly dipping antithetic normal fault forms in the east of the basin (Fig. 5.19b). The Ihkes Nuur Formation is deposited comprising small alluvial fans derived from the hanging wall dip slope in the east and large alluvial fans in the west sourced from the footwall. The largest alluvial fan is seen in the Sandstorm Section and Green Valley Section and flows north, again this may record the influx of a fluvial system through a transfer ramp

---

**Figure 5.19** (following page) – Cross-sections showing an extensional model for the evolution of the Dariv Basin A) Regional crustal tension creates a Jurassic half-graben. B) An antithetic normal fault forms in the Cretaceous confining Cretaceous sediments within the central part of the Dariv Basin. C) Tectonic quiescence and regional peneplanation in the Palaeogene. D) Onset of transpressional uplift of Sutai Uul and Dariv Nuruu in the Oligocene. Many new faults form with only the Central Ridge fault reactivated and inverted as a thrust fault. E) Ongoing transpression results in intrabasinal deformation by foreberg evolution and uplift of the Central Ridge. Deformation causes uplift and erosion of the basin fill and its redeposition downslope.



between two fault segments or another topographic low. Following deposition of the Ihkes Nuur Formation, the basin fill fines upward, perhaps in response to a decreasing subsidence rate. Palaeoflow indicators in the Cretaceous indicate that the basin became internally drained and a divergence of palaeoflow in the south suggests that the Dariv and Shargyn basins became separate depocentres. This may relate to tectonic uplift, however it is also possible that intrabasinal lows developed in the north and south of the Mesozoic basin due to differential motion on the bounding normal faults. This might produce two distinct lakes surrounded by an alluvial plain. Upward-fining basin fill is characteristic of an extensional basin and the absence of pre-Cenozoic contractional deformation of the basin fill further supports an extensional model. The Central Ridge fault has remained active since its formation and controls the eastern basin margin. The extensional model best explains the marked asymmetry of the basin fill. The major problem with this model is assumption that a basin bounding normal fault or faults originally defined the western basin margin. The model (Fig. 5.19) requires thrust truncation and burial of this assumed normal fault during uplift of the Cenozoic Tonhil Nuruu.

#### 5.3.4 Summary

While it is not possible to prove either model, the extensional model is more consistent with the observations and data presented here and is favoured. This model also fits with the conclusions drawn from the Dzereg Basin study (Howard *et al.*, 2003) where there is more structural evidence for Mesozoic extension. It is also significant that the predominantly sedimentological evidence in the Dariv Basin best supports the extensional model interpretation.

## 5.4 Synthesis of Cenozoic basin evolution incorporating sedimentary and structural data.

Following a regional peneplanation event in the Palaeogene, the Altai was reactivated and uplifted in response to northeast-southwest compression derived from the Indo-Eurasia collision. The principle difference between the two evolutionary models (Figs. 5.18 & 5.19) is the degree to which inherited Mesozoic structures may have been reactivated. Sutai Uul is the highest peak in the region and lies at a stepover zone between two regionally important strike-slip faults. It is interpreted to be the initial locus of uplift adjacent to the basin. South of Sutai Uul, uplift along the Tonhil fault occurred across a developing westerly vergent flower structure. Dariv Nuruu is uplifted by a north-eastward-directed thrust fault on its north-eastern side (Figs. 5.18d and 5.19d). In the case of a Mesozoic compressional basin (Fig. 5.18d), northeast-southwest directed shortening in the Cenozoic may be accommodated on reactivated Mesozoic thrust faults. However if the Mesozoic Basin was extensional (Fig. 5.19d) the initiation of new faults on the southwest side of the Dariv Basin that offset the original basin bounding normal fault is necessary.

In comparison with the Dzereg Basin, there is a time lag between the onset of basin margin deformation in the Oligocene and widespread deposition of coarse sediment within the Dariv Basin. The minor angular unconformity observed in the east of the Dariv Basin is interpreted to record minor erosion of tilted Mesozoic strata prior to peneplanation. Oligocene fluvial sandstone and gravel beds with siltstone overbank deposits (Red Hill Formation) overlie the unconformity surface. Long-lived stable channels are seen in most sections, these rivers flowed axially southeast through the Dariv Basin and a lateral change from proximal to more

distal deposits is observed. This fluvial system flowed between the Dariv and Shargyn basins based on palaeocurrent data, indicating that the Dariv and Shargyn basins were again linked following peneplanation. This suggests that uplift along the Shargyn fault occurred later in the basin's evolution. This initial pulse of sediment is the equivalent of the Oasis Unit in the Dzereg Basin and the Beger Suite of Devjatkin, (1981). In the Dzereg Basin, the Cenozoic succession coarsens upward as the adjacent ranges develop, however, in the Dariv and Shargyn basins the Red Hill Formation fines upward. The lack of a significant coarse pulse of sediment overlying this unit is unexpected and requires explanation. The North Foreberg Section records the only well exposed section through Cenozoic strata. The Miocene Eagle Valley Formation records a broad alluvial plain periodically flooded by distal sheetfloods and rarely by more persistent lakes. Extensive palaeosol development indicates slow sedimentation and, aside from a few fringing alluvial fans, the basin is interpreted to have been dominated by a sand dominated fluvial system. Sutai Uul is proximal to the North Foreberg locality and was supplying large amounts of coarse sediment into the Dzereg Basin during the Miocene (the Tan and Yellow Conglomerate Units). This prompts the question "Why was the Dariv Basin receiving only limited coarse sediment during the Miocene?" Two major drainages shown in Fig. 5.2 incise the east ridge of the Sutai Massif and link this evolving catchment area to the Dariv Basin. If these drainages formed later in the basin's evolution, perhaps during the upper Miocene, this might explain the lack of coarse sediment in the Dariv Basin during the Miocene. In the east, Dariv Nuruu preserves a major peneplanation surface, and consequently is not considered to be a major post-Palaeogene sediment source to the Dariv Basin. The Eagle Valley Formation coarsens in its upper part as fluvial fans prograded southeast into the northern Dariv Basin,



perhaps related to uplift of Sutai Uul and headward erosion of river systems cutting into the range on its east and southeast side. However, the first major input of conglomeratic sediment does not occur until the Pliocene/lower Pleistocene. From the widespread distribution of the Eagle Valley Formation it is clear that there was little active deformation in the North Foreberg at this time. The Shargyn Section however, received increasingly coarse sediment that is interpreted to record sediment proximal to a new source in the north and northeast of this section based on palaeocurrent data. This source is interpreted to relate to a period of uplift along the Shargyn Fault and the final separation of the Dariv and Shargyn basins.

The Eagle Valley Conglomerate Member records a major alluvial fan prograding southeast from Sutai Uul from a new catchment along the northwest basin margin. The Eagle Valley conglomerate may have been sourced from the same catchment eroding today and, if so, progressive uplift of the Eagle Valley Anticline has led to successive fans being deflected southward as the anticline upwarped preceding fan surfaces producing an offlap structure. As intrabasinal deformation became more intense, uplift of the North and South Forebergs and Central Ridge initiated erosion and redeposition of the basin fill. Uplift of the thrust ridges is associated with incision by antecedent drainages and, where these drainages could not keep up with tectonic uplift, streams were either diverted (as seen in the South Foreberg Ridge) or sediment ponded behind the ridges (e.g. the Dariv (e) Formation). The Dariv (e) Formation is undated, but probably contains the youngest Cenozoic sediments investigated within the Dariv Basin.

## 5.5 The Future

The absence of a thrust bound eastern margin to the Dariv Basin suggests that the Dariv basin's preservation potential is greater than the Dzereg Basin, which is overthrust and closing from opposite sides. Continued eastward directed thrusting from Sutai Uul and continued shortening in both the North and South Forebergs is possible. Even if outward thrusting and uplift occurred along the Tonhil fault and a major range developed south of Sutai Uul, it is likely that uplifted and eroded basin fill would be redeposited locally, onlapping Dariv Nuruu. The Central Ridge zone, which contains no evidence for recent activity, may be able to accommodate further east-west compression. If major uplift were to occur along the Central Ridge, the preservation potential for the Dariv Basin fill would be significantly reduced.

The Dariv Basin is an intracontinental basin positioned between a major restraining bend and at the intersection of a major conjugate fault system. The modern basin is simultaneously receiving sediment whilst undergoing active deformation by block uplift, folding and vertical axis rotations that leads to erosion and redeposition of the basin fill. The basin provides a snapshot of the complex interplay of major regional fault systems, local intrabasinal structures and evolving depositional systems.

## 5.6 The Shargyn Basin

### PREVIOUS WORK

The conjugate strike-slip faults that bound the Shargyn Basin were first recognised on satellite imagery by Tapponnier & Molnar (1979). Schlupp (1996) includes the Shargyn Basin in his study of the structural geology of the Altai region based on satellite image interpretation. Schlupp (1996) includes detailed fault maps of the Shargyn Basin but no specific discussion relating to its evolution.

### DESCRIPTION

The Shargyn Basin is considerably larger than the Dariv Basin (approximately 2970 km<sup>2</sup> and 360 km<sup>2</sup> respectively). Field data for the Shargyn Basin include one detailed stratigraphic and structural section on the flanks of Tsetseg Dariv Uul (described in chapter 4), and structural observations made on the north-eastern basin margin. Cenozoic faults that bound the Shargyn Basin are visible on satellite imagery and, along with documented sediment exposure, are shown on published geological maps.

The Shargyn Basin is located within a discrete crustal block bound by conjugate strike-slip faults and linked thrusts (Fig. 5.20). The sinistral Shargyn fault forms the northern margin of the Shargyn Basin, and bounds the southern flanks of the Dariv range to the northwest. To the northeast the trace of the Shargyn fault is marked by springlines (Fig. 5.20). Uplift of the Dariv range adjacent to the Shargyn Basin indicates that the Shargyn fault has a dip-slip component. However, the straight fault trace and absence of uplift in the east suggest that movement is predominantly strike-slip.

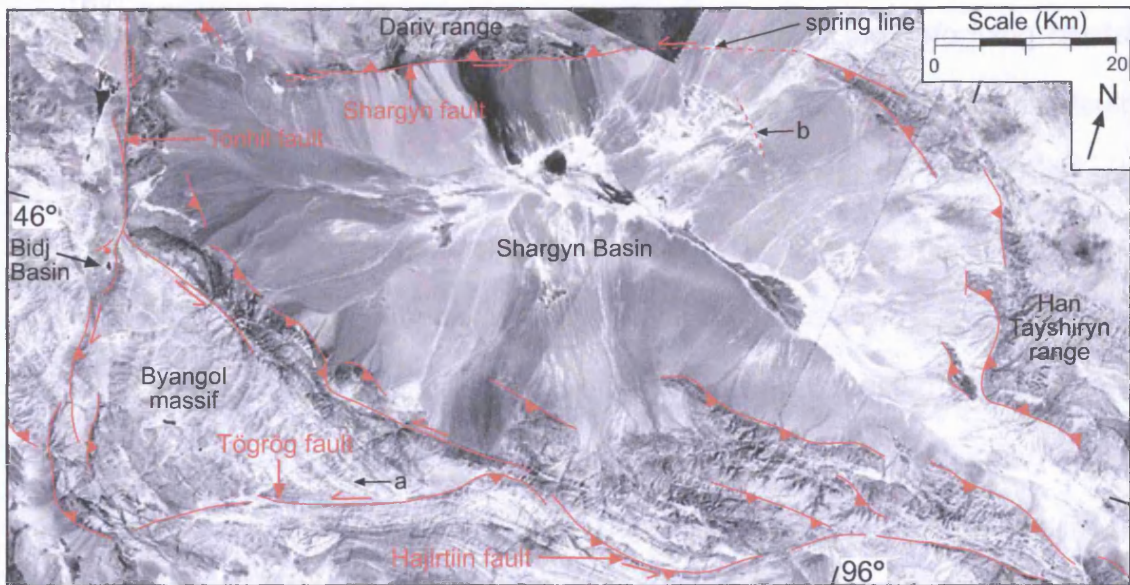


**Figure 5.20** - Interpreted Landsat TM montage of the Shargyn Basin showing major thrust and strike-slip faults bounding the adjacent ranges. a - arcuate and deflected basement structural grain suggests sinistral motion on the Tögrög fault. b - surface lineament picked out by channel nick points, possibly records movement on a blind fault at depth.

The dextral Tonhil fault forms the western margin of the deforming crustal block. The low relief Tonhil range, uplifted by thrusting linked to the Tonhil fault, forms the western basin margin. The sinistral Tögrög and Hajirtiin faults (Schlupp, 1996) form the southern margins of the fault block. The Byangol massif is uplifted where the Tögrög fault intersects the Tonhil fault in the southwest. The Byangol massif is triangular in plan view and bound on its north-eastern and western margins by outward directed thrust faults. Small basins have formed along segments of the Tonhil and Tögrög faults that bound the Bayangol massif, these include the Bidj Basin, a small pull apart (Fig. 5.20; Schlupp, 1996).

A series of en-echelon northeast directed thrust faults, which uplift forebergs occur along the southern margin of the Shargyn Basin (Fig. 5.20). Within the unnamed ranges south of the Shargyn Basin, the arcuate trend of basement structural grain adjacent to the Hajirtiin and Tögrög faults suggests sinistral drag (Fig. 5.20). Faults that control the Shargyn Basin's eastern margin are less clear on the imagery, but a number of basinward-directed thrust faults are visible and an eastward directed, basinward dipping, thrust fault was identified in the field on the north-western flanks of the Han Tayshiryn range.

The basin interior is a broad, low-relief desert plain that receives <50 mm a year of rainfall (Arakawa, 1969; Lehmkuhl, 1998). At present, sediment is derived from adjacent ranges and transported into the basin by ephemeral streams which deposit alluvial fans around the basin margins. The basin is internally drained and there is a broad marshy area in the basin centre (Fig. 5.21a). Away from the marshy area, the basin floor is dominated by active aeolian dunefields (Fig. 5.21b). Exposure of Neogene sediments occurs throughout the basin (Tomurtogoo, 1999), however exposure of the older basin fill is more limited. Mesozoic strata are documented only in the exposure described in chapter 4, on the north-western



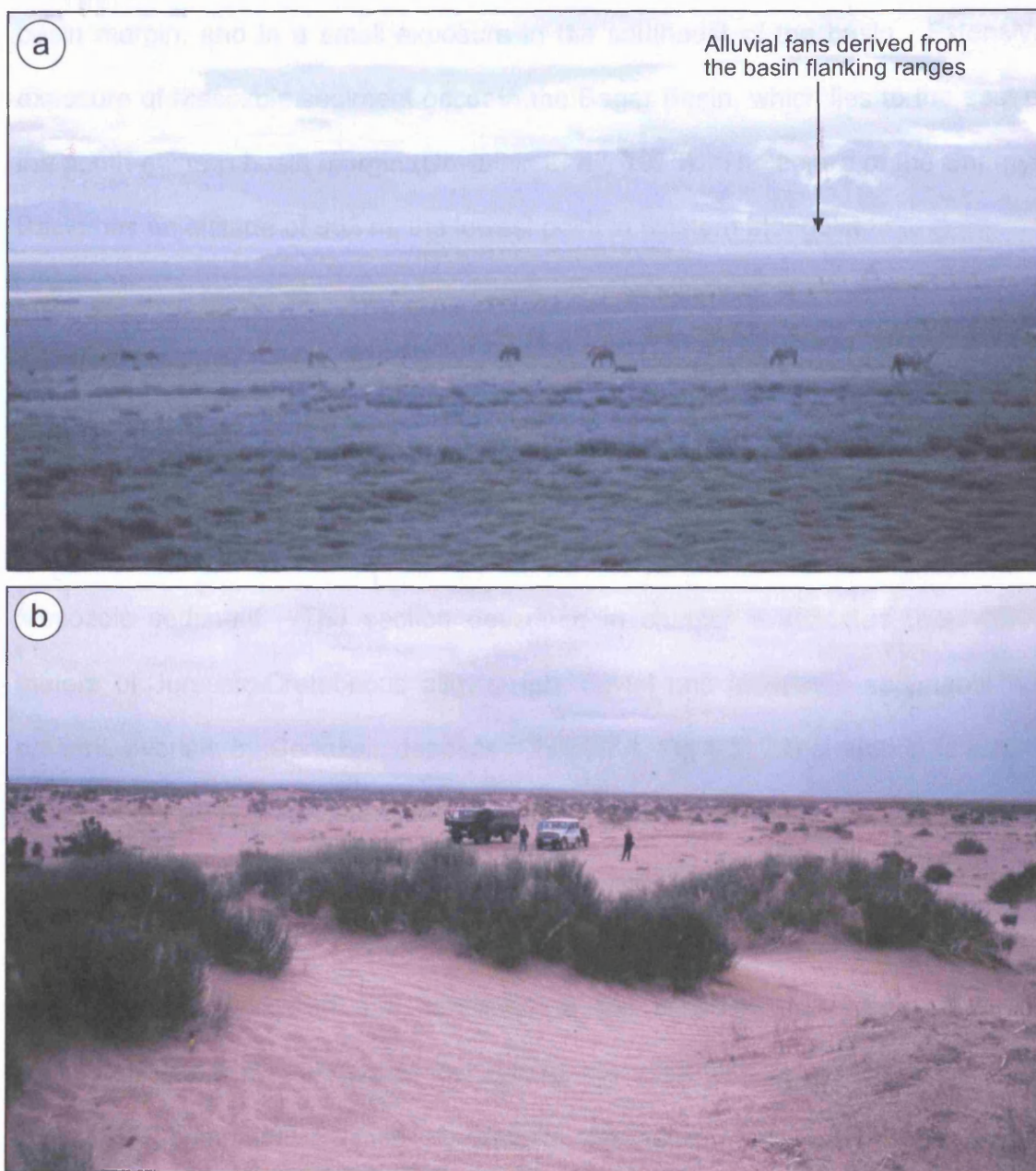


**Figure 5.21a** - View across the Shargyn Basin showing the broad marsh area in the basin centre, and in the background, alluvial fans derived from adjacent ranges. **5.21b** - Active aeolian dune fields within the northwest Shargyn Basin.

basin margin, and in a small exposure in the southeast of the basin. Extensive exposure of Mesozoic sediment occur in the Beger Basin, which lies to the east of the south-eastern basin margin (Devjatkin *et al.*, 1975). The centre of the Shargyn Basin has an altitude of 963 m, the lowest point in western Mongolia.

## 5.6.2 INTERPRETATION

### 5.6.2.1 The Mesozoic Shargyn Basin.

Little is known about the Mesozoic evolution of the Shargyn Basin due to the absence of any known Mesozoic structures and the limited exposure of Mesozoic sediment. The section described in chapter 4 indicates that >1500 meters of Jurassic-Cretaceous alluvial fan, fluvial and lacustrine sediments are present, overlain by Cenozoic deposits (Chapter 4, Fig 4.3). The section reveals a similar stratigraphy to that documented in the Dariv and Dzereg basins. Palaeocurrent data suggest that the Dariv and Shargyn basins were linked periodically during their evolution. When rivers linked the Dariv and Shargyn basins, they flowed from the northwest to the southeast suggesting that the Shargyn Basin was a regional low during the Jurassic-Cretaceous as well as during the Cenozoic. While no definite conclusions may be reached, the similarities between the Shargyn and Dariv Basin fill suggest that the Shargyn Basin may represent the southward continuation of the Mesozoic extensional or transtensional basin system interpreted for the Dariv and Dzereg basins.

### 5.6.2.2 The Cenozoic Shargyn Basin

Cenozoic reactivation of the Shargyn Basin is concentrated around the basin margins. Intrabasinal deformation is limited to small thrust ridges in the southeast of the basin and a distinct lineament, marked by channel nick point



incision, that may record surface uplift relating to a fault at depth (Fig. 5.21). The Cenozoic development of the Shargyn Basin has been controlled by its position within a conjugate fault system which may be generalised as a deforming rhomboid. The rhomboid encompasses both the Shargyn Basin and the Bayangol massif and is bound by the major conjugate strike-slip faults. A simple model whereby the rhomboid is subjected to northeast-southwest compression predicts many of the features observed within the Shargyn Basin (Fig. 5.22). With the assumption that vertical block rotations commonly occur adjacent to strike-slip faults (Cobbold & Davy, 1988; England and Molnar, 1990; Thomas *et al.*, 2002), this model predicts shortening parallel to SHmax stress and possible vertical axis rotations of the strike-slip faults that bound the basin block. Deformation suggested by this simple model generally corresponds with fault patterns observed in and around the Shargyn Basin. Thrust faults observed along the north-eastern basin margin, and those in the southwest that uplift the Bayangol massif, accommodate shortening of the deforming block parallel to SHmax. Strike-slip faults on the basin margins accommodate block rotation and possible northwest-southeast stretching. The low altitude of the basin floor, suggests that the Shargyn Basin may be subsiding. There are at least two ways in which this might be occurring. The simple model of a deforming rhomboid (Fig. 5.22) suggests a component of northwest-southeast extension related to the rotation and stretching of the basin block. This extensional component may be accommodated by normal faults parallel to SHmax. Normal faulting would explain the observed low level of the basin floor however the absence of evidence for internal faults oriented northeast-southwest is a problem, although they could be obscured by modern sediment. In the absence of extensional faulting within the deforming block, subsidence may result from down-warping of the basin floor by crustal flexure in

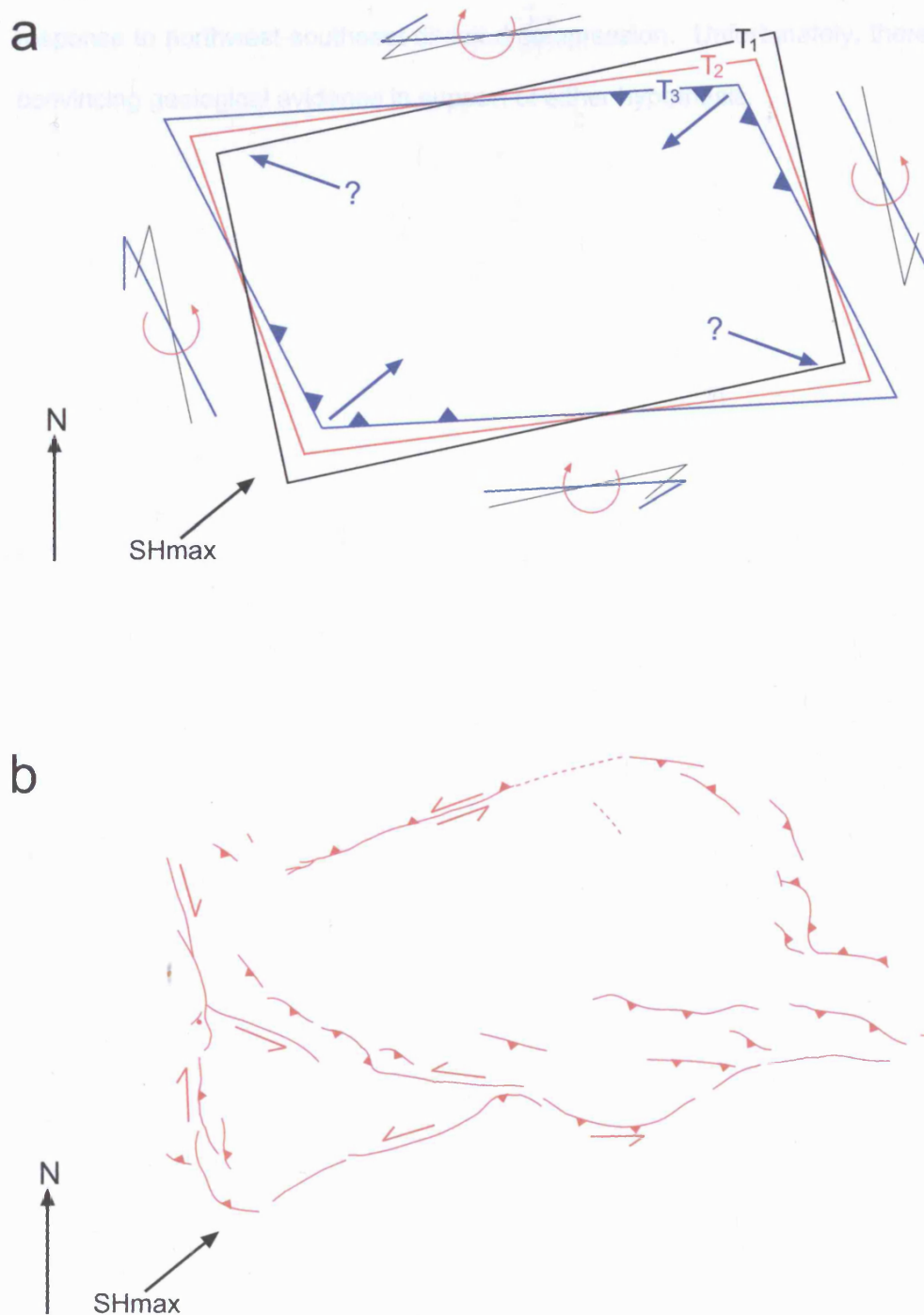


**Figure 5.22a** - Simple model for block rotation in a conjugate strike-slip fault system. Northeast directed shortening results in compressional deformation in the southwest and northeast, vertical axis rotation of strike-slip faults that bound the fault block and possible northwest-southeast orientated extension. **5.22b** - Actual fault geometry of the Shargyn Basin. Note how faults within the Shargyn Basin correspond broadly with the model above. Thrust faults accommodating northeast-southwest shortening dominate the northeast and southwest corners of the basin. There is no clearly defined strike-slip fault on the eastern margin of the Shargyn Basin, and thrust faults dominate the basin's southeast corner. In the northwest, strike-slip faults dominate with minor thrust displacements.

response to northwest-southeast directed compression. Unfortunately, there is no convincing geological evidence in support of either hypothesis.



## Chapter 6

### Conclusions and Wider Implications

#### 6.1 Introduction

This concluding chapter summarises existing literature on transpressional basins, both within Asia and on other continents. Models developed for the Oligocene to present day transpressional evolution of the three western Mongolia basins investigated in this study are then compared with existing models and field studies.

Transpressional basins vary in size and in the distribution, orientation and sense of movement on basin bounding faults. These variations make the development of generalised models for their evolution difficult. Intracontinental transpressional basins are, therefore, compared with other generalised models for a variety of basin types (rift, foreland etc.), in order to establish criteria for the recognition of transpressional basins in the rock record. The variation observed between different transpressional basins requires that a range of attributes, combined with an understanding of the regional tectonic framework, be used to identify an ancient transpressional basin.

#### 6.2 Review of transpressional basin types

Transpressional basins are described in both interplate and intraplate settings. Interplate transpressional basins have been more extensively studied because they tend to be larger, deeper and potentially hydrocarbon bearing, e.g. the San Joaquin, Ventura, Santa Maria and Santa Lucia basins, California

(Namson & Davis, 1988; Nilsen & Sylvester, 1995; Sorlien *et al.*, 1995; Miller & Meltzer, 1995) and the Azua and Enriquillo basins, Hispaniola (Mann *et al.*, 1991).

Intraplate transpressional basins are less commonly documented, perhaps because these basins tend to be smaller and have less obvious economic potential. Existing studies describe a broad spectrum of intraplate transpressional basins that form a continuum from dominantly strike-slip to compressional settings. Transpressional basins are bound by oblique-slip and thrust faults and there is a grey area between basins controlled predominantly by strike-slip faults and foreland basins with minor strike-slip faulting. A transpressional basin should contain strong evidence, e.g. fault plane solutions or reliable kinematic indicators, supporting a significant strike-slip component on the faults controlling basin formation.

One of the most widely quoted models for interplate/intraplate transpressional basin evolution is the restraining bend model of Nilsen and Sylvester (1995; 6.1a). This model describes basin formation due to flexural loading adjacent to a restraining bend uplift in a discrete strike-slip fault zone. An example of a dominantly strike-slip intraplate transpressional basin, which corresponds to this model, is the As Pontes Basin, Spain, which developed adjacent to an evolving restraining bend along the Pedroso-As Pontes-Moiñonovo strike-slip fault system (Cabrera *et al.*, 1996; Fig 6.1b & c). Flexural loading, adjacent to basinward-directed thrust faults along one margin, controls basin subsidence. One intrabasinal normal fault enhances flexural subsidence, but most intrabasinal deformation is compressional, and is especially intense adjacent to the basin bounding thrust faults.

Transpressional basins bound by basinward-directed thrust faults on each basin margin represent another common group. Basins with this geometry have

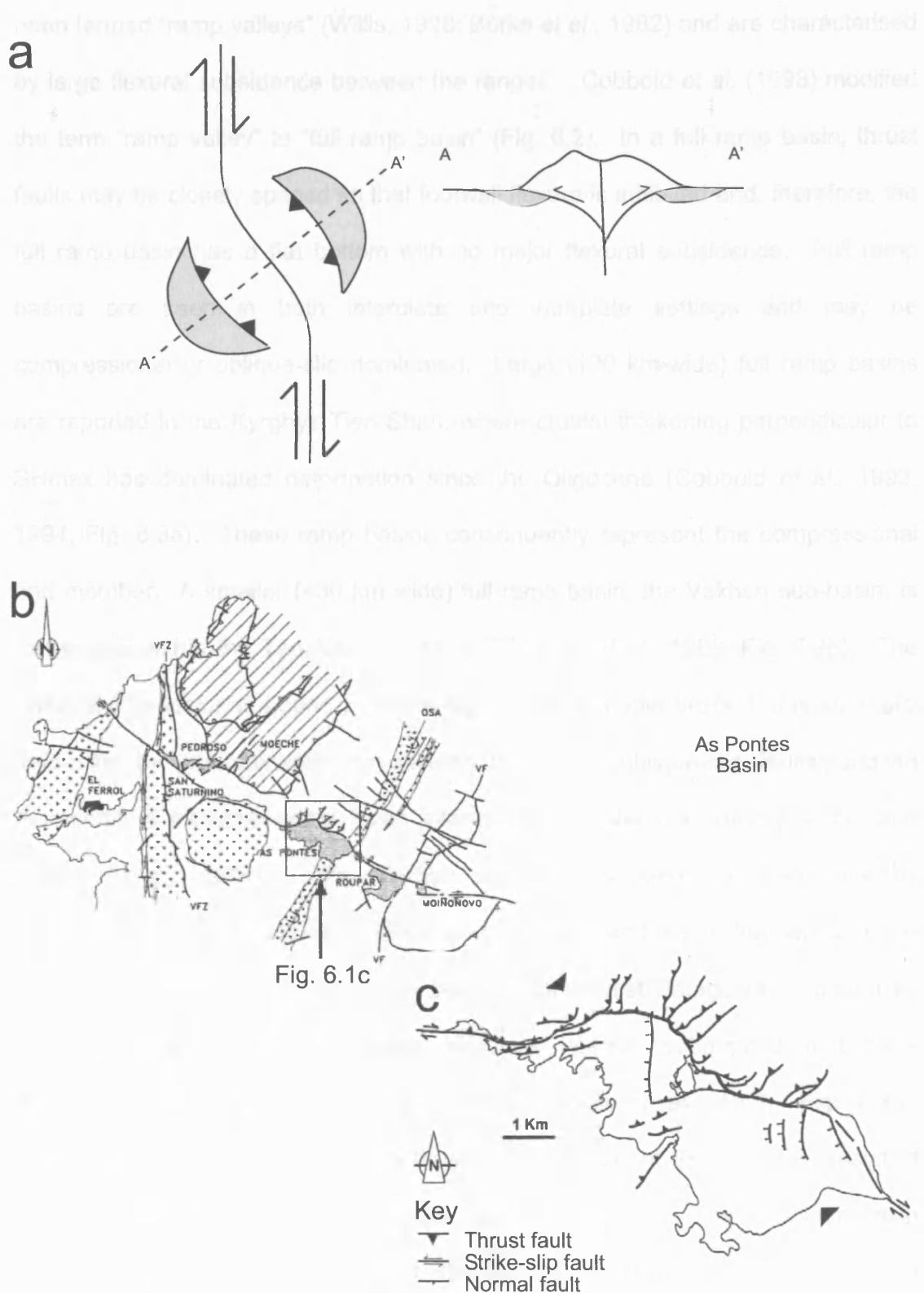


**Figure 6.1a** – Model for transpressional basin development at a restraining bend. Grey areas are areas of flexural subsidence adjacent to a range developed as a positive flower structure. Modified from Nilsen & Sylvester (1995). **6.1b** - Map showing the main structural features of the Pedroso-As Pontes-Moinonovo fault zone and the location of the As Pontes Basin. Modified from Sáez & Cabrera (2002) **6.1c** - Sketch map of the As Pontes Basin, Spain which corresponds well with model “a” above. The basin formed predominantly by flexural subsidence adjacent to a restraining bend on the Pedroso-As Pontes-Moinonovo fault zone. Modified from Sáez & Cabrera (2002).

been termed “ramp valleys” (Willis, 1928; Burke *et al.*, 1982) and are characterised by large flexural subsidence between the ranges. Cobbold *et al.* (1993) modified the term “ramp valley” to “full ramp basin” (Fig. 6.2). In a full ramp basin, thrust faults may be closely spaced so that footwall flexure is inhibited and, therefore, the full ramp basin has a flat bottom with no major flexural subsidence. Full ramp basins are seen in both interplate and intraplate settings and may be compressional or oblique-slip dominated. Large (100 km-wide) full ramp basins are reported in the Kyrghyz Tien Shan, where crustal thickening perpendicular to SHmax has dominated deformation since the Oligocene (Cobbold *et al.*, 1993, 1994; Fig. 6.3a). These ramp basins consequently represent the compressional end member. A smaller (<30 km wide) full ramp basin, the Vakhsh sub-basin, is recognised within the Tadzhik depression (Thomas *et al.*, 1996; Fig. 6.3b). The Tadzhik depression is bound by strike-slip and oblique-slip faults, but is internally deforming by predominantly thin-skinned thrust and oblique-slip faults, and so represents a transpressional basin intermediate between a compressional and pure strike-slip setting. The Vakhsh sub-basin is bound on each side by basinward-directed thrust faults which cut basement, and lies in the centre of the Tadzhik depression. The El Bolson Basin, in northwest Patagonia, is bound by transpressional ranges with flower structure internal geometries that have developed along dextral strike-slip faults (Diraison *et al.*, 1998; Fig. 6.3c). Basinward-directed thrust faults, both within and adjacent to the basin, result in intense contractional deformation of the basin fill (Fig. 6.3c). The El Bolson Basin is an example of a ramp basin controlled by uplift along oblique-slip faults. Full ramp basins are most common where uplift, on oblique-slip or thrust faults, occurs along multiple parallel faults. They occur throughout the Altai (Chapter 2). Basins with full ramp geometry need not undergo major subsidence for significant

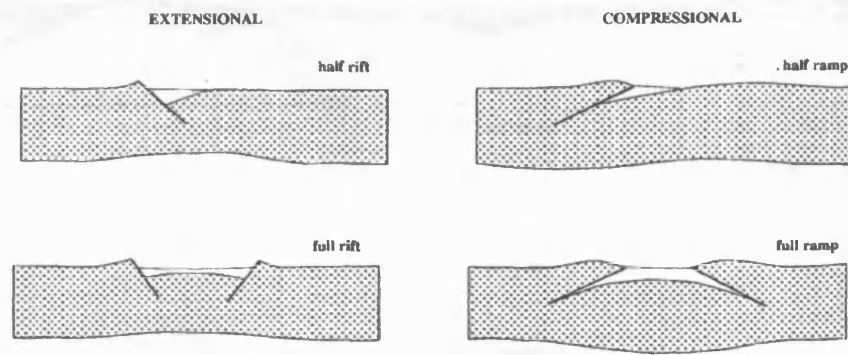


**Figure 6.2** – sketch cross-sections showing the orientation of basin bounding faults in ramp and full ramp basins and their extensional counterparts (Cobbold *et al.*, 2003).



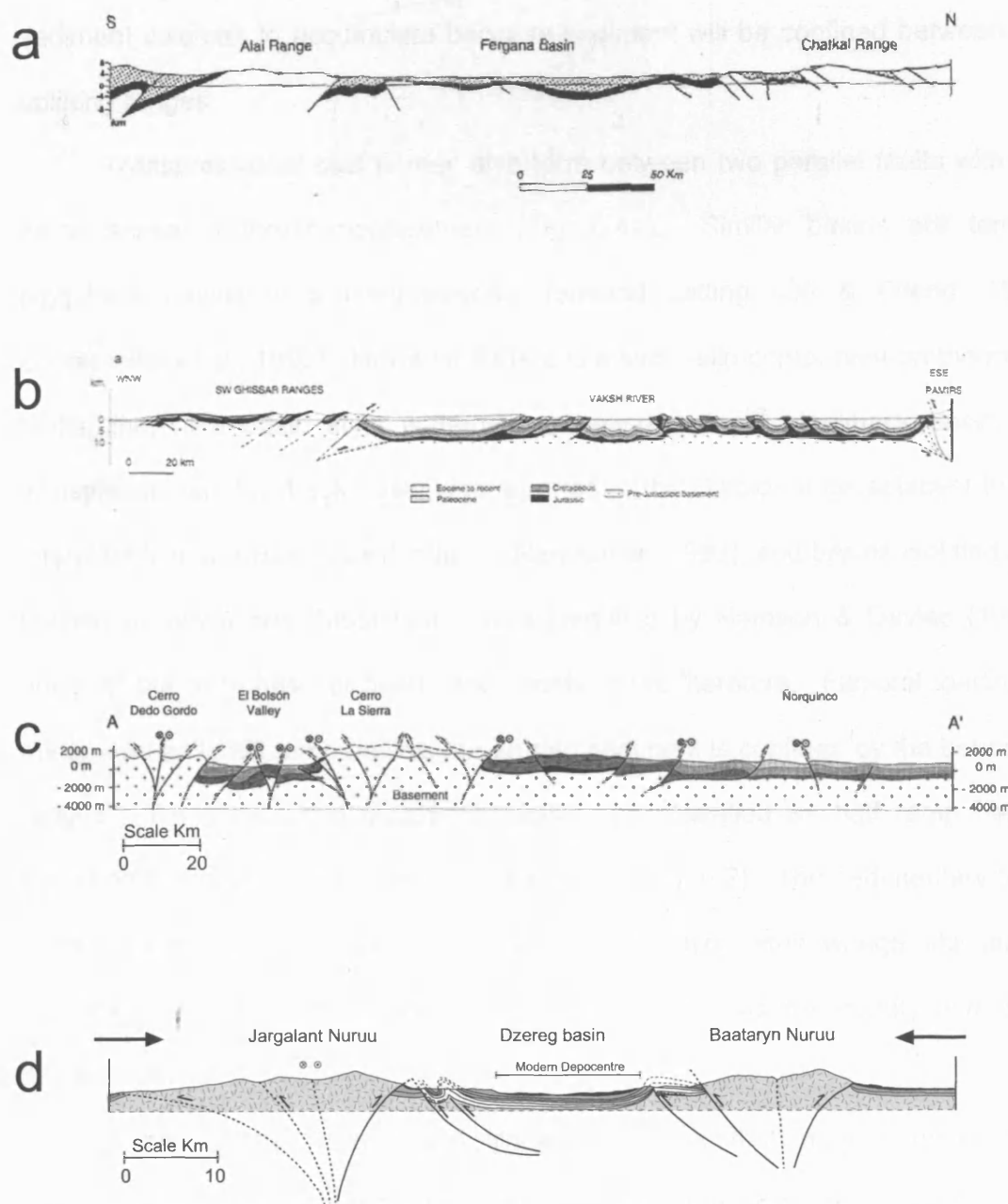


**Figure 6.3** - Cross-sections through the transpressional basins with a full ramp geometry discussed in the text. **6.3a** - The >100 km wide Fergana Basin in the Kyrghyz Tien Shan (Cobbold *et al.*, 1994). **6.3b** - The Tadzhik depression containing the 30km wide Vaksh sub-basin (Thomas *et al.*, 1996). **6.3c** - The 20 km wide El Bolson Basin adjacent to the large Niriuhau foreland (modified from Diraison *et al.*, 1998). **6.3d** - The Dzereg Basin (Howard *et al.*, 2003; chapter 3).

sediment volumes to accumulate because sediment will be confined between the uplifting ranges.

Transpressional basins may also form between two parallel faults with the same sense of thrust displacement (Fig. 6.4a). Similar basins are termed piggyback basins in a compressional foreland setting (Ori & Friend, 1984; Zoetemeijer *et al.*, 1993). However if there is a strike-slip component on the major faults, then this basin style is termed a transpressional piggyback basin. A transpressional piggyback basin was reported in the Diablo range adjacent to the interplate Ventura Basin, California, by Rentschler (1986), and basins isolated and uplifted by advancing thrust faults were identified by Namson & Davies (1988), however the term has not been used widely in the literature. Flexural loading is minor, and as in full ramp basins, the eroded sediment is confined by the bounding ranges. Transpressional piggyback basins are classified as half ramp basins based on the orientation of their bounding faults (Fig. 6.2). The sedimentary fill of a transpressional piggyback basin will form an asymmetric wedge, thickening towards the active basin margin. This distribution contrasts the broadly symmetric full ramp basin.

Transrotational basins are strike-slip basins that may form in both transpressional and transtensional settings. They form adjacent to shear zones between discrete crustal blocks that rotate around vertical or subvertical axis. Block rotation may create triangular or rhomb shaped depressions between blocks in which sediment may accumulate. Internal deformation within the rotating basement block, by either crustal flexure or extension, may also be an important mechanism for basin formation (Chapter 5).

In summary transpressional basins may vary significantly in shape and size, and differences relate predominantly to the distribution of bounding faults and fault

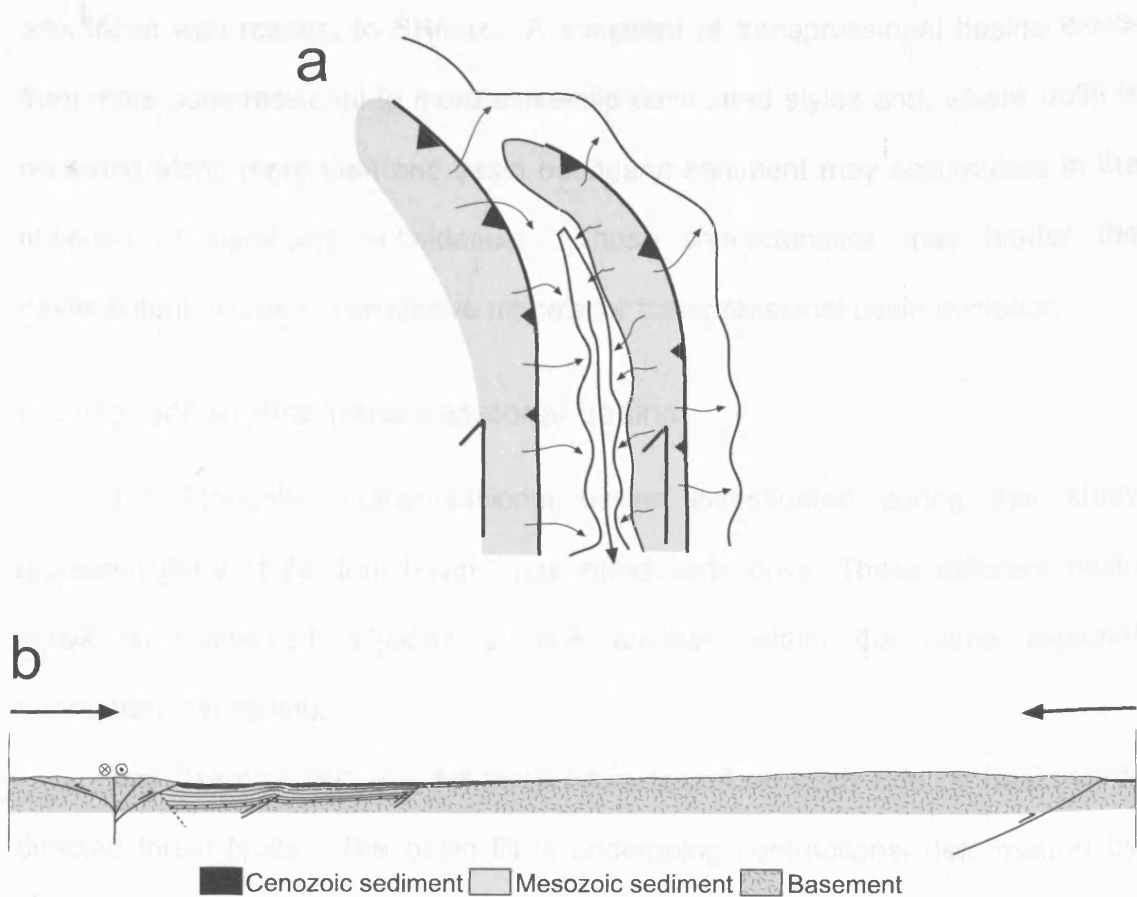


**Figure 6.4a** - Sketch model showing a basin developing between basement blocks (grey) uplifted at the thrust termination zones of two parallel strike-slip faults. This basin is not subsiding but sediment is stored in the depression between the uplifted ranges. The basin is bound by active faults on one side only. **6.4b** - Cross-section interpretation for the early Cenozoic evolution of the Dariv Basin which is an actively deforming transpressional piggyback basin. Note the asymmetry of the Cenozoic basin fill.

orientation with respect to SHmax. A spectrum of transpressional basins exists from more compressional to more strike-slip dominated styles and, where uplift is occurring along more than one basin boundary, sediment may accumulate in the absence of significant subsidence. These characteristics may hinder the development and use of predictive models for transpressional basin evolution.

### 6.3 Mongolian Altai transpressional basins

The Mongolian transpressional basins investigated during this study represent three of the four basin types introduced above. These different basin styles have evolved adjacent to one another, within the same regional transpressional setting.

The Dzereg Basin is a full ramp basin bound on each side by basinward-directed thrust faults. The basin fill is undergoing contractional deformation by folding and faulting, both internally and adjacent to the basin margins. Since flexural subsidence is considered minor (Cunningham, 1998), sediment is accumulating passively between the uplifted ranges. Based on these characteristics, the Dzereg Basin is considered an excellent example of an active, intraplate, transpressional full ramp basin, in the early stages of uplift and basin destruction (Fig. 6.3d). The 20 km wide Dzereg Basin is of a similar scale to the 25-30 km wide El Bolson Basin, and both are undergoing similar intrabasinal contractional deformation (Fig. 6.3c & d). The tectonic settings of the two basins are, however, very different, because the El Bolson Basin is located in the central Andes, where strike-slip and thrust sense displacements are partitioned adjacent to the large Ñirihuau foreland basin.

The Dariv Basin is located between two active ranges, uplifted by eastward-directed thrust faults on their eastern margins. Consequently the basin is actively

deforming only along its western margin and by east directed thrust faults within the basin. Sediment is accumulating between the two ranges. The basin floor, appears to be actively uplifting rather than subsiding, based on the altitude of the basin floor relative to adjacent basins. The lower rate of basin uplift, relative to uplift of the bounding mountain ranges, produces the accommodation. The Dariv Basin is a rare example of an actively deforming, intraplate transpressional piggyback basin (Fig. 6.4b).

The Shargyn Basin lies within a zone of conjugate strike-slip faulting. Conjugate strike-slip faulting and associated block rotations can provide space for sediment accumulation and basin development (Mann & Burke, 1982; Garfunkel & Ron, 1985, Nilsen and Sylvester, 1995). Block rotation may be accompanied by internal block deformation. Subsidence in the Shargyn Basin is probably related to internal deformation, either by crustal flexure and downwarping of the basin or by crustal thinning, during block rotation adjacent to the Tonhil and Shargyn strike-slip faults (Chapter 5, page 173). The Shargyn Basin is classified as a transrotational basin because of the interpreted link between block rotation and basin formation.

The restraining bend model of Nilsen and Sylvester (1995) is not applicable to any of the three basins studied in the Altai because it attributes basin formation to flexural subsidence. In the Altai, a network of sub parallel strike-slip, oblique-slip and thrust faults accommodate active dextral deformation. In such broad deforming zones with numerous spaced faults discrete, spaced mountain ranges are uplifted and are separated by depressions where sediment can accumulate. Full ramp, piggyback and rotational transpressional basin types are, therefore, likely to develop. Basins corresponding to the flexural restraining bend model of Nilsen and Sylvester (1995) are more likely to form where deformation is focussed on a single strike-slip fault, or within a narrow and discrete deforming belt.



## 6.4 Identification of transpressional basins in the rock record

Major criteria for the identification of different types of intracontinental basins may include their areal extent, their depth and sediment volume, the style of bounding faults, vertical changes in facies architecture and the presence of internal deformation or interstratified volcanic rock (Table 6.1). The various transpressional basin types are bound by different fault geometries and show consequent variation in the sedimentary facies architecture and the style and distribution of intrabasinal deformation. However, the different styles of transpressional basin identified in this study may form within the same tectonic setting. Consequently, there is no single characteristic feature distinguishing transpressional basins from other major basin types in the rock record.

Preserved transpressional basins are unlikely to be mistakenly interpreted as the deposits from a rift or transtensional basin. Rift or transtensional basins are bound by extensional faults and, consequently, tend to be deep and lack evidence for significant compressional deformation, either at their margins or within the basin. Volcanic material can be interstratified with the sedimentary fill of rift basins and large transtensional basins that accommodate significant crustal stretching. Volcanic material is not, however, generally observed in transpressional basins (Table 6.1). Rift basins are also characterised by their large areal extent, their elongate trough shaped geometry and their great sediment volume that distinguish them from transpressional basins.

Differentiation between transpressional basins and other major basin types is likely to prove more difficult. For example a two-dimensional section (e.g. a seismic line) through a transpressional basin may appear similar to a compressional foreland or broken foreland basin. A flexural foreland basin will generally be deep, contain a large sediment volume and have a broad lateral extent. These characteristics should allow them to be easily distinguished from transpressional basins. However differentiation between a broken foreland basin and a transpressional basin may be more difficult.

Transpressional basins will generally be shallow and contain a coarsening upward succession of texturally immature, coarse alluvial sediment derived from the basin margins. Away from the margins predominantly alluvial sediments will commonly fine into lacustrine or marsh deposits in the basin centre. Evidence for contractional deformation by faults or folding, both within and adjacent to the basin, results from basinward-directed thrust faults that bound one or more basin margins. Abrupt lateral facies changes and internal unconformities record uplift of the basin fill adjacent to the bounding structures, and result in progressive offlap of younger sediment toward the basin centre. Unfortunately none of these sedimentary or structural features are unique to transpressional basins, and they could equally describe a broken foreland setting.

If the basin bounding faults can be identified, they provide further evidence

---

**Table 6.1** (following page) – Table compares the general characteristics of idealised intracontinental basins. The first order characteristics of different continental basin types are used to identify the major differences between them. These features will aid the differentiation of basin types in the rock record. References: General – Allen & Allen, 1990; Busby & Ingersoll, 1985; Nilsen & Sylvester, 1996; Leeder, 1999. Foreland Basins – Macqueen & Leckie, 1992, and references therein; DeCelles & Giles, 1996; Mascle et al., 1998, and references therein. Broken foreland basins – Dickinson et al., 1998; Kraemer et al., 1999. Rift Basins – Prosser, 1993. Transtensional Basins – Mann et al., 1982; Christie-Blick & Biddle, 1985; Waldron, 2003. Transpressional Basins – Cobbold et al., 1993; Diraison et al., 1998; Howard et al., 2003.

**Table 6.1**

	Foreland	Broken foreland	Extensional rift	Transtensional	Transpressional
Bounding faults	A compressional orogen bound by basinward directed thrust faults forms one basin margin.	A compressional orogen bound by basinward directed thrust faults forms one basin margin, with subsidiary-basement cored uplifts, bound by basinward directed thrust faults, uplifted within the flexural basin.	Normal faults form one or more basin margins.	Strike-slip, oblique-slip or normal faults bound each basin margin.	Thrust, strike-slip and oblique-slip faults bound one or more basin margins.
Flexural component of subsidence	Large	Large	Late stage thermal subsidence	Minor – moderate	Minor
Aerial extent	1000's – 100000's km <sup>2</sup>	1000's – 100000's km <sup>2</sup>	1000's – 100000 km <sup>2</sup>	10's -1000's km <sup>2</sup>	10's - 1000's km <sup>2</sup>
Intrabasinal deformation	Intense contractional deformation adjacent to the advancing thrust wedge.	Potentially intense contractional deformation adjacent to all basin bounding thrust faults.	Large rollover anticlines commonly develop adjacent to the basin bounding normal faults. Fault propagation anticlines develop above normal faults. Intrabasinal deformation by antithetic faults and folds is common.	Rollover anticlines develop adjacent to extensional basin bounding faults. Fault propagation anticlines develop above normal faults. Potentially complex faulting may develop antithetically to basin bounding normal and strike-slip faults. Compressional deformation is minor.	Intense compressional faulting and folding adjacent to basin bounding thrust faults. Internal deformation away from the basin margins increases as the basin evolves.
Internal fill	Tapering sediment wedge thinning and fining away from the advancing orogen. The basin fill commonly coarsens upward as the relief of the adjacent orogen increases and greater volumes of sediment are eroded. Cyclical sedimentation reflecting intermittent uplift in the adjacent fold and thrust belt is common.	Variable, dependent on an individual basin's proximity to the advancing orogen and the interconnectivity of basins. Axial fluvial systems are common in the basin centre and alluvial fans flank the basin margins. However, basins may be internally drained and dominated by lake sediments with coarse fringing alluvial fans.	Highly variable dependent on the geometry of basin bounding faults. An asymmetric sediment wedge is characteristic of a half graben. Commonly the footwall is bound by fringing alluvial fans that prograded into an axial fluvial or lacustrine system. Finer sediment is supplied down the hanging wall dip slope. Basin fill may fine or coarsen upward dependant on sediment supply.	Highly variable, but usually coarse and dominated by alluvial fans. Generally reflects rapid infill of the developing basin. Lacustrine sediments are common in the basin centre.	Varied, dominated by coarse alluvial fan sediments derived from the evolving basin margins. Lacustrine sediments can be volumetrically important in internally drained basins. Overall the succession tends to coarsen upward as the basin evolves and closes.
Relative potential for interstratified volcanic rock	Low	Low	High	moderate	Low
Sediment volume	Large	Medium	Large	Medium-large	Low
Overall preservation potential	High	High	High	moderate	Low

to distinguish between broken foreland and transpressional basin types. Broken foreland basins are bound primarily by thrust faults, so evidence for strike-slip or oblique-slip faulting on basin bounding faults provides strong evidence for a transpressional basin. However, transpressional basins may be bound by thrust faults, so the basin bounding faults do not provide conclusive evidence. The regional, rather than basin proximal, tectonic setting may be easier to discern than the kinematic history of individual basin bounding faults. The presence of an adjacent compressional orogen provides strong evidence for a broken foreland basin, and its absence, particularly if strike-slip motion is identified, suggests a transpressional basin. The difficulties in distinguishing transpressional and broken foreland style basins mean that it is important to know the regional context.

Transpressional basins, especially those that are small intramontane basins (< 30 km wide), may be particularly difficult to identify in the rock record because intense deformation and uplift of the basin fill is part of the basin's life cycle. Therefore, preserved sediments from these basins will be both structurally and sedimentologically complex, requiring detailed investigation of the three-dimensional geometry to unravel their depositional history.

## 6.5 Future work

Most of the western Mongolian sedimentary basins remain relatively understudied and there remain many unanswered questions. The following points are suggestions for future work that would build on this project, and improve understanding of transpressional basins in Mongolia and elsewhere.

- A seismic investigation of the Altai flanking basins and Valley of Lakes would clarify the geometry of subsurface structures and enable rough calculations of the volume of sediment within the basins. These data would expose the relationship between sedimentary units and structures at depth, and aid the correlation of stratigraphic units between exposed sections. Unconformable surfaces and lateral variations in unit thickness could also be identified. These interpretations would cast light on both the Mesozoic and Cenozoic history of the region.

- Investigation of the depressions of the high Altai, using borehole/seismic data would determine whether an older Cenozoic basin sediments are preserved beneath the modern cover. The sediment contained within these basins could record the earliest stages of Cenozoic range growth. Insights into the evolving depositional environment, intrabasinal deformation and basin preservation potential might be expected.

- The Shargyn Basin represents one of the most interesting tectonic features in western Mongolia. Its unusual depth and size suggests that it may contain a large volume of sediment. It is currently classified as a transrotational



basin in which some crustal extension is suspected, but unproven. A detailed study of the Shargyn Basin using seismic data and fieldwork might document crustal thinning in the basin centre. Borehole data would also be useful to trace facies variations within the basin, and to correlate formations (in conjunction with seismic data), given the limited outcrop away from the basin margins.

- A detailed GPS study in the southern Altai area would quantify rates and kinematics of fault motion and block rotations. This could provide supporting evidence for the models presented in chapter 4.

- Many aspects of the sedimentology deserve further investigation. For example:

A detailed palaeo-environmental study of the lake sediments of the Gurven Ereen Formation and examination of the suspected cyclicity in the millimetre-scale laminated succession would yield a great deal of data on the changing water composition. In turn this would probably provide information on Cretaceous climate

A detailed palaeontological investigation focussing on the fossil rich Gurven Ereen and Dzereg Formation lake sediments might provide fauna characteristic of particular environmental conditions. This would allow palaeo-environmental interpretations presented in Chapter 4 to be further tested and refined.

Palaeosols, particularly from the Red Hill Formation, are well preserved and laterally extensive. By mapping out these exposure surfaces and potentially correlating them across the different exposure in the North Foreberg a more detailed understanding of the evolving depositional system could be gained. Many

of the palaeosols are also candidates for palaeontological dating which would provide further age control for Cenozoic strata.

- Geomorphological mapping of uplifted and tilted surfaces within the three Mongolian basins and cosmological dating could better constrain the displacement rates of the faults and folds deforming the basin sediments.

## 6.6 Summary of major conclusions

### LANDSAT INVESTIGATION OF THE GREATER ALTAI AREA (CHAPTER 2)

- A hierarchy of depocentres linked by major river systems are identified in the Altai. These depocentres store sediment eroded from the range and may contain an important record of sequential range uplift.

- Approximately 50% of the Altai surface area is drained by two major river systems. The Khovd river, which has a catchment area of 14,100 km<sup>2</sup>, supplies sediment to the northern Dzereg Basin. The Ob river has its source in the Russian Altai and its various tributaries extend throughout most of that range.

- The Chinese Altai forms a continuous, unbroken range along the Mongolian Chinese border. The range is uplifted by west directed thrust faults but few faults with known Cenozoic movement have been identified. River systems drain well-defined, deeply incised catchment areas and supply sediment directly into the eastern margins of the Junggar Basin. The sediment is then transported west by major rivers. The absence of a thick sediment wedge along the north-eastern margin of the Junggar Basin suggests that the high topography may have formed in the Mesozoic with limited Cenozoic reactivation.

- Range flanking transpressional basins, including the Dzereg, Dariv and Shargyn basins, represent the major sediment sinks within the Altai region. The large flanking basins (Valley of Lakes and the Junggar Basin) receive little sediment from the range interior at the present time, although they may have received more in the past.

- The decrease in altitude from west to east and coincident decrease in both drainage basin maturity and evidence for past glaciations, combined with the concentration of known Cenozoic faults in the Mongolian Altai, suggest that uplift of the Altai began in the west, and that the range is progressively growing eastwards.

#### THE DZEREG BASIN (CHAPTER 3)

- Mesozoic sediment is found only within Cenozoic basins. The absence of Mesozoic sediment in any uplifted ranges suggests that the basins represent older Mesozoic depocentres. Complete erosion of Mesozoic strata from the Cenozoic ranges is possible but not considered likely since erosion of the Cenozoic ranges is not yet advanced.

- Mesozoic sedimentary successions fine upward and are dominated by the deposits of a meandering river system that flowed to the southeast within an elongate trough. Alluvial fans shed from the basin margins extended into the axial river system, or into periodic lakes developed within the basin.

- The geometry of faults and folds within the Dzereg Basin, combined with the distribution of Mesozoic sediments and the fining upward succession, suggest

that the main intrabasinal faults may be inverted Mesozoic normal faults, and that the Mesozoic Dzereg Basin was controlled by an extensional or transtensional tectonic regime.

- The Cenozoic reactivation of the Dzereg Basin began in the Oligocene, as a far field response to the Indo-Eurasian collision, and continues to the present. The ranges are bounded by outwardly propagating thrust faults which deform the basin margins, and active folding and thrust faulting occurs within the basin. Cenozoic strata coarsen upward, and are dominated by alluvial fans shed from the adjacent ranges.

#### THE STRATIGRAPHY OF THE DARIV AND SHARGYN BASINS (CHAPTER 4)

- Mesozoic strata within the Dariv Basin fine upward and record southeast flowing axial river systems, fed by flanking alluvial fans and overlain by lacustrine sediment deposited in a long-lived lake. Mesozoic formations thicken markedly westward within the basin forming an asymmetric wedge.

- Cenozoic strata within the Dariv Basin fine upward into the Upper Miocene, above which the strata coarsen as sediment is derived from the adjacent ranges. This is in contrast to the Dzereg Basin, which coarsens upward from the Oligocene, and is interpreted to reflect a delay in major drainages developing in the Dariv Basin across the regional northwest-southeast fault trend.

- Paleocurrent data measured throughout the Dariv Basin record the evolution of both internal and external drainage systems. Axial river systems linking the Dariv and Shargyn basins developed during the Upper Jurassic and

again in the Oligocene. At other times the location of the main depositional low within the Dariv Basin is indicated by the centripetal drainage pattern.

- Utilising palaeosols, fossil flora, and the sedimentary interpretations relating to evolving river systems and fluctuating lake levels, long-term trends in palaeoclimate are recognised. The Mesozoic climate became increasingly arid overall while there appears to have been little variation throughout the Cenozoic until the Pleistocene ice age events. These data support existing models/predictions (e.g. Parrish *et al.*, 1982) for the palaeoclimate of Asia.

#### THE STRUCTURE OF THE DARIV BASIN (CHAPTER 5)

- The Dariv Basin contains only one potentially reactivated Mesozoic normal fault, the Central Ridge Fault. However this, combined with marked thickness variations in the Mesozoic sediment from east to west, the absence of compressional deformation within the Mesozoic basin fill and the fining upward Mesozoic succession, supports deposition in an extensional basin. The master bounding fault(s) are interpreted to be obscured by Cenozoic sediment or advancing thrust wedges.

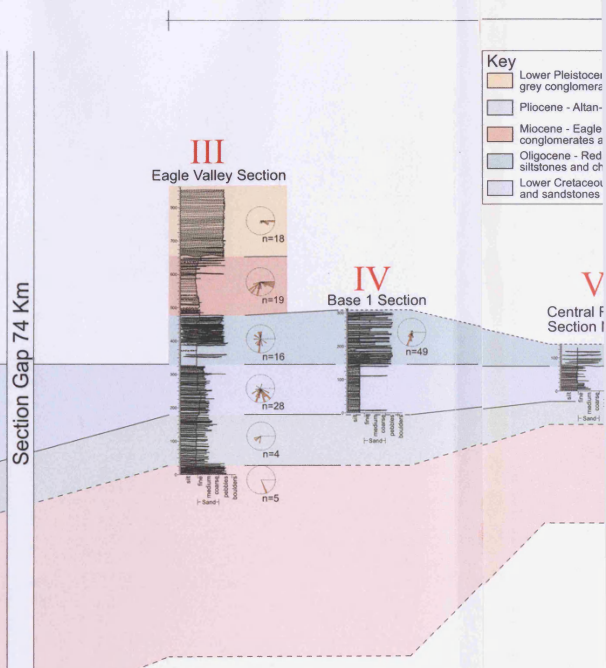
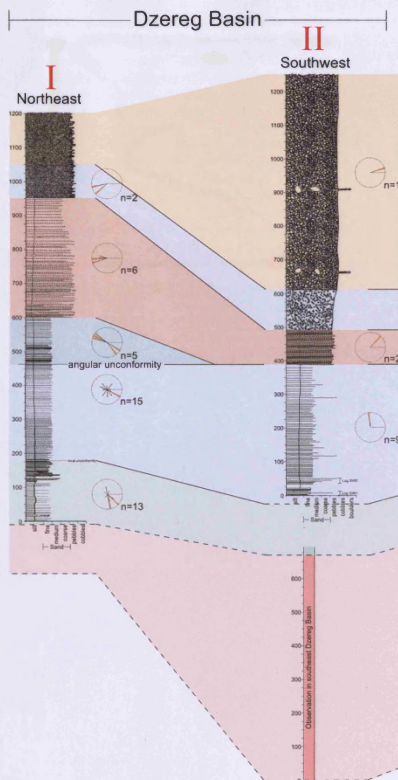
- The Cenozoic Dariv Basin is internally deformed and uplifted in discrete zones which define a rhomboid of active deformation, adjacent to the Tonhil strike-slip fault. This deformation records the complexities of basin formation between major conjugate strike-slip faults, adjacent to an evolving restraining bend. Deformation continues and the basin is still receiving sediment.



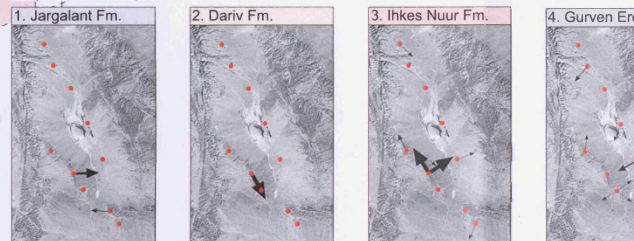
## WIDER IMPLICATIONS OF THE PROJECT (CHAPTER 6)

- The three adjacent basins investigated have each developed a different structural style. The Dzereg Basin is a full ramp basin, the Dariv Basin is a transpressional piggyback basin and the Shargyn Basin is a transrotational basin. This reflects the variation in basin types that develop in an intraplate transpressional mountain belt, different thrust and strike-slip fault linkage geometries.

- Transpressional basins are bound by thrust, oblique-slip or strike-slip faults and are shallow, intensely deformed by contractional structures and have limited preservation potential. They are consequently difficult to recognise in the rock record. Transpressional basins are most likely to be misinterpreted as broken foreland basins if the presence of an adjacent contractional orogen cannot be ruled out.



Maps 1-6 show palaeocurrent data from the lower 6 formations



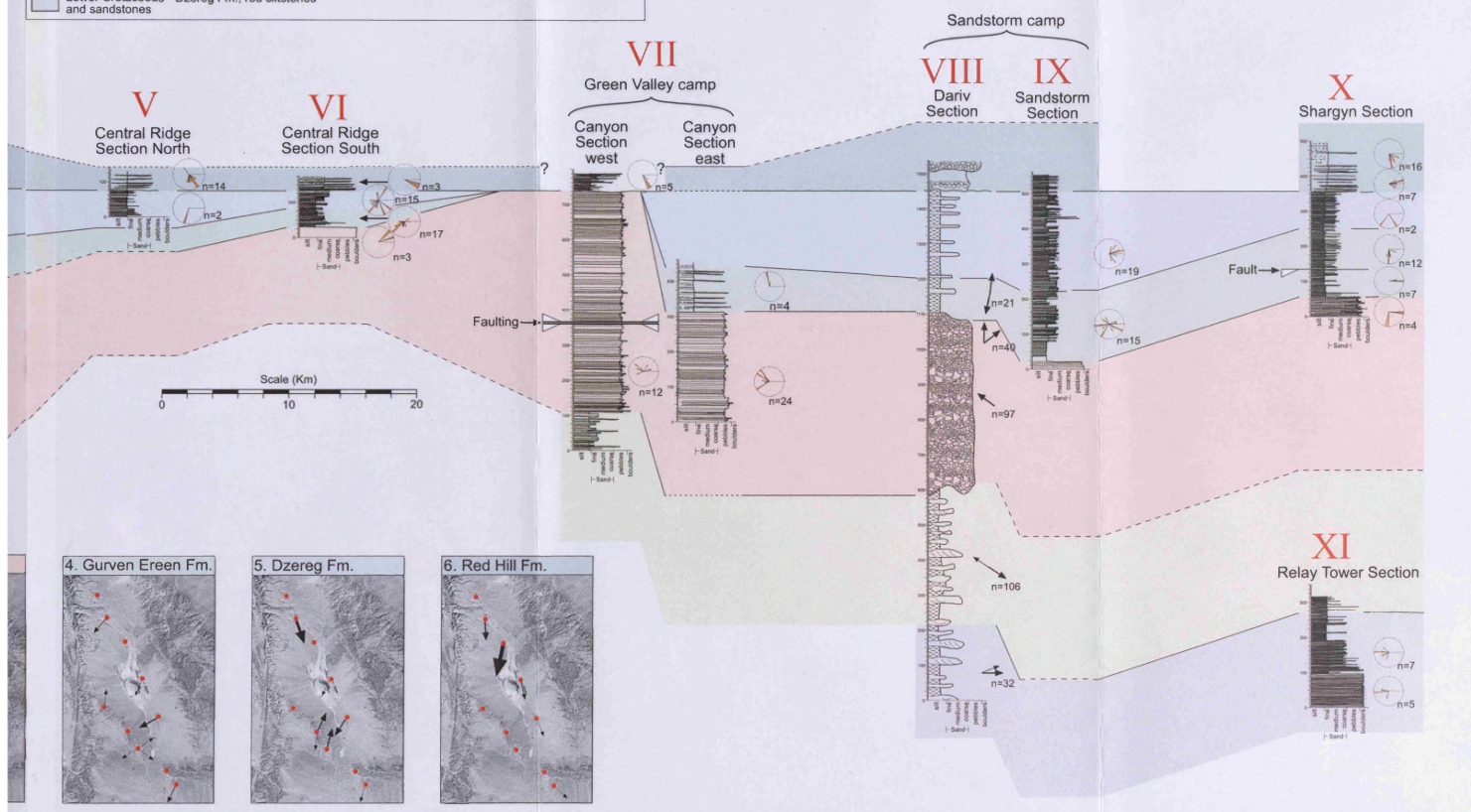
Key to paleocurrent maps  
 → n = <5  
 → n = 6-15  
 → n = 16-25  
 → n = 26-35  
 → n = >36

Key  
 Lower Pleistocene - grey conglomerates  
 Pliocene - Altan  
 Miocene - Eagle conglomerates and sandstones  
 Oligocene - Red siltstones and chert  
 Lower Cretaceous - sandstones

# Dariv Basin

# Shargyn Basin

<b>Key</b> Lower Pleistocene - Goshu Fm., massive grey conglomerates Pliocene - Altan-Teel Suite, yellow conglomerates Miocene - Eagle Valley Fm. (Oshin suite), channelised conglomerates and grey siltstone Oligocene - Red Hill Fm. (Beger Suite), red siltstones and channelised sandstones Lower Cretaceous - Dzereg Fm., red siltstones and sandstones	Lower Cretaceous - Gurven Ereen Fm., grey siltstone and fine sandstone Upper Jurassic/Lower Cretaceous - Ihkes Nuur Fm., matrix supported conglomerate Upper Jurassic - Dariv Fm., channelised sandstone and red siltstone Middle Jurassic - Jargalant Fm., channelised green sandstone and siltstone
---	--



## Appendix 3

Loose leaf copies of large figures in envelope on back cover:

**Figure 2.4** - Interpreted TM Landsat montage showing major Cenozoic faults and known kinematics. Interpretation based on image analysis, ground truthing and historical seismicity.

**Figure 2.5** - Interpreted TM Landsat montage showing catchment areas, drainage divides and major rivers in the greater Altai area. Inset map shows the upstream catchment areas for major river systems.

**Figure 2.6** - Interpreted TM Landsat montage showing major drainage divides and the distribution of major sedimentary basins. Five major types of sedimentary basin are distinguished.

**Figure 4.3** – Correlation panel showing generalised stratigraphic sections from the Dzereg, Dariv and Shargyn Basins, Section VIII, the Dariv Section is taken from Sjostrom, 2001. Inset map shows the location of sections. Formation names correspond to those of Devjatkin, 1981. Correlation is based on palaeontological data (listed in appendix 1), field mapping of formations and major changes in lithology. The direction of measured palaeocurrent is shown on sections and on 6 inset maps.

**Table 3.1 and 4.2** – Facies chart for major stratigraphic units identified in the Dzereg, Dariv and Shargyn basins.

## Reference List

- Ahnert, F. 1998. Introduction to Geomorphology, Arnold, London, pp 360.
- Allen, M. B. & Vincent, S. J. 1997. Fault reactivation in the Junggar region, Northwest China; the role of basement structures during Mesozoic-Cenozoic compression. *Journal of the Geological Society*, London, **154**, 151-155.
- Allen, M. B., Sengor, A. M. G. & Natal'in, B. A. 1995. Junggar, Turfan and Alakol basins as Late Permian to ?Early Triassic extensional structures in a sinistral shear zone in the Altaid orogenic collage, Central Asia. *Journal of the Geological Society*, London, **152**, 327-228.
- Allen, P. A. & Allen J. R. 1990. Basin Analysis, Principles and applications, Blackwell, Oxford, pp 451.
- Anadón, P., Cabrera, L. Colombo, F., Marzo, M. & Riba, O. 1986. Syntectonic intraformational unconformities in alluvial fan deposits, eastern Ebro Basin margins (NE Spain). In: Allen, P. A. & Homewood, P. (eds) Foreland Basins, International Association of Sedimentologists Special Publications, **8**, 259-270.
- Arakawa, H. (Ed.) 1969. Climates of Northern and Eastern Asia. World Survey of Climatology Volume 8. Elsevier, Amsterdam, pp 248.
- Ashley, G. M. 1990. Classification of large-scale subaqueous bedforms: a new look at an old problem. *Journal of sedimentary petrology*. **60**, 160-172.
- Badarch, G., Cunningham, D. & Windley, B. 2002. A new terrane subdivision for Mongolia: implications for the Phanerozoic crustal growth of Central Asia. *Journal of Asian Earth Sciences*, **21**, 87-110.
- Baljinnyam, I., Bayasgalan, A., Borisov, B. A., Cisternas, A., Den'yanovich, M. G., Ganbaatar, L., Kochetkov, V. M., Kurushin, R. A., Molnar, P., Philip, H. & Vashchilov, Y. Y. 1993. Ruptures of major earthquakes and active deformation in Mongolia and its surroundings. *Geological Society of America Memoirs*, **181**, pp 68.



- Bayasgalan, A., Jackson, J., Jean-François, R. & Carretier, S. 1999a. 'Forebergs', flower structures, and the development of large intracontinental strike-slip faults: the Gurvan Bogd fault system in Mongolia. *Journal of Structural Geology*, **21**, 1285-1302.
- Bayasgalan, A., Jackson, J., Ritz, J. F. & Carretier, S. 1999b. Field examples of strike-slip fault terminations in Mongolia and their tectonic significance. *Tectonics*, **18**, 394-411.
- Blair, T. C. & McPherson, J. G. 1994. Alluvial fan processes and forms. In: Abrahams, A. D. & Parsons A. J. (eds) *Geomorphology of desert environments*, Chapman & Hall, London, 354-402.
- Burch, D. E. 1992. Petrology and stratigraphy of the Upper Triassic-Lower Jurassic Eagle Mills Formation, Choctaw County, Alabama. Masters Thesis, University of New Orleans, pp 234.
- Burchfiel, B. C. & Stewart, J. H. 1966. 'Pull-apart' origin of the central segment of Death Valley, California. *Geological Society of America Bulletin*, **77**, 439-441.
- Burke, K., Mann, P. & Kidd, W. 1982. What is a ramp valley? International Congress on Sedimentology, **11**, International Association of Sedimentologists, page 40 (Summary only).
- Busby, C. & Ingersoll, R. 1995. *Tectonics of sedimentary basins*. Blackwell, Oxford, pp 578.
- Cabrera, L., Ferrúa, B., Sáez, A., Santanach, P. F. & Bacelar, J. 1996. Onshore Cenozoic strike-slip basins in NW Spain. In: Friend, P. & Dabrio, C. (eds) *Spanish Tertiary Basins*, Cambridge University Press, Cambridge, 247-253.
- Carroll, A. R., Graham, S. A., Hendrix, M. S., Ying, D. & Zhou, D. 1995. Late Paleozoic tectonic amalgamation of northwestern China: sedimentary record of the northern Tarim, northwestern Turpan and southern Junggar basins. *Geological Society of America Bulletin*. **107**, 571-594.
- Chen, B. & Jahn B. 2002. Geochemical and isotopic studies of the sedimentary and granitic rocks of the Altai origin of northwest China and their tectonic implications. *Geological Magazine*, **139**, 1-13.

- Chlachula, J. 2001. Pleistocene climate change, natural environments and Palaeolithic occupation of the upper Yenisei area, south-central Siberia Lake Baikal and surrounding regions. *Quaternary International*, **80-81** 101-130.
- Christie-Blick, N. & Biddle, K. T. 1985. Deformation and Basin Formation along Strike-slip Faults. In: Biddle, K. T. & Christie-Blick, N (eds) Strike-slip Deformation, Basin Formation and Sedimentation. Society of economic paleontologists and mineralogists, Special Publication **37**, 1-34.
- Cobbold, P. R. & Davy, P. 1998. Indentation tectonics in nature and experiment: 2. *Central Asian Bulletin of Geology*, **14**, 143-162.
- Cobbold, P. R., Sadybakasov, E. & Thomas, J. C. 1994, Cenozoic transpression and basin development, Kyrghyz Tianshan, central Asia. In: Roure, F., Ellouz, N., Shein, V. S. & Skvortsov, I. (eds) Geodynamic Evolution of Sedimentary Basins, International Symposium, 181-202.
- Cobbold, P., Davy, P., Gapais, D., Rossello, E. A., Sadybakasov, E., Thomas, J.C., Tondji, J.J. & de Urreiztieta, M. 1993. Sedimentary Basins and Crustal Thickening. *Sedimentary Geology*, **86**, 77-89.
- Collinson, J. D. 1996. Alluvial sediments. In: Reading, H. G. (ed) Sedimentary environments; processes, facies and stratigraphy (3<sup>rd</sup> edition), Blackwell Science, Oxford, 37-82.
- Cunningham, W. D., Davies S. & Badarch, G. 2003. Crustal architecture and active growth of the Sutai Range, western Mongolia: a major intracontinental, intraplate restraining bend. *Journal of Geodynamics*, **36**, 169-191.
- Cunningham, W. D., Dijkstra A., Howard. J.P., Quarles A. & Badarch, G. 2002. Active Intraplate Strike-Slip Faulting and Transpressional Uplift in the Mongolian Altai. In: Holdsworth, R. E. & Salvini, F. (eds) Intraplate strike-slip deformation belts. Geological Society, London, Special Publications, **210**, 65-87.
- Cunningham, W. D. 1998. Lithospheric controls on late Cenozoic construction of the Mongolian Altai. *Tectonics*, **17**, 891-902.

- Cunningham, W., Windley, B.F., Dorjnamjaa, D., Badamgarov, G. & Saandar, M. 1996a. A structural transect across the Mongolian Western Altai: active transpressional mountain building in central Asia. *Tectonics*, **15**, 142-156.
- Cunningham, W. D., Windley, B. F., Dorjnamjaa, D., Badamgarov, G. & Saandar, M. 1996b. Late Cenozoic transpression in southwestern Mongolia and the Gobi Altai-Tien Shan connection, *Earth and Planetary Sciences*, **140**, 67-82.
- de Urreiztieta, M., Gapais, D., Le Corre, C. Cobbold, P. R. & Rossellio, E. 1996. Cenozoic dextral transpression and basin development at the southern edge of the Puna Plateau, northwestern Argentina. *Tectonophysics*, **254**, 17-39.
- DeCelles, P. G. & Giles, K. A. 1996. Foreland Basin Systems. *Basin Research*, **8**, 105-123.
- Dehandschutter, B., Vysotsky, E., Delvaux, D., Klerkx, J., Buslov, M. M., Seleznev, V.S. & De Batist, M. 2002. Structural evolution of the Teletsk graben (Russian Altai). *Tectonophysics*, **351**, 139-167.
- Delvaux, D., Klerkx, J. De Batist, M. & Dobretsov, N. L. 2002. Tectonic control of continental sedimentary basins in Altai-Baikal, Central Asia: introduction. *Tectonophysics*, **351**, 1-2.
- Devjatkin, E.V. 1981. The Cenozoic of Inner Asia Stratigraphy Combined Soviet-Mongolian Scientific Research Geological Expeditions Transactions, **27**, Nauka, Moscow, pp. 274 (In Russian).
- Devjatkin, E.V., Nagibina, P. & Khosbayar. 1975. Neotectonic structures of western Mongolia. In: Yanshin, A. L. (ed) Mesozoic and Cenozoic Tectonics and Magmatism of Mongolia. Combined Soviet-Mongolian Scientific Research Geological Expeditions Transactions, **11**, Nauka, Moscow, 44-102, (In Russian).
- Devjatkin, E. V. 1970. Mesozoic and Cenozoic geology of western Mongolia. Joint Soviet-Mongolian: Scientific Research Geological Expeditions Transactions, **1**, Nauka, Moscow, pp. 322 (In Russian).
- Dickinson, W. R., Klute, M. A., Hayes, M. J., Janecke, S. U., Lundin, E. R., McKittrick, M. A. & Olivares, M. D. 1998. Paleogeographic and paleotectonic

setting of Laramide sedimentary basins in the central rocky-mountain region. *Geological Society of America Bulletin*, **100**, 1023-1039.

- Diraison, M., Cobbold, P. R., Rosello, E. A. & Amos, A. 1998. Neogene dextral transpression due to oblique convergence across the Andes of northwestern Patagonia, Argentina. *Journal of south American Earth Sciences*, **11**, 519-532.
- Diraison, M., Cobbold, P. R., Rosello, E. A., Amos, A. J. & Lopez Gamundi, O. R. 1998. The Niriuhau Basin (Patagonia, Argentina); its Mesozoic rifting and Neogene architecture due to dextral Andean Transpression. *AAPG Bulletin*, **82**, (summary only).
- Dirik, K., Goncuoglu, M. C. & Kozlu, H. 1999. Stratigraphy and pre-Miocene tectonic evolution of the southwestern part of the Sivas Basin, central Anatolia, Turkey. In: Bozkurt, E. (ed) *Advances in Turkish geology; Part II*, *Geological Journal*, **34**, 303-319.
- Dumitru, T. A. & Hendrix, M. S. 2001. Fission-track constraints on Jurassic folding and thrusting in southern Mongolia and their relationship to the Beishan thrust belt of northern China. In: Hendrix, M. S. & Davis, G. A. (eds), *Palaeozoic and Mesozoic tectonic evolution of Central and Eastern Asia, from continental assembly to intracontinental deformation*. Geological Society of America Memoir, **194**, 215-229.
- Dumitru, T. A., Zhou, Da, Chang, E. Z. Graham, S. A., Hendrix, M. S., Sobel, E. R. & Carroll, A. R. 2001. Uplift, exhumation, and deformation in the Chinese Tian Shan. In: Hendrix, M. S. & Davis, G. A. (eds), *Palaeozoic and Mesozoic tectonic evolution of Central and Eastern Asia, from continental assembly to intracontinental deformation*. Geological Society of America Memoir, **194**, 71-99.
- England, P. & Molnar, P. 1990. Right lateral shear and rotation as an explanation for strike-slip faulting in eastern Tibet. *Nature*, **344**, 140-142.
- Farrell, K. M. 1987. Sedimentology and facies architecture of overbank deposits of the Mississippi River, False River region, Louisiana. In: Ethridge, F. G. Flores, R. M. & Harvey, M. D. (eds), *Recent developments in fluvial*

sedimentology. Society of Economic Palaeontologists and Mineralogists Special Publication **39**, 111-120.

Fastovsky, D. E., Badamgarav, D., Ishimoto, H., Watabe, M. & Weishampel, D. B. 1997. The Paleoenvironments of Tugrikin-Shireh (Gobi Desert, Mongolia) and Aspects of the Taphonomy and Paleoecology of *Protoceratops* (Dinosauria: Ornithischia), *Palaios*, **12**, 59-70.

Fedeneva, I. N. & Dergacheva, M. I. 2003. Paleosols as the basis of environmental reconstruction in Altai mountainous areas. *Quaternary International*. **106-107**, 89-101.

Florensov, N. A. & Korzhnev, S. S. 1982. Geomorphology of Mongolian Peoples Republic. Joint Soviet-Mongolian scientific research geological expeditions, Transactions, **28**. pp. 183 Nakau, Moscow, (in Russian).

Garfunkel, Z. & Ron, H. 1985. Block rotation and deformation by strike-slip faults; 2, The properties of a type of macroscopic discontinuous deformation. *Journal of Geophysical Research B*, **90**, 8589-8602.

Gibling, M. R., Nanson, G. C. & Maroulis, J. C. 1998. Anastomosing river sedimentation in the Channel Country of central Australia. *Sedimentology*, **45**, 595-619.

Gierlowski-Kordesch, E. & Rust, B. R. 1994. The Jurassic east Berlin Formation, Hartford Basin, Newark Supergroup (Connecticut and Massachusetts): a saline lake-playa-alluvial plain system. In: Renaut, R. W. & Last, W. M., (eds), Sedimentology and geochemistry of modern and ancient saline lakes. Society for Sedimentary Geology Special Publication, **50**, 249-265.

Gloppen, T. G. & Steel, R. J. 1981. The deposits, internal structure and geometry in six alluvial fan-fan delta bodies (Devonian-Norway) – a study in the significance of bedding sequence in conglomerates. Society for Sedimentary Geology Special Publications, **31**, 49-69.

Graham, S. A., Hendrix, M. S., Barsbold, R., Badamgarav, D., Sjostrom, D., Kirschner, W. & McIntosh, J. S. 1997. Stratigraphic occurrence,



paleoenvironment, and description of the oldest known dinosaur (late Jurassic) from Mongolia. *Palaios*, **12**, 292-297.

Greene, T. J., Carroll, A. R., Hendrix, M. S., Graham, S. A., Warts, M. A. & Abbink, O. A. 2001. Sedimentary record of Mesozoic deformation and inception of the Turpan-Hami Basin, Northwest China. In: Hendrix, M. S. & Davis, G. A. (eds), Palaeozoic and Mesozoic tectonic evolution of Central and Eastern Asia, from continental assembly to intracontinental deformation. Geological Society of America Memoir, **194**, 317-340.

Grunert, J., Lehmkuhl, F. & Walther, M. 2000. Paleoclimatic evolution of the Uvs Nuur basin and adjacent areas (Western Mongolia). *Quaternary International*, **65/66**, 171-192.

Hardie, L. A., Smoot, J. P. & Eugster, H. P. 1978. Saline lakes and their deposits: a sedimentological approach. In: Matter, A. & Tucker, M. E. (eds), Modern and Ancient Lake Sediments: International Association of Sedimentologists Special Publication, **2**, 7-41.

Hartley, A. J. 1993. Sedimentological response of an alluvial system to source area tectonism; the Seilao Member of the Late Cretaceous to Eocene Purilactis Formation of northern Chile. In: Marzo, M. & Puigdefabregas, C. (eds) Alluvial sedimentation. Special Publication of the International Association of Sedimentologists, **17**, 489-500.

Hartley, A. J., Flint, S., Turner, P. & Jolley, E. J. 1992. Tectonic controls on the development of a semiarid alluvial basin as reflected in the stratigraphy of the Purilaetis group (Upper Cretaceous-Eocene), northern Chile. *Journal of South American Earth Sciences*, **5**, 273-294.

Harvey, A. M., Foster, G., Hannam, J. & Mather, A. E. 2003. The Tabernas alluvial fan and lake system, southeast Spain: applications of mineral magnetic and pedogenic iron oxide analysis towards clarifying the Quaternary sequences. *Geomorphology*, **50**, 151-171.

Harvey, A. M. 1988. Controls of alluvial fan development: the alluvial fans of the Sierra de Carraschoy, Murcia, Spain. In Harvey A. M. & Sala, M. (eds),

Geomorphic processes, environments with strong seasonal contrasts, Volume 2, Geomorphic Systems. Catena supplement, **13**, 123-137.

Hendrix, M. S. & Davis, G. A. (eds), 2001. Palaeozoic and Mesozoic tectonic evolution of Central and Eastern Asia, from continental assembly to intracontinental deformation. Geological Society of America Memoir, **194**, 361-388.

Hendrix, M. S., Graham, S. A., Amory, J. Y. & Badarch, G. 1996. Noyon Uul syncline, southern Mongolia: Lower Mesozoic sedimentary record of the tectonic amalgamation of central Asia. *Geological Society of America Bulletin*, **108**, 1256-1274.

Hendrix, M. S., Graham, S. A., Carroll, A. R., Sobel, E. R., McKnight, C. L., Schulein, B. J. & Wang, Z. 1992. Sedimentary record and climatic implications of recurrent deformation in the Tien Shan: Evidence from Mesozoic strata of the north Tarim, south Junggar, and Turpan basins, northwest China. *Geological Society of America Bulletin*, **104**, 53-79.

Hoey, T. B. 1992. Temporal variations in bedload transport rates and sediment storage in gravel-bed rivers. *Progress in Physical Geography*, **16**, 319-338.

Holdsworth, R. E., Butler, C. A. & Roberts, A. M. 1997. The recognition of reactivation during continental deformation. *Journal of the Geological Society*, **154**, 73-78.

Howard J. P., Cunningham W. D., Davies S. J. & Badarch G. 2003. The stratigraphic and structural evolution of the Dzereg Basin, western Mongolia: clastic sedimentation, transpressional faulting and basin destruction in an intraplate, intracontinental setting. *Basin Research*, **15**, 45-72.

Johnson, C. L., Webb, L. E., Graham, S. A., Hendrix, M. S. & Badarch, G. 2001. Sedimentary and structural records of late Mesozoic high-strain extension and strain partitioning, East Gobi basin, southern Mongolia. In: Hendrix, M.S. & Davis, G.A. (eds), Paleozoic and Mesozoic tectonic evolution of central and eastern Asia from continental assembly to intracontinental deformation: Geological Society of America Special Paper, **194**, 413-435.

- Keller, A. M. & Hendrix, M. S. 1997. Paleoclimatologic Analysis of a Late Jurassic Petrified Forest, Southeastern Mongolia. *Palaios*, **12**, 282-291.
- Kelly, S. B. & Olsen, H. 1993. Terminal fans – a review with reference to Devonian examples. *Sedimentary Geology*, **85**, 339-379.
- Khil'ko, S. D., Kurushin, R. A., Kochetkov, V. M., Balzhinnyam, I. & Monkoo, D. 1985. Strong Earthquakes, Paleoseismogeological and Macro seismic data. Nauka, Moscow, 19-83.
- Khosbayer, P. 1973. New Data on Upper Jurassic and Lower Cretaceous Sediments of Western Mongolia. *Academy of Sciences of USSR, Doklady Earth Sciences Section*, **208**, 115-116.
- Komatsu, G., Brantingham, P. J., Olsen, J. W. & Baker, V. R. 2001. Paleoshoreline geomorphology of Böön Tsagaan Nuur, Tsagen Nuur and Orog Nuur: the Valley of Lakes, Mongolia. *Geomorphology*, **39**, 83-98.
- Kraemer, B., Adelman, D., Alten, M., Schnurr, W., Erpenstein, K., Kiefer, E., van den Bogaard, P. & Görler, K. 1999. Incorporation of the Paleogene foreland into the Neogene Puna plateau: The Salar de Antofalla area, NW Argentina. *Journal of South American Earth Sciences*, **12**, 157-182.
- Kraus, M. J. & Brown, T. M. 1988. Pedofacies analysis; A new approach to reconstructing ancient fluvial sequences. In: Reinhart J. & Sigleo W. R. (eds) *Paleosols and Weathering through Geologic Time*, Geological Society of America Special Paper, **216**, 143-152.
- Leeder, M. R. 1999. *Sedimentology and sedimentary basins: from turbulence to tectonics*, Blackwell, Oxford, pp 608.
- Lehmkhul, F., Haselein, F. 2000. Quaternary paleoenvironmental change on the Tibetan Plateau and adjacent areas (Western China and Western Mongolia). *Quaternary International*, **65/66**, 121-145.
- Lehmkhul, F. (1998) Quaternary Glaciations in Central and Western Mongolia. In: Owen, L.A. (Ed): *Mountain Glaciations. Quaternary Proceedings*, **6**, 153-167.

- Link, M. H. & Osbourne, R. H. 1978. Lacustrine facies in the Pliocene Ridge Basin Group: Ridge Basin, California. In: Matter, A. & Tucker, M. E. (eds), *Modern and Ancient Lake Sediments: International Association of Sedimentologists Special Publication*, **2**, 7-41.
- Lowe, D. R. 1975. Water escape structures in course-grained sediments, *Sedimentology*, **22**, 157-204.
- Machette, M. N. 1985. Calcitic soils of the south-western United States. *Geological Society of America Special Paper*, **203**, 1-21.
- Mack, G. H. & James, W. C. 1994. Paleoclimate and the global distribution of plaeosols. *Journal of Geology*, **102**, 360-366.
- Mack, G. H., James W.C., Monger, H. C. 1993. Classification of paleosols. *Geological Society of America Bulletin*, **105**, 129-136.
- Mack, G. H., Cole, D. R., Giordano, T. H., Schaal, W. C. & Barcelos, J. H. 1991. Paleoclimatic controls on stable oxygen and carbon isotopes in caliche of the Abo Formation (Permian) south-central New Mexico, USA. *Journal of Sedimentary Petrology*, **61**, 458-472.
- Macqueen, R. W. & Leckie, D. A. 1992. Foreland Basins and Fold Belts. *American Association of Petroleum Geologists Memoir*, **55**, pp 460.
- Mann, P., Draper, G. & Lewis, J. F., 1991. An overview of the geologic and tectonic development of Hispaniola. In: P. Mann, G. Draper & J.F. Lewis (Eds), *Geologic and Tectonic Development of the North America-Caribbean Plate Boundary in Hispaniola*. *Geological Society of America Special Paper* **262**, 1-28.
- Mann, P., Hempton, M. R., Bradley, D. C. & Burke, K. 1983. Development of pull-apart basins. *Journal of Geology*, **91**, 529-554.
- Mann, P. & Burke, K. 1982. Basin formation at intersections of conjugate strike-slip faults; examples from southern Haiti. *The Geological Society of America*, 95<sup>th</sup> annual meeting Abstracts with programs, page 14, (summary only).

- Masclé, A., Puigdefàbregas, C., Luterbacher, H. P. & Fernández, M. (eds) 1998. Cenozoic Foreland Basins of Western Europe. Geological Society, London, Special Publication, **134**, pp 400.
- McClay, K. & Bonora, M. 2001. Analog models of restraining stepovers in strike-slip fault systems. *American Association of Petroleum Geologists Bulletin*, **85**, 233-260.
- McKnight, C. L., Graham, S. A., Carroll, A. R., Gan, Q., Dilcher, D. L., Zhao, M. & Liang, Y. H. 1990. Fluvial sedimentology of an Upper Jurassic petrified forest, Shishu Formation, Junggar Basin, Xinjiang, China. *Palaeogeography, Palaeoclimatology, Palaeoecology*, **79**, 1-9.
- Meng, Q. 2003. What drove late Mesozoic extension of the northern China-Mongolian tract?. *Tectonophysics*, **369**, 155-174.
- Miall, A.D. 1996. The Geology of Fluvial Deposits: Sedimentary Facies, Basin Analysis, and Petroleum Geology, Springer, Berlin, pp 582.
- Miller, K. C. & Meltzer, A. S. 1995. Structure and tectonics of the offshore central Santa Maria and Santa Lucia Basins, California: Results from the PG&E/EDGE seismic reflection survey. In: Keller, M. A. (ed), Evolution of sedimentary basins/onshore oil and gas investigations – Santa Maria Province. United States Geological Survey Bulletin, 1995, chapter Z.
- Namson, J. S. & Davies, T. L. 1988. Seismically active fold and thrust belt in the San Joaquin Valley, central California. *Geological Society of America Bulletin*, **100**, 257-273.
- Nanson, G. C., Young, R. W., Price, D. M. & Rust, B. R. 1988. Stratigraphy, sedimentology and late-Quaternary chronology of the Channel Country of western Queensland. In: Warner, R. F. (ed), Fluvial geomorphology of Australia, Academic Press, London, 151-175.
- Nanson, G. C., Rust, B. R. & Taylor, G. 1986. Coexistent mud braids and anastomosing channels in an arid-zone river: Cooper Creek, central Australia. *Geology*, **14**, 175-178.



- Natsagdorj, L., Jugder, D. & Chung, Y. S. 2003. Analysis of dust storms observed in Mongolia during 1937-1999. *Atmospheric Environment*, **37**, 1401-1411.
- Nemec, W. & Postma, G. 1993, Quaternary alluvial fans in southwestern Crete; sedimentation processes and geomorphic evolution. In: Marzo, M. & Puigdefabregas, C. (eds) Alluvial sedimentation, International Association of Sedimentologists, Special Publication, **17**, 235-276.
- Nemec, W. & Steel, R. J. 1984. Alluvial and coastal conglomerates; their significant features and some comments on gravelly mass-flow deposits. In: Koster, E. H. & Steel, R. J. (eds) Sedimentology of gravels and conglomerates, Canadian Society of Petroleum Geologists, Calgary. 1-31.
- Nilsen, T. H., Sylvester, A. G. 1995. Strike-slip basins. In: Busby, C. J. & Ingersoll, R. V. (eds) Tectonics of Sedimentary Basins. Blackwell, Oxford, 425-457.
- Olsen, P. E. 1991. Tectonic, climatic and biotic modulation of lacustrine ecosystems-examples from the Newark Supergroup of eastern North America. In: Katz, B. J. (ed), Lacustrine Basin Exploration, American Association of Petroleum Geologists Memoir, **50**, 209-224.
- Ori G.G. & Friend P.F. 1984. Sedimentary basins formed and carried piggy-back on active thrust sheets. *Geology*, **12**, 475-478.
- Parkash, B., Awasthi, A.K. and Gohain, K. 1983. Lithofacies of the Markanda river terminal fan, Kurukshetra District, Haryana. International Association of Sedimentologists Special Publication, **6**, 337-344.
- Parrish, J. T. 1993. Climate of the supercontinent Pangea. *Journal of Geology*, **101**, 215-233.
- Parrish, J. T. & Curtis, R. L. 1982. Atmospheric circulation, upwelling, and organic-rich rocks in the Mesozoic and Cenozoic eras. *Palaeogeography, Palaeoclimatology, Palaeoecology*, **40**, 31-66.
- Parrish, J. T., Ziegler, A. M. & Scotese, C. R. 1982. Rainfall patterns and the Distribution of coals and evaporates in the Mesozoic and Cenozoic. *Palaeogeography, Palaeoclimatology, Palaeoecology*, **40**, 67-101.

- Postma, G. & Roep, T. B. 1985. Resedimented conglomerates in the bottomsets of Gilbert-type gravel deltas. *Journal of sedimentary petrology*, **55**, 874-885.
- Prokopenko, A. A., Karabanov, E. B., Williams, D. F. Kuzmin, M. I., Khursevich, G. K. & Gvozdkov, A. A. 2001. The link between tectonic and paleoclimatic events at 2.8-2.5 Ma BP in the Lake Baikal region. *Quaternary International*, **80-81**, 37-46
- Qu, G. & Zhang, J. 1994. Oblique thrust systems in the Altai orogen, China. *Journal of southeast Asian Earth Sciences*, **9**, 277-287.
- Rasnitsyn, A. P. (1985) Fossil insects of Siberia and Mongolia Moscow, Rossiyskaya Akademiya Nauk, Paleontologicheskii Institut, USSR, 103-120 (in Russian).
- Reading, H. G. 1980. Characteristics and recognition of strike-slip fault systems. In: Balance, P. F. & Reading, H. G. (eds) Sedimentation in Oblique-slip Mobile Zones, International association of Sedimentologists Special Publication, **4**, 7-26.
- Rentschler, M. (1986) Transpressional Piggyback Basin in Southern Diablo Range, California. *American Association of Petroleum Geologists Bulletin*, **70**, 476-477 (summary only).
- Retallack, G. 1988. Field recognition of paleosols, in: Reinhart, J. & Sigleo, W. R. (eds) Paleosols and Weathering through Geologic Time, Geological Society of America Special Paper, **216**, 1-20.
- Rust, B. R. & Nanson, G. C. 1989. Bedload transport of mud as pedogenic aggregates in modern and ancient rivers. *Sedimentology*, **36**, 291-306.
- Ryang W. H. & Chough S.K. 1997. Sequential development of alluvial/lacustrine system: Southeastern Eumsung Basin (Cretaceous), Korea. *Journal of Sedimentary Research*, **67**, 274-285.
- Sáez, A. & Cabrera, L. 2002. Sedimentological and palaeohydrological responses to tectonics and climate in a small, closed, lacustrine system: Oligocene As Pontes Basin (Spain), *Sedimentology*, **49**, 1073-1094.

- Sanz, M. E., Rodríguez-Aranda, J. P., Calavo, J. P. & Ordóñez, S. 1994. Tertiary detrital gypsum in the Madrid Basin, Spain: criteria for interpreting detrital gypsum in continental evaporitic sequences. In: Renaut, R. W. & Last, W. M. (eds), *Sedimentology and geochemistry of modern and ancient saline lakes*. Society for Sedimentary Geology Special Publication, **50**, 249-265.
- Schlupp, A. 1996. Neotectonique de la Mongolie occidentale analysee a partir de donnees de terrain, seismologiques et satellitaires. PhD Thesis, Universite Louis Pasteur Ecole et Observatoire de Physique du Globe de Strasbourg, pp 172 (in french).
- Sengör, A. M. C., Natalin, B. A. & Burtman, V. S. 1993. Evolution of the Altaid tectonic collage and Paleozoic crustal growth in Eurasia. *Nature*, **364**, 299-307.
- Shuvalov, V.F. 1969. Continental red beds of the upper Jurassic of Mongolia. *Doklady Akademii Nauka, Moscow*, **189**, 1088-1091.
- Sjostrom, D. J. 2001. Sedimentology and provenance of Mesozoic nonmarine strata in western Mongolia: a record of intracontinental deformation. In: *Palaeozoic and Mesozoic tectonic evolution of Central and Eastern Asia: from continental assembly to intracontinental deformation*. In: Hendrix, M. S. & Davis, G. A. (eds), *Palaeozoic and Mesozoic tectonic evolution of Central and Eastern Asia, from continental assembly to intracontinental deformation*. Geological Society of America Memoir, **194**, 361-388.
- Sjostrom, D. J. 1997. Lower-Middle Jurassic through Lower Cretaceous sedimentology, stratigraphy, and tectonics of western Mongolia, Masters thesis, The University of Washington, pp 189.
- Smoot J. P. & Lowenstein T. K. 1991. Depositional environments of non-marine evaporates. In: Melvin, J. L. (ed), *Evaporites, Petroleum and Mineral Resources*, Elsevier, Amsterdam, 189-347.
- Sorlien, C. C., Nicholson, C. & Luyendyk, B. P. 1995 Miocene extension and post-Miocene transpression offshore of South Central California. . In: Keller, M. A. (ed), *Evolution of sedimentary basins/onshore oil and gas investigations –*

Santa Maria Province. United States Geological Survey Bulletin, 1995, chapter Z.

Stear, W. 1985. Comparison of the Bedform Distribution and dynamics of Modern and Ancient Sandy ephemeral Flood Deposits in the Southwestern Karoo Region, South Africa. *Sedimentary Geology*, **45**, 209-230.

Summerfield, M. A. 1991. Global Geomorphology, Longman, Harlow, pp 537.

Sun, J. 2002. Provenience of loess material and formation of loess deposits on the Chinese Loess Plateau. *Earth and Planetary Science Letters*, **302**, 845-859.

Talbot, M. R., Holm, K. & Williams, M. A. J. 1994. Sedimentation in low-gradient desert margin systems; a comparison of the Late Triassic of Northwest Somerset (England) and the late Quaternary of east-central Australia. In: Rosen M. R. (ed) Paleoclimate and basin evolution of playa systems, Geological Society of America Special Paper, **289**, 97-117.

Tapponnier, P. & Molnar, P. 1979. Active Faulting and Tectonics of the Tien Shan, Mongolia and Baykal Regions. *Journal of Geophysical Research*. **84**, 3425-3459.

Thomas, J. C., Lanza, R., Kazansky, A., Zykin, V., Semakov, N., Mitrokhin, D. & Delvaux, D. 2002. Paleomagnetic study of Cenozoic sediments from the Zaisan basin (SE Kazakhstan) and the Chuya depression (Siberian Altai): tectonic implications for central Asia. *Tectonophysics*, **351**, 119-137.

Thomas, J. C., Cobbold, P. R., Wright, A. & Gapais, D. 1996. Cenozoic tectonics of the Tadzhik depression, Central Asia. In: Yin, A. & Harrison, T. M. (eds), The Tectonic Evolution of Asia, Cambridge University Press, Stanford, 191-207.

Togtoh, B. & Baatarhuyag, A. 1991. Open-File report of the Tonhil mapping project, Ulaan Baatar, pp 59 (In Mongolian).

Tomurtogoo, O. (ed.) 1999, Geological map of Mongolia. scale 1:1 000 000, Nauku, Moscow.

- Traynor, J.J. & Sladen, C. 1995. Tectonic and stratigraphic evolution of the Mongolian People's Republic and its influence on hydrocarbon geology and potential. *Marine and Petroleum Geology*, **12**, 35-52.
- Truc, G. 1978. Lacustrine sedimentation in an evaporitic environment: the Ludian (Palaeogene) of the Mormoiron basin, southeastern France. In: Matter, A. & Tucker, M. E. (eds), *Modern and Ancient Lake Sediments*. International Association of Sedimentologists Special Publication, **2**, 7-41.
- Tunbridge, I. P. 1981. Sandy High-Energy Flood Sedimentation - Some Criteria for Recognition, with an example from the Devonian of S.W. England. *Sedimentary Geology*, **28**, 79-95.
- Turner, B. R. & Munro, M. 1987. Channel formation and migration by mass-flow processes in the Lower Carboniferous fluviatile Fell Sandstone Group, northeast England. *Sedimentology*, **34**, 1107-1122.
- Turner, P. 1980. Continental red beds. *Developments in sedimentology*, **29**, Elsevier Scientific, Amsterdam, pp 562.
- Vincent, S. J. & Allen, M. B. 2001. Sedimentary record of Mesozoic intraxcontinental deformation in the eastern Junggar Basin, northwest China: Response to orogeny at the Asian Margin. In: Hendrix, M. S. & Davis, G. A. (eds), *Palaeozoic and Mesozoic tectonic evolution of Central and Eastern Asia, from continental assembly to intracontinental deformation*. Geological Society of America Memoir, **194**, 345-363.
- Vincent, S. J. & Allen, M. A. 1999. Evolution of the Milne and Chaoshui Basins, China: Implications for Mesozoic strike-slip basin formation in Central Asia. *Geological Society of America Bulletin*, **111**, 725-742.
- Webb, L. E., Graham, S. A., Johnson, C. L., Badarch, G. & Hendrix, M. S. 1999. Occurrence, age, and implications of the Yagan-Onch Hayrhan metamorphic core complex, southern Mongolia. *Geology*, **27**, 143-146.
- Whipple, K. X. & Dunne, T. 1992. The influence of Debris-flow rheology on fan morphology, Owens Valley, California. *Geological Society of America Bulletin*, **104**, 887-900.



- Williams, G. E. 1971. Flood Deposits of the sandbed ephemeral streams of central Australia. *Sedimentology*, **17**, 1-40.
- Willis, B. 1928. Dead Sea problem: rift valley or ramp valley? *Geological Society of America Bulletin*, **39**, 490-542.
- Windley, B. F., Kröner, A., Guo, J., Qu, G., Li, Y., Zhang C. 2002. Neoproterozoic to Paleozoic geology of the Altai orogen, NW China: new zircon age data and tectonic evolution. *Journal of Geology*, **110**, 719-737.
- Wizevich, M. C. 1992. Sedimentology of Pennsylvanian quartzose sandstones of the Lee Formation, central Appalachian Basin: fluvial interpretation based on lateral profile analysis. *Sedimentary Geology*, **78**, 1-47.
- Wright, V. P. 1992. Paleopedology: Stratigraphic relationships and empirical models. In: Martini I. P. & Chesworth W. (eds), *Weathering Soils and Paleosols*, Elsevier, Amsterdam, 475-499.
- Yeats, R. S., Huftile, G. J. & Stitt, L. T. 1994. Late Cenozoic Tectonics of the East Ventura Basin, Transverse Ranges, California. *American Association of Petroleum Geologists Bulletin*, **78**, 1040-1074.
- Yin A. & Harrison T. M. 1996. *The Tectonic Evolution of Asia*. Cambridge University Press. Cambridge, pp 666.
- Young, A. A. 1993, Sheetflood sedimentology and stratigraphy of the middle Proterozoic Revett Formation, Scotchman Peak proposed wilderness area, Montana. Unpublished Masters Thesis, University of Montana pp 345.
- Zaitsev, N.S. 1978. Geological Map of the Mongolian Altai, scale 1:500 000. Combined Soviet-Mongolian Scientific Research Geological Expeditions, Nakau, Moscow, (In Russian).
- Zhang, ZH. M., Liou, J. G. & Coleman, R. G. 1984. An outline of the plate tectonics of China. *Geological Society of America Bulletin*, **95**, 295-312.
- Zoback, M. L. 1992. First- and second-order patterns of stress in the lithosphere: the world stress map project. *Journal of Geophysical Research*, **97**, 11703-11711.

Zoetemeijer, R, Cloetingh, S., Sassi W. & Roure, F. 1993. Modelling of piggyback-basin stratigraphy - record of tectonic evolution. *Tectonophysics*, **226**, 253-269.

# Appendix 1 – Fauna reported from western Mongolian Mesozoic and Cenozoic strata.

Yellow Sandstone Unit. Equivalent to the lower Cretaceous Gurvan Ereen Formation (J <sub>3</sub> -K <sub>1</sub> )		Lower Red Bed Unit and Western Red Bed Unit. Equivalent to the lower Cretaceous Dzereg Formation (K <sub>1</sub> )		Oasis Unit. Equivalent to the Oligocene Beger Suite (P <sub>1-2</sub> )	Tan Conglomerate Unit/ Lower Yellow Conglomerate Unit. Equivalent to the Miocene Oshin Suite (N <sub>1-2</sub> ).	Upper Red Bed Unit/ Upper Yellow Conglomerate Unit and Grey Conglomerate Unit. Equivalent to the Pliocene Altan-teel suite and the lower Pleistocene Goshu Formation (N <sub>1-2</sub> and Q <sub>1</sub> )	
<b>Dzereg Locality Mollusca</b> (Devjatkin <i>et al.</i> , 1975)  Leptesthes (?) bahatiriensis Jak. Valvata sp. Limnocyrena reissi Kol. L. reggens sp. nov. Limnocyrena sp. Cypridea consulta Mand. C. trita Lub. C. zugustaica Scoblo Darwinula sp. Rhinocypris sp. Bairdestheria sinensis (Chi.) Eumograptia pseudoinsperta Step. E. haranurensis Step. Loxopolygrapta zargaica Step. Bairdestheria dahurica Tschern. B. cf. chekiangensis sp. nov. Pseudestheria sp.  <b>Dariv Locality Konhostraca</b> (Devjatkin <i>et al.</i> , 1975)  Bairdestheria middendorffii Jones B. sinensis (Chi.) Liograptia (Kob. Et Kus.)	Palaeoleptestheria wolchonini Nov. P. Baicalia Kras. P. legiminiformis Kras. P. gurbanerensis Step. Palaeoleptestheria sp.  <b>Ostracoda</b> (Devjatkin <i>et al.</i> , 1975)  Daurina mongolica sp. nov. Cypridea vitimensis Mand. C. trita Lub. C. zugustaica Scoblo Mongolionella palmosa Mand. Lycoperocypris sp. Rhinocypris potanini (Gal.)  <b>Fish</b> (Devjatkin <i>et al.</i> , 1975)  Stichopterus popovi sp. nov. Gurvanichthys mongolicus sp. nov.  <b>Insecta</b> (Rasnitsyn, 1985)  Ostracindusia biassica Suk. Corixonesta hosbajari sp. nov. Secrindusia translucens Suk. Baissocovixa Jacjewski J. Pop.	<b>Dzereg Locality Mollusca</b> (Devjatkin, 1981)  Unio tudagoensis Jak Limnocyrena anderssoni pusilla subsp. nov. L. zergensa Limnocyrena sp. Valvata cf. mongolica V. subpiscinalis Leptesthes (?) bahatiriensis Jak  <b>Dariv locality Mollusca</b> (Devjatkin <i>et al.</i> , 1975)  Unio tsentahozensis Jak. U. hangaensis Jak. U. cf. Hangaensis Jak. U. tudagoensis Jak. Leptesthes (?) bahatiriensis Jak. Limnocyrena anderssoni pusilla (Grab.) sub. Sp. nov. L. zergensa Martins. L. anderssoni longa (grab.) sub. sp. nov. Valvata subpiscinalis Martins. V. mongolica sp. nov. Probaicalia vitimensis Martins. P. gerassimovi (Reis.) Bithynia laeochioidea Martins. Guraulus sp. Konhostraca-Bairdestheria dahurica (Tschern.).	<b>Ostracoda</b> (Devatkin <i>et al.</i> , 1975)  Darwinula ex gr. Oblonga (Roemer) D. ex gr. Contracta Mand. D. contracta Mand Cypridea zacustaica Scoblo C. ex gr. Trita Lub. C. tuberculisperga Gal. C. ex gr. Vitimensis Mand. C. gurbanensis Sinita. C. prognata Lub. Cytheridae gen. nov. Rhinocypris ex gr. Jurassica (Mart.) R. ex gr. barunbainensis (Lub.) R. ex gr. tugurigenensis (Lub.) R. potanini (Gal.) Timiriasevia sp.  <b>Insecta</b> (Rasnitsyn, 1985)  Ostracindusia modesta Suk. O. biassica Suk. O. onusta Suk. O. conchifera Suk. Pelindusa ostracifera Suk. P. minae Suk Cristocorixa gurbanica sp. nov.	<b>Dzereg locality Mammalia</b> (Devjatkin, 1981)  Cylindrodontitae Cricetidae Rhizomyidae Ctenodactylidae	<b>Dzereg Locality Mammalia</b> (Devjatkin 1981)  Lagomerycinae gen.? Cervulinia gen.? Baluchitherium mongoliensis Osb. Serridentinus gobiensis Osb Begertherium borissiakii (?) Gomphotheriidae gen.? Elasmotheriinae and Begertheriinae Gazella paotehensis Gervidae Rhinocerotidae Chelonia Iranotherium sp.?  <b>Upper sub suite Mammalia</b> (Devjatkin (1981) Gomphotheriidae gen.? Hipparion theobaldi nagrinis Hipparion mongolicum Elasmotheriinae gen.? Chilootherium sp. Oshinootherium orlovi Crocuta sp. Gazella sp. Chilootherium sp. Hipparion mongolicum Tragoceras sp. Samotherium sp. Gazella mongolica Oioceros sp.  <b>Aves</b> (Devjatkin (1981) Struthio	<b>Valley of lakes and Dzereg localities Mammalia</b> (Devjatkin 1981)  Zygolophodon borzoni Hipparion cf. teobaldi nagriensis Gazella sp. G. paotehensis  <b>Mammalia</b> (Devjatkin, 1981) Chiloterium sp. Hipparion placodus H. hippidioidus Crocuta gigantean Ichitherium sp. Hipparion teobaldi mogoicum H. placodus Chilootherium wimani Sinotherium sp. Samotherium mongoliense Tragoceras sp. Gazella gaudry G. paotehensis Gazelle sp. Palaeoryx sp. Cervavitus sp. Parahizomys hipparionum Sinohippus sp. Proboscidea gen. Hipparion hippidioidus Chelonia sp.	<b>Reptilia</b> (Devjatkin, 1981) Geocheloné askarkuhne

## Appendix 2

Table 1 - Stages of carbonate accumulation in palaeosols, from Retallack, 1988.

Stage	Paleosols Developed in Gravel	Paleosols Developed in Sand, Silt, or Clay
I	Thin, discontinuous coatings of carbonate on underside of clasts	Dispersed powdery and filamentous carbonate
II	Continuous coating all around, and in some cases, between clasts; additional discontinuous carbonate outside main horizons	Few to common carbonate nodules and veinlets, with powdery and filamentous carbonate in places between nodules
III	Carbonate forming a continuous layer enveloping clasts; less pervasive carbonate outside main horizon	Carbonate forming a continuous layer formed by coalescing nodules; isolated nodules and powdery carbonate outside main horizon
IV	Upper part of solid carbonate layer with a weakly developed platy or lamellar structure, capping less pervasively calcareous parts of the profile	
V	Platy or lamellar cap to the carbonate layer strongly expressed; in places brecciated and with pisolites of carbonate	
VI	Brecciation and recementation, as well as pisolites common in association with the lamellar upper layer	

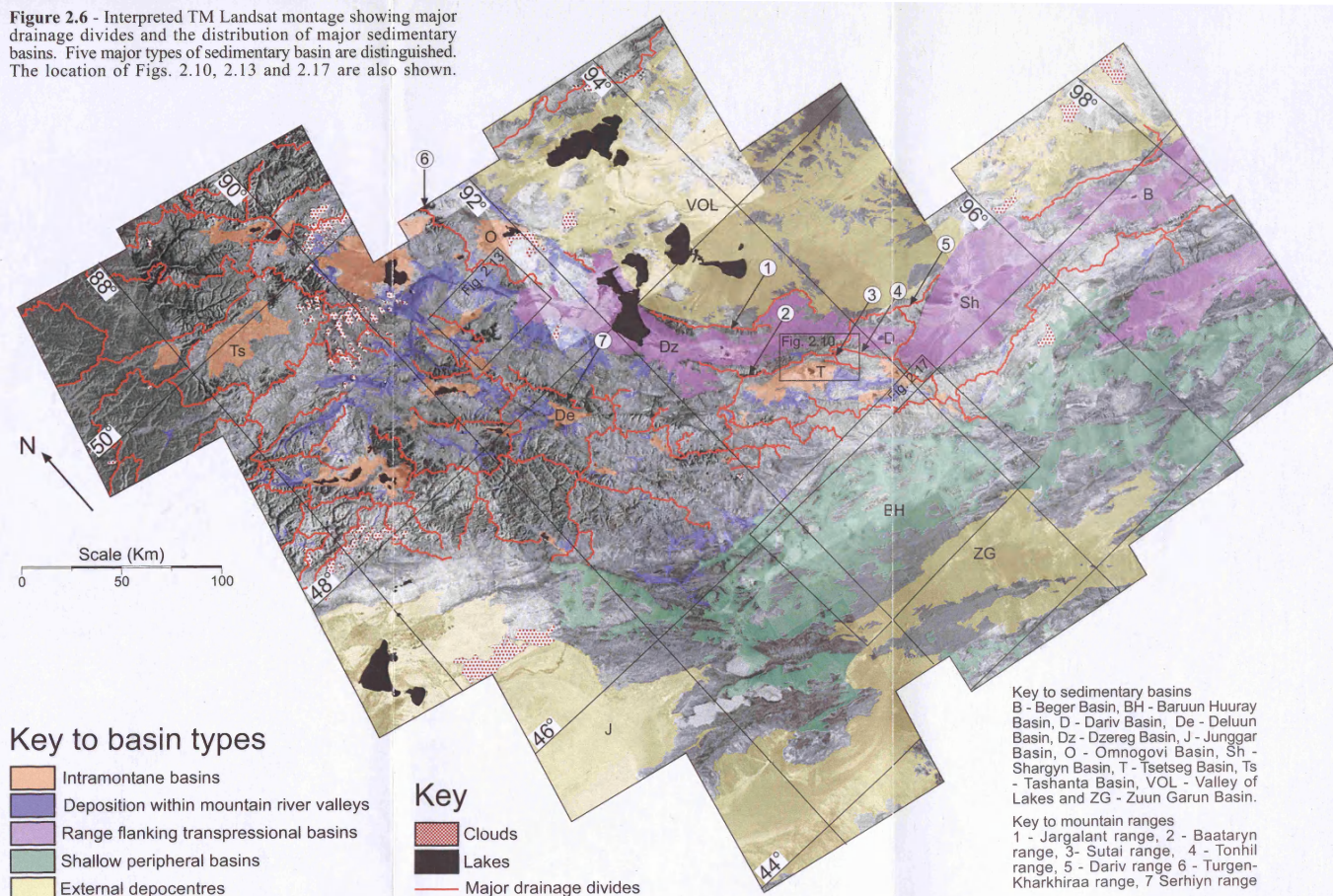
*Note:* This table includes modifications (Machette, 1985) to the scheme proposed by Gile and others (1966).

Table 2 - A short and superficial key to soil orders of the U. S. Department of Agriculture for field identification of palaeosols, from Retallack, 1988.

Features	Order
<b>If paleosol has:</b>	<b>It may be a(n):</b>
• Abundant swelling clay (mainly smectite) to a presumed uncompacted depth of 1 m or to a bedrock contact, together with hummock and swale structure (mukkaru), especially prominent slickensides or clastic dikes	Vertisol
• No horizons diagnostic of other orders, and very weak development (Table 5)	Entisol
• No horizons diagnostic of other orders, but weak development (Table 5)	Inceptisol
• Light coloration (high Munsell value), thin calcareous layer (calcic horizon) close to surface of profile and developed to stage II or more (Table 4), or evidence of pedogenic gypsum or other evaporite minerals	Aridisol
• Organic (but not carbonaceous or coaly), well-structured (usually granular) surface (A) horizon ( <i>mollic epipedon</i> ), usually with evidence of copious biological activity (such as abundant fine root traces and burrows) and with subsurface horizons often enriched in carbonate, sometimes enriched in clay	Mollisol
• Surface organic (O) horizon of carbonaceous shale, peat, lignite, or coal ( <i>histic epipedon</i> ) originally (before compaction) at least 40 cm thick	Histisol
• Thick, well-differentiated (A, Bt, and C horizons) profile, with subsurface (Bt) horizon appreciably enriched in clay ( <i>argillic horizon</i> ) and often red with sesquioxides or dark with humus, and also with evidence (such as effervescence in acid or calcareous nodules or abundance of easily weathered minerals such as feldspar) for high concentrations of nutrient cations (such as Ca <sup>++</sup> , Mg <sup>++</sup> , Na <sup>+</sup> , and K <sup>+</sup> )	Alfisol
• Thick, well-differentiated (A, Bt, and C horizons) profile, with subsurface (Bt) horizon appreciably enriched in clay ( <i>argillic horizon</i> ) and often red with sesquioxides or dark with humus, but also with evidence (such as lack of reaction with acid or abundant quartz or kaolinite) for low concentrations of nutrient cations	Ultisol
• Thick, well-differentiated (A, Bs, and C horizons), with sandy subsurface (Bs or Bh) horizon cemented with opaque iron or aluminum oxyhydrates or organic matter ( <i>spodic horizon</i> ), and always with little or no clay or carbonate	Spodosol
• Thick, well-differentiated to uniform profile, clayey texture, with subsurface horizons highly oxidized and red, and almost entirely depleted of weatherable minerals ( <i>oxic horizon</i> )	Oxisol

*Note:* This key has been simplified for field observation. Precise identification of soils and their diagnostic horizons requires laboratory work and careful reference to Soil Survey Staff (1975).

**Figure 2.6** - Interpreted TM Landsat montage showing major drainage divides and the distribution of major sedimentary basins. Five major types of sedimentary basin are distinguished. The location of Figs. 2.10, 2.13 and 2.17 are also shown.





**Figure 2.4** - Interpreted TM Landsat montage showing major Cenozoic faults and known kinematics. Interpretation based on image analysis (Cunningham pers comm 2003, Cunningham *et al.*, 1996b), ground truthing and historical seismicity (Baljinnyam *et al.*, 1993).

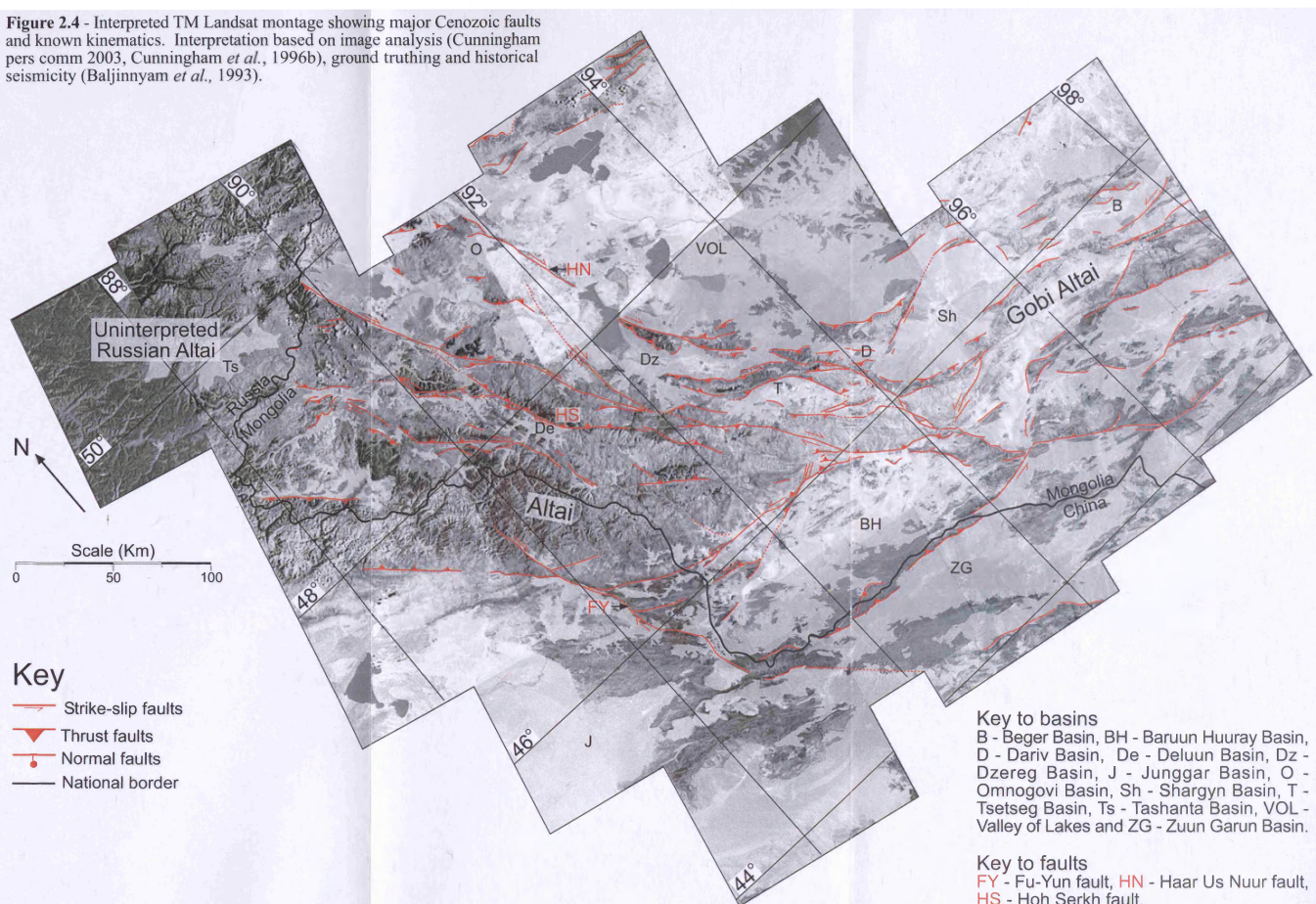


Table 3.1/4.1 – Facies chart for major stratigraphic units identified in the Dzereg, Dariv and Shargyn basins.

Facies	Description	Process	Interpretation
AC	Erosive base. Laterally extensive pebble sheets, massive or upward fining, clast supported and <60 cm thick. Occasional lamination or cross-stratification.	Fining upward indicates waning flow during deposition and lateral extent suggests a broad unconfined flow. Usually associated with Facies AF.	Coarse sheetflood deposit. Massive beds may be hyperconcentrated gravity flow deposits
AF	Sharp, often erosive base. Occasional basal pebble/granule lag overlain by a fining upward sandstone succession. Some/all of a characteristic vertical sequence of sedimentary structures: Laminiae, planar or trough-cross stratification, laminae, massive sandstone. Upper surface may be rippled. Associated with facies EF/EC.	Basal lamination representing upper phase flow overlain by fining upwards sandstone and structures characteristic of waning flow.	Sheetflood deposit.
BC	Massive clast-supported cobble/pebble conglomerate with some interbedded sandstone. Laterally extensive <3 m thick. Rare normal grading. Interbedded with facies AF.	Lateral migration of a cobble dominated channel system. Reworking of sedimentary structures and little preservation of overbank material (Facies AF and EF).	Deposits of a coarse bedload braided river system on a fluvial or alluvial fan.
BF	Massive laterally extensive pebble conglomerate and sandstone sheets with many internal erosion surfaces. Abundant imbrication and cross-stratification and occasional normal grading.	Variable clast size and complex internal structure results from the migration of channel macroforms within a braided gravel-bed river system.	Deposits of a braided river system.
C	15-30 cm thick pebble conglomerate with minor erosive bases and rare cross-stratification. Grade laterally into coarse sandstone. No internal erosion surfaces.	Coarse sediment deposited over the floodplain during a flood event. Slightly channelised base indicated more confined flow than facies AF and AC.	Crevasse splay deposit.
D	Well-defined channels containing clast supported pebbles (rarely cobbles) that fine up between internal erosion surfaces. Interbedded with sandstone sheets. Cross-stratification, lamination and deformation of underlying strata are common. Occasional silt (facies EF) drapes.	Bedload gravel and sand transport in a fluvial system with variable discharge. Gravel and sandstone bodies record the migration of bedforms. Intermittent siltstone (facies EF) horizons indicate flow was ephemeral.	Deposits of an ephemeral, sinuous mixed-load river. Massive beds may represent hyperconcentrated flood gravels.
EF	Intermittently laminated siltstones and rare mudstones. Containing organic material. Large colour variations.	Slow setting of silt from suspension after inundation of the floodplain. Primary lamination is commonly reworked by bioturbation and rooting. Colour variation records hydromorphic processes in action on the floodplain.	Overbank deposits.
EC	Massive silt-rich sandstone or sand-rich siltstone sheets often containing matrix-supported granules.	Deposition either by (1) transport of clay within fluvial systems as sand-grade aggregates (Nanson <i>et al.</i> , 1988; Talbot <i>et al.</i> , 1994), where post depositional breakdown of the aggregates produces a matrix supported sand rich siltstone (2) muddy debris flow (3) reworking of interbedded sandstone and siltstone by bioturbation. These options cannot be distinguished without microscopic analysis of the sediment.	Overbank deposits or debrites.
F	Lenticular sand sheets containing extensive cross-stratification that are laterally extensive over 100's m. > 1 m high foresets are mantled with pebbles and granules with occasional pebble sheets.	Migration of sand-bed channel. Cross-stratification represents both the migration of 3D bedforms and preservation of bank attached foresets resulting in a broad range of measured palaeocurrent.	Deposits of a high sinuosity sand bed river system.
G	Coarsening upward clast supported granule/pebble or pebble/cobble conglomerate.	Deposit of a wet or hyperconcentrated debris flow from which the matrix drained after deposition.	Hyperconcentrated gravity flow deposits.
H	Pebbles and granules supported in a fine sand or siltstone matrix. Massive or coarsening upward.	Cohesive debris flow in which large grains are carried by a dense matrix.	Cohesive debris flow deposit.
I	Sandstone dominated sheets that fine upward from an occasionally pebbly base and contain structures indicating waning flow. Dish and pillar structures or laminations form the upper part of beds. Massive beds are rare and contain evidence of burrowing. Commonly interbedded with lacustrine fines (Facies J & K).	Fining upward with a structure indicative of waning flow suggests the influx of coarse sediment into a lake as an individual flood event. This facies represents sheetflood facies AF entering a lake.	Deposits of a sheetflood entering a lake.
J	Very well laminated siltstone and claystone often showing fine variations between lamina. Individual laminations have a large lateral extent in good exposure. Can be associated with gypsum horizons.	Slow settling of silt or clay particles from suspension in the water column. Background sedimentation with the variation in lamination picking out periodic changes in climate or water column composition. Lack of bioturbation put down to anoxic bottom waters or elevated salinity. Gypsum horizons are precipitated from concentrated water, water concentration varies.	Lacustrine deposits recording conditions hostile to burrowing benthic organisms.
K	Massive siltstone and claystone, occasionally micritic. Sometimes associated with gypsum horizons.	Reworked lacustrine sediments often associated with gypsum. Lamination removed by either sub-aqueous burrowing – suggesting conditions supported benthic life or sub aerial exposure, often difficult to establish which. Gypsum deposited during concentration of water by evaporation.	Lacustrine deposits reworked by burrowing organisms or hydromorphic processes.
Facies association L	LA Coarsening upwards interbedded sandstone and laminated, massive or bioturbated siltstone. Sand beds have sharp planar bases.	Distal influence of prograding fluvial system into lacustrine environment. Preservation of lamination implies anoxic conditions. Bioturbated or massive siltstones suggest oxic conditions.	Prodelta deposits.
	LB Massive or coarsening upward sandstone with low-angle planar lamination or cross-stratification. Commonly affected by small-scale soft sediment deformation e.g. dish and pillar structures and minor slumping.	Deposition of sandstone over the delta surface. Slumping and dish and pillar structures form due to loading of saturated prodelta sediments.	Delta front deposits.
	LC Large (>1 m) trough cross-stratified sandstone beds with erosive bases, often with lag surfaces and occasional siltstone drapes.	The migration of mouth bars close to the mouth of the fluvial system. Silt drapes suggest periodic pauses in fluvial input, possibly seasonal.	Mouth bar deposits.
	LD Ripple cross-stratified sandstone with a coarse lag surface, commonly bioturbated.	Reworking of abandoned delta surface by wind derived currents into ripples etc. Lag surface results from continual reworking of sediment and winnowing of coarse fraction. Bioturbation affects the surface if it is exposed for extended periods.	Reworked delta top deposits.
	LE Erosive based conglomerate sheets and interbedded fine sediment (Facies EF). Commonly hard and resistant to erosion due to intensive caliche formation.	Sub aerial deposits on the delta top. Laterally extensive channels reflect channel migration and the extensive carbonate concretion indicate long-term exposure and non-deposition.	Delta top deposits.
M	Micritic limestone containing ostracods and gastropods.	Deposition of calcium carbonate in a temporary lake environment.	Temporary lake deposits.